AD-A051 925 HONEYWELL INC ST PETERSBURG FL AVIONICS DIV F/G 17/2
ATEC DIGITAL ADAPTATION STUDY, DEVELOPMENT AND FIELD EVALUATION--ETC(U)
JAN 78 T J CAMPBELL, W F ACKER, C L CHRISTNER F30602-75-C-0282
UNCLASSIFIED 1077-14813-VOL-1 RADC-TR-77-431-VOL-1 NL

1 OF 3
AD
A051925

(2)

RADC-TR-77-431, Volume I (of three)
Final Technical Report
January 1978

ATEC DIGITAL ADAPTATION STUDY, Development and Field Evaluation - Digital Automated Technical Control

Mr. T.J. Campbell
Dr. W.F. Acker
Mr. C.L. Christner
Mr. D.T. Doyle
Mr. W.M. Goldstein
Mr. R.L. Tufaner

Honeywell Inc.

Approved for public release; distribution unlimited.

ROME AIR DEVELOPMENT CENTER
Air Force Systems Command
Griffiss Air Force Base, New York 13441

Because of the size of this report, it has been divided into three volumes. Volume I contains Sections 1 through 5. Volume II contains Section 6. Volume III contains Section 7 and Appendices A and B.

The quality of copy of test data and/or results is the best available. The reproduction was the original copy which cannot be duplicated or better copy produced. The test data is not of the highest printing quality but because of economical consideration, it was determined in the best interest of the government that it be used in this publication.

This report has been reviewed by the RADC Information Office (OI) and is releasable to the National Technical Information Service (NTIS). At NTIS it will be releasable to the general public, including foreign nations.

RADC-TR-77-431, Volume I (of three) has been reviewed and is approved for publication.

APPROVED: Arnold E Argenzia

ARNOLD E. ARGENZIA
Project Engineer

APPROVED: Fred I Diamond

FRED I. DIAMOND
Technical Director
Communications and Control Division

FOR THE COMMANDER: John P Huss

JOHN P. HUSS
Acting Chief, Plans Office

If your address has changed or if you wish to be removed from the RADC mailing list, or if the addressee is no longer employed by your organization, please notify RADC (DCLD) Griffiss AFB NY 13441. This will assist us in maintaining a current mailing list.

Do not return this copy. Retain or destroy.

UNCLASSIFIED

SECURITY CLASSIFICATION OF THIS PAGE (When Data Entered)

REPORT DOCUMENTATION PAGE

READ INSTRUCTIONS BEFORE COMPLETING FORM

1. REPORT NUMBER: RADC-TR-77-431, Vol 1 (of three)

2. GOVT ACCESSION NO.

3. RECIPIENT'S CATALOG NUMBER

4. TITLE (and Subtitle): ATEC DIGITAL ADAPTATION STUDY, Development and Field Evaluation - Digital Automated Technical Control.

5. TYPE OF REPORT & PERIOD COVERED: Final Technical Report. Mar 1977 - August 1977

6. PERFORMING ORG. REPORT NUMBER: 1077-14813-Vol-1

7. AUTHOR(s): Mr. T.J. Campbell, Mr. W.F. Acker, Mr. C.L. Christner, Mr. D.T. Doyle, Mr. W.M. Goldstein, ~~Mr. R.L. Tufaner~~

8. CONTRACT OR GRANT NUMBER(s): F30602-75-C-0282 new

9. PERFORMING ORGANIZATION NAME AND ADDRESS:
Honeywell Inc./Avionics Division
13350 U.S. Highway 19
St. Petersburg FL 33733

10. PROGRAM ELEMENT, PROJECT, TASK AREA & WORK UNIT NUMBERS:
33126F
21550101

11. CONTROLLING OFFICE NAME AND ADDRESS:
Rome Air Development Center (DCLD)
Griffiss AFB NY 13441

12. REPORT DATE: January 1978

13. NUMBER OF PAGES: 232 p.

14. MONITORING AGENCY NAME & ADDRESS (if different from Controlling Office):
Same

15. SECURITY CLASS. (of this report): UNCLASSIFIED

15a. DECLASSIFICATION/DOWNGRADING SCHEDULE: N/A

16. DISTRIBUTION STATEMENT (of this Report)

Approved for public release; distribution unlimited.

17. DISTRIBUTION STATEMENT (of the abstract entered in Block 20, if different from Report)

Same

18. SUPPLEMENTARY NOTES

RADC Project Engineer: Arnold E. Argenzia (DCLD)

(See reverse)

19. KEY WORDS (Continue on reverse side if necessary and identify by block number)

Performance Assessment, Fault Isolation, and Trend Analysis (PA/FI/TA) in Digital Transmission Systems
ATEC (Automatic Technical Control) Applicability for PA/FI/TA in the FKV Digital Transmission System
Sudden Service Failure Sensing System (SSFSS)

20. ABSTRACT (Continue on reverse side if necessary and identify by block number)

Subsequent to the completion of the feasibility phase of the ATEC Digital Adaptation Study, existing ATEC hardware and software was adapted or developed to provide Performance Assessment (PA), Fault Isolation (FI) and Trend Analysis for the FKV type digital transmission systems. The resulting DATEC system was then field tested using the facilities of the digital transmission test bed located at Ft. Huachuca, Arizona. The purpose of the field evaluation was to confirm the basic concepts, exercise and test the developed hardware →

DD FORM 1 JAN 73 1473 EDITION OF 1 NOV 65 IS OBSOLETE

UNCLASSIFIED

SECURITY CLASSIFICATION OF THIS PAGE (When Data Entered)

393 215

and software, and verify DATEC's capabilities to accomplish PA/FI/TA in the operational environment of an operating digital transmission system. These DATEC capabilities are directed towards the centralized nodal monitoring of numerous digital transmissions links.

The DATEC field evaluation confirmed both the practicality and advantages inherent in automated digital system monitoring, insofar as enabling the centrally located controller to performance assess, trend analyze and fault isolate the digital transmission system for numerous failure occurrences and patterns and system parameter degradation. DATEC enables technicians to monitor in-service system parameters thereby enhancing system performance and allowing more efficient utilization of maintenance resources.

Block 18. (Continued)

Because of the size of this report, it has been divided into 3 volumes:

Volume I contains Sections 1 through 5.

Volume II contains Section 6.

Vol III contains Sections 7 and Appendices A and B.

SUMMARY

Rome Air Development Center Technical Report, RADC-TR-76-302, dated October 1976, ATEC Digital Adaptation Study, described the monitoring system requirements for PA/FI/TA applicable to a digital data transmission system comprised of microwave radio links and PCM/TDM multiplex terminals interfaced with FDM multiplexers to the subscribers' equipment. The study determined that certain ATEC hardware adaptations would satisfy the monitoring requirements. These adaptations would permit the monitoring of the 3 level partial response radio baseband signal plus the counting and/or latching of transient system and equipment events, e.g., multiplexer frame errors and reframes. Software adaptations provide for system monitor point scans, operator interaction, data analysis, and CRT display generation.

The hardware selected for adaptation were the Converter-Monitor Group, Baseband, OU-116(V)/G commonly referred to as the Baseband Monitor (BBM) which was adapted to measure the 3- level partial response signal and is referred to as a Baseband Eye Monitor (BEM); and the Relay Assembly Group, OK-329(V)1/G, commonly called the Form A Scanner which was converted to a combination of Form A Scanner and event per unit time (EPUT) monitor, commonly referred to as the EPUT.

After successful in-plant testing of the adapted hardware and software, in conjunction with the control hardware, the Digital ATEC (DATEC) system was shipped to Fort Huachuca, Arizona where it was interfaced with the digital data transmission test bed for field evaluation in a simulated operational environment. This report describes the hardware and software development, the results of the field evaluation, and provides recommendations for improved system operating features.

TABLE OF CONTENTS

TABLE OF CONTENTS (Continued)

TABLE OF CONTENTS (Continued)

TABLE OF CONTENTS (Continued)

TABLE OF CONTENTS (Continued)

TABLE OF CONTENTS (Continued)

TABLE OF CONTENTS (Continued)

LIST OF ILLUSTRATIONS

LIST OF ILLUSTRATIONS (Continued)

LIST OF ILLUSTRATIONS (Continued)

LIST OF TABLES

EVALUATION

The Digital Automated Tech Control (DATEC) Adaptation Program sought to answer the questions: (1) What should be monitored for performance assessment, fault isolation and trend analysis (PA/FI/TA) of typical military digital transmission systems. (2) What measurements, data collection and analysis should a digital monitor system perform. (3) Is the present analog Automated Tech Control (ATEC) system capable of satisfying the measurement and analysis requirements, either unmodified or with minor adaptations.

The result is the confidence that the existing ATEC system augmented by minor hardware and software adaptations can satisfy all the PA/FI/TA requirements for the Digital European Backbone phase one (DEB-I) Transmission System. The hardware adaptations permit the monitoring of the 3 level partial response radio baseband signal plus the counting and/or latching of transient system and equipment events, eg., multiplexer frame errors and reframes. The software adaptations provide for the communication system monitor point scans, operator interaction, data analysis and CRT display generation.

The problem addressed in the DATEC program was that of monitoring a communications network composed of unmanned or minimally manned sites. Based upon the different communications system strata of the

DEB-I system a monitor system hierarchy was developed that provides an organized, step-by-step, layer-by-layer assessment of the communications system. The requirement to reduce Operator and Maintenance (O&M) personnel led to the additional concept of "nodal control", which is defined to be the coordination, supervision, operation and maintenance management of portions of the DCS from a central site. Thus, the total concept includes two independent monitoring systems: (1) The Sudden Service Failure System (SSFSS), and (2) The DATEC Monitoring System. The SSFSS is an equipment alarm scanner system that rapidly reports the loss of communications system service to the nodal site. The DATEC Monitoring System is a computer-based system which is used to report communications PA/FI/TA information via a Cathode Ray Tube (CRT) display.

The DATEC field test program was performed on the Ft. Huachuca to Site Sibyl AN/FRC-162 radio transmission test link located at the U.S. Army Electronic Proving Grounds, Ft. Huachuca, Arizona. The test program addressed DATEC system and equipment performance, accuracy, and effectiveness in accomplishing PA/FI/TA on the transmission test link. The system evaluation phase of the test program addressed DATEC PA/FI/TA effectiveness as judged by experienced tech controllers from Ft. Huachuca and Richards-Gebaur AFB who participated as members of the field test team. Typical transmission system failure and degradation scenarios were executed while the tech controllers sought to identify and isolate system and equipment problems. The DATEC system was determined to be effective and of definite value in providing specific transmission system information relative to PA/FI/TA. Additional

testing was conducted using the Avantek DR8A 2 bits/Hz/sec digital radio (the prototype for the Digital Radio and Multiplexer Acquisition - DRAMA - Communications System) in place of the AN/FRC-162 radio communications system.

As the DATEC system is the only digital tech control system capability that has been successfully tested and demonstrated relative to the PA/FI/TA of 12.6MB/s DEB-I and DRAMA-like line of sight communications systems, this system and its capabilities are central to the system control of digital communications systems.

The results of this work, which was done under TPO R3A, have been submitted to the ESD ATEC SPO office in order to assist their efforts relative to the Low Rate Initial Production (LRIP) ATEC acquisition program.

Arnold E. Argenzia

ARNOLD E. ARGENZIA
Project Engineer

Section 1

INTRODUCTION

This report describes the conceptualization, design, implementation, and Field Testing of adaptations of the Automated Technical Control (ATEC) monitor equipment for application to digital transmission communication systems. The report is composed of seven sections in addition to this introduction. Section 2 describes the background of the trend toward total digitization of all forms of communications networks. It also describes the objectives desired by creation of Digital ATEC (DATEC) monitors. Section 3 contains the rationale for adaptation of the ATEC Baseband Monitor to a Baseband Eye Monitor (BEM) and a detailed discussion of the BEM theory of operation. Section 4 deals with the event per unit time (EPUT) monitor in a similar manner as used for the BEM. Software development and application is described in Section 5. Field test results are covered in Section 6. Section 7 provides conclusions and recommendations.

Section 2

BACKGROUND OBJECTIVES

2.1 INTRODUCTION

The ATEC Digital Adaptation Study consisted of three related phases; Analysis and Conceptualization (Phase I), Design and Development (Phase II), and Field Test and Evaluation (Phase III).

The Phase I analysis and conceptualization objectives were: (1) analyze the FKV digital transmission system and identify those system and equipment monitor points which contribute to Performance Assessment (PA), Fault Isolation (FI), and Trend Analysis (TA) of the digital transmission system, (2) determine the monitoring system requirements which permit monitor point data collection and analysis, (3) study and analyze the ATEC system and equipment applicability in satisfying the measurement and analysis requirements for PA/FI/TA, and (4) recommend ATEC hardware and software adaptations, as required, to permit a demonstration of ATEC's digital transmission system monitoring capability in the FKV system. Phase I was completed in March 1976, and the results published in the three volume Final Technical Report (RADC-TR-76-302, October 1976).

Phase II took the Phase I recommendations and implemented them in the form of adaptation of existing ATEC hardware, along with the creation of software to enable nodal control monitoring of a six link digital transmission system (FKV). The nodal control software package included essential parameter and equipment status displays, plus parameter trend analysis information presented in trend analysis displays. Once designed and constructed, the Digitally Adapted ATEC equipment and software was in-plant tested through the use of a digital transmission system site simulator.

Phase III commenced in April 1977, and deployed the Digital ATEC (DATEC) equipment to the US Army Communications Command digital transmission system test bed at Ft. Huachuca, Arizona. There the DATEC nodal control and remote monitoring equipment was field evaluated and its capabilities assessed. Phase III field evaluation was completed in August 1977.

2.2 DIGITIZATION TREND IN THE DEFENSE COMMUNICATIONS SYSTEM

The DCS has gone full circle in the employment of digital time division multiplex equipment (TDM). TDM was initially employed in the early years of the DCS (1955 through 1960) in the form of Pulse Amplitude (PAM) and pulse position (PPM) modulation

schemes. The PAM and PPM of that era had several shortcomings, primarily that of channel capability. Most systems were limited to 24 channels.

In early 1960, the DCS began an upgrade to Frequency Division Multiplex (FDM) equipment, and by 1965 most of the world was FDM analog in one form or another. FDM was selected for several reasons, but primarily for its channel capability and acceptance by the commercial common carrier world. FDM dominated most DCS system segment upgrades over the next 10 year period (1965-1975), but not without the identification of some significant and inherent shortcomings. First, FDM is sensitive to thermal and intermodulation noise variations of both the radio path, link and multiplex equipment. Second, the standard FDM VF channel is information throughput limited by bandwidth. Increased customer data and data rate requirements necessitated the creation of various digital to analog modem devices. Still the most sophisticated of these VF channel devices can only produce maximum throughput data rates on the order of 9.6K bits. This falls short of some customers' requirements, thus slowing down data transfer operation. Finally and possibly most significant, FDM multiplex is subject to covert interception subjecting the VF traffic to analysis, interpretation, or other belligerent power intelligence operations. These and other considerations have prompted the DCA to look for better, more secure means of multiplexing mission traffic.

The nonsecure/intercept problem of FDM was addressed by the Director, Defense Communications Agency in early 1973, when announcing one of his prime objectives was the eventual bulk encryption of all DCA communications systems. State of the art developments in both cipher and TDM pulse code modulation multiplex equipment allows not only bulk encryption of the radio link baseband or Di-Group, but it is to some degree impervious to the thermal noise variations of the radio link equipment. Further, it is not sensitive to traffic signal loading and does not suffer from intermodulation distortion or noise as does FDM equipment.

Current PCM/TDM equipment allows the multiplexing of 8-24 channel Di-Groups, or 192 channels. Digital radio modulation techniques facilitate the stacking of two 192 channel digital streams on the same radio link, thus increasing the total link channel capacity to 384 channels. Other options of the PCM/TDM multiplex allows the direct input of lower speed digital data streams without the need of A/D converters or modems, and at much higher Baud rates than currently used.

The trend now is to move the greater portion of the DCS from the FDM environment into PCM/TDM. The Frankfurt-Koenigstuhl-Vaihingen or FKV digital transmission system currently installed in West Germany was the pilot program involving the installation at six locations of state of the art PCM/TDM multiplex and adapted radio equipment. This is to be followed by the Digital European Backbone upgrade or DEB, during the 1978-1983 time period. The phased DEB implementation program will see the replacement of most of the existing FDM multiplex in Europe with PCM/TDM. This trend is expected to continue throughput the world. Transmission media previously considered unsuitable for PCM transmission such as troposcatter over the horizon radio links will be adapted to PCM use, either through redesign or use of a digital applique unit (DAU) or modem.

This is the current trend in digitization of the DCS, and technical control performance monitoring and assessment, fault isolation and trend analysis must keep pace with the upgrade, and adapt itself to requirements unique to digital transmission systems.

2.3 ANALOG-VERSUS-DIGITAL COMMUNICATIONS PERFORMANCE MONITORING

2.3.1 Major Differences Between FDM and PCM

As shown in the Phase I Technical Report, PCM unlike FDM does not produce corresponding noise increases in the VF channel, for noise increases in radio equipment performance. This on one hand makes PCM far superior operationally to FDM, while on the other hand it complicates the monitoring and assessment of the link using the old method. Varying RSLs or path fades manifest themselves as bit error or framing error occurrences in the PCM link. These may or may not have been seen in the throughput VF channel.

Loading of the baseband or intermodulation noise contribution related to traffic loading is also not a significant factor in the PCM system. Increases in FDM VF channel noise performance as a function of Intermodulation noise-loading is not present in the PCM system.

It remains that little system performance information can be gleaned by monitoring the VF side of the PCM link. Thus, idle channel noise and baseband loading find little application in the PCM world.

2.3.2 Parallels Between FDM and PCM

The greatest commonality between FDM and current PCM systems is that they use the same radio modulation process (FM or PM). Certain FM RF link performance parameters such as RSL and noise retain their importance regardless of whether PCM or FDM multiplex is employed. RSL is critically important to determine what receiver noise performance and the various "eye" margins should be. Noise enables one to confirm that the receiver noise is performing at the level predicted by the RSL.

2.3.3 Summary

In summary, it should be noted that the ability to assess the system from the VF channel level is not present in the PCM world. Lastly, the practice of assessing multilink (hop) systems or routes through the VF channel is also not available in the PCM system. Performance assessment must be on a link by link basis and instrumented accordingly.

A discussion of PCM performance monitor points and parameter follows below.

2.4 MONITOR POINTS

Based on the Phase I analysis of the FKV type digital transmission system, key performance and alarm parameters were identified for all major system components or functional areas. These monitor points are presented in Table 2-1. They are grouped by the following equipment levels or functions:

Radio

Baseband

T1-4000 Multiplexer

T1WB1 Multiplexer

CY-104 Multiplexer

Voice Frequency

For each alarm/parameter listed, a definition, alarm condition (when applicable), and use is listed. These monitor points provide the data which is processed and used by DATEC to perform PA/FI/TA on an FKV type digital transmission system.

TABLE 2-1. COMMUNICATION SYSTEM MONITOR POINTS

AN/FRC-162 Radio Monitor Points

Tx Problem Tx A Tx B	Definition: Tx Problem is the OR function of Power, AFC, and Pilot alarms. Alarm Condition: Occurs if transmitter RF power is below a specified threshold, if AFC voltage is beyond normal control range or phaselock reference is lost, or if pilot level is below a specified threshold. Use: To determine whether or not A or B transmitter is operative or in a degraded or inoperative state.
Rx Problem Rx A Rx B	Definition: Rx Problem is the OR function of Rx Phase lock and Rx Squelch alarms. Alarm Condition: Occurs if receiver local oscillator has lost phaselock with receiver crystal controlled reference or if received signal level is below a preset threshold. Use: Employed to indicate if received signal is in a usable or degraded state. It also can be used for fault isolation since joint occurrence of a Tx Problem and Rx Problem indicates a Tx failure while no Tx Problem and an Rx Problem indicates an RF path or Rx failure.
Rx Squelch Rx A Rx B	Definition: Rx Squelch is the radio receiver squelch alarm output. Alarm Condition: Indicates that received signal level is below a preset threshold. Use: Employed to indicate severe path loss or a degraded signal level caused by Tx or Rx degradation.

TABLE 2-1. COMMUNICATION SYSTEM MONITOR POINTS (Continued)

NOTE

Both Rx Squelch and Rx Problem (which includes Rx Squelch) are useful alarms. Rx Squelch is monitored and correlated with the T1-4000 BER measurement to indicate a high error rate due to RF fade. Occurrence of Rx Problem indicates that no signal is present in the radio receiver or that the signal is below a usable level. Joint occurrence of both Rx Problem alarms indicates a failure of both radio channels and, hence, loss of RF communications.

Maintenance Maintenance A Maintenance B	Definition: This alarm or status indicator indicates that maintenance is in progress on a particular radio equipment. Alarm Condition: Controlled by position of toggle switches located near equipment. Use: If maintenance is known to be in progress on equipment, this knowledge is used to suppress monitoring system response to maintenance-related alarms.
RSL Rx A Rx B	Definition: RSL A and B are receiver analog output voltages which are monotonic functions of respective receiver received signal levels. Alarm Condition: Does not apply to these analog output voltages. Use: RSL is processed by monitoring system to yield value of received signal level. RSL provides path loss information as well as information related to Tx and Rx performance.
Rx Pilot Rx A Rx B	Definition: Rx Pilot is the radio receiver pilot alarm output. Alarm Condition: Indicates loss of radio pilot carrier in radio receiver. Use: Loss of pilot monitor means loss of a usable radio signal. Both A and B Pilot alarms are ANDed to yield SSFSS Radio Rx alarm. Occurrence of Radio Rx alarm indicates loss of both radio channels.

TABLE 2-1. COMMUNICATION SYSTEM MONITOR POINTS (Continued)

Tx In-Service (Unit A or B)	Definition: Tx In-Service is a two-valued status indicator which indicates which of two radio transmitters on a particular link is in-service. Alarm Condition: Monitor point employed to indicate status rather than alarm condition. Use: To determine which transmitter is in operation, mainly for use in fault isolation.
Rx In-Service (Unit A or B)	Definition: Rx In-Service is a two-valued status indicator which indicates which of two radio receivers on a particular link is in-service. Alarm Condition: Monitor point employed to indicate status rather than alarm condition. Use: To determine which receiver is in operation. Long term use of one receiver under conditions of automatic switching may indicate that the receiver that is rarely used is degraded when compared to the high use receiver.
Power Supply Voltages 1-8	Definitions: These are actual values of radio internal voltages. Alarm Condition: This does not apply to analog parameters. Use: For determining power supply degradation before power supply and consequential equipment failure.

TABLE 2-1. COMMUNICATION SYSTEM MONITOR POINTS (Continued)

Baseband Monitor Points

Radio Baseband Eye Rx A Rx B (Noise, Amplitude, and Hits)	Definition: Noise is the eye pattern scatter measured on the 3-level partial response signal as measured at baseband radio output between radio receiver and T1-4000 receiver input. Amplitude is the signal level of the partial response before AGC circuit. Hits are a measure of the burst-like nature of noise in the 3 level eye. Alarm Condition: This does not apply to these analog parameters. Use: Parameters measured here are derived from the baseband signal at the radio receiver outputs. These are analog signals from radio receiver outputs to the diversity switch to the T1-4000 receiver input. Briefly, the baseband waveform is AGCed and filtered to produce a 3 level partial response signal. Measures of the nonAGCed level, composite signal eye scatter or noise and the burst character of the noise are converted to analog voltages which are measured by a MAC. Eye scatter noise is related to multiplexer performance over a BER range of 10^{-3} to 10^{-15} and is used to derive a measure of radio link performance margin. Amplitude of the signal from the radio output is valuable for assessing operation of the multiplexer transmitter and radio link and also is useful for fault isolating to the level of the T1-4000 receiver. Monitoring of baseband eye pattern at T1-4000 radio interface allows a comparison of derived BER performance, at the radio baseband, with the calculated BER from T1-4000 frame error rate. This permits degradation or fault isolation to the analog signal processing portion of the T1-4000. (This includes 3LPR filter and AGC circuits prior to the redigitizing process in the T1-4000 receiver.)

TABLE 2-1. COMMUNICATION SYSTEM MONITOR POINTS (Continued)

Radio Baseband Eye (Cont)	A measure of the burstlike or hit nature of the noise is also made for the purpose of detecting radio frequency interference of an impulse or burst nature. Inclusion of the hit measurement in the baseband monitor effectively removes the requirement for a radio noise burst measurement.
T1-4000 Monitor Points	
Switch Major	Definition: Major alarm output of the switch which controls two T1-4000s. Alarm Condition: Occurs if a transfer from use of one T1-4000 to other T1-4000 fails, if standby multiplexer loses synchronization while transferred, if a remote alarm is received, or in case of a switch or multiplexer power failure. Use: Primarily to indicate a switch failure or failure of a transfer of operation from one T1-4000 to other T1-4000.
Switch Minor	Definition: This is the minor alarm output of the switch which controls two T1-4000s. Alarm Condition: Occurs if operation of receiver or transmitter is transferred, if a receiver or transmitter automatic transfer is disabled, if a unit loses power, or if the standby multiplexer loses synchronization. Use: Primarily to indicate transfer of operation of a multiplexer receiver or transmitter.
Major Alarm Unit A Unit B	Definition: This is the major alarm output of each of two T1-4000s which are served by a switch. Alarm Condition: Occurs if the 3-level error density exceeds a 10^{-5} threshold, if 20 vdc power is lost, if a remote alarm is received, of if main frame or control reframe synchronization is lost in receiver.

TABLE 2-1. COMMUNICATION SYSTEM MONITOR POINTS (Continued)

Major Alarm (Cont)	Use: To indicate failure of a receiver or loss of control or main frame synchronization in a receiver.
Maintenance Unit A Unit B	Definition: This alarm or status indicator indicates that maintenance is in progress on a particular T1-4000 multiplexer. Alarm Condition: Controlled by position of a toggle switch located near respective equipment. Use: If maintenance is known to be in progress on an equipment, this knowledge is used to suppress monitoring system response to maintenance-related alarms.
Main Frame Bit Error Unit A Unit B	Definition: A pulse is generated when the receiver detects an incorrect framing bit. Alarm Condition: This is a monitored system parameter rather than an alarm. Use: Main frame bit error pulses are counted to yield a bit error rate value for T1-4000 Radio path.
Control Reframe Unit A Unit B	Definition: This is an indication given when the receiver undergoes the process of control reframe. Alarm Condition: This is a monitored system parameter rather than an alarm. Use: Latched to provide a measure of multiplexer performance by detecting the occurrence of a control reframe.
Tx In-Service and Rx In-Service (Unit A or B)	Definition: These are two-valued status indicators which indicate which of two multiplexer transmitters and which of two multiplexer receivers is in operation at a given time. Alarm Condition: An alarm condition does not apply to this status indicator.

TABLE 2-1. COMMUNICATION SYSTEM MONITOR POINTS (Continued)

Tx In-Service and Rx In-Service (Cont)	Use: Knowledge of which unit is typically in-service is used to locate degraded in-service or standby units and to fault isolate.
Power Supply Voltage 1-5	Definition: These are the actual values of the multiplexer internal power supply voltages. Alarm Condition: This does not apply to these analog parameters. Use: Useful for determining power supply degradation before power supply and consequential equipment failure.
T1WB1 Monitor Points	
Office	Definition: This is an alarm provided by T1WB1. Alarm Condition: An office alarm is given due to remote alarm, local alarm, bi-polar errors in the receiver, fuse alarm, loop alarm, outgoing alarm cut-off switch or loss of power. A uniform error rate of 2.6×10^{-5} will trigger alarm within 100 msec. Use: Primarily to indicate a loss of power or an abnormally high bi-polar error violation.
Reframe	Definition: This signal indicates that the multiplexer is attempting to acquire frame synchronization. Alarm Condition and Use: Indicates that multiplexer does not have frame synchronization. Use: Latched to provide a measure of multiplexer performance by detecting the occurrence of a reframe.

TABLE 2-1. COMMUNICATION SYSTEM MONITOR POINTS (Continued)

Maintenance	Definition: This maintenance signal indicates that a maintenance function is in progress on the T1WB1. Alarm Condition: Controlled by position of a toggle switch near the multiplexer location. Use: If maintenance is known to be in progress on the equipment, this knowledge is used to suppress monitoring system response to maintenance-related alarms.
Frame Bit Error	Definition: This is a pulse which indicates the presence of a frame bit error in the receiver. Alarm Condition: This is a monitored system parameter rather than an alarm. Use: Frame bit errors are counted to yield a bit error rate value for the respective T1WB1/T1-4000/Radio paths in the FKV.
Power Supply Voltages 1-6	Definition: These are the actual values of the T1WB1 multiplexer internal power supply voltages. Alarm Condition: This does not apply to the analog power supply voltages. Use: To determine power supply degradation before power supply and consequential equipment failure.
CY-104 Monitor Points	
Service	Definition: A composite alarm that indicates when any of the following conditions exist: local alarm, loop alarm, or remote alarm. Alarm Condition: Alarm is activated if any of the above occur.

TABLE 2-1. COMMUNICATION SYSTEM MONITOR POINTS (Continued)

Service (Cont)	Use: For CY-104 fault isolation. If no alarms at the T1-4000 and radio level in the system and a service alarm is activated, failure of a CY-104 is indicated.
Remote	Definition and Alarm Condition: This alarm is activated if the far end CY-104 is not passing valid data. Use: This alarm serves the same use as the Service Alarm. It also serves as a redundant backup alarm since it is available at a different physical location than the corresponding CY-104 Service Alarm.
VF Monitor Points (IQCS Measurements)	
Average Power (dBm)	Definition: This is the average power level observed over a 3 second interval on the VF channel undergoing analysis. Alarm Condition: Alarm condition does not apply to this analog measurement. Use: If no data or voice signal is present, this measurement yields a value for residual system or background noise. If data or voice is present, the measurement yields a value of the average signal level.
Signal to Noise (2600 Hz)	Definition: This is the noise observed on the VF channel after notching out the 2600 Hz tone. Alarm Condition: Alarm condition does not apply to this analog measurement. Use: Yields a SNR for the channel by dividing the total power observed by the notched noise power.

Section 3

FUNCTIONAL DESCRIPTION OF BASEBAND EYE PATTERN MONITOR

3.1 INTRODUCTION

The Phase I ATEC Digital Adaptation Study recommended that a device be developed for monitoring those properties of a digital baseband which directly relate to signal quality. It was further indicated that the existing ATEC Baseband Monitor was a viable candidate for the adaptation for several reasons. First, it provides selectable inputs as would be required in a digital system. Second, the frequency range is correct, except for a possible downward extension of the low frequency range. Lastly, the output circuitry is suitable for providing a performance related voltage for measurement by the existing Measurement Acquisition Controller, of such parameters as eye pattern dispersion, eye hits, and eye amplitude.

Typically, the output from the degradation monitor is either an analog voltage proportional to the degree of eye pattern closure, or a derived bit error rate which is a gross extension of the basic error rate. In either case, the applique unit, of which the degradation monitor is a part, will perform the necessary signal measurement to achieve compatibility with the MTS option interface. The analog voltage output from the first mentioned type should be measured with a resolution on the order of 1 percent, which is possible even with very simple A/D conversion techniques. The pseudo error output from the second type must be counted to give events per unit time, and buffered.

The eye pattern monitors, in general, reflect a "smoothed" measure of system performance. The output of the device itself contains a significant amount of information. It can be easily trended to identify deteriorating system operation. In order to maximize the value of its use, however, the eye pattern data must be correlated with other monitored parameters such as other estimates of bit error rate and radio alarms.

In an all digital network, such as the FKV system, the Bit Error Rate (BER) is to the end user the ultimate measure of communication quality.

The most powerful indirect technique for BER estimation is the use of the eye pattern monitor. The output of the baseband monitor is designed to be compatible with the ATEC MTS option interface. An important feature of this form of BER measurement is that it provides a good estimate even in extremely low ($<10^{-9}$) BER environments.

This section provides the study and design rationale and mathematical proofs involved in the conception, design, construction and testing of the Baseband Eye Monitor (BEM).

3.2 PRELIMINARY CONSIDERATIONS

3.2.1 Inadequacy of Output Error Counting for Degradation Measuring

Digital communication links are intentionally designed to have as large a tolerance to noise and other signal degradations as practicable. A system can have such a large built-in tolerance that it will still run error free even with one or more elements severely degraded. A primary objective of performance monitoring is to detect such degradations so that they may be corrected before the digital link begins to make errors. It is obvious that the desired information for meeting this objective cannot be obtained by examining the digital output because the objective is to detect degradations while this output is still error free. Presumptive tests which remove digital links from service long enough to run test sequences through them for measuring error rate, as well as error detecting and correcting codes, have valid applications in performance monitoring; however, they are not adequate for measuring performance margin under error free conditions because they give no indication of degradations until they have become bad enough to cause errors in the received data. An ideal degradation monitoring technique should be capable of detecting degradations before they become large enough to cause errors in the received data.

The ability to detect signal degradations before they become large enough to cause errors in the received messages is vitally important for both analog and digital channels; however, the channel user's ability to detect gradually increasing degradations and anticipate loss of the channel is far better for analog voice channels than digital communication links. In analog communication links, such as voice channels, the channel induced noise and distortion are delivered to the user along with the desired signal; hence, these degradations can be detected by the user. These degradations are detectable by the user at power levels several decades lower than the level at which they make the channel unusable by lowering the intelligibility index of the voice signal below an acceptable level. Thus, in analog communication channels there is typically a large margin between the level at which noise and distortion is detectable and that at which it becomes intolerable. Furthermore, the user of a voice channel can readily estimate the degree of channel degradation by a qualitative estimate of signal intelligibility. The user of a digital channel is presented with a very different situation because each digital receiver in the communication chain reshapes the digital pulses so that the symptoms of channel noise and distortion are removed before the signal is forwarded.

The primary effect of pulse reshaping between the links of the digital communication chain is to reduce the message error rate by stripping off noise and distortion at each link interface so that these individual link induced distortions are not allowed to accumulate as they would in an analog system. Thus, even if the sum of the noises and distortions for the total number of links is so large as to produce an intolerable error rate for an end-to-end digital system using no intermediate pulse reshaping, it is often possible to reduce the end-to-end error rate to approximately zero by stripping off the noise and distortion and regenerating the digital signal at selected locations in the chain. As long as the cumulative degradation in each individual link is kept below the critical level for that link, each link will run error free, and hence, the end-to-end channel will run error free. On the other hand, if the degradation in one, several, or all of these links is just slightly below the critical level at which it begins to produce errors, there will be no indication of this impending problem in the error-free data stream delivered to the user. Thus, the pulse reshaping in digital systems is advantageous in that it can help reduce the error rate of the system; however, it removes symptoms of channel degradation from the output data signal. Since the digital output signal gives no indication of degradation until errors actually occur in the output, the user who has nothing but the receiver digital signal to work with has no means of estimating how close the channel degradations are to the critical levels until after one or more of those levels has been exceeded.

The inability of the user to detect gradual channel degradations until they are large enough to produce errors in the received digital data stream would be less objectionable if there were a greater separation between the degradation level at which the error rate becomes just barely measurable and that at which it becomes intolerable. Assuming that the degrading factor is additive uncorrelated Gaussian noise, then the amplitude of the noise will be distributed in accordance with the cumulative Normal probability function plotted in Figure 3-1. Observe that the probability, $P(z<t)$, of the normally distributed noise amplitude, z, exceeding an arbitrary threshold, t, decreases so rapidly with increasing t that even when using a seven decade semilog scale, the probability function crosses the plot vertically more than seven times (indicating more than 49 decades) as the amplitude of t is changed less than 24 db (1.2 decades). As a consequence of this extremely rapid change of $P(z>t)$ with respect to t, the bit error rate of a digital receiver can change very rapidly with respect to small changes in the amplitude of the additive Gaussian noise. For an ordinary PAM (pulse amplitude modulated) signaling, it can be shown that the BER (Baud error rate; that is, probability of receiving one or more bits incorrectly in one Baud) for additive uncorrelated Gaussian noise can be computed from the following relations.

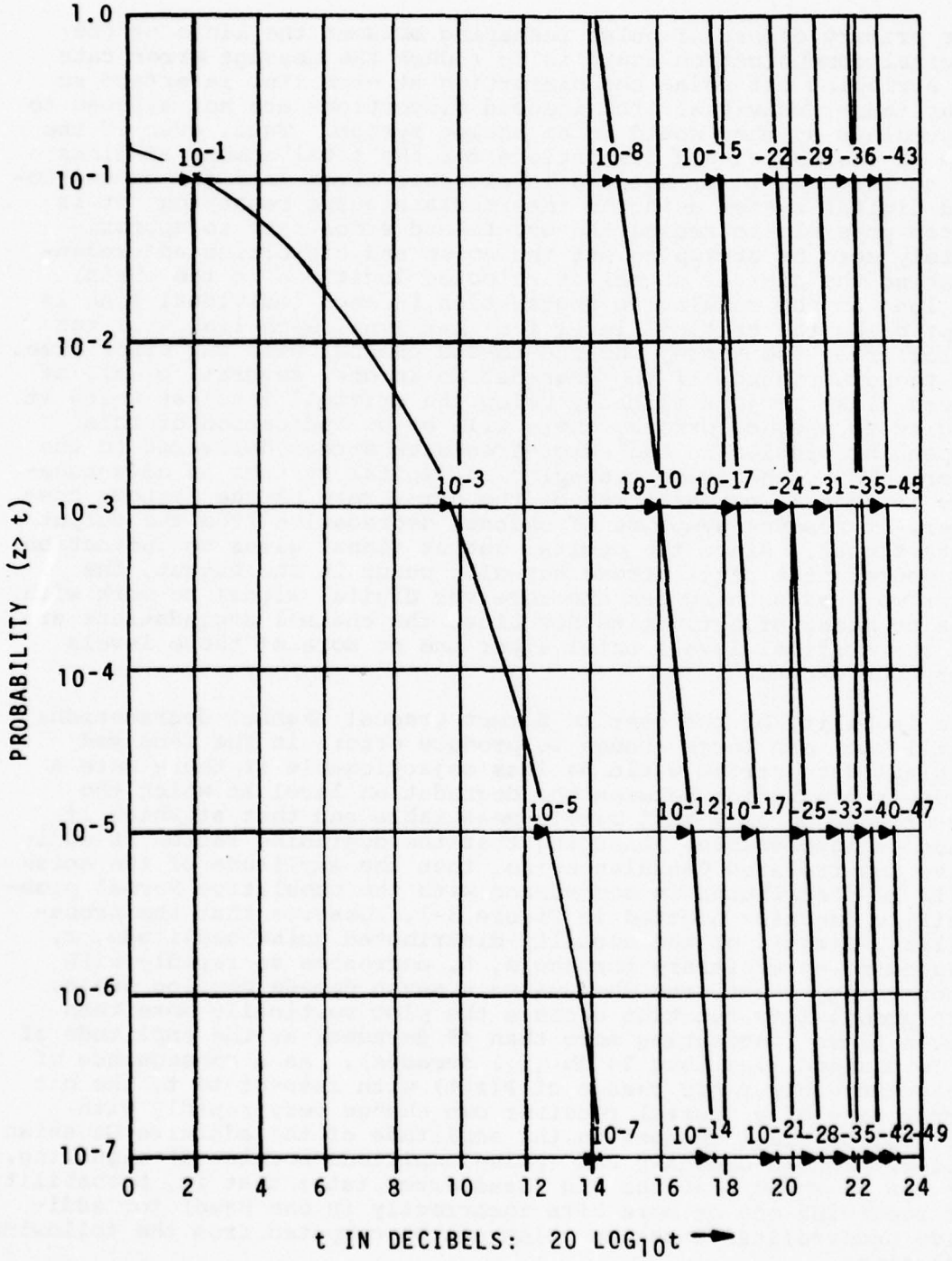

FIGURE 3-1. PROBABILITY THAT z > t GIVEN THAT z IS NORMALLY DISTRIBUTED WITH MEAN = 0 AND VARIANCE = 1

$$BER = 2\left(1 - \frac{1}{L}\right) P\left(z > \sqrt{\frac{3}{(L^2 - 1)} \frac{S^2}{N^2}}\right) \quad (1)$$

where

$L \equiv$ number of levels per Baud

$z \equiv$ normally distributed random variable with mean = 0 and variance = 1.

$S^2 \equiv$ signal power at decision circuit.

$N^2 \equiv$ noise power at decision circuit.

$P(z>\cdots) \equiv$ the probability plotted in Figure 3-1.

For the most common types of partial response signaling (Class I with n=2 and Class IV with n=3 per Reference 9), the BER can be computed using the similar relationship shown below:

$$BER^* = 2\left(1 - \frac{1}{M^2}\right) P\left(z > \sqrt{\frac{3}{2(M^2 - 1)} \frac{S^2}{N^2}}\right) \quad (2)$$

where

$$M \equiv \frac{L + 1}{2} \quad (3)$$

*The reason that the above equation for BER requires a 0.91210 db higher signal to noise ratio than that given on page 89 of Reference 10 is that Lucky, Salz & Weldon's equation was derived for measuring SNR at the receiver input with half of the partial response shaping in the transmitter and half in the receiver, whereas the above equation is for SNR measured at the decision circuit regardless of how the partial response filtering is partitioned.

To clearly illustrate how the BER can change from a value essentially equal to zero to a value so large as to be intolerable for a relatively small change in signal to noise ratio, the BER for a three-level 12.5 meg bit/sec partial response signal has been computed and the results are presented in Table 3-1.

TABLE 3-1. BER COMPUTATION

Errors/Time	BER	Signal/Noise) db
10,000 errors/second	8×10^{-4}	13.31
100 errors/second	8×10^{-6}	15.89
1 error/second	8×10^{-8}	17.52
1 error/minute	1.33×10^{-9}	18.60
1 error/hour	2.22×10^{-11}	19.46
1 error/day	9.26×10^{-13}	20.04
1 error/year	2.54×10^{-15}	20.94
1 error/century	2.54×10^{-17}	21.53

Table 3-1 shows that the difference in signal to noise ratio (SNR) for 100 errors per second and for one error per century is only 5.64 db. For a reasonably accurate performance measurement it is necessary to observe a significant number of errors because the standard deviation of the number of errors measured per sample is essentially equal to the square root of the average number of errors measured per sample. For example, if the average number of errors per sample is 100, then the standard deviation is computed as $\sqrt{100} = 10$, which means that the BER is being measured with error of about 10 percent, one sigma. For measurement periods of one hour, the computed error rate will be based on error observations which on the average are half an hour old at the time the computation is made. Also, for one hour long measurements, the percentage error in the measurement will increase rapidly as the error rate drops below 1 error per minute. The signal to noise ratio producing one error per minute is only 2.71 db lower than that producing 100 errors per second which is not considered to be a very good margin for a performance degradation detector that is intended to predict rather than confirm system failure. If a larger error sample is taken to increase the margin (measured in db) of the monitor, the measurement will take longer causing an even longer delay in the monitoring process. The conclusion is that counting errors in the output data stream as a means of predicting the failure of a digital system suffering gradual degradation leaves a lot to be desired. Fortunately, more powerful degradation detection techniques are available as will be described in the next section.

3.2.2 Eye Pattern Measurements for Degradation Monitoring

The eye pattern shown in Figure 3-2 was obtained by taking a time exposure of an oscilloscope presentation of the voltage at the input to the decision circuit of a VICOM T1-4000 multiplexer. At the sampling times the voltage ideally would be exactly at one of

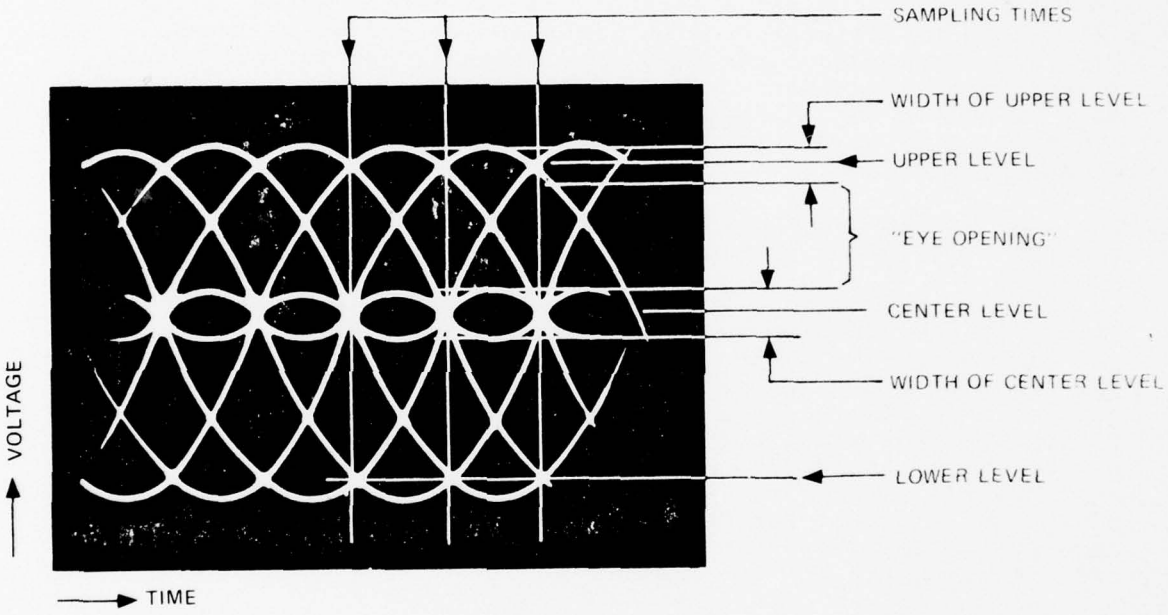

FIGURE 3-2. EYE PATTERN FOR THREE LEVEL
PARTIAL SIGNAL RESPONSE

three distinct levels; hence, this is called a three-level eye. Ideally, the decision circuit will sample the eye pattern voltage at each of the sampling times and decide whether an upper, center, or lower level signal was intended to be received at that sampling time. Additive noise will cause the voltages to deviate from their ideal values, thus widening the lines on the oscilloscope picture in the vertical direction. As the noise increases, the images corresponding to the upper, middle, and lower levels widen. When the images of the levels become so wide that there is no longer a clear separation between levels, the decision circuit will begin to misinterpret the intended message which causes errors. The spaces separating the images of the various levels at the sampling points are called the "eyes". When signal degradations become so bad that these spaces shrink to zero, the "eyes" are said to "close". When the eyes are closed, the receiver will be making errors.

The size of the eye openings relative to the distances between the centers of adjacent levels expressed as a "percentage of eye opening" has long been used as a figure of merit for performance measurement and it is a good one if its limitations are understood. First, if the decision voltage levels of the decision circuit are not located in the center of the eye vertically and, second, if the sampling times are not centered in the eyes horizontally, then the receiver will begin to make errors before the eye is totally closed. Third, since the noise typically has a Gaussian amplitude distribution, the width of the levels (and hence the percentage of eye opening) is not sharply defined because the level width image on the oscilloscope can be varied from about ±1 sigma depending upon the intensity setting of the oscilloscope and the length of the time exposure for averaging time).

These three limitations may be overcome by proper system design as will be discussed in the following paragraphs. The techniques to be discussed apply to eye patterns with any number of levels; however, the discussions will be concentrated primarily on the three-level case because the two-level case is too simple to display generality while examples involving more than three levels would make the explanation more cumbersome without adding any significant degree of insight.

Conceptually, what the eye pattern monitor should do is to measure the probability density function of the signal perturbations from the ideal levels so that the desired error rates and performance margins can be computed. In actual practice, point by point determination of the probability density function is too expensive. A practical alternative is to assume that the distribution of the perturbation amplitudes is Gaussian and make some measurement from which the rms amplitude of the distribution may be inferred. Since there are several common conditions such as additive tones, highly correlated intersymbol interference, and impulse noise for which the distribution of the perturbations deviates significantly from Gaussian, it is desirable to augment

the first amplitude measurement with a second measurement which can either indicate that the distribution is Gaussian or indicate the nature of its deviation from Gaussian.

To measure the signal perturbations from the nominal levels, it is first necessary to determine the exact amplitude of the nominal levels so that when we measure the distances from the nominal reference levels to the observed signals we will be measuring signal perturbations only-- not perturbations plus or minus the error in measuring the nominals. Automatic gain control systems based on measurement of signals biased by noise (References 4, 6, and 8) have been used for this purpose but the nominal level of the signal which they control will necessarily change as the amount of noise changes. Another example of how the signal level may become dependent upon noise amplitude is the VICOM T1-4000 multiplexer which uses a peak clipping circuit for its amplitude sensing signal so that the larger the noise the smaller the signal will be. The system concept proposed here for measuring the nominal levels in the eye pattern degradation monitor is to adjust the reference level of a comparator with a feedback loop such that 50 percent of the samples associated with that level fall above that level and the other 50 percent fall below that level. The hardware needed to implement this concept is reasonably simple.

Conceptually, it would be possible to subtract the nominal levels from the observed levels to obtain the perturbation amplitudes, compute the rms value of these amplitudes, and assume that the perturbations are normally distributed with a mean of zero and a standard deviation equal to the measured rms value. In actual practice it would be difficult to mechanize the above system for a 12.5 megaBaud/sec receiver. Also, it would be desirable to make some additional measurement (such as rectified average versus rms) to test the distribution for deviation from Gaussian. For building a device which will measure eye quality at 12.5 megaBaud/sec, a system which uses one or more additional comparators offset from the nominal levels to sense the amount of signal perturbation from nominal seems to be a practical compromise between complexity and performance.

The offset threshold monitors described in References 5 and 6 use comparators with offset thresholds as described above to measure signal quality and, therefore, they have been carefully analyzed to determine their capabilities and limitations. From an operational viewpoint, one of the biggest disadvantages of this mechanization is that its quality output signal has no absolute scale such that a specific output voltage would have a specific meaning. The calibration of the device is accomplished after it is attached to the specific multiplexer which it is to monitor. In accordance with the calibration procedure, all monitors on all multiplexers are adjusted to indicate a signal quality of 0.10 volt at the end of calibration regardless of individual variations in the operating conditions of the various multiplexers at time of calibration. To take an absurd example, if a signal quality monitor indicated a problem with a multiplexer, the first troubleshooting step

might be to check the calibration of the degradation monitor by repeating the calibration procedure; in which case the symptom of trouble would automatically disappear regardless of the condition of the multiplexer. Assuming that a calibration technique could be developed for circumventing the above problem, the existing offset threshold monitor is still not recommended because it uses a fixed (adjusted by a potentiometer during calibration) offset from the nominal reference level as a reference voltage for the comparator used to measure "pseudo error rate". With the aid of Figure 3-3, the measured "pseudo error rate" may be defined as equal to the number of samples observed between upper data decision threshold at +d volts and the upper offset threshold at + (2d-a) volts plus the number of samples observed between corresponding pair of lower thresholds -d, and -(2d-a) divided by the number of sampling periods over which the count was made. When a fixed threshold offset, a, is used, "pseudo error rate" measurements suffer from the same rapid changes for small changes in signal to noise ratio as previously described for counting actual errors. If the offset, voltage, a, is made too large, the pseudo error rate will be too small to make accurate measurements of low level degradations. If the offset voltage, a, is made too small the error rate will change rapidly for small degradations but tend to remain nearly constant at nearly 25 percent (assuming that the outer signaling levels are used 50 percent of the time) for large noise levels in the amplitude range of greatest interest where the system just begins to make actual errors. In either case, the error rate variation versus noise level is a highly nonlinear function which is not readily interpreted.

The recommended solution to the dilemma as to how large to make the voltage offset, a, for measuring "pseudo error rate" is to design a closed loop system which adjusts the voltage offset, a, as required to keep the pseudo error rate constant. From Figure 3-3 it may be seen that the thresholds for the upper pair of pseudo error comparators at 2d-a and d volts are a volts and d volts, respectively, below the nominal upper signal level. If, at a point where the signal is supposed to be at its upper level, it suffers a perturbation in the negative direction larger than a and less than d, the level of the perturbed signal will fall between the limits defined by the upper pair of pseudo error comparators and, thus, be counted as a pseudo error. The exact probability of counting a pseudo error is not determined here, but for the present discussion an approximate analysis will be meaningful. Assuming that perturbations larger than d volts are so rare compared with those larger than a as to be negligible, the probability of counting a pseudo error when the signal is nominally at the upper level is equal to the probability that the amplitude perturbation, ε, is more negative than a. To maintain the same pseudo error rate when the rms amplitude of ε is doubled, the amplitude of a must be doubled. Thus, within the limits of our approximation, it is obvious that when a is adjusted to keep the pseudo error rate constant that a is directly proportional to the rms amplitude of the perturbations ε.

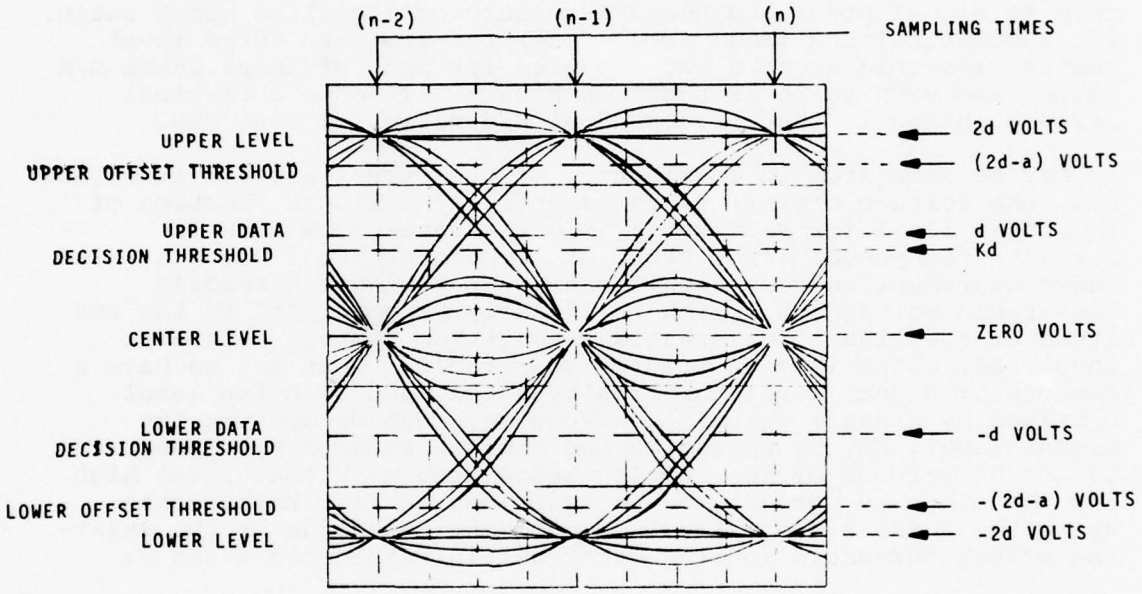

FIGURE 3-3. DEFINITION OF LEVELS FOR OFFSET THRESHOLD MONITORING OF THREE LEVEL EYE

The results of the exact derivation for constant pseudo error rates of 10 percent and 1 percent are plotted in Figure 3-4. For the exact derivation, the voltage offset, a, and the rms voltage, N, of the perturbations are both divided by d volts, half of the outer level signal voltage, in order to generalize the results. The normalized voltage offset a/d is plotted as a function of the normalized rms noise amplitude N/d and both of these quantities are dimensionless. The ordinates for the two a/d versus N/d curves were computed for the seven N/d values: 1/3, 1/4, 1/5, 1/6, 1/7, 1/8, and 1/20. Notice that N/d is a measure of noise power relative to signal power and hence a measure of signal to noise ratio. The theoretical BER (Baud error rate) for standard three level partial response signals was computed for each of these seven N/d values and each value is shown on Figure 3-4 above a vertical arrow pointing to the corresponding N/d ratio for that BER.

As may be seen from an examination of the curves plotted in Figure 3-4, the voltage offset, a, is essentially a linear function of rms noise level for receiver Baud error rates from zero to 2×10^{-3} for pseudo error rates of 10 percent and 1 percent. The above statement is very significant. We now have a readily measurable voltage, a, which is linearly proportional to the rms level of the signal perturbations about the nominal reference level, 2d, which is also readily measurable. That is, we have a measure of signal level unbiased by noise, and of noise level unbiased by signal; assuming, of course, that we measure the signal level, 2d, by adjusting the nominal reference comparator to get 50 percent of the samples associated with that level high and the other 50 percent low as described earlier rather than using the noise biased signal measurement technique of the existing offset threshold monitor described in References 6 and 7.

We now have a measurement of the signal amplitude and the noise amplitude. Still needed is a test to determine whether or not the probability density function of the noise fits the Gaussian probability distribution. This capability can be readily provided to two pseudo error detectors which are controlled to two different pseudo error rates such as 1 percent and 10 percent, for example. If the probability density function is truly Gaussian, then the voltage offsets a_1 and a_2 of the two pseudo error detectors should maintain a constant ratio with respect to each other, which is 2.441 for the 1 percent and 10 percent example. For noise probability density functions, such as those caused by single tone interference which have short tails, the ratio between b_1 and b_2 will be smaller than 2.441, and for distributions with larger tails the ratio will be larger than 2.441. By using a larger number of pseudo error detectors set at a larger number of levels, the shape of the probability density function could be determined with greater precision; however, a point of diminishing returns is quickly reached. For the present, it is suggested that the eye pattern degradation monitor have three analog voltage outputs: one to indicate the signal, 2d; one to indicate the amplitude of the perturbations, a_1; and second perturbation measure of a_2, made

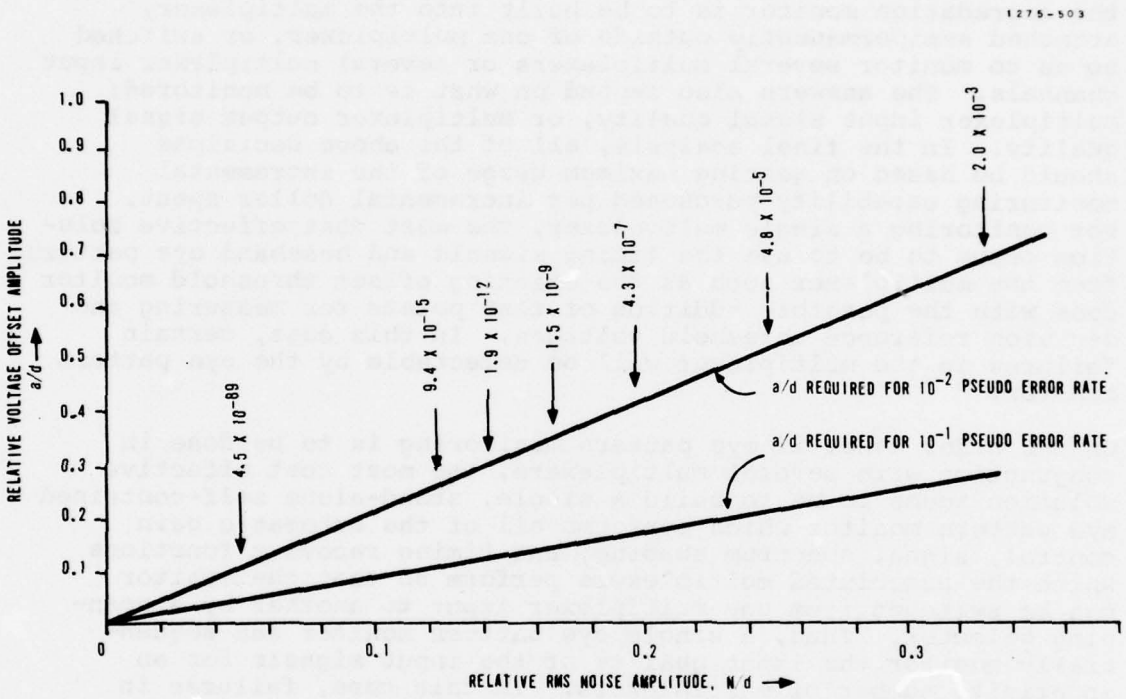

FIGURE 3-4. VOLTAGE OFFSET AMPLITUDE VERSUS NOISE FOR CONSTANT PSEUDO ERROR RATE (THREE LEVEL)

at a different pseudo error rate but scaled differently so that a_1 is equal to a_2 when the probability distribution is Gaussian.

The next question to be addressed is how should we determine the voltage level and sample timing in the multiplexer relative to the eye opening. The answers to this depend greatly upon whether the degradation monitor is to be built into the multiplexer, attached semipermanently outside of one multiplexer, or switched so as to monitor several multiplexers or several multiplexer input channels. The answers also depend on what is to be monitored; multiplexer input signal quality, or multiplexer output signal quality. In the final analysis, all of the above decisions should be based on getting maximum usage of the incremental monitoring capability purchased per incremental dollar spent. For monitoring a single multiplexer, the most cost effective solution seems to be to use the timing signals and baseband eye pattern from the multiplexer such as the existing offset threshold monitor does with the possible addition of test points for measuring the decision reference threshold voltages. In this case, certain failures in the multiplexer will be detectable by the eye pattern monitor.

On the other hand, if eye pattern monitoring is to be done in conjunction with several multiplexers, the most cost effective solution seems to be to build a single, stand-alone self-contained eye pattern monitor which performs all of the automatic gain control, signal spectrum shaping, and timing recovery functions which the associated multiplexers perform so that the monitor can be switched from one multiplexer input to another by a scanning selector. Thus, a single eye pattern monitor can sequentially monitor the input quality of the input signals for an indefinite number of multiplexers. In this case, failures in the multiplexers (other than dead shorts at the inputs, etc.) would not alter the output of the eye pattern monitor.

3.2.3 Derivation of Voltage Offset Versus Noise for Constant Pseudo Error Rates

We now derive the relationship shown in Figure 3-4 which indicates how the voltage offset a (normalized by dividing it by d) must be adjusted to keep the pseudo error rate constant as the rms noise level N (normalized by dividing it by a) changes. This relationship is derived for the three level partial response signal shown in Figure 3-3. It is assumed that noise at the sample points is normally distributed with a mean equal to zero and a standard deviation equal to N.

It is further assumed that two pairs of comparators are used. One pair measures the number of samples between d and (2d-a) volts; the other measures the number of samples between -d and -(2d-a) volts. In actual practice, the pseudo error rate measured by the upper pair of comparators may differ from that measured by the lower pair because the signal waveform may be distorted by clipping or saturation in such a manner that only one side is distorted. For this reason, it is considered necessary to use two sets of comparators so as to test both the top and bottom levels of the signal.

In the idealized case which we are considering here, the upper and lower comparator sets would both obtain the same average number of pseudo errors; hence, in this derivation, we shall derive the average rate for the top pair alone and then multiply by two to obtain the total pseudo error rate.

The magnitude of each received voltage sample is equal to its nominal intended magnitude +2d, 0, or -2d volts plus the magnitude of the signal perturbation, ε. In accordance with our previous assumption, ε must be a normally distributed random variable with mean equal to zero and a standard deviation equal to N. The probability of a particular sampled voltage amplitude falling between d and 2d-a volts, assuming that the nominal intended level was 2d, is equal to the probability that ε is of the proper size to cause the sampled voltage to fall within the specified range.

$$P(\text{upper pair detects pseudo error} \mid \text{intended level} = 2d)$$

$$= P(d \leq 2d + \varepsilon < 2d - a)$$

$$= P(-d \leq \varepsilon < -a)$$

$$= P[-d/N \leq \varepsilon/N < -a/N \mid \varepsilon/N \sim N(0,1)]$$

$$= P[d/N < z \leq a/N \mid z \sim N(0,1)]$$

$$= Q(a/N) - Q(d/N) \qquad (4)$$

where

$$Q(t) \triangleq P[z > t \mid z \sim N(0,1)]$$

= P (z > t) given z is normally distributed with mean = 0 and variance = 1.

The conditional probability of the upper pair of comparators detecting a pseudo error given that the intended level was zero may be computed simularly.

$$P(\text{upper pair detects pseudo error} \mid \text{intended level} = 0)$$

$$= P(d < 0+\varepsilon \leq 2d-a)$$

$$= P[d/N < \varepsilon/N \leq (2d-a)/N \mid \varepsilon/N \sim N(0,1)]$$

$$= Q(d/N) - Q(2d-a)/N \tag{5}$$

Likewise,

$$P(\text{upper pair detects pseudo error} \mid \text{intended level} = -2d)$$

$$= P(d < -2d+\varepsilon \leq 2d-a)$$

$$= P(3d < \varepsilon \leq 4d-a)$$

$$= P[3d/N < \varepsilon/N \leq (4d-a)/N \mid \varepsilon/N \sim N(0,1)]$$

$$= Q(3d/N) - Q(4d-a)/N \tag{6}$$

For the three-level partial response signal considered here, the probability of level +2d, 0, or -2d being intended is 1/4, 1/2, or 1/4, respectively. Therefore, the probability of the upper pair of comparators detecting a pseudo error is as follows.

$$P(\text{upper pair detects pseudo error})$$

$$= 1/4\ \{Q(a/N) - Q(d/N)\}$$

$$+ 1/2\ \{Q(d/N) - Q[(2d-a)/N]\} \tag{7}$$

$$+ 1/4\ \{Q(3d/N) - Q[(4d-a/N]\}$$

$$= 1/4\ \{Q(a/N) + Q(d/N) - 2Q[(2d-a)/N] + Q(3d/N) - Q[(4d-a)/N]\}$$

Given that both an upper pair (2d-a and d) and a lower pair (-2d+a and -d) of pseudo error comparators are to be used, and assuming that both pairs detect the same average number of errors, the total pseudo error rate will be twice that derived above.

P (pseudo error)

$$= 1/2 \{Q(a/N) + Q(d/N) - 2Q[2d-a)/N] + Q(3d/N) - Q[(4d-a)/N]\} \quad (8)$$

Using the above equation, we may solve explicitly for P (pseudo error) as a function of the two normalized variables a/N and d/N (or N/d if preferred). To obtain the points required to plot a/N as a function of N/d for a constant value of pseudo error, as shown in Figure 3-4, it would be convenient to have an equation expressing a/N as an explicit function of P (pseudo error) and N/d. Not having such an explicit relationship for a/N, the above equation was solved iteratively for each fixed value of N/d by adjusting a/N successively until the desired value of P (pseudo error) was obtained to the desired accuracy. The initial value of a/N for each series of iterations could be solved for explicitly using the following approximation which neglects the last three terms of the equation.

$$P \text{ (pseudo error)} \approx 1/2 \; Q(a/N) + Q(d/N) \quad (9)$$

$$Q(a/N) \approx 2 \; P \text{ (pseudo error)} - Q(d/N) \quad (10)$$

$$a/N \approx Q^{-1} [2 \; P \text{ (pseudo error)} - Q(d/N)] \quad (11)$$

For the points shown in Figure 3-4, the above approximation is quite accurate.

For example, the approximation is poorest at N/d = 1/3 and P (pseudo error) = 0.01, at which point the approximation gives

$$a/N \approx Q^{-1} [0.02 - Q(3)] = 2.0829 \quad (12)$$

After iterative solutions to find an improved value for a/N, we obtain a/N = 2.0805. Substituting a/N = 2.0805 and N/d = 1/3 into the precise equation for P (pseudo error), we obtain the following numerical solution.

P (pseudo error)

$$= 1/2\{Q(2.0805 + Q(3) - 2Q(3.9195 + Q(9) - Q(9.9195)\}$$

$$= 1/2\{0.0187398 + 0.0013500 - 0.0000888 + 1.15 \times (10)^{-19}$$

$$- 1.75 \; (10)^{-23}\}$$

$$= 1/2 \; (0.0200010) = 0.0100005 \quad (13)$$

Notice that the fourth and fifth terms of the exact expression were truly negligible at this point and the effect of the third term was small, only changing a/N from 2.0829 to 2.0805; that is, 0.1 percent.

It is significant to check the accuracy of the one term approximation for P (pseudo error) because the one term approximation produces a linear relationship between a and N which is convenient for interpreting the output of the degradation monitor.

$$P \text{ (pseudo error)} \approx 1/2\ Q(a/N) \tag{14}$$

$$a/N \approx Q^{-1}\ [2\ P \text{ (pseudo error)}] \tag{15}$$

for

$$P \text{ (pseudo error)} = 0.01 \tag{16}$$

$$a \approx N\ Q^{-1}\ (0.02) = 2.0542\ N \tag{17}$$

$$a/D \approx 2.0542\ N/d \tag{18}$$

The above equation defines the asymptote which the 0.01 pseudo error rate curve on Figure 3-4 approaches as N/d approaches zero. Collecting results where P (pseudo error) = 0.01 and N/d = 1/3,

Using all five terms, $a/N \approx 2.0805$, exact (19)

Using three terms, a/N 2.0805, negligible error (20)

Using two terms, a/N 2.0829, 0.1 percent high (21)

Using one term, a/N 2.0542, 1.3 percent low. (22)

Since the P (pseudo error) = 0.01, N/d = 1/3 point was selected as the point farthest away from the one term asymptotic approximation for all points computed in plotting Figure 3-4, the one term approximation is adequate for most purposes over the range of values plotted.. Using this approximation, the rms noise level is directly proportional to the measurable voltage with a known scale factor; hence, we have a means for determining the rms noise level.

The actual (not pseudo) Baud error rate for the transmitted data may be conveniently computed from the following equations, which are equivalent to those given earlier except that the rms signal power parameter, S, has been replaced with the closely related parameter, d, which as defined previously as equal to half of the voltage difference between adjacent levels.

For ordinary (that is, all levels equally probable) PAM signaling with L levels,

$$\begin{aligned} BER &= 2(1 - 1/L)\ P(\varepsilon > d). \\ &= 2\ (1 - 1/L)\ P[\varepsilon/N > d/N \mid \varepsilon/N \sim N(0,1)] \\ &= 2\ (1 - 1/L)\ Q(d/N) \end{aligned} \tag{23}$$

Similarly, for the most common types of partial response signaling (Class I with n=2 and Class IV with n=3),

$$BER = 2(1 - 1/M^2)\ Q(d/N)$$

where

$$M \equiv \frac{L + 1}{2} \qquad (24)$$

Note that d and N are both measured by the proposed eye pattern monitor and that L is simply the number of signaling levels; hence, the eye pattern monitor output signals are sufficient for computing the actual error rate assuming that the distribution of the perturbation is Gaussian.

3.3 BASEBAND EYE PATTERN MONITOR CIRCUIT DESCRIPTION

3.3.1 Baseband Eye Monitor Overall View

The circuits presently implemented in the Baseband Eye Monitor are shown in the "Baseband Eye Pattern Monitor Functional Block Diagram", Figure 3-5. The BEM evaluates the quality of the baseband input signal (shown entering at the upper left) in the performance measurement function of the digital ATEC system. In this application, the "baseband" input signal is the output of a radio receiver. The term "baseband" (for PCM/TDM) means that the demodulation processes have been completed to the degree that no further frequency translations are required. In the presently developed BEM application, the communication system consists of VICOM TI-4000 series multiplexers connected through radio links (AN/FRC-162). The baseband signal which the BEM analyzes has a three level, PAM (pulse amplitude modulated) format. When the received analog voltage is observed with a properly synchronized oscilloscope, the resulting eye pattern for the three level partial response signal at the VICOM TI-4000 should look like that shown in Figure 3-3.

In the VICOM system, the partial response shaping filters are divided into two approximately equal parts located in the MUX transmitter and the MUX receiver. The BEM receives the same signal as the receive multiplexer and must perform the same partial response filtering in order to obtain the same eye pattern. In the multiplex receiver the quality of the eye pattern is affected by the quality of the AGC (automatic gain control) and Baud timing recovery systems. To produce an eye pattern, the BEM must perform the same functions as the MUX receiver. If the BEM performs the partial response filtering, AGC, and timing recovery functions better than the VICOM receiver, then the BEM eye pattern will be better than that of the VICOM. In such a case the BEM quality measurements would not be directly applicable to predicting VICOM receiver performance. On the other hand, if VICOM TI-4000 circuit

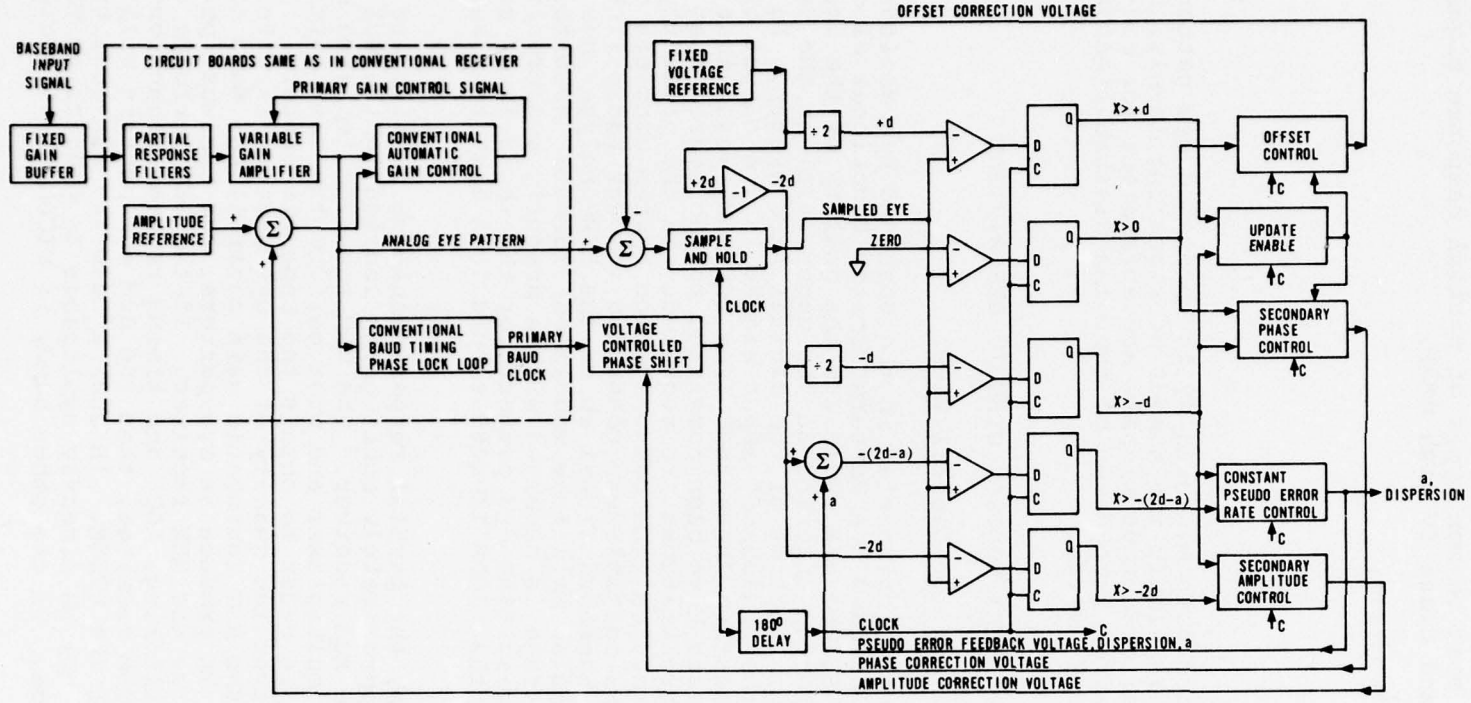

FIGURE 3-5. BASEBAND EYE PATTERN MONITOR FUNCTIONAL BLOCK DIAGRAM

boards are used for partial response filtering, AGC, and timing recovery, the BEM would be excessively sensitive to temperature fluctuations since the temperature sensitivities of the VICOM boards exceed those allowable for the BEM application.

After careful consideration of these factors it was decided that the best solution was a compromise between building improved filter, AGC, and timing recovery circuits and using the VICOM circuit boards. It was decided that the BEM quality measurements would be most useful for predicting VICOM performance if actual VICOM circuit boards were used. However, narrow bandwidth (slowly responding) secondary control loops would be needed to correct for variations of the control points of the VICOM AGC and Baud timing systems caused by temperature changes and other influences. The BEM Functional Block Diagram shows the functions performed by VICOM circuit boards (enclosed within dashed lines). A secondary, but significant, advantage of the use of MUX receiver boards is that this simplifies logistics and makes it easier to configure the BEM to monitor different types of MUX receivers.

3.3.2 Automatic Gain Control Systems

The incoming baseband signal to the BEM passes through a fixed gain buffer amplifier to the standard VICOM receiver circuit boards. The standard partial response shaping filters are used even though the resulting eye pattern shows degradation from intersymbol interference; which would not occur if the filter shaping were ideal. It was discovered that the degree of degradation of the filter shaping varied as the gain of the variable gain amplifier (VGA) changed; as the amplifier gain was increased, amplifier bandwidth decreased causing amplifier phaseshift to increase.

A new wideband VGA was developed but it was decided that the original VGA should be used. That way the variation of the eye pattern quality versus input signal level for the BEM would more nearly match that of the VICOM receiver. In the VICOM system the signal for adjusting the VGA gain is obtained by monitoring the positive peaks of the baseband eye pattern signal with a peak detector. Whenever the signal exceeds a positive reference level, current flows into a low pass filter, dc amplifier circuit. Part of the reference voltage for the gain control is dependent on diode or base emitter junction voltages which are temperature sensitive; therefore, the signal level of the VICOM AGC system varies with temperature.

The amplitude of the desired portion of the eye pattern signal also varies as a function of the noise level. The peak amplitude detecting controller attempts to adjust the gain so that the peak amplitude for the composite data and noise signal is equal to that desired for data alone. The result is that the data signal shrinks as the noise increases. In order to maintain the same dynamic response as the VICOM AGC system but eliminate the essentially steady state errors, an extremely slow secondary AGC system is built into the BEM which adds a quasi dc signal to the reference

voltage used in the VICOM AGC. This quasi dc signal from the secondary AGC system adjusts the control point of the primary (VICOM circuit board) AGC system to remove steady state gain errors without altering the dynamic response of the primary system. Except for this one modification, which requires the addition of one resistor, the portion of the BEM Functional Block Diagram inside the dashed line rectangle uses the same circuit boards used in the standard MUX receiver, for the communication channel which the BEM is monitoring.

3.3.3 Frequency and Phase Lock Systems

The standard MUX receiver circuit boards used in the BEM have two output signals. One is the analog eye pattern signal and the other is the Baud timing clock, used in the MUX receiver to control the timing of the sampling process which converts the eye pattern analog into a digital signal. Like the signal level from the AGC circuit, the phase of the Baud timing recovery circuit changes as a function of temperature and noise level. A secondary phase control system with an intentionally very slow response is used to correct for the steady state phase errors in the primary phase lock loop without significantly altering the dynamic response. The phase adjustment is accomplished by passing the primary Baud timing clock signal through a voltage controlled phaseshift device to obtain the necessary quasi-steady-state phase correction needed to satisfy the secondary phase control system. The voltage controlled phaseshift circuit produces a phase shift directly proportional to the applied voltage.

3.3.4 Phase Shifting Module

A technique for building a voltage controlled phase shift module is shown in Figure 3-6. The square wave clock signal, A, is passed through an integrator to form triangular wave signal, B, which is connected to one input of a comparator. The quasi-steady-state phase control voltage, C, is applied to the other input. When the dc component of waveform B crosses the level of phase control voltage, C, the comparator output is switched. Assuming both signals, B and C, have no dc bias, the comparator output becomes a 50 percent duty cycle square wave, D. Increasing the phase control voltage, as shown by C', causes the switching times of the comparator to change, changing the comparator output signal from a 50 percent duty cycle square wave to an unequal duty cycle, rectangular wave, D'. The rising edges of D' are delayed by a fixed phase relative to D and the falling edges of D' are advanced relative to D by the same amount.

If the circuits using the clock can tolerate an uneven duty cycle clock, the output of the comparator can be used directly as the new clock. If an equal duty cycle clock is required the frequency of the uneven clock, D', can be divided by two using a flip-flop which only clocks on the rising (or falling) edges of D' so that output, E', becomes a 50 percent duty cycle, phase adjustable clock at half the frequency of the input clock, A. When a clock at double

the required output frequency is available for an input to the phase shifter, and a maximum phase adjustment range of 90 degrees peak-to-peak is sufficient, this technique provides excellent performance with minimal hardware complexity.

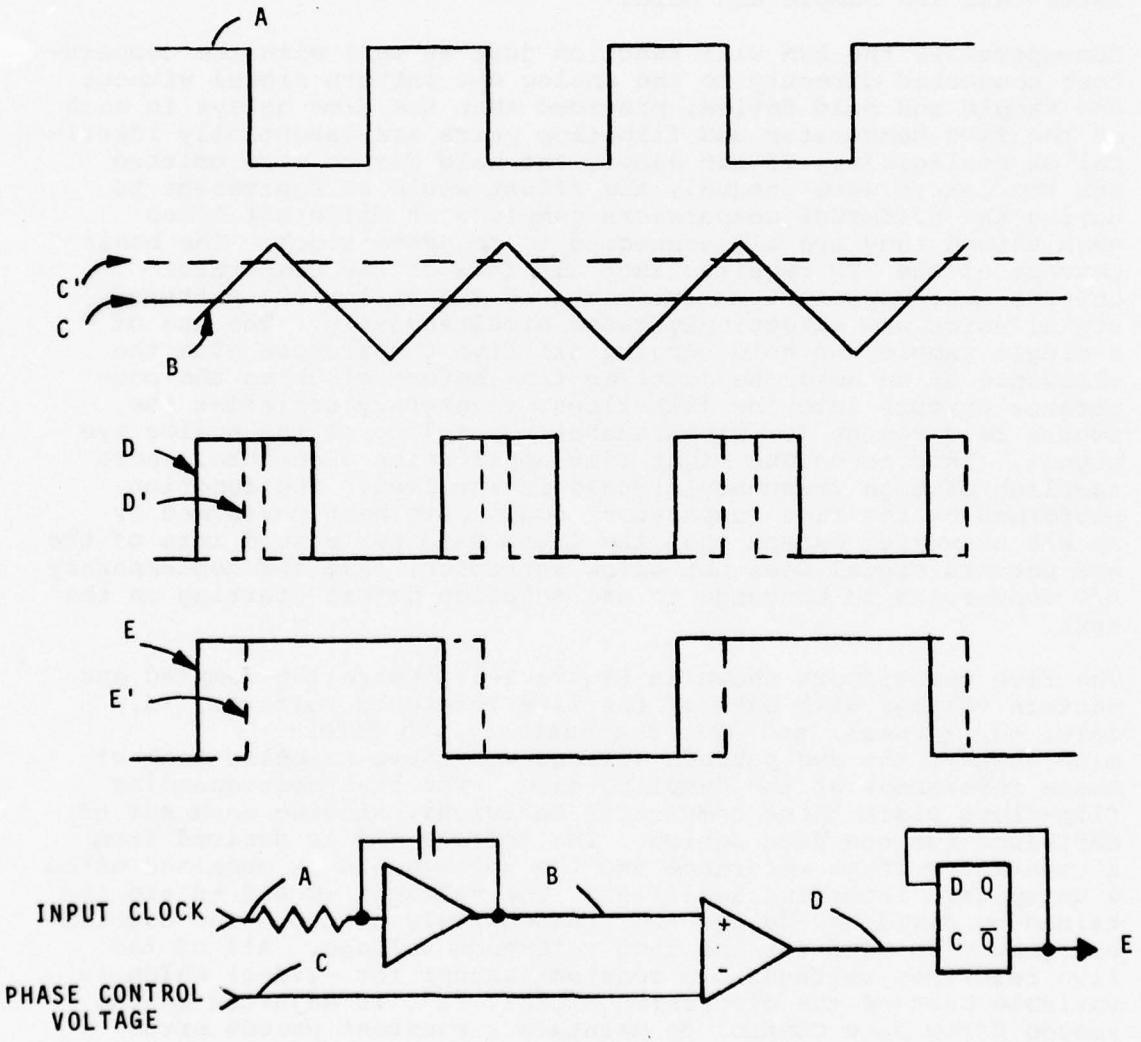

FIGURE 3-6. A VOLTAGE CONTROLLED PHASESHIFT CIRCUIT

3.3.5 Sample and Hold For Simultaneous Comparator Samples

The Baud timing clock from the voltage controlled phase shift module controls the timing of the sample and hold module which samples the analog eye pattern signal. The output of the sample and hold goes to the noninverting input of each of five comparators (Figure 3-5). Each of the comparator outputs is sampled and stored by a flip-flop which is clocked one half a Baud period later than the sample and hold.

Conceptually, the BEM will function just as well with the comparators connected directly to the analog eye pattern signal without the sample and hold device, provided that the time delays in each of the five comparator and flip-flop pairs are essentially identical or negligible. If the sample and hold device were omitted and the delays were unequal, the effect would be equivalent to having the different comparators sampling at different times even though they are all connected to the same clock. The basic concept of the BEM requires that all five of the comparator outputs must represent measurements of the analog eye pattern signal which are effectively taken simultaneously. The use of a single sample and hold serving all five comparators plus the allowance of an adequate settling time before clocking the comparator outputs into the flip-flops, rigorously satisfies the severe requirement for simultaneously sampling of the analog eye signal. This technique might find application elsewhere, where sampling of high frequency signals is involved. The function performed by the five comparators could have been performed by an A/D converter except that the 12.5M Baud per second rate of the eye pattern signal does not allow sufficient time for contemporary A/D converters to converge to one solution before starting on the next.

The five comparators shown in Figure 3-5 compare the sampled eye pattern voltage with each of the five reference voltages, +d, zero, -d, -(2d-a), and -2d, respectively, to determine whether the eye pattern voltage was above or below each of these references at the sampling time. The five corresponding flip-flops clock these comparator decisions, storing each set of decisions for one Baud period. The voltage -2d is derived from a constant voltage reference and the voltage -2d is obtained using a unity gain inverting amplifier. The voltages +d and -d are obtained by dividing +2d and -2d, respectively by two. The electrical ground is used for the zero reference voltage. All of the five reference voltages are constant except for -(2d-a) which is variable because the dispersion signal, "a", is adjusted by the Pseudo Error Rate Control to maintain a constant pseudo error rate. The time constant for the Pseudo Error Rate Control Loop is equal to a few million Baud periods; therefore, for events taking only a few thousand Baud periods or less the comparator reference voltage -(2d-a) may be considered to be essentially constant. The variable reference voltage, -(2d-a), is equal to the sum of the fixed reference voltage, -2d, and the dispersion voltage, "a".

An ordinary summing amplifier combines these two signals to obtain the pseudo steady state -(2d-a) comparator voltage reference. The outputs of the five comparators contain the needed information for correcting the dc offset, sampling phase, amplitude, and pseudo error rate of the sampled signal, as will be explained.

3.3.6 Zero Crossing Detector For Offset and Phase Controls

Errors in the eye pattern sampling clock phase can be detected by observing samples taken at the time the eye pattern voltage is supposedly passing through the zero volt level as shown in Figure 3-3. If the voltage is rising at sampling time, (n-1), sampling late will cause the sampled voltage to exceed zero, producing a 1, "true" output from the X > 0 comparator and flip-flop. On the other hand, if the eye pattern voltage were falling at the sampling time, sampling a zero crossing late would produce a false output (zero) from the X > 0 output. Therefore, to detect the direction of a phase error, it is necessary to know: first, that the eye pattern voltage sample in question was taken at or close to a zero crossing; and second, whether the sampled voltage was rising or falling when the sample was taken. Figure 3-3 shows that both of these conditions are met whenever the preceding sample, (n-2), fits the upper level and the following sample, (n), fits the lower level, or when, (n-2), fits the lower and, (n-1) fits the upper. In both cases, the voltage passes through zero at the sampling time, (n-1), and in the first case the voltage is falling at the sample time while in the second case it is rising. The logic circuit shown in Figure 3-7 detects these two patterns to allow phase corrections only when the zero crossings with maximal slopes occur.

Referring to Figure 3-3, the received analog signal, "Y", corresponding to the received three-level eye pattern will be defined as equal to +1 for an upper level signal, zero for a center level signal, and -1 for a lower level signal. The two patterns to be detected for sample phase correction as defined in the preceding paragraphs correspond to Y_{n-2}, Y_{n-1}, Y_n equal +1, 0, -1 or -1, 0, +1 respectively (Figure 3-7). When the $X_n > +d$ input in Figure 3-7 is true the received value for Y_n is equal to +1, so this is called the $Y_n = +1$ signal as shown at the input of flip-flop 2. When the $X_n > -d$ input signal is false, Y is equal to -1, so the $X_n > -d$ signal is inverted to produce the $Y_n = -1$ signal. Flip-flops 2 and 6 store the previous values of the $Y_n = +1$ signal so that the $Y_{n-1} = +1$ signal and $Y_{n-2} = +1$ signals are available at their outputs. Flip-flops 3 and 7 provide the $Y_{n-1} = -1$ and $Y_{n-2} = -1$ signals in a like manner. If the value of Y is neither +1 nor -1 then it must be 0; therefore, NOR gate 5 produces a $Y_{n-1} = 0$ signal when the $Y_{n-1} = +1$ and $Y_{n-1} = -1$ signals are connected to the input. Three-input AND gate 8

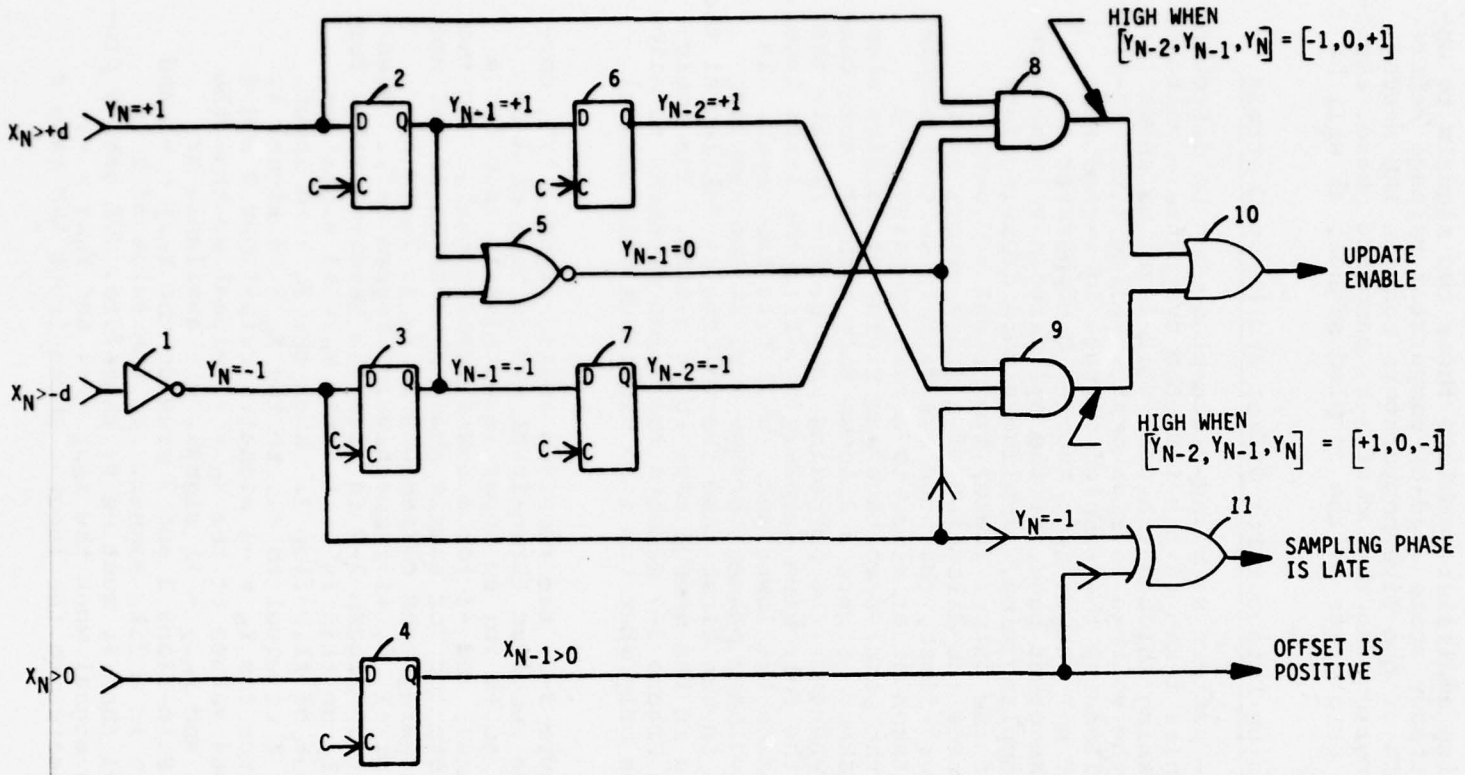

FIGURE 3-7. UPDATE ENABLE LOGIC AND THE OFFSET ERROR AND PHASE ERROR SIGNALS WITH THE CORRESPONDING TIMING

detects a zero crossing with rising voltage at sample time n-1 and gives a true output whenever the three inputs, $Y_{n-2} = -1$, $Y_{n-1} = 0$, and $Y_n = +1$ are simultaneously true. Three-input AND gate 9 detects a zero crossing with falling voltage at sample time n-1 and gives a true output whenever the three inputs, $Y_{n-2} = +1$, $Y_{n-1} = 0$, and $Y_n = -1$ are simultaneously true. The positive and negative slope zero crossing detection signals from gates 8 and 9 respectively are combined by OR gate 10 so that if either one type zero crossing or the other is detected at sample time n-1 the output of OR gate 10 will be true. Therefore, a true output from gate 10 indicates that a maximum slope zero crossing has been detected at sample time n-1.

The phase correction and dc offset correction voltages are adjusted only when maximum slope zero crossings are detected, so the signal from gate 10 is used to enable or prohibit the updating of these corrections. The true state of the gate 10 output permits the phase and dc offset corrections to be updated; therefore, this signal is called "update enable".

3.3.7 Offset Control

If the sample timing is correct but there is a positive dc offset, then the measured value of X at the time of a zero crossing will be positive regardless of the direction (increasing or decreasing) of the voltage change at the zero crossing; therefore, a true value of the $X > 0$ signal (Figure 3-5) measured at the zero crossing time indicates that the dc offset is positive. At the time that the "update enable" signal is true, the X sample corresponding to the detected zero crossing is X_{n-1}; therefore, flip-flop 4 (Figure 3-7) is used to delay the $X_n > 0$ signal one Baud period to obtain the $X_{n-1} > 0$ signal labeled "offset is positive" which is used along with the "update enable" signal to adjust the dc offset correction voltage as shown in Figure 3-8. The clock input, C, to the digital counters in Figure 3-8 would cause them to count one increment per Baud period if it were not for the "update enable" signal which permits them to count only when zero crossings are detected. The signal labeled "offset is positive" controls the direction of the counting so that the number in the counter is increased one count whenever $X_{n-1} > 0$ is true when a zero crossing is detected, and decreased one count whenever $X_{n-1} > 0$ is false when a zero crossing is detected. The most significant bits of the counter are connected to the digital to analog converter which produces the analog "offset correction voltage" signal that is subtracted from the analog eye pattern signal prior to the sampling process as shown in Figure 3-5. The counter was designed to handle binary numbers several bits longer than the D/A converter so that many LSB (least significant bit)

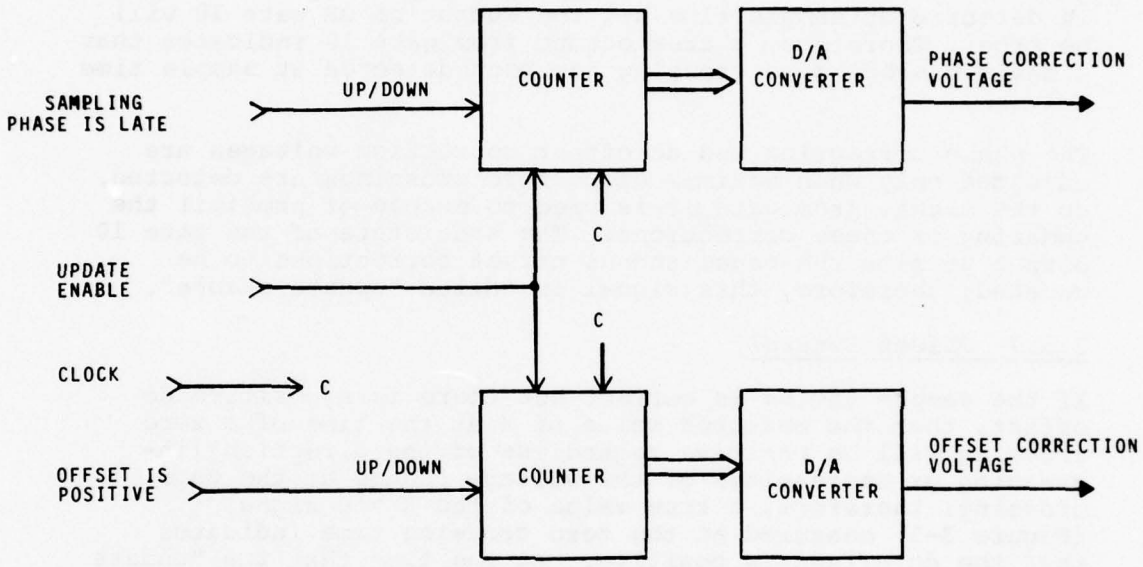

FIGURE 3-8. OFFSET CONTROL AND SECONDARY PHASE CONTROL EXCEPT FOR PORTION SHOWN WITH UPDATE ENABLE LOGIC

counts are required into the counter in order to change the A/D output by one LSB. This difference in the size of the LSBs slows the rate of response for the closed loop correction thereby decreasing the noise level in the offset correction voltage.

3.3.8 Secondary Phase Control

The phase correction loop uses essentially the same design as the offset correction loop except for the exclusive OR gate (modulo two adder), gate 11 of Figure 3-7. If the $Y_n = -1$ signal into gate 11 is true when the "update enable" signal is true, this indicates that the sampled voltage was decreasing with respect to time when the zero crossing was detected. Therefore, when negative going zero crossing is sampled late, the zero crossing sample, X_{n-1} will be negative causing, $X_{n-1} > 0$ to be false and $Y_n = -1$ to be true. These two unlike input states into gate 11 make the output signal, called "sampling phase late", true. Similarly, if a positive going zero crossing is sampled late, the $Y_n = -1$ signal will be false and the sample near the zero crossing, X_{n-1}, will be positive so that $X_{n-1} > 0$ will be true. Once again the states of the two input signals into gate 11 are unlike causing the output signal called "sampling phase late" to be true. Thus, in both zero crossing cases, sampling late will produce a true state for the "sampling phase is late" signal while the "update enable" signal is true. Similarly, it may be shown that sampling a zero crossing early will cause the "sampling phase is late" signal to be false when the "update enable" signal is true. The up down counter and D/A converter portions of the phase correction system shown in Figure 3-8 work in essentially the same manner as the equivalent components in the offset control system and, therefore, require no further explanation.

3.3.9 Secondary Amplitude Control

As explained previously, the secondary amplitude control (Figure 3-9) changes the size of the voltage reference which the primary amplitude control uses as the standard to which the signal level should be controlled. If the signal level detected by the secondary control is too small, the secondary control obtains the desired increase by increasing the size of the voltage reference used by the primary control. For the BEM to measure dispersion of the baseband eye pattern signal about the lower level accurately, the lower level of that signal must be accurately centered about the -2d voltage reference level. The secondary amplitude control adjusts the signal amplitude as needed to accomplish this centering. The secondary amplitude control block diagram, Figure 3-9, shows how the amplitude error signal is obtained and how the amplitude correction voltage is adjusted. The $X > -d$ signal is inverted to obtain a signal which is true only when the received value of X is closer to the level than any other level; therefore, this inverted signal

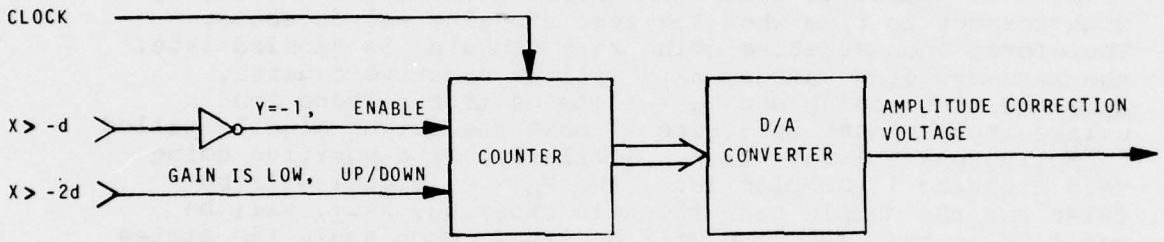

FIGURE 3-9. SECONDARY AMPLITUDE CONTROL

is called the Y = -1 signal. The function of the secondary amplitude control is to adjust the signal amplitude so that half of the lower level sample points are below the -2d voltage reference level and the other half are above that reference; therefore, the Y = -1 signal is connected to the enable input of the counter so that only X samples corresponding to lower level samples are permitted to affect the counter. The X > -2d signal is used to control the direction of the counter. When the baseband eye pattern signal is small the X > -2d signal will be true more often than false for lower level samples causing the counter to count up more often than down. The net surplus of upward counts relative to downward counts causes the counter digital output to increase thereby increasing the amplitude of the analog voltage out of the D/A converter. As said before, increasing the amplitude correction voltage out of the D/A converter causes the eye pattern signal amplitude to increase. Thus, the secondary amplitude control adjusts the signal amplitude as needed to cause half of the lower level samples to occur below the -2d level and half above.

The original BEM system plan called for adjusting the center of the upper level of the eye pattern signal to +2d volts, the center level to zero volts, and the lower level to -2d volts so that offset threshold measurements could be made to the upper level as well as the lower level. However, it was learned during laboratory testing that it was impossible to center all three levels simultaneously as intended because the levels were not equally spaced. The cause of the unequal spacing was traced to unequal duty cycles for positive and negative output pulses in the VICOM transmitter. Since improving all of the VICOM transmitters was an impractical solution, the BEM system plan was changed to accommodate this unexpected form of signal distortion. One attractive approach was to center the upper and lower levels about +2d and -2d respectively so that offset threshold measurements could still be made about both the upper and the lower levels; however, the chosen secondary phase adjustment system was not designed to tolerate dc offset of the center level. When the unsymmetrical VICOM signal problem was discovered, it was too late to add all of the system complexity needed to make the secondary phase adjustment system insensitive to center level dc offset errors. The most practical remaining option was to control the center level and either the upper or lower level, but not both. The lower level was selected for control and monitoring for reasons involving component layout and noise in the existing circuit boards. Deleting the AGC and pseudo error input signals previously supplied by measurements about the upper level cut the data rates into these control loops in half, thereby doubling the time constants for these loops; however, the loop responses are still fast enough to satisfy all of the requirements of the BEM application.

3.3.10 Pseudo Error Rate Control

The final module to be explained in the BEM functional diagram is the constant pseudo error rate controller shown as a single box in Figure 3-5 and shown in greater detail in Figure 3-10. The function of this controller is to adjust the magnitude of the offset threshold voltage, a, as the signal quality changes so that a constant percentage of the X voltage samples distributed around the lower level are above the adaptive pseudo error threshold voltage, -(2d-a).

The controller in Figure 3-10 determines how many X samples belong to the lowest level by inverting the X > -d digital signal to obtain a Y = -1 signal and using this signal to enable the 2048 counter which is clocked at the Baud rate so that it increments one count every time an X sample voltage more negative than -d volts is obtained. The 2048 counter overflows when its count reaches 2048 thereby inputting a true signal into flip-flop 1 which is clocked at the Baud rate. When the overflow = true signal is clocked to the output of flip-flop 1, it resets the 2048 counter to zero and the counter overflow returns to false. Thus, flip-flop 1 outputs a single one Baud wide true signal every time 2048 lower level X samples are counted. The reset signal to the counter is not essential if the ratio (2048) selected for input pulses versus output pulses is an even power of two because binary counters are available which, when clocked one more time after reaching the all 1's state, will automatically output an overflow signal and return to the all zero's state. However, the presence of flip-flop 1 and the reset signal makes it possible to reset the counter to some initial state other than all zero's thereby providing a wider choice in countdown ratios.

The function of flip-flop 2 is to output a single Baud baud wide true signal every time the voltage of one of the lower level X samples is more positive than the offset threshold, -(2d-a) volts. When X is one of the lower level samples, the Y = -1 signal will be true, and when the sample value is more positive than the offset threshold, the X > -(2d-a) signal will also be true; therefore, using an AND gate to combine these two signals and clocking the AND gate output through flip-flop 2 with a Baud rate clock produces the desired output. This signal is called the pseudo error signal because it indicates the presence of unusually large eye pattern deviations in the direction which would produce errors in the VICOM T1-4000 receiver if the deviation amplitudes were larger than the true decision margin, d volts, rather than merely larger than the pseudo decision margin, a volts. Each Baud width true signal clocked out of flip-flop 2 is therefore called one pseudo error.

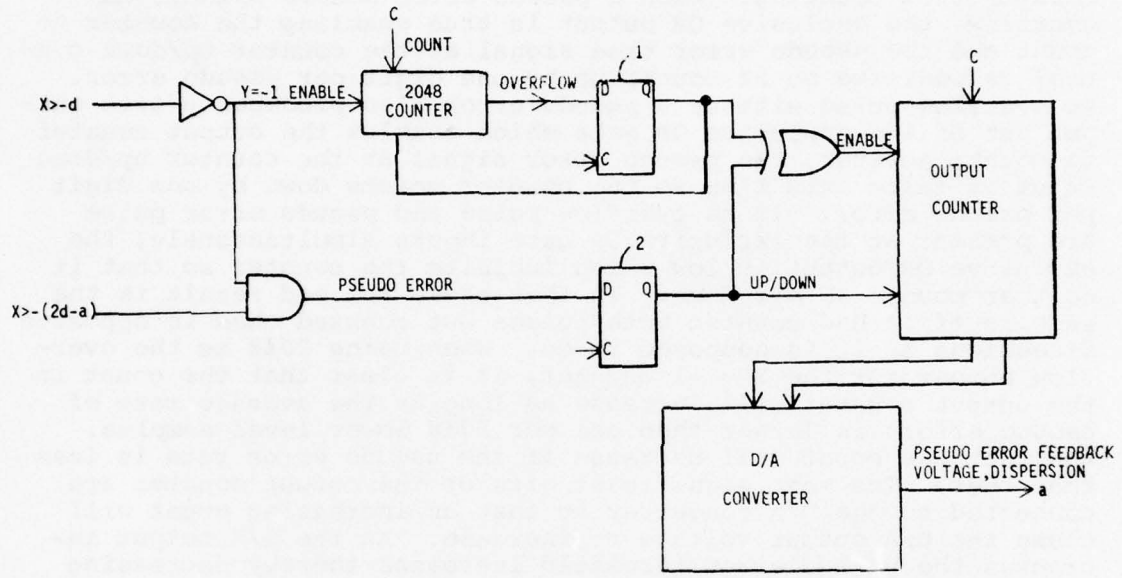

FIGURE 3-10. CONSTANT PSEUDO ERROR RATE CONTROL

The pseudo error feedback voltage, a volts, from the D/A converter is adjusted automatically by the system shown in Figure 3-10 until the average rate at which pseudo errors are clocked out of flip-flop 2 is equal to the rate at which overflow pulses are clocked out of the 2048 counter. When neither an overflow pulse nor a pseudo error pulse appear at the input of the exclusive OR gate, the output of that gate is false, which prevents the output counter from counting. When a pseudo error occurs without an overflow, the exclusive OR output is true enabling the counter to count and the pseudo error true signal at the counter up/down control is positive so it counts up by one digit per pseudo error. An overflow pulse without a pseudo error also produces a true output out of the exclusive OR gate which enables the output counter to count; however, the pseudo error signal at the counter up/down input is false this time so the counter counts down by one digit per pseudo error. If an overflow pulse and pseudo error pulse are present at the exclusive OR gate inputs simultaneously, the exclusive OR output is low which inhibits the counter so that it neither counts up nor down. In this case, the end result is the same as if it had counted both pulses but counted them in opposite directions as it is supposed to do. When using 2048 as the overflow number for the Y = -1 counter, it is clear that the count in the output counter will increase as long as the average rate of pseudo errors is larger than one per 2048 lower level samples, and that the count will decrease if the pseudo error rate is less than that. The most significant bits of the output counter are connected to the D/A converter so that an increasing count will cause the D/A output voltage to increase. As the D/A output increases the pseudo error threshold increases thereby decreasing the pseudo error rate. If the pseudo error rate is less than one pseudo error per 2048 lower level samples, the output counter will count down thereby decreasing the pseudo error margin, a, which causes the pseudo error rate to increase. If the deviations of the sampled values from their nominal levels is normally distributed with a mean value of zero and a standard deviation equal to sigma, then the one per 2048 rate for pseudo error versus lower level samples will be obtained when the pseudo error margin is equal to about 3.3 sigma. Thus, for normally distributed errors the pseudo error margin, a, is a measure of sigma. The number of sigma which the pseudo error margin, a, represents can be altered by changing the overflow level of the lower level sample counter from 2048 to some other number.

3.3.11 "Three-Level Eye Pattern" Found to Have Nine Levels

In the VICOM TI-4000 signals observed during BEM tests, the dispersions in the eye pattern were not made up of purely normally distributed components but also of strongly quantized components caused by non-ideal partial response filters. The filters produced so much adjacent symbol interference that the eye pattern signal appeared to have nine levels rather than three levels. The six undesired levels occurred slightly above and slightly below the three ideal levels. Once this departure from the normal

distribution was identified and inserted into the math models it became demonstratably possible to predict VICOM TI-4000 performance accurately from BEM pseudo error margin measurements, a; however, the means for accomplishing this are the subject of another subsection (3.4).

3.3.12 Baseband Eye Monitor Adaptability to Other Applications

The BEM uses two circuit boards from a VICOM TI-4000 receiver so that if improvements are made in these VICOM receiver cards the BEM can be updated to predict the new improved performance by replacing the old receiver cards with new ones. If the new boards are not interchangeable with the old ones, it should still be possible to accommodate the BEM to them by making appropriate modifications to the board connectors and associated wiring. During the BEM design and fabrication processes, the specialized BEM functions were made as independent from the conventional receiver boards as was practical so as to make the BEM adaptable for the measurement of other communication eye patterns.

In this report, the BEM mechanizations have been explained as applied exclusively to one particular three-level eye pattern. Also, only one adaptive threshold comparator, -(2d-a), is used in the present mechanization. Using an offset of amplitude, a, six possible locations for the pseudo error threshold were considered both separately and jointly for the present three-level, +2d, zero, -2d, eye application. Use of pseudo error thresholds at +(2d +a) and/or at -(2d +a) was an attractive possibility, both because it minimizes the sensitivity the sampling phase errors, and because the nominal data levels are all on one side (or all on the other side) of each of these pseudo error thresholds so that signal deviations larger than d from one level do not look like deviations smaller than d from a different nominal level. Use of these pseudo error thresholds was rejected because amplitude clipping in the signal path could clip off the noise peaks which the BEM should be measuring while leaving all of the noise which causes errors in received data. This, coupled with the higher than average tolerance for phase errors, could cause performance predictions based on +(2d +a) and -(2d +a) pseudo error threshold measurements to be excessively optimistic. Use of pseudo error thresholds at +a and/or, at -a was an attractive concept because there are nominally twice as many data samples at the zero level as at either of the other levels; however, since nonlinear distortion, signal clipping, and associated transient ringing could degrade response at the outer levels without increasing dispersion measurements made about the center level, it was considered uncautious to base performance predictions on center level dispersion measurements alone. The above arguments leave only two pseudo error threshold levels, +(2d -a) and -(2d -a) as being reliable for detecting degradations from signal clipping with and without noise. These are the two pseudo error thresholds selected for mechanization in the BEM.

As originally built, the BEM used two pseudo error detection windows: one from +(2d -a) to +d and the other from -(2d -a) to -d; however, the MUX transmitter had unequal duty cycles for positive and negative pulses so that the distance from the zero level to the upper level (nominally +2d) was not equal to the distance from the zero level to the negative level (nominally -2d). At present, the offset control adjusts the signal so that the center level is centered with respect to the zero referenced comparator, and the gain control adjusts the eye pattern so that the lower level is centered with respect to the -2d referenced comparator. The constant pseudo error rate adaptive threshold -(2d -a), measures upward perturbations from the lower level. Because of the MUX transmitter distortion, the upper eye pattern level is not centered with respect to the +2d comparator reference; however, pseudo error measurements could still be taken around the upper level if an additional adaptive loop were added to adjust the voltage, 2d', (approximately equal to 2d) until half of the upper level samples were above +2d' and half were below. Then the appropriate pseudo error detection window would extend from +(2d' -a) to d' or from +(2d' -a') to d', depending on whether the loop for adjusting the offset threshold a, were the same as that used for the lower level offset threshold, or separate. The present implementation saves hardware by measuring pseudo errors only around the lower level; however, it can be used to measure dispersion about the upper level instead by the simple expedient of inverting the signal prior to applying it to the BEM input.

The per sample pseudo error rate (ratio of pseudo errors detected on one side of level per sample observed at that level) was chosen to correspond to approximately the three sigma point on the Gaussian (normally distributed) probability function. The pseudo error rate, and hence, the measured point on the Normal curve, may be changed by changing the countdown ratio. Ideally, more than one pseudo error threshold would be used per level so that more than one point on the Normal curve could be measured simultaneously. This would be helpful in determining whether the errors are actually normally distributed or not. Unfortunately, space and power supply limitations made it impractical to include this dual threshold feature in the existing BEM. A less desirable but cheaper alternative for testing the shape of the error distribution would be to use a single pseudo error threshold as is presently used, but to make the pseudo error rate adjustable by computer command rather than fixed as it is presently.

The BEM implementation techniques presented here have been explained solely with respect to the present three-level eye multiplexer application; however, the techniques can clearly be adapted to apply to two-, four-, five-, six-, ... level eyes found in other communication systems such as the seven-level eye pattern test point provided by the AN/USC-26 modem for monitoring purposes.

To adapt the present BEM hardware to allow monitoring and BER determination of a system utilizing the AN/USC-26 modem, certain circuit changes would be required. The GDM D/A diagnostic output would be the monitor point to which the BEM would be connected. The clock generated in the GDM would be used in place of the Baud timing recovery circuits in the BEM. Also, the phase correction loop circuits in the BEM could be disabled because the sampling time is not as critical with the square wave appearing eye pattern of the GDM. When the GDM is operating in the three level mode, the pseudo error rate sampling window (+(2d-a) to +d) circuits would remain substantially the same. However, when the GDM operates in the seven level mode, this sampling window and associated circuits would change. In the seven level eye pattern, two levels fall between the zero level and both the upper and lower outer levels. One location for the sampling window would be in a zone defined by $+(L_1-a)$ and $+L_1/2$. Where L_1 is the first positive voltage level above zero and $L_1/2$ is the decision threshold voltage for the first level; "a" as before is the measure of dispersion. This mechanization would make maximum use of the BEM circuits with minimum change since this dispersion meter would be treating the first positive level of the seven level GDM eye as the present BEM dispersion meter uses the upper level in the three level eye. The circuits in the BEM which now regulate the "2d" (upper level) voltage could also be disabled since the GDM measures and regulates the first level voltage independent of noise content as the BEM regulates the "2d" level.

The software to implement such a modified BEM would be of the same type, and the data base tables relating the measured dispersion voltage to BER would have to be developed in the same manner as presently used.

3.4 PERFORMANCE PREDICTION FROM BASEBAND EYE PATTERN MONITOR MEASUREMENTS

3.4.1 Introduction

3.4.1.1 Need for Sensitive Degradation Detection

The BEM (baseband eye pattern monitor) is a device for measuring degradation of signal quality in digital communication links. When gradual degradation of signal quality occurs in an analog communication link such as an ordinary telephone voice channel, this degradation is observable in the quality of the analog output signal when it is still 20 or 30 dB below the level at which it renders the channel unusable. However, when the same channel is used for digital data transmission, the channel noise and distortion components are intentionally stripped off of the digital signals before they are outputted from the receiver; therefore, low levels of channel distortion are not readily detectable by observing the output signals of digital receivers. Deterioration in the quality of output digital signals may be unobservable when the channel deterioration is only a few dB away from the level at which the quality of the digital output signals becomes unacceptably degraded. Thus, when channel conditions degrade gradually, the quality of received analog signals also degrades gradually; however, the quality of received digital signals continues to show no apparent degradation for a long time and then changes rapidly to such a highly degraded condition that the received signal is unusable. It often appears that analog channels degrade gradually while digital chanels fail suddenly with little or no warning. The function of the BEM is to provide warning of impending failure in digital communication links prior to the point where the deterioration is observable by close scrutiny of the digital output signal and to continue measuring channel degradation up to levels at which the digital output becomes unusable.

3.4.1.2 General Principle of BEM Operation

The BEM monitors signal quality by measuring the amount of noise which is superimposed on top of the desired digital signal. For the VICOM TI-4000 series multiplexer, a three-level partial response PAM (Pulse Amplitude Modulation) signal format is used; therefore, at the times that the received signal is sampled to obtain the transmitted digital information, the received signal should be at one of three specific voltage levels. If the data transmission system is running perfectly with no noise, the received signal will be precisely equal to one of these three voltage levels at each sampling time. A small amount of distortion or additive noise in the channel will cause the received voltages to vary slightly from their ideal values. As the amplitude of the noise or distortion increases, this variation also increases. The BEM is designed to make precise measurements of these undesired voltage variations in VICOM TI-4000 multiplexer links. The hardware mechanizations of the various control loops employed by the BEM in making these precision measurements have

been described previously. The following sections explain how system bit error rate can be predicted from BEM measurements. The word "predicted" is appropriate because error rates of one error per minute, hour, day, or year can be predicted using systems in the BEM which have time constants in the order of one second. Obviously, it is impossible to measure bit error rates in the order of one error per hour by counting the number of errors made within a few seconds; therefore, to obtain information relating to such low error rates within a few seconds of time, the error rates must be predicted rather than measured directly.

3.4.1.3 Preview of Following Sections

The mathematical tools and techniques for predicting digital system performance from BEM outputs evolved gradually over a period of about a year and a half. As would be expected, the initial math model is the simplest one and each time a new factor is identified and included in the math model to improve the prediction accuracy, the math model becomes more complex. In order to lead the reader gradually from the simple to complex and to build a sense of history, the material in this report is arranged in approximately historical order.

Paragraph 3.4.2 presents analyses assuming that an ideal three-level partial response eye pattern is used. When samples of the VICOM TI-4000 series multiplexer boards were received and tested, it was discovered that the actual eye pattern, instead of having three precise levels as intended, had three broad levels. On closer examination it became apparent that each of these three broad levels consisted of three smaller levels so that the total result was a nine-level eye rather than a three-level eye as intended. The cause of this distortion of three levels into nine was determined and included in the nine-level eye math model used in the analyses presented in Paragraph 3.4.3. Paragraph 3.4.4 describes a set of interlocking computer programs which were written to produce performance prediction tables for the nine-level eye math model disclosed in Paragraph 3.4.3. As would be expected, the VICOM TI-4000 multiplexers had other imperfections in addition to the nine-level eye effect. Paragraph 3.4.5 describes laboratory experiments performed to isolate and identify the most significant of these effects. Paragraph 3.4.6 presents a procedure for identifying the magnitudes of the more significant multiplexer deficiencies and including them in the math models so that the performance prediction tables can be adjusted to produce accurate predicitons based on theoretically sound corrections. Paragraph 3.4.7 presents the results of actual experience in preparing performance prediction tables in the field using the theoretical tables and theoretical corrections as a guide. These field techniques greatly reduce the amount of work required to produce actual prediction tables from theoretical ones while obtaining the same prediction accuracy which the more complicated correction procedures produced. Design analysis and testing of the hit counter was performed concurrently with the work outlined

above; however, discussion of this work is presented separately in consolidated form in Paragraph 3.4.8 in Section 8 to make the explanations easier to locate and follow.

3.4.2 BEM Analyses Assuming a Three-Level Partial Response Eye

3.4.2.1 Definitions

The classical partial response three-level eye pattern is shown in Figure 3-11. This figure represents the pattern which would be obtained on the face of an oscilloscope if the analog eye pattern voltage were connected to the vertical inputs and the horizontal time base were synchronized with Baud timing so that each sweep would start with the same Baud timing phase. If the sweep time were adjusted to cover several Baud periods, then the proper sampling times would become apparent as they are in the figure. At the proper sampling times, the analog voltage is equal to one of three values: 2d, 0 or -2d volts. These three voltage levels, and five additional levels, making eight voltage levels in all, are shown in Figure 3-11. By using eight voltage comparators, with these eight voltage levels as references, it is possible to determine whether the voltage was above or below each of these eight levels at each sampling time. Two of these levels, the upper and lower offset thresholds, are adjustable by changing the value of the offset voltage, a. The level Kd is determined by selecting the constant K as explained in Paragraph 3.4.8. For the purposes of the present discussions, the level Kd can be ignored. The other five levels are constant.

Several detailed analyses for this eye pattern have been reported in Appendix A of the ATEC Digital Adaptation Study, RADC-TR-76-302. For the reader's convenience, that appendix has been revised to make it consistent with the present nomenclature and is included in the present report in Paragraph 3.2. In this appendix and in all of the mathematical analyses up to and including the writing of the computer programs, it was assumed that two zones would be used for counting pseudo errors. The upper pseudo error zone extends from d to (2d-a) volts, and the lower pseudo error zone extends from -d to -(2d-a) volts. For the math models used in the mathematical analyses and computer programming, the pseudo error rates for the upper and lower zones are equal; therefore, the total error rate for the two zones is equal to twice the pseudo error rate for either of the single zones. The VICOM eye pattern used during laboratory testing was found to be so asymmetrical that it was necessary either to use a single pseudo error zone on one side of the signal, ignoring the other side, or to provide the hardware with additional degrees of freedom and control loops so that both sides of the signal could be tracked separately. Because of power, size, and schedule constraints, it was decided to use only a single pseudo error zone. Most of the mathematical analyses and computer programs had been finished at the time that the asymmetry was discovered; therefore, all pseudo error rates in these documents are expressed as two zone or "two sided" pseudo error rates unless otherwise specified. Interpreting results stated in terms of the two-zone pseudo error rate

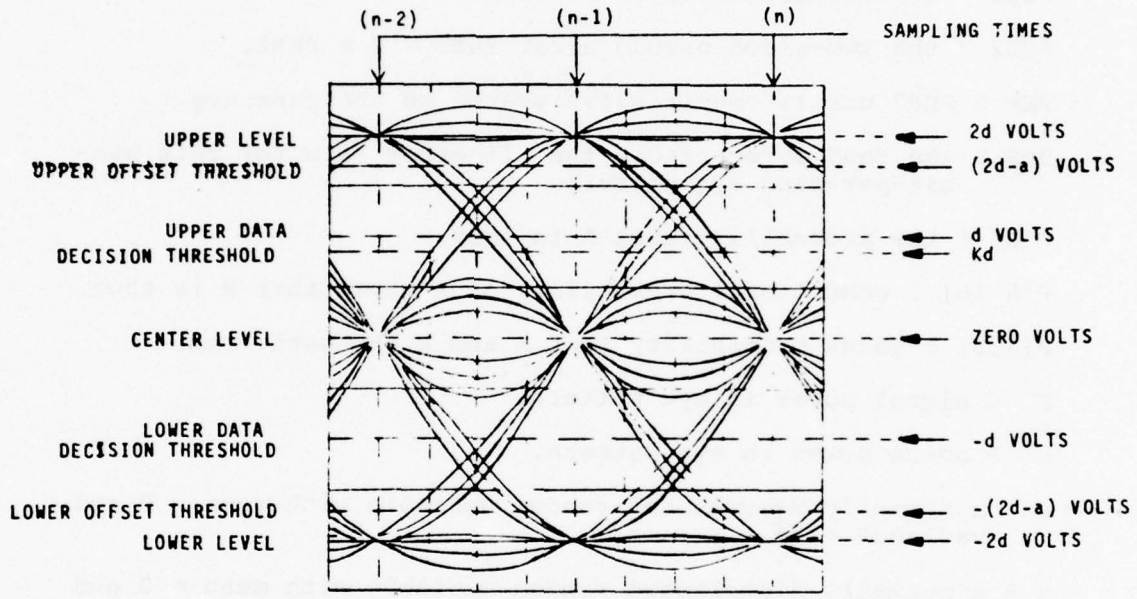

FIGURE 3-11. DEFINITION OF LEVELS FOR OFFSET THRESHOLD MONITORING OF THREE LEVEL EYE

definition will cause no hardship as long as it is remembered that the single-sided pseudo error rate is equal to half of the two-sided pseudo error rate. In this report the number 1 or 2 will follow the letters PER to designate whether a one-sided or two-sided pseudo error rate is intended. When old work is reproduced, the letters PER may appear without the number 1 or 2 following, in which case, it is the two-sided error rate which is being referred to. These and some other useful definitions are listed below:

PER1 ≡ the one-sided pseudo error rate.

PER2 ≡ the two-sided pseudo error rate = 2 x PER1.

PER ≡ PER2 unless specifically stated to the contrary.

BER ≡ the Baud error rate = the bit error rate for this one-bit-per-Baud eye pattern.

P[A] ≡ the probability that A is true.

P[A |B] ≡ conditional probability of A given that B is true.

P[A,B] ≡ joint probability that A and B are both true.

S^2 ≡ signal power in eye pattern.

N^2 ≡ noise power in eye pattern.

ε ≡ a normally distributed random variable with mean = 0 and variance = N^2.

z ≡ a normally distributed random variable with mean = 0 and variance = 1.

Q(x) ≡ P[z>x|z~N(0,1)] which is to be read as "the probability z is greater than x, given that z is a normally distributed random variable with mean equal to zero and variance equal to one."

$Q^{-1}(p)$ ≡ [x[Q(x)=p] which is read as "Q inverse of p is defined as equal to the value of x for which Q of x equal to p."

$Q'(x) \equiv \frac{d}{dx} Q(x)$ which is equal to minus the density function of the N(0,1) distribution at point where the random variable is equal to x.

3.4.2.2 Signal-To-Noise Ratio Computation

It was stated near the close of Paragraph 3.2.3 that there is a specific relationship between the amplitude of d and the signal power. That relationship will be derived here. The average signal power is equal to the probability that it is at the upper level

times the power at that level, plus the probability that it is at the center level times the power at that level, plus the probability that it is at the lower level times the power at that level as given below.

$$S^2 = P\,[L=2d]\;[POWER|L=2d] + P\,[L=0]\;[POWER|L=0] + P\,[L=-2d]\;[POWER|L=-2d] \quad (25)$$

Since the power at any particular level is equal to the voltage at that level squared and the probabilities of the upper, center, and lower levels are 1/4, 1/2, and 1/4 respectively, the above equation can be rewritten as below.

$$S^2 = 1/4\;(2d)^2 + 1/2\;(0)^2 + 1/4\;(-2d)^2 = 2d^2 \quad (26)$$

The signal-to-noise ratio, then, is simply equal to the signal power divided by the noise power as shown below.

$$S^2/N^2 = 2(d/N) \quad (27)$$

Using this relationship, the signal-to-noise ratio in decibels, dB, can be obtained directly from the d/N ratio.

$$SNR \equiv 10\;LOG_{10}\;(S^2/N^2)\;dB = [3.0103 + 20\;LOG_{10}\;(d/N)]\;dB \quad (28)$$

3.4.2.3 Baud Error Rate Computation

In general, SNR is more convenient for empirical investigations, and d/N is more convenient for statistical analyses. For instance, the Baud error rate can be readily derived in terms of d/N. A Baud error occurs whenever the amplitude of the random noise fluctuation, epsilon, causes the transmitted signal intended for one level to be misinterpreted as belonging to a different level. The values of epsilon which will cause errors are different for the three different levels; therefore, they will be calculated separately and summed together as was done for the power calculations using the following relationship.

$$BER = P[L=2d]\;P\,[ERROR|L=2d] + P\,[L=0]\;P\;[ERROR|L=0] + P\,[L=-2d]\;P\;[ERROR|L=-2d] \quad (29)$$

If an upper level is transmitted and epsilon is more negative than -d, the received symbol will be interpreted as a center or lower level; hence, values of epsilon more negative than -d will cause errors. There is no level above the upper level; therefore, positive values of epsilon are not harmful. The probability of error, given that an upper level was transmitted, is equal to the probability that the value of epsilon will be less than -d.

$$P[ERROR|L=2d] = P[\varepsilon<-d] = P[\varepsilon>+d] \quad (30)$$

The probability of the value of epsilon being less than -d is equal to the probability of its being more than +d because the distribution of epsilon is symmetrical about 0. Dividing both sides of the inequality by the positive definite constant N does not alter the validity of the inequality.

$$P[ERROR|L=2d] = P[\varepsilon/N > d/N] \quad (31)$$

Since epsilon by definition is normally distributed with a mean equal to 0 and a variance equal to N^2, dividing epsilon by N produces a random variable which is normally distributed with a mean of 0 and a variance of 1.

$$P[ERROR|L=2d] = P[z > d/N | z \sim N(0,1)] \quad (32)$$

This probability by definition is equal to Q(d/N).

$$P[ERROR|L=2d] = Q(d/N) \quad (33)$$

The probability of error given that a lower level signal is transmitted is equal to the probability that the value of epsilon will be sufficiently large in the positive direction to cause the signal to be misinterpreted as a 0 or upper level symbol. This will happen if the error voltage epsilon is larger than d.

$$P[ERROR|L=-2d] = P[\varepsilon>+d] \quad (34)$$

Since the right hand side of Equation 34 looks like that of Equation 30, it is obvious that it is also equal to the right hand side of Equation 33.

$$P[ERROR|L=-2d] = Q(d/N) \quad (35)$$

If a center level signal is transmitted, there are two ways in which an error can be made in the receiver. If the error voltage, epsilon, is more positive than d, the received signal will be interpreted as an upper level symbol and if it is more negative than -d, it will be interpreted as a lower level symbol.

$$P[ERROR|L=0] = P[\varepsilon>d] + P[\varepsilon<-d] \quad (36)$$

This is obviously equal to the sum of Equations 30 and 34.

$$P[ERROR|L=0] = 2Q(d/N) \quad (37)$$

Substituting Equations 33, 35 and 37 into Equation 29 and remembering the probabilities of the upper, center, and lower levels are 1/4, 1/2, and 1/4 respectively, the following result.

$$BER = (1/4)Q(d/N)+(1/2)2Q(d/N)+(1/4)Q(d/N) \quad (38)$$

Combining terms, the desired result can now be obtained in an elegantly simple form.

$$BER = (3/2)Q(d/N) \tag{39}$$

An equivalent formula for bit error rate was given in Equation 2, Paragraph 3.2.1 of this section, but the derivation was not shown and it was expressed in terms of signal-to-noise ratio and a variable number of levels so it has a more complicated appearance.

3.4.2.4 Pseudo Error Rate Equation

The pseudo error rate for the three-level eye was derived in Paragraph 3.2.3 with the results for the one-sided and two-sided solutions being stated in Equations 31 and 32 respectively. The one-sided solution is presented below for convenience.

$$PER1 = (1/4)\ \{Q(a/N)+Q(d/N)-2Q\ [(2d-a)/N] \\ +Q(3d/N)-Q[(4d-a)/N]\} \tag{40}$$

3.4.2.5 Computation of Dispersion Amplitude

Using Equations 39 and 40, it is possible to compute the dispersion, a/d, for a fixed pseudo error rate, PER1, for a given noise level, N/d, or a given bit error rate, BER. Examples of these relationships are shown in Figure 3-4 and 3-12. Equation 40 could not be solved explicitly for dispersion; therefore, it was solved iteratively by hand calculations at first, and later by computer. When solving these equations it is convenient to express Equation 40 in terms of three variables: pseudo error rate, PER1; dispersion, a/d; and decision level to noise ratio, d/N.

$$PER1 = (1/4)\ \{Q[(a/d)(d/N)] + Q(d/N)-2Q[2(d/N)-(a/d)(d/N)] \\ +Q\ [3(d/N) - Q\ [4(d/N)-(a/d)(d/N)]\} \tag{41}$$

When solving for dispersion iteratively, either by hand or by machine, it is convenient to have the partial derivative of the pseudo error rate with respect to dispersion. This relationship may be determined by inspection from Equation 41.

$$\partial PER1/\partial(a/d) = (1/4)\{Q'[(a/d)(d/N)] + 2Q'[2(d/N)-(a/d)(d/N)] \\ +Q'[4(d/N)-(a/d)(d/N)]\}(d/N) \tag{42}$$

The BEM has an automatic gain control system to keep the amplitude of d constant; therefore, PER1 in Equations 41 and 42 is a function of only two variables, a and N. Thus, if the pseudo error rate, PER1, is held constant, the magnitude of a is dependent on only one variable, N. Thus, the amplitude of a can be used as a measure of the noise amplitude, N.

3.4.2.6 Pseudo Error Rate Loop Analysis

A block diagram of the control loop for holding the pseudo error rate constant is shown in Figure 3-13. The three parameters which affect the loop are shown entering at the left hand side of Figure 3-13. These three parameters are the Baud rate, B, the rms noise level, N, and the signal level, d. For the system presently under study, the Baud rate, B, is equal to 12,552,600 Baud/sec. The signal level, d, is held constant by an AGC system. Thus, the only variable entering the pseudo error rate control loop is the rms level of the noise, N.

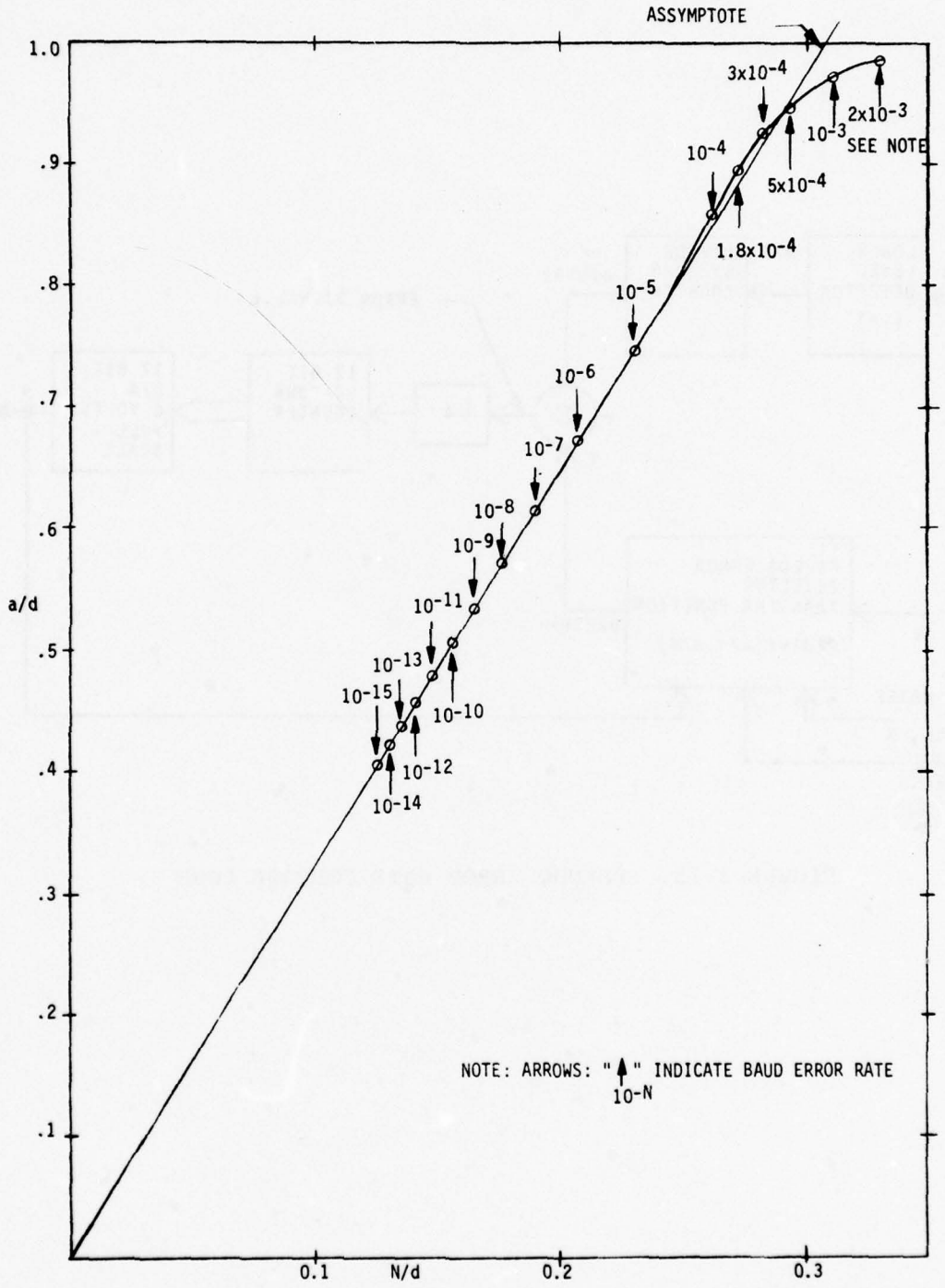

FIGURE 3-12. a/d VERSUS N/d FOR PER1 = 1.5×10^{-4} AND 3 LEVEL PARTIAL RESPONSE

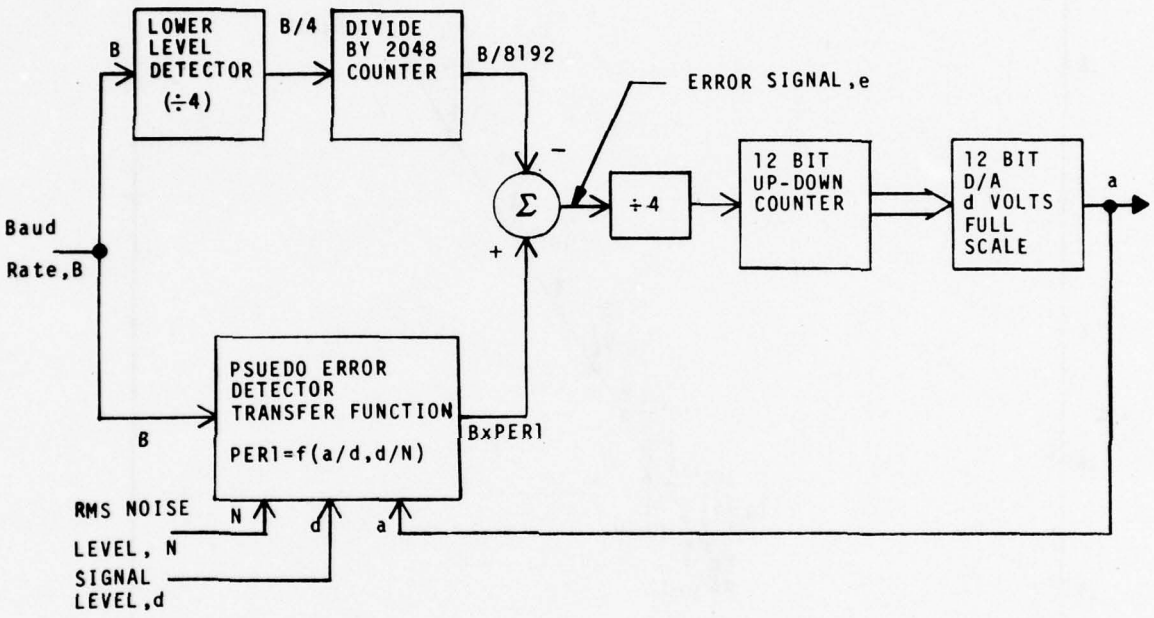

FIGURE 3-13. PSEUDO ERROR RATE CONTROL LOOP

In order to keep the amplitude of the output, a, dependent upon only one variable, N, the control loop in Figure 3-13 must keep the pseudo error rate, PER1, constant. The summing device is an up-down counter in which pulses into the lower input cause it to count up, pulses into the upper input cause it to count down, and simultaneous pulses into both inputs cause it to do nothing. The lower input into the summing device is the output of the pseudo error detector which transmits one pulse for each pseudo error. The average number of pseudo error pulses transmitted per second is equal to the Baud rate, B, times the pseudo error probability per Baud, PER1. The upper input to the summing device is obtained by dividing the output of a lower level detector by 2048. The reason for using the lower level detector is that the pseudo error detector in this system looks for pseudo errors only around the lower level. When the probability of receive bauds being at the lower level is 1/4, the lower level detector can be replaced by a divide by 4 counter. Normal data patterns are sufficiently random that a lower level probability will be 1/4; however, the lower level detector is used in preference to a divide by 4 counter in order to keep the ratio of pseudo errors made per Baud tested constant even in the presence of special test patterns. For normal data patterns, the average rate out of the lower level detector is equal to 1/4 the Baud rate, B/4, so that the average rate out of the divide by 2048 counter is B/8192. The average rate of the error signal, e, out of the summing device is equal to the difference between the rates of the lower and upper inputs.

$$e = B \times PER1 - B/8192 \tag{43}$$

Assuming that the control loop drives the error signal, e, to zero, and that the baud rate, B, is not equal to zero, the pseudo error rate can be determined from Equation 43.

$$PER1 = 1/8192 \text{ given } e=0,\ B\neq 0 \tag{44}$$

The pseudo error rate can be readily adjusted by changing the count down ratio in the 2048 counter.

For computation of the dynamics of the pseudo error rate control loop, the equations will be simplified by defining two new variables, A and D, to replace the three variables, a, d, and N.

$$\text{Define } A \equiv a/d \tag{45}$$

$$\text{and} \quad D \equiv d/N \tag{46}$$

$$\text{where} \quad d \equiv \text{a system constant} \tag{47}$$

An equation for the pseudo error rate in terms of these two new variables may be obtained by substituting Equations 45 and 46 into Equation 41.

$$PER1 = (1/4)\ \{Q(AD)+Q(D)-2Q[(2-A)D] + Q(3D)-Q[(4-A)D]\} \quad (48)$$

Given the magnitude of the pseudo error rate, PER1, and the data to noise ratio indicator, D, there is only one value of dispersion, A, which will satisfy Equation 48. The value of A which satisfies Equation 48 for a given value of D when PER1 is equal to 1/8192 will be defined as A_D for convenience.

$$A_D \equiv [A \mid PER1(A,D) = 1/8192] \quad (49)$$

To determine the value of dispersion, A_D, which satisfies Equation 49 for a given value of D, Equation 48 is solved iteratively, using the given value for D, and sequential estimates of the value A_D in the place of A until the desired value for the pseudo error rate PER1 is obtained. The rate of convergence of the sequential estimation process can be improved by using a partial derivative of the pseudo error rate with respect to dispersion in a Newton Raphson iterative solution process. The required partial derivative may be obtained by inspection of Equation 48.

$$\partial PER1/\partial A = (D/4)\{Q'(AD)+2Q'[(2-A)D] +Q'\ [(4-A)D]\} \quad (50)$$

Using the information given above and in the block diagram, Figure 3-13, it is also possible to determine the time constant of the pseudo error rate control loop. Since the D/A converter full scale voltage is equal to d volts, the scale factor for the 12 bit up/down counter and the converter is $[2d/(2^{12}-1)]$ volts per count. When the average amplitude of the loop error signal is represented by e, the net difference in counts per second between the lower and upper inputs to the summing point, then clearly e/4 counts per second are applied to the 12-bit counter so that the output voltage, a, from the D/A converter changes at an average rate of $(e/4)\ [d/(2^{12}-1)]$ volts per second.

$$\dot{a} = e\ d/\{4(2^{12}-1)\} \quad (51)$$

Using the relationship in Equation 45, and recalling that d is a constant, Equation 51 may be put into a simpler form

$$\dot{A} = \dot{a}/d=e/\{4(2^{12}-1)\} \quad (52)$$

The gains around the pseudo error rate control loop have now been computed from the location of the summing point error signal, e, to the pseudo error detector dispersion input, A. To complete the expression for the loop gain it is now necessary to determine the gain from the location of A to that of e. The expression for the amplitude of e in terms of A is given in Equation 43 in which the term PER1 is a function of A and D as given in Equation 48. The relationship between e and A is nonlinear in A and is also a function of D.

It is assumed that the noise level changes so slowly relative to the pseudo error loop time constant that D can be treated as a constant. To facilitate analysis of the loop response for small excursions of A about the steady state value A_D a new term, ΔA, is defined such that

$$A = A_D + \Delta A \tag{53}$$

Equation 43 can be rewritten explicitly showing the dependency of PER1 on the values of A and D,

$$e = B[PER1(A,D) - (1/8192)] \tag{54}$$

Assuming that ΔA is small,

$$PER1(A,D) \approx PER1(A_D,D) + \Delta A \left\{ \frac{\partial}{\partial A} \left[PER1 \,|\, A=A_D, D=CONST \right] \right\} \tag{55}$$

From Equation 49,

$$PER1(A_D,D) = 1/8192 \tag{56}$$

Substituting Equations 56 and 50 into 55 yields the following result.

$$\begin{aligned} PER1(A,D) \approx (1/8192) + \Delta A(D/4)\{&Q'(A_D\ D) \\ &+2Q'[2-A_D)D] + Q'[(4-A_D)D]\} \end{aligned} \tag{57}$$

Substituting Equation 57 into 54 gives

$$\begin{aligned} e = \Delta A \frac{BD}{4} \{&Q'(A_D\ D) + 2Q'[(2-A_D)D] \\ &+Q'[(4-A_D)D]\} \end{aligned} \tag{58}$$

Recall that D is assumed to be constant so that A_D is constant so

$$\frac{d}{dt} A = \frac{d}{dt} (A_D + \Delta A) = \frac{d}{dt} (\Delta A) \tag{59}$$

Substituting Equation 59 into Equation 52, produces Equation 35

$$\frac{d}{dt} (\Delta A) = e \left[\frac{1}{4(2^{12}-1)} \right] \tag{60}$$

Finally, substituting Equation 58 into 59 gives the rate of correction for a dispersion error, ΔA.

$$\frac{d}{dt}(\Delta A) = (\Delta A)\frac{BD}{4}\{Q'(A_D D) + 2Q'[(2-A_D)D] + Q'[(4-A_D)D]\}\frac{1}{4(2^{12}-1)} \tag{61}$$

The above result is recognized as belonging to the class of differential equations obtainable from the response below.

$$x = x_o e^{-(t/T)} \tag{62}$$

Where T = the system time constant, and x_o = the value of x when t=0.

The relationship between Equations 61 and 62 can be made more obvious by performing the following operations.

Differentiating both sides of Equation 62 with respect to time, t, gives Equation 63

$$\dot{x} = \frac{-1}{T} x_o e^{-(t/T)} \tag{63}$$

Next, Equation 62 is substituted into Equation 63.

$$\dot{x} = \left(\frac{-1}{T}\right) x \tag{64}$$

Note that the factor multiplied by ΔA in Equation 61 corresponds to (-1/T) in Equation 63. Equating these two factors and solving for T gives the following expression for the time constant of the pseudo error rate control loop.

$$T = \frac{-4}{BD}\{Q'(A_D D) + 2Q'[(2-A_D)D] + Q'[(4-A_D)D]\}^{-1} 4(2^{12}-1) \tag{65}$$

When the noise is not zero; N, a, d, A, and D are positive definite; all of the Q( )'s are positive definite; and all of the Q'( )'s are negative definite. The Baud rate, B, is also positive definite. The negative sign on the right hand sign of Equation 61 cancels the negative signs of the Q'( )'s; therefore, the time constant of the loop is positive definite which guarantees that the loop will be stable.

Table 3-2 has been prepared to show the range over which the loop time constant varies for a selection of BER values which adequately covers the range over which the BEM is intended to operate. The results in this table were computed first by hand and then by computer to check the series of computer programs to be described later. Each row starts with an assumed value for the Baud error rate, BER. Substituting Equation 46 into 39 gives

$$BER = (3/2Q(D) \tag{66}$$

Rearranging terms,

$$Q(D) = (2/3)BER \tag{67}$$

TABLE 3-2. LOOP TIME CONSTANT VERSUS BER COMPUTED FOR LOOP CONSTANTS SHOWN IN FIGURE 3-13

BER (Error/Baud)	D	A_D	T (Sec)
$1.0x10^{-3}$	3.2087	0.97743	0.248
$1.8x10^{-4}$	3.6728	0.90768	0.792
$1.0x10^{-4}$	3.8203	0.87108	0.832
$5.0x10^{-5}$	3.9880	0.83127	0.792
$1.0x10^{-15}$	7.9927	0.41253	0.376
$1.0x10^{-23}$	10.015	0.32922	0.300

Then using the definition of $Q^{-1}(p)$

$$D = Q^{-1}\ (2/3\ BER) \tag{68}$$

The magnitude of D can be determined from that of BER using Equation 68 and a computer program or an appropriate set of tables for performing the $Q^{-1}(p)$ operation on (2/3) BER.

Then, given the magnitude of D and PER1 (which is 1/8192) the magnitude of A_D may be determined by Newton Raphson iteration (which can be a tedious process if done by hand). Given the Baud rate, B, and the values of D and A_D, the time constant, T, can be determined from Equation 65 using a computer program or an appropriate set of tables to evaluate the Q'(x) terms.

3.4.2.7 Selection of a Pseudo Error Rate

The last subject to be discussed in this section is the selection of an appropriate value for PER1. An examination of Figure 3-12, which shows a/d plotted versus N/d for a PER1 value of 1.5×10^{-4}, reveals that as the amplitude of a/d decreases, the computed values of dispersion a/d versus N/d asymptotically approach a straight line which passes through the origin. If the pseudo error rate, PER1, is decreased, the asymptote will become more nearly vertical but it will still pass through the origin as may be verified by Figure 3-4. The optimal slope for a given application is usually close to the slope which causes the asymptote to cross the a/d = 1.0 level at the maximum BER value which the BEM is expected to monitor. For convenience this maximum BER will be defined as equal to G.

$$G \equiv \text{Max}[BER \mid BER \text{ in useful range}] \tag{69}$$

Next, define d/N_G as the value of d/N which makes the Baud error rate equal to G. Then substituting G and (d/N_G) into Equation 39 gives

$$G = (3/2)Q(D/N_G) \tag{70}$$

Rearranging factors

$$Q(d/N_G) = (2/3)G \tag{71}$$

After solving a few a/d versus N/d curves by hand for constant PER1 using Equation 41, it becomes obvious that the equation for the asymptote can be obtained by deleting all but the first Q ( ) term on the right.

$$PER1 = (1/4)Q[(a/d)(d/N)], \text{ for asymptote} \tag{72}$$

To force a/d to equal one when the bit error rate is equal to G, substitute Equations 73 and 74 into Equation 72 to obtain Equation 75.

$$a/d = 1 \tag{73}$$

$$d/N = d/N_G \tag{74}$$

$$PER1 = (1/4)Q(d/N_G) \tag{75}$$

Then substitute Equation 71 into 75

$$PER1 = (1/4)(2/3)G \tag{76}$$

$$PER1 = G/6, \text{ where } G = BER_{MAX} \tag{77}$$

To test this result on Figure 3-12, G is computed from the value of PER1 which is 1.5×10^{-4}.

$$G = 6\ PER1 = 9 \times 10^{-4}, \text{ for Figure 3-12.} \quad (78)$$

From Figure 3-12, the value of BER at which the asymptote crosses the a/d = 1 level is about 4/5 of the way from the 5×10^{-4} line to the 10×10^{-4} (that is 1×10^{-3}) which is as expected from Equation 78. When additional factors begin to affect the operation of the BEM, Equation 77 may not give the exact value for the optimal PER1, but even then it is a good starting point for an iterative solution.

From Equation 78, PER1 is equal to 1.5×10^{-4}, which is one error in every 1667 Bauds received. To simplify hardware design and provide a relatively close match with the optimal PER1, a sample size of 2048 was chosen. With this sample size one error represents approximately 0.05% and corresponds to an error margin of 99.95% or 3.3 sigma for normally distributed errors.

3.4.3 Analyses Including the VICOM T1-4000 Nine-Level Eye Distortion

3.4.3.1 Description of the Nine-Level Eye

The VICOM 4000 series multiplexer nominally has a three-level eye pattern. However, because of intersymbol interference, the eye pattern accidentally has nine levels. As shown in Figure 3-14, each of the three nominal levels, 2d, 0, and -2d, has an additional level above it, 2d+i, i, and -2d+i, respectively, and an additional level below it, 2d-i, -i, and -2d-i, respectively. Because of intersymbol interference, the voltage received at any sampling time, such as n-1, will be dependent not only upon the symbol intended for the n-1 sampling time but also upon the symbols transmitted at the adjacent sampling times n-2, and n. Since this type of distortion causes the received voltage to be affected by the voltage of the adjacent symbols, this type of distortion is called intersymbol interference. If the intersymbol interference extends over a sufficiently long time period that the voltage at the n-1 sampling time is affected by other samples in addition to the n-2 and n sample then the intersymbol interference eye pattern becomes more complex than that shown in Figure 3-14 and the number of levels obtained will be greater than nine. When the additional effects become large enough, adjacent levels such as the +i, 0, and -i levels will become blurred together and indistinguishable from each other. In the VICOM TI-4000 eye pattern, the intersymbol interference between adjacent Bauds is so much larger than all of the other eye pattern degrading effects that all nine levels are distinct and clearly separated from each other.

In order to perform mathematical analyses for the nine-level eye pattern equivalent to those performed in the previous section for the three-level eye pattern, it is necessary to have the probabilities of each eye pattern level. The values of these probabilities, which have been determined by analysis and confirmed by observations, are given below in Equations 79 through 87 and their sum is equal to 1 as shown in Equation 88.

$$P(L = 2d+i) = 1/16 \tag{79}$$

$$P(L = 2d) = 2/16 \tag{80}$$

$$P(L = 2d-i) = 1/16 \tag{81}$$

$$P(L = 0+i) = 2/16 \tag{82}$$

$$P(L = 0) = 4/16 \tag{83}$$

$$P(L = 0-i) = 2/16 \tag{84}$$

$$P(L = -2d+i) = 1/16 \tag{85}$$

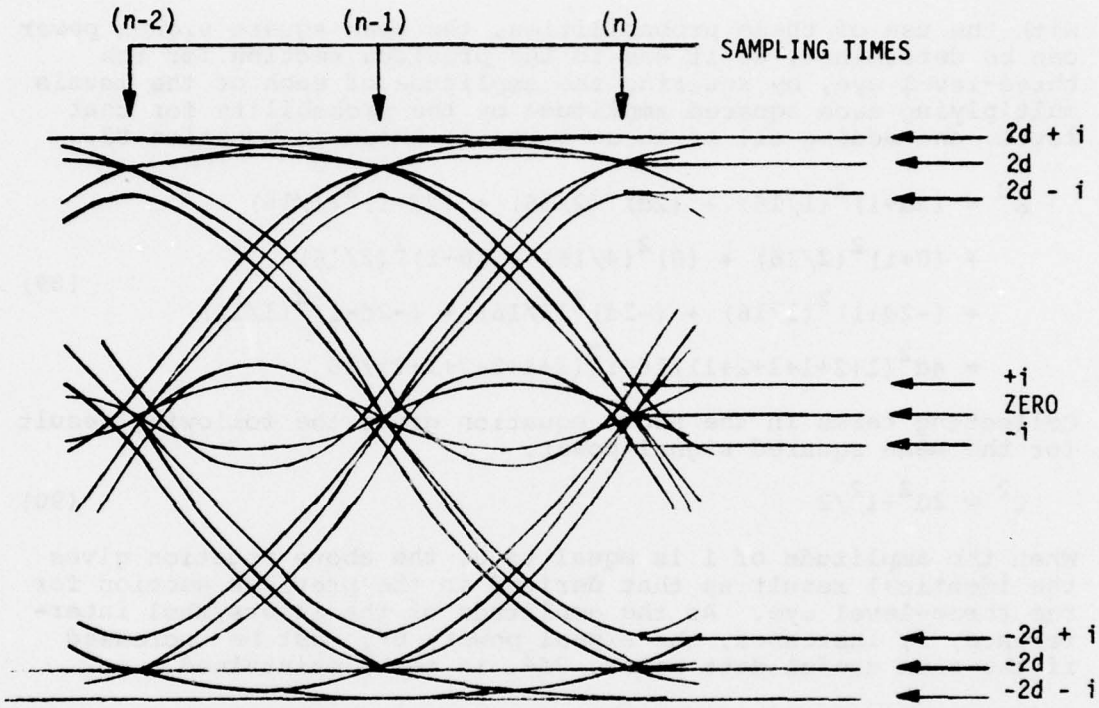

FIGURE 3-14. THREE LEVEL EYE DISTORTED TO NINE LEVELS BY INTERSYMBOL INTERFERENCE

$$P(L = -2d) = 2/16 \tag{86}$$

$$P(L = -2d-i) = 1/16 \tag{87}$$

$$\text{Sum of the above} = 1 \tag{88}$$

With the use of these probabilities, the mean square signal power can be determined, as it was in the previous section for the three-level eye, by squaring the amplitude of each of the levels, multiplying each squared amplitude by the probability for that level, and adding all of these terms as shown in Equation 89.

$$\begin{aligned} S^2 &= (2d+i)^2(1/16) + (2d)^2(2/16) + (2d-i)^2(1/16) \\ &\quad + (0+i)^2(2/16) + (0)^2(4/16) + (0-i)^2(2/16) \\ &\quad + (-2d+i)^2(1/16) + (-2d)^2(2/16) + (-2d-i)^2(1/16) \\ &= 4d^2(1+2+1+1+2+1)/16+i^2(1+1+2+2+1+1)/16 \end{aligned} \tag{89}$$

Collecting terms in the above equation gives the following result for the mean squared signal power.

$$S^2 = 2d^2+i^2/2 \tag{90}$$

When the amplitude of i is equal to 0, the above equation gives the identical result as that derived in the previous section for the three-level eye. As the amplitude of the intersymbol interference, i, increases, the signal power, S^2, must be increased if the same useful data power, $2d^2$, is to be maintained.

3.4.3.2 Computation of BER

The Bit Error Rate probability may be calculated by using the same technique which was used for the three-level eye which is to multiply the probability of occurrence for each level by the probability of baud error given that that level was transmitted, and sum these individual probability terms to determine the total bit error rate. This operation is shown in Equation 91 in which the contributions of the nine separate levels are shown on nine separate lines.

$$\begin{aligned} BER = (1/16)\ \{ & \ Q[(d+i)/N] \\ & +2Q[\ \ d\ /N] \\ & + Q[(d-i)/N] \\ & +2Q[(d-i)/N] + 2Q[(d+i)/N] \\ & +4Q[\ \ d\ /N] + 4Q[\ \ d\ /N] \\ & +2Q[(d+i)/N] + 2Q[(d-i)/N] \\ & + Q[(d-i)/N] \\ & +2Q[\ \ d\ /N] \\ & + Q[(d+i)/N]\} \end{aligned} \tag{91}$$

This result may be simplified by collecting terms.

$$BER = (1/16)\{6Q[(d+i)/N] + 12Q(d/N) + 6Q[(d-i)/N]\} \quad (92)$$

Notice that when the value of i is set equal to 0 that the above equation gives the same bit error rate, (3/2) Q(d/N), as was obtained previously for the three-level eye.

3.4.3.3 Computation of Pseudo Error Rate

The pseudo error rate for the nine-level eye, PER1, is derived as before by multiplying the probability of each level occurring by the probability that a pseudo error will be made if that level occurs, and summing the contributions over the nine levels to obtain the total pseudo error rate. This operation is performed in Equation 93 in which the contribution of each level is shown on a separate line.

$$\begin{aligned} PER1 = (1/16)\ \{ & Q[(a+i)/N] - Q[(d+i)/N] \\ & +2Q[a/N] - 2Q[d/N] \\ & +Q[(a-i)/N] - Q[(d-i)/N] \\ & +2Q[(d-i)/N] - 2Q[(2d-a-i)/N] \\ & +4Q[d/N] - 4Q[(2d-a)/N] \\ & +2Q[(d+i)/N] - 2Q[(2d-a+i)/N] \\ & +Q[(3d-i)/N] - Q[(4d-a-i)/N] \\ & +2Q[3d/N] - 2Q[(4d-a)/N] \\ & +Q[(3d+i)/N] - Q[(4d-a+i)/N]\} \end{aligned} \quad (93)$$

The above result may be simplified by collecting terms as shown in Equation 94.

$$\begin{aligned} PER1 = (1/16)\ \{ & +Q[(a-i)/N]+2Q[a/N]+Q[(a+i)/N] \\ & +Q[(d-i)/N]+2Q[d/N]+Q[(d+i)/N] \\ & -2Q[(2d-a-i)/N]-4Q[(2d-a)/N]-2Q[(2d-a+i)/N] \\ & +Q[(3d-i)/N]+2Q[3d/N]+Q[(3d+i)/N] \\ & -Q[(4d-a-i)/N]-2Q[(4d-a)/N]-Q[(4d-a+i)/N]\} \end{aligned} \quad (94)$$

Notice that if the value of i is set equal to zero that the three separate terms on each of the five rows merge into a single term and once again the result is identical to that which was obtained for the three-level eye.

3.4.3.4 Analysis of the Pseudo Error Threshold Control Loop

To determine the value of the dispersion, a/d, given the magnitude of the pseudo error rate, PER1, and the value of d/N, it is convenient to have the partial derivative of the pseudo error rate, PER1, with respect to the offset threshold amplitude, a. This partial derivative may be obtained by inspection from Equation 95.

$$\frac{\partial PER1}{\partial a} = (16N)^{-1}\{\ Q'[(\ \ a-i)/N]+2Q'[\ \ \ a\ /N]+\ Q'[(\ \ a+i)/N]$$
$$+2Q'[(2d-a-i)/N]+4Q'[(2d-a)/N]+2Q'[(2d-a+i)/N] \quad (95)$$
$$+\ Q'[(4d-a-i)/N]+2Q'[(4d-a)/N]+\ Q'[(4d-a+i)/N]\}$$

When the magnitude of the intersymbol interference, i, is set equal to zero, each of the three lines of Equation 95 collapses to a single term and these three terms are identical to those obtained in the three-level eye pattern analysis. The dispersion amplitude for a given noise level, A_D, and the corresponding time constant, T, for a nine-level eye pattern can be determined by using the same techniques which were developed for the three-level eye but using the nine-level equations in place of the three-level ones. One complexity resulting from the use of the nine-level equation is that they introduce a new parameter, the intersymbol interference amplitude, i. Fortunately, the magnitude of the intersymbol interference, i, appears to be essentially constant for any given application so that it may be treated as a constant when solving for the dispersion, A_D, and the time constant, T.

3.4.4 Computer Program to Produce Performance Prediction Tables

3.4.4.1 Introduction

One of the primary functions of the mathematical analyses described here is to perform real time prediction of VICOM TI-4000 series multiplexer bit error rate, BER, from BEM dispersion measurements, a/d. Using the nine-level eye equations previously derived, tables of dispersion versus bit error rate can be prepared for various values of intersymbol interference. Explicit solutions for dispersion, given bit error rate, are unavailable so that the equations which do exist must be solved iteratively. The number of terms in these equations is so large that even if a small number of iterations per point were adequate it would not be practical to prepare the required tables by hand. Since it was considered possible that additional tables might be needed at a later date and that it might be necessary to use a different computer in preparing these tables, all of the programs in the family were written using the Structured Programming techniques. These programs are completely documented on comment cards contained within the programs themselves so that their operation can be readily understood and they may be easily modified to reflect future changes in the math models or to run on different machines. The complete set of programs consists of one trunk program called TRUNK, three regular subroutines, and a group of five-function type subroutines to produce five different parameters related to the NORMAL distribution.

The computer program and sample printout is contained in Appendix B.

3.4.4.2 The Main Program: TRUNK

The first function of the TRUNK program is to read the input data cards to determine the value of the Baud error rate and pseudo error rate for which the analyses are to be performed. Next, it reads a list of the bit error rate values, each of which is used once per table. Then, it reads a list of intersymbol interference values, i/d, for which it is to produce one table each. For the first intersymbol interference value and bit error rate, the TRUNK program calls Subroutine DNR9LE to determine the value of d/N which corresponds with a given value of Baud error rate, BER. The TRUNK then calls Subroutine ADR9LE to determine the value of a/d which corresponds with the given value of d/N for the specified pseudo error rate. This subroutine also computes the time constant of the dispersion loop. When the TRUNK program has finished computing all of the values for one table, it calls Subroutine TABLE which does the actual printing. The TRUNK program continues to compute and print tables until it has exhausted the list of intersymbol interference values; then it stops.

3.4.4.3 The Gaussian Distribution Function Type Routines

These subroutines are written in function style so that they do not have to be called explicitly. Examples of such routines already existing in the computer library are: sine, cosine, and square root functions. The functional programs written for this analysis correspond to $Q(x)$, $Q^{-1}(x)$, $Q'(x)$, and two additional programs which work with $(1-Q)$ rather than Q itself. If greater detail is desired, it may be found within the programs themselves.

3.4.4.4 Subroutine DNR9LE

Subroutine DNR9LE determines the value of d/N, that is A_D, which will produce the specified value of BER. It obtains this d/N value by a Newton Raphson iterative solution of Equation 91 using the specified values for BER and intersymbol interference amplitude, i/d.

3.4.4.5 Subroutine ADR9LE

Subroutine ADR9LE solves Equation 94 iteratively to determine the amplitude of the dispersion, a/d, which satisfies that equation for the given values of d/N, i/d, and pseudo error rate. As a biproduct, this subroutine also determines the derivative of the pseudo error rate with respect to dispersion, and using this value computes the time constant of the dispersion loop.

3.4.4.6 Subroutine TABLE

Subroutine TABLE prints the information obtained by the TRUNK program in tabular form with proper headings and definitions so that each table is complete in itself and of suitable dimensions for storing in an 8-1/2 x 11 inch file folder or notebook.

3.4.5 Differences Between Computer Math Model and Actual Hardware Identified Through Laboratory Testing

3.4.5.1 Introduction

For pragmatic reasons, the various differences which were discovered between the real world and the simplified math model in the computer will be classified in accordance with the ways in which they affect the various predictions. It was found that each of the deviations can be assigned to one of three general categories. Factors in the first category cause the dispersion value, a/d, to be larger than zero even when the amplitude of the noise added for test purposes is equal to zero. The second class of factors cause the slope of the dispersion versus noise, N/d, to deviate from the mathematically predicted slope. Factors of the third type cause the observed bit error rate, BER, to be greater than the values predicted on the basis of dispersion, a/d, measurements. These three different types of factors will be described in the following subsections.

3.4.5.2 Factors Affecting No Noise Dispersion

Tests were performed in the laboratory to measure dispersion, a/d, versus added noise. A summing amplifier was added between the output of the VICOM TI-4000 multiplexer transmitter and the input of the associated multiplexer receiver. The BEM was connected in parallel with the receivers so that the receiver and BEM both shared the same input signal. Noise was added in the summing amplifier, and the multiplexer bit error rate and BEM output dispersion voltage were both noted. When the added noise was reduced to zero it was found that dispersion did not go to zero. This phenomena was partially explained by intersymbol interference which produces the results shown in Figure 3-15. The expression AIDR used in Figure 3-15 is equivalent to the previously defined quantity, i/d. AIDR is a mnemonic used in the computer program and other documentation which stands for amplitude of intersymbol interference to d ratio. The dispersion versus noise characteristics, shown as solid lines in Figure 3-15, are plotted from computer outputs and show the affect of different AIDR values on the nine-level eye math models. If the AIDR ratio is 0.2, then for the computer math model the dispersion, a/d, will be equal to 0.2 when the noise, N/d, is equal to zero. However, in the real world, the dispersion, a/d, with no noise added to the channel, may be larger than the AIDR value. Laboratory tests were performed to determine what factors could cause the zero noise dispersion amplitudes to vary from the mathematical predictions. One of the first factors identified was a gain bandwidth interaction in the variable gain amplifier of the VICOM multiplexer receiver. As the amplitude of the input signal to the receiver was decreased, the variable amplifier gain was automatically increased to obtain a constant amplitude level at the VICOM comparators. The increase in gain caused the bandwidth of the variable gain amplifier to decrease thereby increasing the phase lag

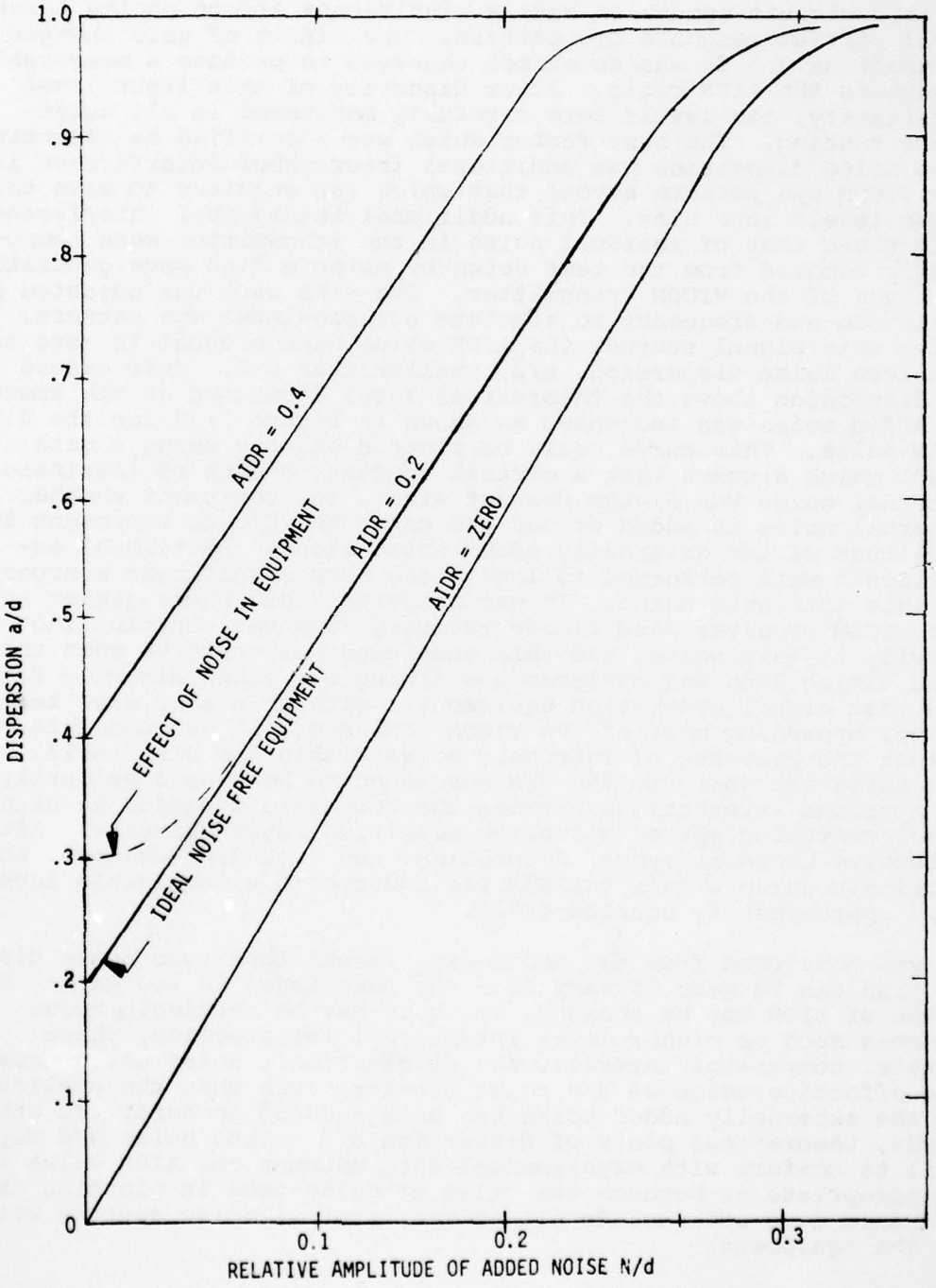

FIGURE 3-15. FACTORS AFFECTING ZERO NOISE DISPERSION

AD-A051 925 HONEYWELL INC ST PETERSBURG FL AVIONICS DIV F/G 17/2
ATEC DIGITAL ADAPTATION STUDY, DEVELOPMENT AND FIELD EVALUATION--ETC(U)
JAN 78 T J CAMPBELL, W F ACKER, C L CHRISTNER F30602-75-C-0282
UNCLASSIFIED 1077-14813-VOL-1 RADC-TR-77-431-VOL-1 NL

2 OF 3
AD
A051925

in this circuit enough to have a significant effect on the three-level partial response eye pattern. The effect of gain changes as small as 0.5 dB was sometimes observed to produce a measurable change in the AIDR ratio. After discovery of this input level sensitivity, the levels were carefully monitored in all subsequent testing. The next factor which was identified as affecting zero noise dispersion was additional intersymbol interference in the VICOM eye pattern beyond that which was required to make the three levels into nine. This additional intersymbol interference effect and that of residual noise in the transmitter were temporarily removed from the test setup by using a sine wave generator in place of the VICOM transmitter. The sine wave was adjusted in amplitude and frequency to simulate a three-level eye pattern. Using this signal source, the AIDR value became equal to zero and the zero noise dispersion, a/d, smaller than 0.1. This excess of dispersion above the theoretical level decreased as the amount of added noise was increased as shown in Figure 3-15 for the 0.2 AIDR value. This curve could be plotted exactly using a math model which assumes that a certain constant amount of intrinsic internal noise was always present within the equipment whether external noise is added or not and using the N/d to represent the amplitude of the externally added noise alone. Additional experiments were performed to locate the more significant sources of this intrinsic noise. It was suspected that phase jitter in the VICOM receiver Baud timing recovery loop was contributing heavily to this noise, and this suspicion was verified when the Baud timing loop was bypassed and timing was taken directly from the test signal generation equipment. With this sine wave test setup, bypassing most of the VICOM equipment, it was possible to detect the presence of intrinsic noise within the BEM itself. The noise intrinsic to the BEM was found to be caused primarily by spurious interactions between the comparators caused by high level switching spikes affecting sensitive input circuits. After extensive board relayout, decoupling, and grounding changes, the intrinsic noise within the BEM was reduced to a negligible level (a/d approximately equaled 0.02).

It was concluded from the above experiments that zero noise dispersion can be made to vary from the math model in two ways: the value of AIDR may be changed, or there may be intrinsic noise sources such as higher level intersymbol interference, phase jitter, comparator interactions, or electronic noise which cause the effective value of N/d to be non-zero even when the amplitude of the externally added noise has been reduced to zero. In other words, theoretical plots of dispersion a/d versus noise N/d may fail to conform with experimental data because the AIDR value is inappropriate or because the value of noise used in plotting the N/d axis does not include all of the internal noise sources within the equipment.

3.4.5.3 Factors Affecting Dispersion Versus Noise

Factors affecting the zero noise intercept of the dispersion versus noise curves were discussed in the preceding paragraphs. Now factors will be considered which make the slope of the dispersion versus noise curves vary from those predicted by the computer math models. The slopes of the dispersion versus noise curves plotted from early laboratory data were always greater (more nearly vertical) than those predicted by theory. As additional tests were performed to learn the cause of this variation, it was gradually learned that multiplicative noise mechanisms are present in the VICOM multiplexer receiver. These multiplicative effects were isolated almost entirely to the Baud timing recovery circuits. The computer math models are constructed using the assumption that the Baud timing recovery operation is performed perfectly, so that the only errors present in the eye sampling process are those caused by additive noise being present on top of the desired eye pattern signals. For many receivers this is a good assumption because the Baud timing recovery phase lock loops typically use a very narrow bandwidth to reject almost all of the undesired noise so that the sample timing in the receiver is very nearly jitter free. In the VICOM receiver, an appreciable portion of the noise does get through to affect the sample timing so that the quality of the sampled voltage values decreased more rapidly with increasing noise than it would if additive noise were the only degrading effect present. The BEM could be made to ignore this phase jitter sensitivity of the VICOM receiver Baud timing loop by ignoring the output of the VICOM Baud timing loop and developing its own Baud timing signals independently; however, the function of the BEM is to predict VICOM performance, not theoretical performance, so it was considered advantageous to retain the VICOM Baud timing loop noise sensitivity within the dispersion measuring system. The effect of this noise sensitivity in the Baud timing loop can be seen in Figure 3-16 in which the lower solid line curve represents the dispersion predicted by the computer model for an AIDR value and the upper solid curve shows the actual measured dispersion. The lower dashed line represents the straight line asymptote for the theoretical dispersion versus noise and the upper dashed line represents the straight line asymptote for the measured dispersion versus noise. The 0.088 offset between the upper solid line and the upper dashed line at zero noise was caused by the intrinsic noise effects described previously. This figure will be referred to again when techniques for fitting curves to real data are discussed. The purpose for including it here is to show an actual example of the increased slope in the dispersion asymptote (asymptotes shown as dashed lines) caused by noise induced jitter in the VICOM Baud timing recovery system. In this case, the increase in slope is about 22 percent or 1.75 dB in effective noise power. This 1.75 dB increase in the slope of the dispersion curve versus added noise indicates that the effective noise in the eye pattern samples is 1.75 dB higher than it would be with a jitter free timing recovery circuit. When tests were run with the timing recovery circuit

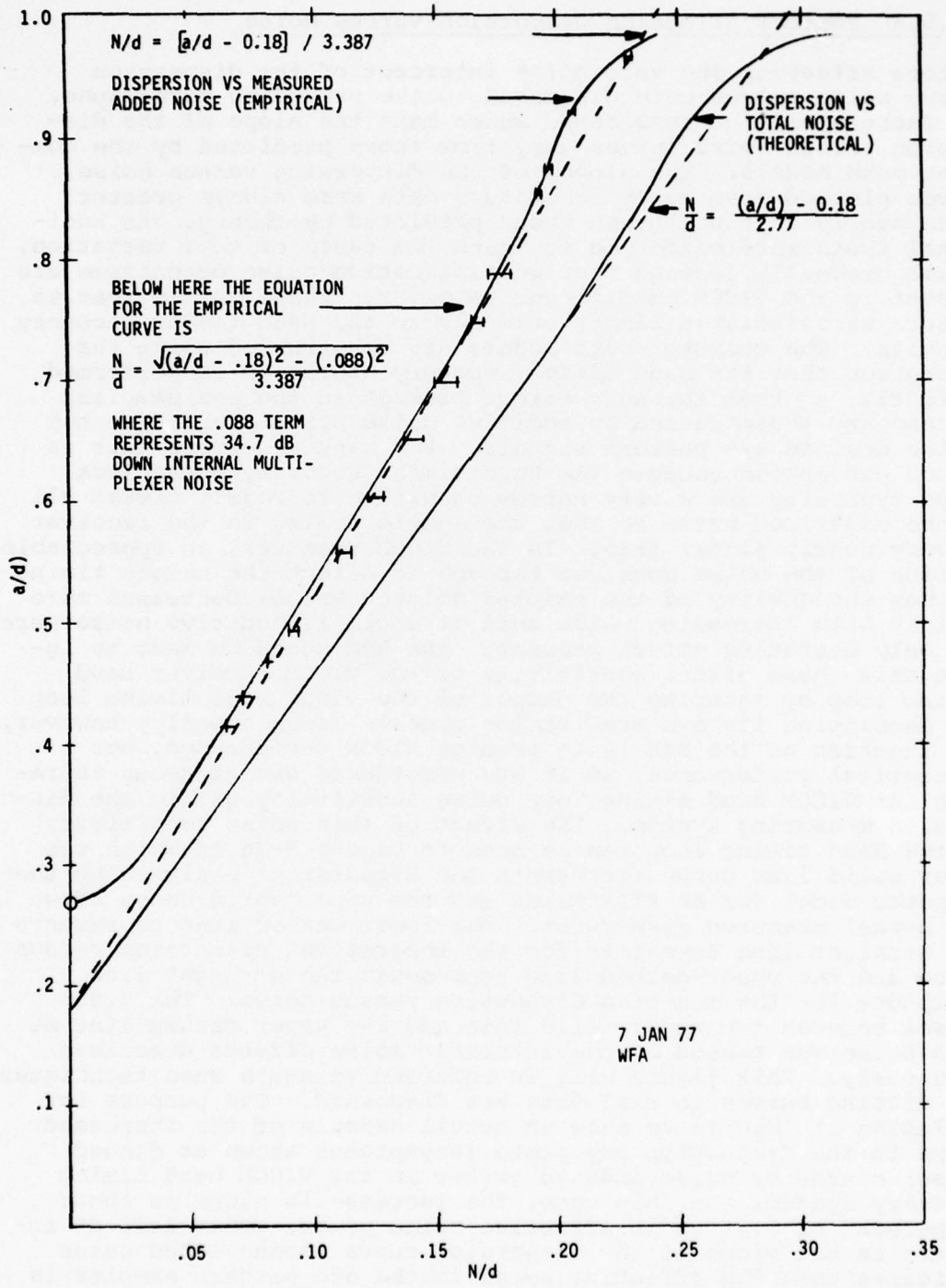

FIGURE 3-16. DISPERSION VERSUS NOISE

bypassed, the measured slope was essentially equal to the mathematical predicted slope. Thus, the increase in slope furnishes a useful measurement of the degradation produced by imperfections in the Baud timing loop.

During dispersion versus noise testing, an additional effect of phase jitter was sometimes observed which does not appear in Figure 3-16. During some of the tests a dispersion versus noise curve was found to be relatively straight with a constant slope as shown in Figure 3-16 up to a dispersion, a/d, amplitude of 0.7 to 0.9 and then undergo an abrupt increase in slope which occasionally was so nearly vertical as to be unmeasurable. The most extreme example of this phenomenon occurs when the test signal and the test noise are both sine waves. The cause of this jump was once again traced to phase jitter in the Baud timing loop. The reason for this jump becomes obvious after a careful examination of the effect of phase jitter on the pseudo error rate detector using the levels defined in Figure 3-11. The lower pseudo error rate detection zone extends from -(2d-a) volts to -d volts. The constant pseudo error rate loop adjusts the amplitude of a as necessary to maintain a constant pseudo error rate. When the noise level, N, is small relative to the decision level, d, of the signal decoding comparators, the distance, a, between the lower boundary of the pseudo error zone and the lower data level will be much smaller than the distance, d, between the upper boundary of the pseudo error zone and the center data level; therefore, the number of pseudo errors caused by lower level signals crossing the lower pseudo error boundary will greatly exceed the number of pseudo errors caused by the center level signals crossing the upper pseudo level boundary. That is, for small noise levels the number of pseudo errors obtained from upper boundary crossings is negligible so that the distance, a, between the lower boundary and the lower level is directly proportional to the noise level, N. As the amplitude of the noise increases, the distance, a, between the lower pseudo error zone boundary and the lower signal level also increases becoming more nearly equal to the distance, d, between the upper pseudo error zone boundary and the center level signal; therefore, the probabilities of signals erroneously crossing these two boundaries becomes more nearly equal causing the dispersion versus noise curves to depart from the straight line asymptote as shown in Figure 3-16. Thus, even when the Baud timing is ideal, as it was in the computer math models, the slope of the dispersion versus noise curve begins to increase for dispersion amplitudes, a/d, greater than about 0.75 in order to reduce the number of lower boundary pseudo errors to compensate for the increase in the number of pseudo errors coming from the center level (recalling that the number of pseudo errors coming from the center level was heretofore negligible). When phase jitter is present, the probability of center level signals crossing the upper pseudo error zone boundary is greatly increased relative to the probability of lower level signals crossing the lower boundary because of the shape peculiar to the eye pattern in Figure 3-11. If the eye pattern is sampled

with perfect timing, the distances from the center level and the lower level to the decision comparator voltage, d volts, are equal. However, looking at the voltage versus time traces on the oscilloscope eye pattern presentation, it is obvious that if the timing becomes increasingly early or late that the vertical distance between the decision level, -d volts, decreases more rapidly for the center level than for the lower level. When the number of pseudo errors from the center level begins to become significant relative to the number from the lower level, the slope of the dispersion versus noise curve will begin to increase; and, if the probability of center level errors reaching -d greatly exceeds that of lower level errors reaching -d, the increase in dispersion will be very abrupt. The most extreme example of this abrupt jump occurred when an unsynchronized sine wave signal was used in the place of a Gaussian noise source to simulate added noise. This sine wave signal induced enough jitter into the VICOM Baud timing loop to cause a large number of center level eye samples to deviate below the -d threshold while the deviation of the samples about the lower level was approximately 0.7d. With this test setup, as the amplitude of the sine wave noise was gradually increased the dispersion versus noise characteristic followed a straight line to a dispersion amplitude of about 0.7, and then the dispersion jumped abruptly to an amplitude of approximately 1.0 for an unmeasurably small additional increase in noise. The underlying cause producing this jump and the point at which the jump occurred could be deduced and predicted by watching oscilloscopic presentations of the eye pattern with appropriate Baud timing as the dispersion versus noise data points were taken. It was determined theoretically that this jump could be avoided by moving the pseudo error zone from its present location, -d to -(2d-a) volts, to a new location adjacent to the center level such as -a to -d volts. If this new pseudo error zone location were used, the dispersion would be even steeper than it is now because of the increased phase jitter sensitivity. When the sine wave noise source was replaced with a Gaussian noise source the jump became more difficult to detect or disappeared altogether as may be seen by looking at Figure 3-16. It was established that dispersion readings obtained using the present pseudo error zone location produced excellent error prediction results. Therefore, changing the hardware so as to move the pseudo error zone was considered not only unjustifiable on the basis of proven performance, but also an unnecessary risk since the hardware was already proven to work with the present pseudo error zone location and had not been tested using one of the alternate locations.

3.4.5.4 Factors Affecting Error Rate Prediction From Dispersion Measurements

Since dispersion measurements indicate the total effective noise level, including such effects as phase jitter and not just the amplitude of the applied noise alone, they would be expected to, and actually do, furnish a better basis for predicting pseudo error rates than do added noise level measurements. However, the Baud error rates predicted on the basis of dispersion measurements are still lower than the measured Baud error rates. The technique for predicting Baud error rates from dispersion measurements is to use the nine-level eye math model to compute the noise level, d/N, which will produce the indicated dispersion, and then to compute the Baud error rate, BER, which corresponds to the computed value of d/N and the assumed value of intersymbol interference AIDR. In order to make the predicted BER values agree with the observed BER values, it was necessary to increase the noise level computed from the dispersion measurements by a constant factor, approximately equal to 3 dB, before using these noise values to compute the predicted BER values. That is, for any particular Baud error rate, the VICOM receiver appeared to need a signal to noise ratio at the comparator inputs approximately 3 dB better than that required for a theoretically perfect comparator detection process. The VICOM receiver was examined to determine the cause of this 3 dB degradation with respect to ideal, and three significant factors were identified. First, the comparator decision thresholds were not set midway between the inner and outer eye pattern levels as was done in the computer math model but were located nearer to the outer levels, probably to take advantage of the extra width (in the time domain) of the eye pattern at those locations as shown by Figure 3-11. Second, the AGC system caused the amplitude of the eye pattern to shrink as the noise level increased because it used the peak amplitude of the signal plus noise as a reference rather than gain controlling on the amplitude of the signal alone. Third, the BEM used a dc phase correction technique so that there was never any steady state phase error in the eye pattern sampling; however, the VICOM receiver used a factory selected phase offset adjustment which was not necessarily optimal at the time of the performance tests for the ambient temperature, signal noise level, and other conditions under which those tests were conducted.

3.4.6 Laboratory Developed Performance Table Fitting Techniques

3.4.6.1 Fitting the Dispersion Versus Noise Curve with Three Constants

The laboratory-developed technique for fitting dispersion versus noise characteristics is illustrated by the example in Figure 3-16. The circles in Figure 3-16 represent the empirical measurements of dispersion versus added noise. For dispersion values larger than 0.75, the dark line fitted to the empirical points was drawn by selecting the best fitting segments of a French curve; however, the portion below the dispersion value of 0.75 was fitted by selecting the appropriate constants in a theoretically derived equation for computing the noise level, N/d, from the measured dispersion, a/d. This equation can be derived by making use of two relationships. First, the amplitude of the noise which affects the dispersion is equal to the total noise power, N_t^2, which is obtained by adding the power of the noise added in at the summing junction, N_s^2, to the power of the intrinsic noise, N_i^2, which is already present in the system.

$$N_t^2 = N_i^2 + N_s^2 \tag{96}$$

The second relationship is that, for dispersion amplitudes, a/d, less than 3/4, the dispersion is approximately equal to the intersymbol interference constant, AIDR, plus a constant times the rms amplitude of the total noise.

$$(a/d) = AIDR + k(N_t/d) \tag{97}$$

Moving the AIDR term to the left hand side of Equation 97, squaring both sides, substituting Equation 96 into the result and rearranging terms gives the following result.

$$[(a/d)-AIDR]^2 = k^2[(N_i/d)^2+(N_s/d)^2] \tag{98}$$

The theoretical equation used for fitting the curve in Figure 3-16 may be obtained by solving Equation 98 for the value of N_s/d.

$$(N_s/d) = \{\sqrt{[(a/d)-AIDR]^2 - k^2(N_i/d)^2}\}/k \tag{99}$$

Corresponding dispersion, a/d, versus added noise, N_s/d, measurements obtained empirically and are shown by the circled data points on Figure 3-16. The values of intersymbol interference, AIDR, intrinsic noise, N_i/d, and dispersion versus noise slope, k, were determined by iteratively trying different values for these parameters to determine which set of values produced the

best fit to the circled points. Once these best fit constants were determined, the solid line through these points was constructed by using the approximation equation to compute as many points as were necessary to completely determine the locus of the dispersion versus noise curve.

Since the error rate to be predicted is a function of the total rms noise amplitude, N_t, rather than the rms amplitude of the summed in noise, N_s, the dispersion value, a/d, is used to predict the amplitude of N_t. In order to accomplish this prediction, Equation 97 is solved for the value of N_t.

$$(N_t/d) = [(a/d)-AIDR]/k \qquad (100)$$

This equation uses only two of the values previously solved for by the recursive curve fitting technique. The upper dashed line in Figure 3-16 is obtained by plotting Equation 100 for an intersymbol interference amplitude, AIDR, of 0.18, and a dispersion versus noise slope, k, of 3.387, which were the values of these constants determined by the successive curve fitting technique. The significant feature about this upper dashed line is that it intersects the dispersion axis at a point equal to the amplitude of the intersymbol interference, AIDR, which in this case is equal to 0.18. Of the three parameter values determined by the iterative curve fitting technique, the intersymbol interference amplitude, AIDR, is the only parameter value to be retained for the prediction of error rate. The lower solid line shown in Figure 3-16 was obtained using the computer math models with the amplitude AIDR set equal to 0.18. The lower dashed line is a straight line approximation to the computer solution. The equation for this line is similar to that given for the upper line by Equation 100, however, in this case, it is the effective rms noise level, N_e, rather than the total rms noise level, N_t, which is being solved for, so the previous slope constant, k, must be replaced by a new slope constant, k_2.

$$(N_e/d) = [(a/d)-AIDR]/k_2 \qquad (101)$$

As may be seen by inspecting Figure 3-16, Equation 101 gives a simple but accurate means of computing the effective noise amplitude, N_e, from dispersion measurements, a/d, for dispersion values up to approximately 0.75. The largest dispersion value used in the BER prediction tables developed and tested in the laboratory was an a/d amplitude of 0.72 which indicated a Baud error rate of 1×10^{-3}. Since no values of a/d larger than 0.75 were used, the straight line approximation given by Equation 101 was adequate for predicting the effective rms noise amplitude, N_e/d.

3.4.6.2 Predicting BER From Dispersion

The first step in predicting the Baud error rate, BER, from the dispersion measurements, a/d, was to use Equation 101 and the previously determined values for AIDR and k_2 to compute the effective noise ratio, N_e/d, from the dispersion measurement, a/d. The results of several of these calculations are shown in column 2 of Table 3-3. It was mentioned in previous discussions that these noise levels must be increased by approximately 3 dB in order to predict the observed BER values. To determine the proper amount by which to increase these noise values, the procedure shown in Table 3-3 was used. The first two columns of Table 3-3 have already been explained. The third column shows the BER values measured under the same conditions as measured dispersion values in the first column. Column 4 shows the values of d/N_{BER} obtained by the computer math models using the assumed value of AIDR (0.18) and the value of BER given in column 3. The ratio of the column 2 figures to the column 4 figures expressed in decibels is computed and written in column 5. Ideally, all of the figures in column 5 would be identical. The mean and standard deviation for these figures were both computed and found to be equal to 3.20 dB and 0.11 dB, respectively. This means that the noise level, N_{BER}, required for predicting bit error rate was typically 3.20 dB higher than the noise level, N_e, computed from the dispersion value when it was assumed that the intersymbol interference amplitude, AIDR, was equal to 0.18 in both cases. Assuming that the dispersion readings are used to compute an effective noise level, N_e, which is then increased by a 3.2 dB factor to obtain an estimate of the noise amplitude, N_{BER}, the standard deviation between this estimated noise amplitude and the desired noise amplitude is computed to be 0.11 dB. On the basis of this preliminary result it was judged that the accuracy of the above outlined computational technique would be better than that necessary for the required purposes. To test this assumption, a table with 61 pairs of BER versus dispersion values was computed using the above techniques and used for bit error rate prediction. The BER values in the table range from 1×10^{-3} to 1×10^{-15} with five BER values given per decade. For observed dispersion values between values given in the table, the predicted BER values were determined by simple linear interpolation. The adequacy of these tables combined with the interpolation process became readily apparent when the predicted and measured BER values were always found to agree closely over the widest range of test conditions reasonably attainable in the laboratory.

3.4.7 Table Fitting Technique Development Under Field Conditions

3.4.7.1 Introduction

The table fitting technique which was developed under laboratory conditions worked quite accurately; however, several factors changed during field testing which made this laboratory table inappropriate. One of the most significant parameters which

TABLE 3-3. BER COMPUTATIONS

Measured a/d	Estimate 1 d/Ne Computed from a/d	Measured BER	Estimate 2 d/NBER Computed from BER	20LOG 10 (NBER/Ne)
8.522	4.1208	5.7 E-03	2.8308	3.2616 dB
7.477	4.9047	1.55 E-03	3.3246	3.3774 dB
6.971	5.3568	5.3 E-04	3.7037	3.2053 dB
6.019	6.5655	3.85 E-05	4.5445	3.1957 dB
5.570	7.3475	5.1 E-06	5.1231	3.1321 dB
4.942	8.8160	6.63 E-08	6.2113	3.0418 dB
4.647	9.7295	4.8 E-09	6.7924	3.1214 dB
4.360	10.820	2.3 E-10	7.4114	3.2868 dB
	Mean	= 3.20 dB		
	Standard Deviation = 0.11 db			

changed was the intersymbol interference measuring parameter, AIDR. Several factors which can cause a change in the intersymbol interference of the three-level eye pattern are changes in the amplitude and phase versus frequency response of the channel, change of signal amplitude into the multiplexer receiver, variations from transmitter to transmitter and receiver to receiver, variations with temperature or time for a given receiver, and even changes in the transmitter and receiver designs. Since changes in most of these factors not only occurred but were detected during BEM testing at Ft. Huachuca, there was ample motivation and practice to improve on the laboratory developed table fitting techniques described previously. The final tables resulting from both techniques are essentially identical; however, the field developed technique requires a smaller number of steps to reach the same end result. The field developed technique also avoids the use of the digital computer programs in the field by assuming that tables showing the theoretical dispersion values, a/d, for all of the desired BER values have been printed out and are available for all intersymbol interference values, AIDR, which will be encountered. The field procedure requires the identification of the amplitudes of only two constants: the intersymbol interference amplitude, AIDR, and an effective noise to dispersion slope ratio, k_3, similar to the constant, k_2, used in the laboratory fitting procedure.

In the field, as in the laboratory, a summing amplifier is inserted in the path between the multiplexer transmitter and receiver so that Gaussian noise may be injected in order to measure the variation of BER versus added noise. Fortunately, it was possible to develop a procedure which makes it unnecessary to know the amplitude of the summed-in noise relative to the signal amplitude, N_s/d, or even the gain of the path through which the added noise passes before being summed in with the signal. The required data for computing the values of AIDR and k_3 consists of several sets of three numbers each in which the first number indicates the amplitude of the summed-in noise measured with some unknown but constant scale factor; the second number indicates the dispersion value, a/d, measured at that noise condition; and the third number is the corresponding BER measurement.

3.4.7.2 Determination of AIDR

The first step in the AIDR determination is to plot the observed dispersion values, a/d, versus the corresponding added noise measurements. If these points are connected by a smooth curved line, the result should look very much like the upper solid curve in Figure 3-16. As was explained previously, Equation 99 was used to subtract out the effect of the background channel and intrinsic noise, N_i, so that the adjusted data points would fall on a straight line such as the upper dashed line in Figure 3-16. To perform this transformation using Equation 99, it was necessary to determine the values of three constants; the relative intersymbol interference amplitude, AIDR, the relative intrinsic noise amplitude, N_i/d, and a dispersion to noise slope ratio, k. The values of these parameters were arrived at by the iterative process of using the new parameter set in Equation 99 to compute a new set of adjusted data points, plotting these points, and adjusting the estimated parameter values to improve the fit. The only parameter value in the above set needed for the field curve fitting technique is AIDR; therefore, an iterative curve fitting technique was developed in which only one parameter, AIDR, is used. Only one equation, Equation 106, is needed for the field technique; however, since it may be helpful to understand the derivation of this equation, that derivation is presented here.

A useful equation which fits all but the top portion of the observed dispersion versus added noise characteristic (upper solid line in Figure 3-16) can be obtained by substituting Equation 96 into Equation 97.

$$a/d = AIDR + k\sqrt{(N_i/d)^2 + (N_s/d)^2} \qquad (102)$$

Notice that Equation 102 contains three parameters of unknown amplitudes, AIDR, k, and N_i/d, not to mention the unknown scale factor on the N_s/d measurement. The N_i/d term can be evaluated in terms of other parameters by taking advantage of the fact that when the amplitude of the added noise, N_s, is equal to zero, the

second term on the right hand side of Equation 102 reduces to $k(N_i/d)$. To take advantage of this simplification, one of the sets of data points for calibration was always a measurement of the dispersion amplitude, a/d, with zero noise added. The BER measurements taken under this condition were generally so close to zero as to be inaccurate and, therefore, were of little or no value for curve fitting purposes. By using the symbol A_0 to represent the amplitude of the a/d measurement made when the added noise amplitude was equal to 0, substituting A_0 into Equation 102, setting N_s equal to zero, and simplifying, the following relationship is obtained.

$$A_0 \triangleq [a/d|N_s=0] = AIDR + k(N_i/d) \tag{103}$$

The value of the intrinsic noise dependent expression can be solved for in terms of two other parameters: A_0, the zero noise dispersion measurement, and AIDR, the parameter value which is to be solved for iteratively.

$$k(N_i/d) = A_0 - AIDR \tag{104}$$

Substituting the equality in Equation 104 into Equation 99 and multiplying both sides by the factor, k, yields the following result.

$$k(N_s/d) = \sqrt{[(a/d)-AIDR]^2 - [A_0-AIDR]^2} \tag{105}$$

The left hand side of Equation 105 is equal to a constant times the amplitude of the summed-in noise; therefore, if the amplitude of the right-hand side is evaluated correctly at the data points and these values are plotted against the amplitude of the summed-in noise, these new points should fall in a straight line. Everything necessary to evaluate the right-hand side of Equation 105 is already known except the amplitude of the AIDR parameter which may be determined by the iterative process of guessing different values until an AIDR value is found which will make the computed values of the right-hand side of Equation 105 fall in a straight line when plotted against the amplitude of the added noise. Thus, the amplitude of the AIDR parameter could be determined by using Equation 105; however, in practice, it is proven to be more convenient to use the slightly more complicated expression in Equation 106 which can be obtained from Equation 105 by adding the term AIDR to both sides. At the zero noise point, a/d is equal to A_0 so the right-hand side of Equation 105 is equal to zero and that of Equation 106 is equal to AIDR; therefore, when a family of curves is plotted for several AIDR ratios, the curves plotted using Equation 106 all start (at zero noise) from their respective AIDR values, so there is no need to label which curve goes with which AIDR value as there would be if Equation 105 had been used.

$$k(N_s/d) + AIDR = AIDR + \sqrt{[(a/d) - AIDR]^2 - [A_0 - AIDR]^2} \qquad (106)$$

The step by step procedure for using Equation 106 to determine the value of the AIDR parameter, given measurements of a/d and BER for various values of added noise including zero, starts with a plotting of the dispersion measurements versus added noise, which should give a result similar to the upper solid line in Figure 3-16. The next step is to lay a straight edge along the side of this newly plotted line and adjust this straight edge to estimate the location which the straight line dispersion versus noise curve will take when the effect of the intrinsic noise has been subtracted out by the use of Equation 106. The dispersion value given by this straight line estimate for zero added noise is used for the initial estimate of the AIDR parameter amplitude. Given this initial AIDR estimate and the measured amplitude A_0 of the zero noise dispersion from the test data, the only variable on the right-hand side of Equation 106 is the dispersion amplitude, a/d. The right-hand side of Equation 106 is evaluated at each plotted value of a/d and the resulting value, the adjusted dispersion, is plotted directly under the measured dispersion for each data point. A line is now drawn through these data points which has a zero noise dispersion amplitude equal to the assumed AIDR amplitude. If the assumed AIDR amplitude was correct, the resulting curve should look like the upper dashed straight line in Figure 3-16. If the adjusted dispersion curve is still concave upward in the low noise region, similar to the unadjusted dispersion curve, a smaller amplitude for AIDR should be assumed for the next iteration. If the resulting curve is concave downward, a larger AIDR value should be tried. Laying a straight edge along the adjusted curve to obtain a revised AIDR estimate has been found to produce such accurate estimates that this iterative procedure usually converges to a solution in only two or three iterations.

3.4.7.3 Determination of k_3

Having determined the amplitude of the AIDR parameter, the next and last parameter value to be determined is that of the slope ratio, k_3. It may be noted that the two straight dashed line characteristics in Figure 3-16 both have the same zero noise dispersion noise amplitude but that they have different slopes. In the laboratory curve fitting procedure, not only were both of these slopes identified, but also a slope constant of approximately 3 dB was identified to adjust for the fact that the measured multiplexer BER values corresponded with noise levels approximately 3 dB higher than the theoretical noise levels indicated by the dispersion measurements. This two-step procedure was appropriate in the laboratory where each individual step was carefully checked against additional empirical measurements; however, data for checking these intermediate results could not

conveniently be taken in the field and would have been irrelevant if taken because the correctness of the intermediate operations in the BEM had already been established.

For the field procedure, the only result sought is a table of 61 preselected BER values, each paired with the dispersion measurement corresponding with that value. Therefore, the field procedure bypasses the intermediate steps of computing the theoretical N/d ratio, and then the effective N/d ratio needed to obtain the observed BER value and goes, instead, directly from the observed a/d ratio to the a/d ratio which the computer tables indicate as corresponding with the observed BER value. For convenience, the term, $(a/d)_{BER}$, will be used to represent the dispersion amplitude which the nine-level eye computer math model would show as corresponding with the observed bit error rate for the assumed AIDR value.

$$(a/d)_{BER} \triangleq [a/d \mid BER(a/d, AIDR) \text{ from computer table} = \text{observed BER}] \tag{107}$$

Notice that at this point in the field curve fitting procedure the value of the AIDR parameter has already been determined; which means that we are now dealing with a single computer printout table rather than a family of tables. Also, for the two straight line dispersion versus noise plots in Figure 3-16, notice that when the AIDR constant is subtracted from the dispersion that the dispersion varies linearly with the noise amplitude. Therefore, if the effective noise in terms of BER performance is 1.4 times larger than the noise corresponding with the measured dispersion, then the dispersion corresponding with this effective noise will be 1.4 times further from the AIDR value than the original dispersion was. If this 1.4 factor is represented by the symbol, c, then the above statement can be represented in mathematical form as follows.

$$c = [(a/d)_{observed} - AIDR]/[(a/d)_{BER} - AIDR] \tag{108}$$

Three parameter values appear in the right-hand side of Equation 108: AIDR, which was determined previously; $(a/d)_{observed}$, which is the observed dispersion value for a given added noise amplitude; and $(a/d)_{BER}$, which is the dispersion value given by the nine-level eye computer program for the observed error rate, BER. Using Equation 108, the amplitude of the slope ratio coefficient, c, can be computed from the data obtained under several added noise conditions. Ideally, all of these values of c will be identical; however, as may be seen by examining the similar calculations performed in Table 3-3, these various slope ratios are very close to each other but are not quite equal. These multiple values for the slope coefficient, c, may be converted to dB and averaged as was done in Table 3-3, or the same results can be obtained by performing the geometric mean computation in which

all n different values of c are multiplied together and then the n^{th} root is taken as shown in Equation 109.

$$k_3 \triangleq \left[\pi_{j=1}^{j=n}\right]^{-n} \tag{109}$$

The average slope thus obtained will be represented by the symbol, k_3, which will be used to produce the desired dispersion tables. Notice that both the actual dispersion versus noise characteristics and the computer model dispersion versus noise characteristics depart from the straight line approximation used in Equation 108 at the higher noise levels, as may be seen by inspecting Figure 3-16. Therefore, values for the slope coefficient, c, which are obtained from Equation 108 using observations involving large dispersion amplitudes will be found to vary appreciably from the rather consistent values obtained using test data in which lower dispersion amplitudes were involved. Only the consistent values for the slope coefficient, c, should be used in Equation 109 to compute the value of the coefficient, k_3.

3.4.7.4 Computation of the Performance Prediction Table

As stated previously, once the value of the parameter, AIDR, is known, a computer printout is obtained for that AIDR value and this computer printout already has the 61 desired BER values. However, the dispersion, a/d, values corresponding with these 61 BER values must be adjusted to compensate for the fact that the real multiplexer equipment suffers from degradations which are not present in the ideal nine-level eye computer math model. The required equation for performing this adjustment can be obtained by solving Equation 108 for the parameter, $(a/d)_{observed}$.

$$(a/d)_{observed} = AIDR + c[(a/d)_{BER} - AIDR] \tag{110}$$

In its original form Equation 110 was used to compute the value of the slope coefficient, c, given the dispersion observation, $(a/d)_{observed}$; however, when the previously unknown value of the slope coefficient, c, is replaced by the known slope coefficient, k_3, the equation can now be used to compute the values of the dispersion observations, $(a/d)_{observed}$, which are needed to construct the new bit error rate versus dispersion table.

$$(a/d)_{new\ table} = AIDR + k_3[(a/d)_{BER} - AIDR] \tag{111}$$

For each of the 61 bit error rates in the computer printout for the specified AIDR value, Equation 111 can be used to compute the dispersion value for the new performance prediction table, $(a/d)_{new\ table}$, from the theoretical dispersion value in the computer printout, $(a/d)_{BER}$. As was mentioned previously, for large dispersion values, the dispersion versus noise characteristics depart from the straight line approximation as shown in Figure 3-16.

When this departure occurs, the value of c determined by Equation 108 begins to vary from its asymptotic value, k_3, so that Equation 111 is no longer accurate. This situation did not occur during the preparation of the laboratory prediction tables because the VICOM multiplexer error rate reached the 10^{-3} upper BER limit of the table before the curve shown in Figure 3-16 exceeded a dispersion amplitude, a/d, of 0.73. All of the laboratory testing was done using only FKV (Frankfurt, Koenigstuhl, and Vaihingen) type VICOM multiplexer boards; however, in the field testing at Ft. Huachuca, revised DEB (Digital European Backbone) type VICOM multiplexer boards were encountered. Normally, if the BEM is to be used to predict DEB type multiplexer performance, DEB type multiplexer receiver boards should be used in the BEM. However, it was not convenient to change these boards during field testing, so in this case, FKV type boards inside the BEM were used for predicting the performance of multiplexers using DEB type boards. Since the DEB boards were considerably superior to the FKV boards, the 10^{-3} BER performance occurred at a much higher BEM dispersion level than it did in the laboratory tests. Because of this board mismatch, which caused the BEM to be used at a higher than normal dispersion level, and because of the presence of phase jitter which caused the dispersion versus noise slope to be greater than normal at high dispersion values (as explained in paragraph 3.4.5.3), the BEM dispersion values began to depart from the straight line math model used in Equation 111 for dispersion values larger than 0.75. Equation 111 worked satisfactorily for all observed dispersion values equal to or less than 0.75. Very little effort was required to obtain the proper performance table values for dispersions greater than 0.75 for two reasons. First, there were not many dispersion points in the table with amplitudes greater than 0.75. Second, the error rates associated with these large dispersion values were so large that very little time was needed to obtain accurate error rate measurements. If the BEM had used the same improved quality receiver boards that were used in the multiplexer, it is expected that there would have been few, if any, values in the performance table which could not have been adequately determined by using Equation 111. In the laboratory, where the same types of boards were used both in the BEM and the multiplexer, the straight line math model assumed in Equation 111 was used to compute every dispersion value in the performance table with excellent results.

The following example is presented in order to illustrate the method of developing a table of derivied BER versus dispersion. The data in Table 3-4 is actual data from the Ft. Huachuca field test.

TABLE 3-4. BEM TEST DATA

Dispersion Voltage	Noise/Signal	BER
-3.98	0.002	$<10^{-8}$
-4.29	0.032	$<10^{-8}$
-4.90	0.0586	2×10^{-8}
-5.10	0.0649	2.1×10^{-7}
-5.30	0.0715	5.5×10^{-7}
-5.60	0.0774	2.5×10^{-6}
-5.73	0.0892	4.9×10^{-6}
-6.21	0.104	3.1×10^{-5}

The data presented in Table 3-4 is plotted in Figure 3-17. The purpose of plotting the data is to determine the AIDR value using Equation 106 and assumed values of AIDR until the resulting data plot is a straight line. Using a straight edge, the first assumed value of AIDR is seen to be equal to 0.3. Using the assumed value of AIDR = 0.3, solve Equation 106 at the dispersion points listed in Table 3-4 for dispersion values up to 6.21 volts.

$$K(N_s/d) + AIDR = AIDR + \sqrt{(Disp - AIDR)^2 - (A_0 - AIDR)^2}$$

A_0 = 0.398 (the "no noise added" point of intersection with the Dispersion axis)

AIDR = 0.3 (assumed)

The resulting data is plotted in Figure 3-17 and has an intersection on the dispersion axis at 0.3. Similar plots are made for AIDR = 0.2 and AIDR = 0.1. The AIDR = 0.2 is a straight line, hence the AIDR = 0.2 table will be used to derive the dispersion versus BER table. Note that the AIDR = 0.3 curve is concave upward indicating a lower value AIDR should be tried and the AIDR = 0.1 curve is concave downward indicating that a higher value AIDR should be tried.

The next step after determining AIDR is to determine the constant necessary to relate the field data with the theoretical results. Using the AIDR = 0.2 table and Equation 108

$$C = [(Disp)_{observed} - AIDR]/[(Disp)_{BER} - AIDR],$$

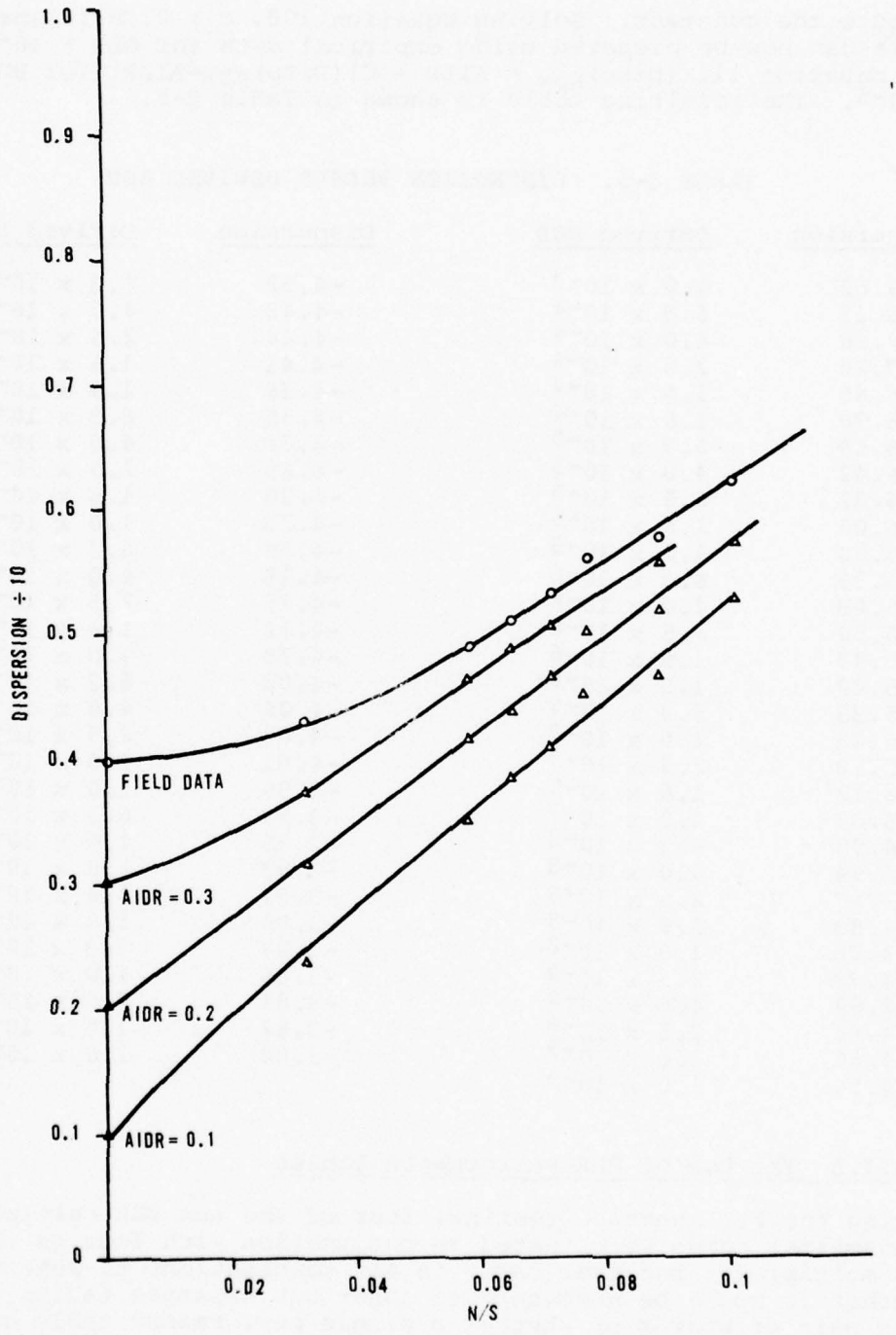

FIGURE 3-17. DISPERSION VERSUS NOISE TO SIGNAL RATIO

compute the constant. Solving Equation 108, C = 0.781. The table can now be prepared using empirical data for BER > 10^{-5} and Equation 111 $(Disp)_{New} = AIDR + C[(Disp)_{BER} - AIDR]$ for BER $\leq 10^{-5}$. The resulting table is shown in Table 3-5.

TABLE 3-5. DISPERSION VERSUS DERIVED BER

Dispersion	Derived BER	Dispersion	Derived BER
-9.62	1.0×10^{-3}	-4.52	6.3×10^{-10}
-8.15	6.3×10^{-4}	-4.48	4.0×10^{-10}
-7.60	4.0×10^{-4}	-4.44	2.5×10^{-10}
-7.20	2.5×10^{-4}	-4.41	1.6×10^{-10}
-6.86	1.6×10^{-4}	-4.38	1.0×10^{-10}
-6.76	1.0×10^{-4}	-4.35	6.3×10^{-11}
-6.59	6.3×10^{-5}	-4.32	4.0×10^{-11}
-6.42	4.0×10^{-5}	-4.29	2.5×10^{-11}
-6.32	2.5×10^{-5}	-4.26	1.6×10^{-11}
-6.05	1.6×10^{-5}	-4.23	1.0×10^{-11}
-5.90	1.0×10^{-5}	-4.20	6.3×10^{-12}
-5.79	6.3×10^{-6}	-4.18	4.0×10^{-12}
-5.68	4.0×10^{-6}	-4.15	2.5×10^{-12}
-5.58	2.5×10^{-6}	-4.12	1.6×10^{-12}
-5.49	1.6×10^{-6}	-4.10	1.0×10^{-12}
-5.40	1.0×10^{-6}	-4.08	6.3×10^{-13}
-5.33	6.3×10^{-7}	-4.06	4.0×10^{-13}
-5.25	4.0×10^{-7}	-4.03	2.5×10^{-13}
-5.18	2.5×10^{-7}	-4.01	1.6×10^{-13}
-5.12	1.6×10^{-7}	-3.99	1.0×10^{-13}
-5.05	1.0×10^{-7}	-3.97	6.3×10^{-14}
-4.99	6.3×10^{-8}	-3.95	4.0×10^{-14}
-4.94	4.0×10^{-8}	-3.93	2.5×10^{-14}
-4.87	2.5×10^{-8}	-3.91	1.6×10^{-14}
-4.83	1.6×10^{-8}	-3.89	1.0×10^{-14}
-4.78	1.0×10^{-8}	-3.87	6.3×10^{-15}
-4.72	6.3×10^{-9}	-3.86	4.0×10^{-15}
-4.69	4.0×10^{-9}	-3.84	2.5×10^{-15}
-4.64	2.5×10^{-9}	-3.82	1.6×10^{-15}
-4.60	1.6×10^{-9}	-3.80	1.0×10^{-15}
-4.56	1.0×10^{-9}		

3.4.7.5 The Use of PAR Performance Tables

During the Ft. Huachuca testing, four of the new DEB multiplexer transmitter cards were tested in conjunction with four of the new DEB multiplexer receiver cards in all combinations to determine whether it would be necessary to construct separate tables for each pair of boards or whether a single performance table could be used for the entire set. It was discovered that two of these transmitter boards were significantly better than the other two

and approximately equivalent to each other. The same statement was found to be true regarding two of the four receiver boards. When either of these two receiver boards was used with either of the two transmitter boards (making four possible combinations), approximately the same error rate versus noise performance was obtained. A performance table was prepared based on tests run with a single pair of these boards and then this table was shown in further testing to give adequate performance prediction for all four combinations of up to par boards. This was then called a PAR Performance Table, indicating that if everything in the system is up to par the system performance will be equal to the predicted performance. When one or more of the sub-par boards was inserted into the system, the observed BER performance was poorer than the predicted performance for a PAR system. It was further concluded that the use of a single PAR Table for a system should be given preference over the use of a separate table for each multiplexer transmitter and receiver pair for two excellent reasons. First, it is much easier to compute, catalog, file, recall, and update a single table than it is to maintain a library of tables with a different table for each multiplexer transmitter and receiver board combination. Second, the use of a single PAR Performance Table will reveal inferior boards for what they are-- inferior-- rather than disguising this inferiority by comparing the performance of each board combination only against it's previous performance so that bad combinations are awarded a handicap advantage which makes them look as good relative to BEM predictions as PAR boards would look.

The BEM monitors the received signal rather than the receiver; therefore, it should tell what the receiver should be doing rather than what the receiver is doing. If a transmitter is below par, a BEM using a PAR Table will indicate the resulting deficiency in the receiver signal quality; however, the BEM has no way of detecting whether the receiver is even turned on. Thus, the concept of adjusting the BEM prediction tables to fit different receivers seemed inappropriate and the concept of using a single PAR Performance Table seems to be not only the easiest technique to implement but also the technique which yields the most meaningful results.

3.4.8 Theory, Testing, and Use of the Hit Counter

3.4.8.1 Hit Probability Versus BER Derivations

The mathematics of the hit counter pseudo error threshold, K, are extremely similar to those of the dispersion loop pseudo error threshold, a/d. The locations of these two thresholds are shown in Figure 3-11. The dispersion loop pseudo error threshold is located at a distance, a volts, above the lower eye pattern level, and the hit counter pseudo error threshold is located at a distance, Kd volts, above the center eye pattern level. The dispersion loop pseudo error threshold, a is adjusted by a control loop which holds the pseudo error rate constant in the pseudo error zone from -(2d-a) to -d volts. On the other hand, the offset threshold voltage, Kd, of the hit counter pseudo error zone has a fixed value which is set by selected resistors. Therefore, the parameter, K, for the hit counter pseudo error loop is a constant while the pseudo error rate for that loop, P[HIT], is a variable. Following the same procedure which was used for determining the dispersion loop pseudo error rate, PER1; the hit counter pseudo error rate, P[HIT], is computed by multiplying the probability of each submitted eye pattern level occurring by the probability that the received voltage will lie in the hit counter pseudo error region between K volts and d volts given that the specified eye pattern level did occur, and summing these resulting joint probability products over all possible transmitted levels to obtain the average hit counter pseudo error probability, P[HIT], for all typical random data patterns. These operations are performed below in Equation 113 in which the effect of each of the nine levels in the nine-level eye pattern is shown on a separate line.

$$R \triangleq AIDR \tag{112}$$

$$\begin{aligned} P[HIT] = (1/16)\ \{ & Q[(1+R)d/N] - Q[(2-K+R)d/N] \\ & +2Q[(1)d/N] - 2Q[(2-K)d/N] \\ & + Q[(1-R)d/N] - Q[(2-K-R)d/N] \\ & +2Q[(K-R)d/N] - 2Q[(1-R)d/N] \\ & +4Q[(K)d/N] - 4Q[(1)d/N] \\ & +2Q[(K+R)d/N] - 2Q[(1+R)d/N] \\ & + Q[(2+K-R)d/N] - Q[(3-R)d/N] \\ & +2Q[(2+K)d/N] - 2Q[(3)d/N] \\ & + Q[(2+K+R)d/N] - Q[(3+R)d/N]\} \end{aligned} \tag{113}$$

By combining like terms, the 18 terms in the above equation can be combined into five groups of three terms each as shown below.

$$\begin{aligned} P[HIT] = (1/16)\{ & 2Q[(K-R)d/N]+4Q[(K)d/N]+2Q[(K+R)d/N] \\ & - Q[(1-R)d/N]-2Q[(1)d/N]- Q[(1+R)d/N] \\ & - Q[(2-K-R)d/N]-2Q[(2-K)d/N]-2Q[(2-K+R)d/N] \\ & + Q[(2+K-R)d/N]+2Q[(2+K)d/N]+ Q[(2+K+R)d/N] \\ & - Q[(3-R)d/N]-2Q[(3)d/N]- Q[(3+R)d/N]\} \end{aligned} \tag{114}$$

The hit counter pseudo error rate for a three level eye can be determined from Equation 114 by setting the intersymbol interference amplitude, AIDR, which is represented above by R, equal to 0. After this substitution, the 15 terms in Equation 114 can be merged into the five terms shown below.

$$P[HIT|AIDR = 0] = (1/4)\{2Q[(K)d/N] - Q[(1)d/N] - Q[(2-K)d/N] + Q[(2+K)d/N] - Q[(3)d/N]\} \quad (115)$$

For the three-level eye, the variation of the hit counter pseudo error probability, P[HIT], and the Baud error probability, BER, can be determined by using Equation 115 and the previously derived Baud error probability equation.

$$BER = (3/2)Q(d/N) \quad (116)$$

Solving the above equation for the decision level to noise ratio, d/N, produces the following result which can be evaluated with the aid of an extensive table of probabilities for the normal distribution or an inverse normal computer subroutine.

$$d/N = Q^{-1}[(2/3)BER] \quad (117)$$

The hit probability versus Baud error rate characteristics for several values of K are shown in Figure 3-18. These characteristics were obtained by using Equation 117 to determine the values of d/N for many Baud error rates in a range from 10^{-1} to 10^{-18} and then using these resulting d/N values with several different values of K in Equation 115 to determine the hit probabilities for those conditions. The resulting hit probabilities were plotted against Baud rate in Figure 3-18, and the points for each particular value of K were connected by smooth lines which are almost straight except in the lower left hand corner.

3.4.8.2 Selection and Laboratory Testing of the Hit Counter Threshold, K

The amplitude of the hit counter threshold, K, is set by calibration resistors and may be changed if this is found to be desirable; however, on the basis of a theoretical analysis, the value was initially set equal to 0.85 which has worked well enough that no additional values have been tested. The 0.85 value was selected on the assumption that the hit counter should just barely begin to detect hits when the Baud error rate is equal to 10^{-12}. The counter counts the number of pseudo errors occurring in a 120 second time interval at a data rate of 12.55M bits per second, which means there are about 1.5×10^9 Baud per measurement interval. To obtain an average of one pseudo error per hit counter interval, the hit counter pseudo error probability, P[HIT], would have to be equal to 6.6×10^{-10}. A small circled point is plotted on Figure 3-18 for a hit probability of 6.6×10^{-10} and a Baud error rate probability of 10^{-12}. The pseudo error versus

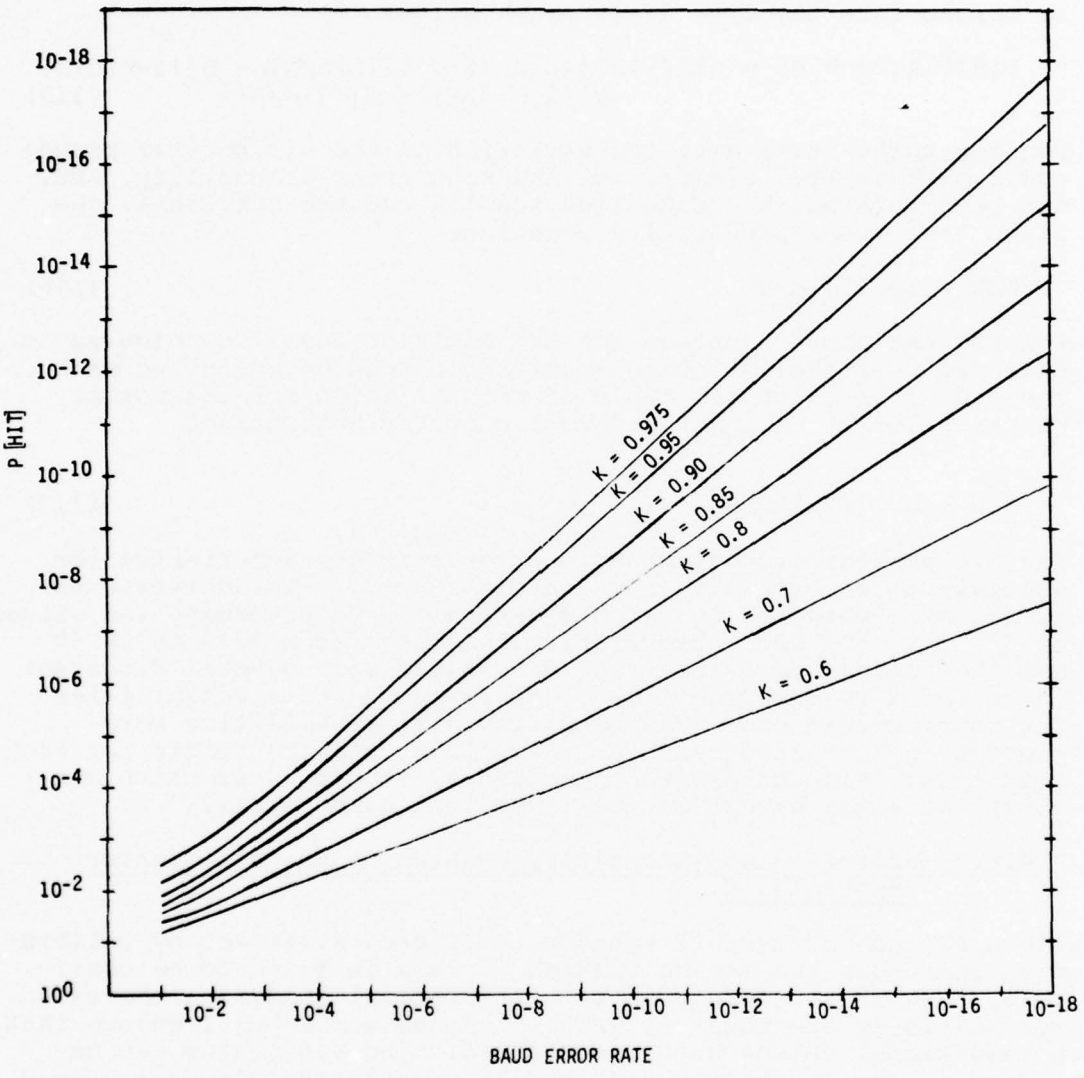

FIGURE 3-18. HIT COUNTER PSEUDO ERROR RATE, P [HIT] VERSUS BER FOR SEVERAL OFFSET THRESHOLD VALUES, K

Baud error curve coming closest to this point is the one with an offset threshold value, K, equal to 0.85, and that is why this value was selected. During laboratory testing, the observed number of hits per interval for various test conditions were in agreement with the theoretically predicted counts. No reason for change in the amplitude of K in either direction could be found, so it was left at 0.85 for field testing.

3.4.8.3 Interpretation of Hit Counter Output

The hit counter and dispersion meter are quite similar; however, they perform different functions when used separately, and when the outputs of these two devices are compared with each other an extra dimension of fault isolation capability becomes available which is not present when both devices are used simultaneously but individually. One very significant difference between these two measurements is that the hit counter has a 120-second averaging interval whereas the dispersion meter has a time constant which is typically a little less than 1 second. Therefore, the hit counter can remember impulses and dropouts which the dispersion meter has long forgotten. If one reads out the dispersion value only once in several minutes and each value represents only about a 1-second sample, a line may be suffering occasional hits for a long period of time before a hit finally affects one of the sampled dispersion readings. The hit counter is less forgiving. Thus, even if the hit counter and dispersion meter were making identical measurements, the difference in their averaging times would make their outputs differ both in appearance and in utility for various functions.

Theoretical analysis predicts that using the hit counter and dispersion meter jointly and comparing the readings should yield valuable diagnostic information for fault isolation. For example, if the channel is being disturbed by Gaussian noise, then the dispersion meter will predict the Baud error rate correctly and the hit counts versus Baud error rate will follow a known characteristic such as that shown in Figure 3-18 so that a particular dispersion meter Baud error rate estimate should always be accompanied by the same hit counter output within small random error limits. In a sense, the hit counter and dispersion meter working together can, to an extent, perform the test for Gaussian noise which previously was going to be performed by using two dispersion meters simultaneously with two different pseudo error rates. The twin dispersion meter technique would give more information; however, it would also be more expensive. Thus, when the dispersion meter and hit counter outputs are compared closely to determine whether or not the disturbance is normally distributed, a cheap approximation to the dual threshold dispersion meter technique is being employed.

If the disturbance is caused by a low amplitude sine wave such as one of the beacons often present in the radio channels, the sine wave amplitude is not large enough to cause any hits; however, the dispersion meter is very sensitive to this type of channel degradation. The dispersion meter is also far more sensitive than the hit counter to changes in the frequency response of a channel which alter the intersymbol interference of the data signal. On the other hand, if some phenomenon is causing narrow impulses to occur in the communication channel, these impulses may be so narrow as to produce only a few pseudo errors each and occur at a low enough rate to be negligible relative to the pseudo error rate in the dispersion meter, which is several thousand errors per second. In this case, the impulses would produce a rather substantial effect on the outputs of the hit counter but be essentially negligible as far as the dispersion output is concerned. In summary, sine waves and intersymbol interference would affect the dispersion meter far more than the hit counter, normally distributed noise would affect both with a known relationship such as that shown in Figure 3-18, and narrow spikes at a fairly low frequency would have very little effect on the dispersion meter and a very large effect on the hit counter. These relationships, and a few others, can be substantiated by theoretical analysis after making some plausible assumptions; however, the real proof of the usefulness of making correlations between the hit counter output and the dispersion meter output will be obtained only by actual experience in the field.

3.5 BEM CIRCUIT BOARD DESCRIPTIONS

BEM circuit board descriptions are presented in the following paragraphs. Refer to Schematics and Board Assembly Drawings.

3.5.1 Circuit Board Description: Interface Unit (A15)

The Interface Unit (A15) is one of two modified VICOM boards in the BEM. These two boards (A14 and A15) contain the circuits used in the on-line multiplexer to receive the radio baseband signal, filter, provide automatic gain control, and derive a phase locked clock. The clock is derived on the Receiver Input board (A14); the other functions are provided by A15.

A block diagram of the Interface Unit (A15) is shown in Figure 3-19.

The partial response filter provides frequency spectrum shaping to generate the three level partial response "eye pattern" that is to be monitored for dispersion and hits.

The variable gain amplifier and automatic gain control circuitry provides amplification of the eye pattern to a somewhat constant output peak amplitude. This output signal, VICOM Eye, is transmitted to the Sample and Hold board (A5) for further processing.

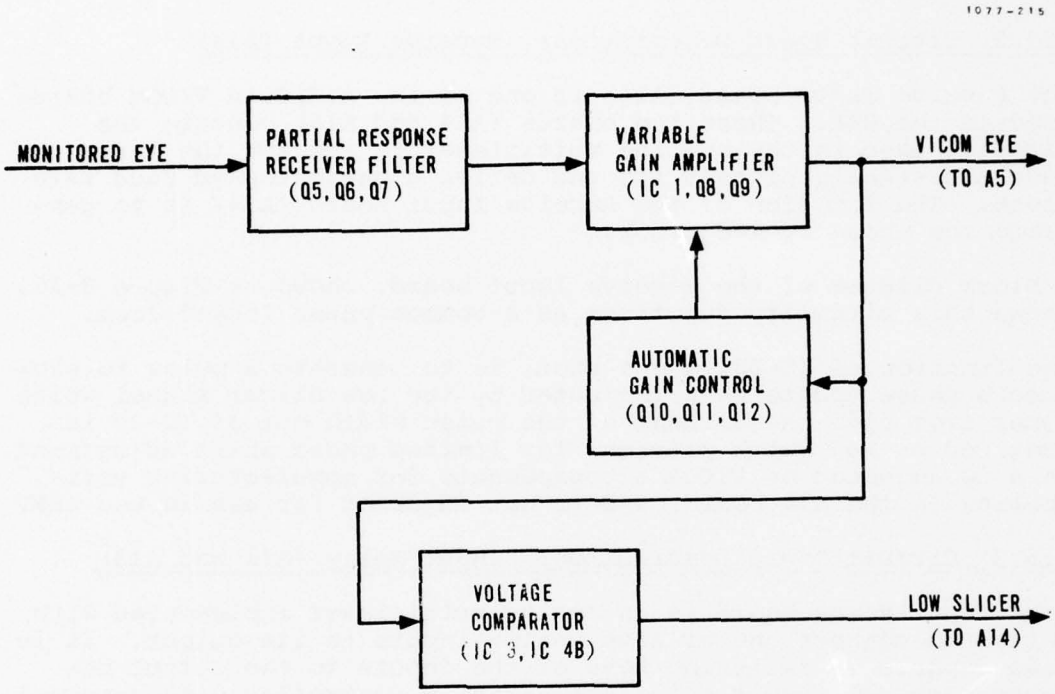

FIGURE 3-19. INTERFACE UNIT (A15) BLOCK DIAGRAM

The VICOM Eye signal is also compared to a fixed negative voltage level by a voltage comparator to detect the negative outer level of the VICOM Eye pattern. The comparator output signal, Low Slicer, is transmitted to the Receiver Input board (A14) for use in deriving the phase locked Baud rate clock.

3.5.2 Circuit Board Description: Receive Input (A14)

The Receive Input board (A14) is one of two modified VICOM boards used in the BEM. These two boards (A14 and A15) contain the circuits used in the on-line multiplexer to receive the radio baseband signal, process it, and derive a phase locked Baud rate clock. The function of the Receive Input board (A14) is to generate the phase locked clock.

A block diagram of the Receive Input board, shown in Figure 3-20, shows this circuitry functions as a common phase locked loop.

The function of IC-20, a one shot, is to generate a pulse to produce a phase update when indicated by the Low Slicer signal which comes from A15. Adjustment of the pulse width out of IC-20 is provided by R61 which provides for limited phase shift adjustment. This is adjusted by VICOM to compensate for manufacturing variability on the A14 board, and is not adjusted for use in the BEM.

3.5.3 Circuit Board Description: Input Relay (A12 and A13)

Each Input Relay board is an analog multiplexer implemented with relays to connect one of five analog inputs to its output. It is also capable of switching none of the inputs to the output because each relay switch is independently controlled with external signals. Two Input Relay boards are used in the BEM assembly providing a capability of selecting one of ten different inputs.

3.5.4 Circuit Board Description: Input Board (A11)

The Input Board (A11) provides two major functions. It contains the circuitry for measuring the RMS voltage amplitude of the input signals to the BEM and the circuitry to provide voltage controlled phase shift for the phase correction loop. Incidentally, it also provides a location to electrically connect the outputs of the two Input Relay boards (A12 and A13). This signal is transmitted to the Interface Unit (A15).

A Burr Brown 4130K, RMS to dc voltage converter is used to implement the RMS measurement. Operational amplifiers at locations 1H and 2L are also part of this circuit.

The voltage controlled phase shifter comprises the remaining circuitry on the Input Board.

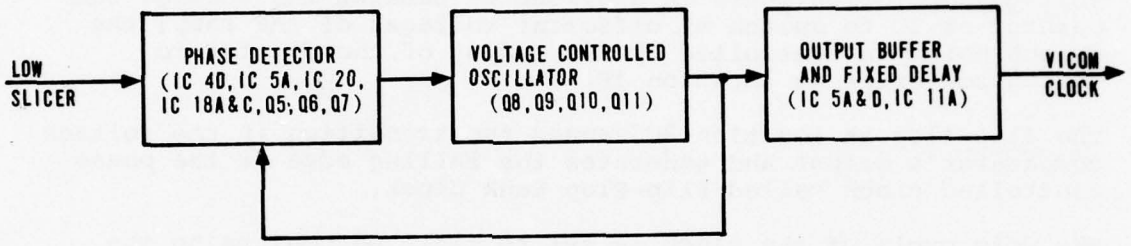

FIGURE 3-20. RECEIVE INPUT (A14) BLOCK DIAGRAM

The outputs of the Phase Locked Loop Control (A10) are converted to a control voltage by the digital to analog converter at location 1E. This voltage is compared to a clock phase related ramp waveform by a voltage comparator at location 1C. The ramp is generated for one half of the VICOM Clock period by charging capacitor C24 with a current source implemented with Q1. The output of the current source is shorted by Q2 during the other half cycle of VICOM Clock to reset the ramp.

Various fixed time delays are strap selectable using integrated circuit locations 2A and 2B.

Voltage controlled phase is provided by causing the voltage comparator at 1C to switch at different voltages of the ramp; the switch point is controlled by the output of the digital to analog converter at location 1E.

The flip-flop at location 2C senses the transition in the voltage comparator's output and generates the falling edge of the phase controlled clock called Flip-Flop Bank Clock.

The duty cycle of the clock is set to fifty percent using the circuitry involved with the voltage comparator at location 1D. That is, this circuitry provides the rising edge of Flip-Flop Bank Clock.

This is implemented by allowing C35 to charge for one half cycle of the output clock, at which time its voltage will exceed the reference at the other input of the comparator. The comparator will then trigger and reset the flip-flop at 2C and cause the rising edge in Flip-Flop Bank Clock.

3.5.5 Circuit Board Description: Phase Locked Loop Control (A10)

The Phase Locked Loop Control Board (A10) contains the digital circuitry that provides control of the phase shifter on A11 to implement automatic phase adjustment of the VICOM Clock and the Sampled Eye.

A block diagram of Phase Locked Loop Control board circuitry is given in Figure 3-21.

The phase locked loop updates on eye pattern zero crossing when the crossing is preceded one Baud earlier by an outer level and followed by the opposite outer level one Baud later. The middle level sample is processed to determine if the clock was early or late relative to the zero crossing and a phase update is generated.

This is implemented by the Extreme Transition Detector of the block diagram.

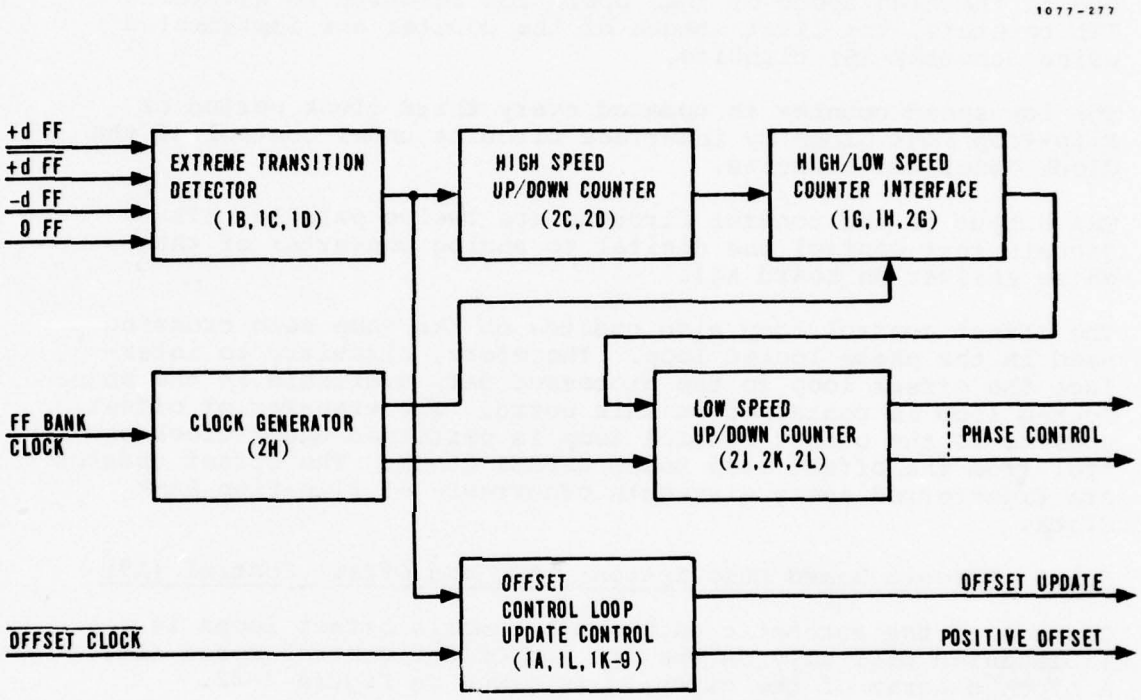

FIGURE 3-21. PHASE LOCKED LOOP CONTROL BOARD (A10) BLOCK DIAGRAM

The individual updates are integrated over time to generate the control signal for the phase shifter. This integration is accomplished with a binary up/down counter.

Due to the high speed of this operation relative to available TTL counters, the first stages of the counter are implemented using Schottky SSI circuits.

The low speed counter is updated every third clock period of Flip-Flop Bank Clock by interface circuits under control of the Clock Generator circuits.

The output of the control circuits are twelve parallel TTL signals that control the digital to analog converter of the phase shifter on board A11.

The offset control loop also updates on the same zero crossing used in the phase locked loop. Therefore, circuitry to interface the offset loop to the processed data available in the phase locked loop is contained on this board. The transfer of offset updates to the offset control loop is performed under clock control from the offset loop using OFFSET CLOCK. The offset updates are transferred every sixteenth occurrence of Flip-Flop Bank Clock.

3.5.6 Circuit Board Description: AGC and Offset Control (A9)

Control of the automatic gain and automatic offset loops is implemented digitally on the AGC and Offset Control Board (A9). A block diagram of the circuits is given in Figure 3-22.

Offset voltage in the sampled eye pattern is reduced by monitoring the center level and forcing its average value to zero. The Offset Update and Positive Offset signals from the Phase Locked Loop board (A10) control an up/down counter which integrates the offset updates. These updates to the counter occur every sixteenth occurrence of Flip-Flop Bank Clock.

The gain of the BEM is controlled so that half of the negative outer level samples are more negative than -2d volts (-1.8 volts dc). The Gain Adjust Update Control function, shown in the block diagram, samples $-\overline{dFF}$ and -2DFF signals every sixteenth occurrence of Flip-Flop Bank Clock under control of the Clock Generator function.

Gain updates are integrated in an up/down counter which adjusts the output voltage of a digital to analog converter as shown in the block diagram. This output voltage adjusts the reference level used in the other automatic gain control circuit on the Interface Unit (A15). This in turn adjusts the control voltage and gain of the variable gain amplifier on A15.

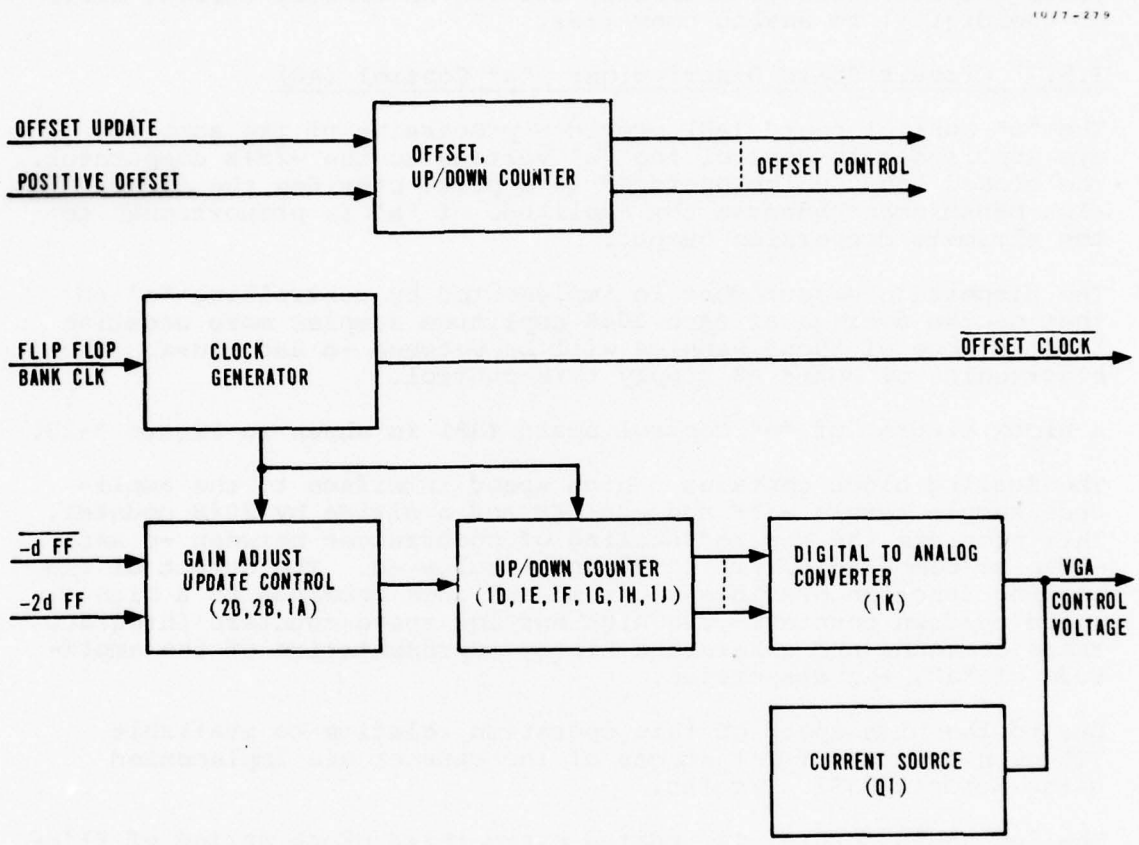

FIGURE 3-22. AGC AND OFFSET CONTROL BOARD (A9) BLOCK DIAGRAM

The current source at the output of the digital to analog converter is used to supply the nominal current required with zero volts output. This is necessary due to the limited current drive of the digital to analog converter.

3.5.7 Circuit Board Description: "a" Control (A8)

The "a" Control board (A8) provides processing of the sampled eye amplitudes to control the "a" voltage to the -2d+a comparator. The closed loop, which board A8 is a part, provides the dispersion measurement because the amplitude of "a" is proportional to the ultimate dispersion output.

The dispersion measurement is implemented by controlling "a" so that on the average of each 2048 amplitude samples more negative than -d, one of those samples will be between -d and -2d+a. The electronics of board A8 supply this control.

A block diagram of "a" Control board (A8) is shown in Figure 3-23.

The Scaling block contains a high speed interface to the amplitude sample levels -dFF and -2d+aFF and a divide by 2048 counter. This provides the desired scaling of occurrences between -d and -2d+a as compared to all occurrences below -d. The output of the scaling function provides count up and down commands to a high speed up/down counter. The high and low speed counters integrate these commands and generate a binary representation of the amplitude of "a", the dispersion.

Due to the high speed of this operation relative to available TTL counters, the first stages of the counter are implemented using Schottky SSI circuits.

The low speed counter is updated every third clock period of Flip-Flop Bank Clock by interface circuits under control of the Clock Generator circuits.

The output of the control circuits are twelve parallel TTL signals that control the digital to analog converter that generates the "a" voltage.

3.5.8 Circuit Board Description: Plus Comparator Board (A7)

The Plus Comparator board (A7) has been modified and no longer contains active comparators. The board does provide the digital to analog converter that produces the "a" Control voltage (2E location) and an amplifier (2L) that amplifies "a" and provides the Dispersion measurement output.

The voltage reference used to generate all other dc reference voltages is generated by diode VR1 and amplifier 1B.

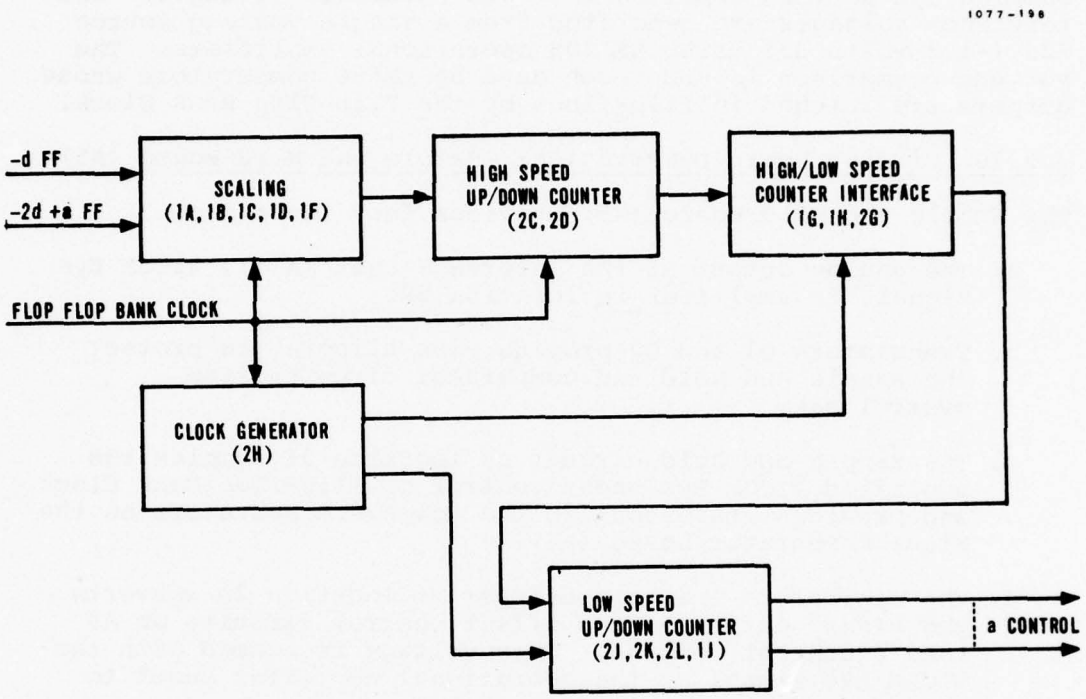

FIGURE 3-23. BLOCK DIAGRAM OF "a" CONTROL BOARD (A8)

3.5.9 Circuit Board Description: Minus Comparator Board (A6)

The Minus Comparator board (A6) provides comparison of the sampled eye pattern amplitudes to six reference voltages. The reference voltages are generated from a single voltage source -2d (-1.8 volts dc) using LM 208 operational amplifiers. The voltage comparison is made each Baud by AM686 comparators whose outputs are latched in flip-flops by the Flip-Flop Bank Clock.

3.5.10 Circuit Board Description: Sample and Hold Board (A5)

The Sample and Hold Board (A5) provides four functions:

a. The analog output of the Interface Unit (A15), VICOM Eye signal, is amplifier in location 2K.

b. Transistors Q1 and Q2 provide peak clipping to protect the sample and hold and comparator circuits from overvoltage.

c. The sample and hold circuit at location 1E samples the amplified VICOM Eye under control of Flip-Flop Bank Clock and provides its output to the voltage comparators on the Minus Comparator board (A6).

d. The digital to analog converter at location 2A converts the binary output of the offset control circuits on A9 into a control voltage. This voltage is summed with the VICOM Eye signal at the operational amplifier input to provide offset capability.

3.5.11 Circuit Board Description: EPUT Counter (A2)

Hits are counted over a strap selectable time base using the EPUT Counter board (A2) and EPUT Time Base board (A1). The EPUT counter board (A2) provides the counters and output coding.

A block diagram of the EPUT Counter board (A2) is given in Figure 3-24.

The Input Conditioning circuits process the sampled eye amplitudes to delete occurrences between -Nd and -d, and generate count pulses to update the counter. These circuits also provide for self-test of the counter by counting Self-Test Clock.

The Counter function is a binary counter with sixteen stages.

The Exponent Counter provides a binary number that equals the number of the stage of the binary counter that has the most significant logic one level.

FIGURE 3-24. EPUT COUNTER BOARD (A2) BLOCK DIAGRAM

The Buffer Register is loaded with the number in the Exponent Counter from the last time period while a new count is being accumulated. This number is coded into a negative dc voltage output by the Digital to Analog Converter function which includes the μA741 output amplifier.

3.5.12 Circuit Board Description: EPUT Time Base A1)

Hits are counted over a strap selectable time base using the EPUT Time Base board (A1) and EPUT Counter board (A2). The EPUT Time Base (A1) supplies control for this function.

A block diagram of the EPUT Time Base board (A1) is given in Figure 3-25.

The length of time during which hit counts are accumulated is controlled by strapping the appropriate clock from the Count Down Chain to the Control function. At the end of each time base period, the hit counters on A2 are stopped by STOP COUNT signal, and the count is transferred to the buffer on A2. The hit counters are then cleared and restarted. The details of this operation are the same as any other Events Per Unit Time (EPUT) monitor.

The additional functions in the BEM-EPUT time base are Measurement Reset and Master Reset. Following a Scanner Address Change or Power Reset, a Master Reset is generated for several milliseconds and a Measurement Reset is generated for thirty seconds.

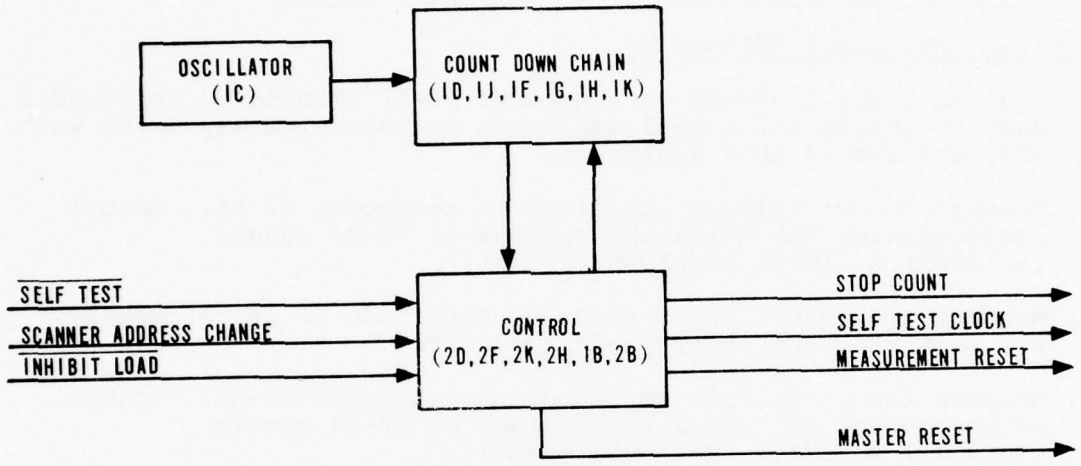

FIGURE 3-25. EPUT TIME BASE BOARD (A1) BLOCK DIAGRAM

3.6 CALIBRATION OF BASEBAND EYE MONITOR (BEM)

The following setup instructions are for the Honeywell Baseband Eye Monitor, and facilitate board alignment and calibration. Refer to the schematics and board assembly drawings for parts location.

3.6.1 Calibration Procedure For Input Board (A11)

3.6.1.1 RMS Level Adjustment

a. Apply a 1 MHz sinewave to connector P2-A1 (Monitored Baseband). Measure and adjust signal amplitude to approximately 0.122 volt RMS, and record this amplitude

b. Measure the dc voltage amplitude at connector P2-A4. Adjust potentiometer R10 until the voltage at P2-A4 equals (-8.2023) x (INPUT AMPLITUDE, VRMS).

c. Measure and adjust input sinewave amplitude to approximately 1.1 volt RMS, and record this amplitude.

d. Measure the dc voltage amplitude at connector P2-A4. Adjust potentiometer R11 until the voltage at P2-A4 equals (-8.2023) x (INPUT AMPLITUDE, VRMS).

e. Repeat steps a through d until the measured dc voltages at connector P2-A4 are within 0.1 percent of the expected values for both steps b and d, following the last adjustment of the potentiometers.

3.6.1.2 Clock Phase Shifter Adjustment

a. Adjust a 2K ohm potentiometer to 900 ohms and place it in the circuit as R33. This is the Digital to Analog Converter gain select resistor.

b. Supply a TTL clock signal having a frequency of 12.5526 MHz nominal to connector pin P2-A3 (VICOM Clock). This signal should be a square wave having logic 1 and 0 pulse widths of 39.8 ±0.5 nanoseconds measured at 1.4 volts.

c. Strap 2B-10 to 2A-1 and 2A-11 to 2B-2.

d. Supply a TTL logic 1 signal to connector pins P1-2 through P1-6 and P1-12 through P1-18.

e. Monitor the clock signal at 2C-9 with an oscilloscope. Adjust potentiometer R32, which is the D/A converter offset adjustment, until the clock signal is at the threshold of becoming a steady logic level.

f. Measure and record the dc voltage amplitude at test point 4. The nominal value is zero.

g. Adjust R32 until the dc voltage at test point 4 is 0.15 volt more positive than measured in step f.

h. Supply a TTL logic 0 signal to connector pins P1-2 through P1-6 and P1-12 through P1-18.

i. Monitor the clock signal at 2C-9 with an oscilloscope. Adjust the potentiometer in the R33 location until the clock signal is at the threshold of becoming a steady logic level.

j. Measure and record the dc voltage amplitude at test point 4. The nominal value is 1.8 volts.

k. Adjust R33 until the dc voltage at test point 4 is 0.15 less positive than measured in step j.

l. Supply a TTL logic 1 signal to connector pins P1-2 through P1-6 and P1-12 through P1-18.

m. Adjust R32 until the dc voltage at test point 4 is 0.15 volt more positive than measured in step f.

n. Supply a TTL logic 1 signal to connector pins P1-2 through P1-6 and P1-12 through P1-18.

o. Adjust the potentiometer in R33 location until the dc voltage at test point 4 is 0.15 volts less positive than measured in step j.

p. Repeat steps l through o until the dc voltages measured in steps m and o are within 0.01 volt of the desired amplitude.

q. Remove the potentiometer from R33 location and measure its value.

r. Place an RN55C resistor, with the standard resistance value closest to that measured in step q, into location R33.

s. Confirm the results of step o.

3.6.1.3 Duty Cycle Adjustment

a. Supply a TTL logic 1 signal to connector pin P1-2 and a TTL logic 0 signal to connector pins P1-3 through P1-6 and P1-12 through P1-18.

b. Monitor the clock signal at connector pin P1-23 for logic 0 pulse width. The duty cycle control circuit sets the time period of the logic 0 portion of this clock.

c. Place a 500 ohm potentiometer in the R26 location and adjust it until the logic 0 pulse width of the clock is 39.8 ±0.5 nanoseconds.

d. Remove the potentiometer from the R26 location and measure its value. Place an RN55C resistor, with the standard resistance value closest to that measured, into location R26.

e. Confirm the logic 0 pulse width at connector pin P1-23 to be 39.8 ±0.5 nanosecond.

3.6.2 Calibration Procedure For Minus Comparator Board (A6)

a. Insert 10 ohms, RN55C resistors in R5 and R8 locations. Leave R6 open. Temporarily connect a 0.1 µf, CK06 capacitor or equivalent to the signal side of R8, not the comparator side.

b. Connect a precision dc voltage source to connector pin P2-A2 (+2d) and adjust it to give +1.8000 ±0.0005 volt dc.

c. Connect a second precision dc voltage source set to zero volt to connector pin P2-A3 (SAMPLED EYE).

d. Monitor 2G-5 with an oscilloscope and slowly decrease the voltage at P2-A3 until the signal at 2G-5 switches to a logic 0.

e. Measure and record the dc voltage at P2-A3 to within 0.1 millivolt.

f. Decrease the voltage at P2-A3 to approximately -1.9 volts dc.

g. Increase the voltage at P2-A3 until this signal at 2G-5 changes state to a logic 1.

h. Measure and record the dc voltage at P2-A3 to within 0.1 millivolt.

i. Average the measurements of steps e and h to calculate the comparator's switch voltage. This is the average of the switch voltage for increasing and decreasing voltage waveforms. For this reason, it is important that the switch points be approached monotonically in steps d and g.

j. Subtract the nominal threshold voltage for the comparator from the average calculated in step i. In this case the nominal threshold is -0.9 volt. If the absolute value of the result is 0.25 millivolt or less, further calibration is not required, go to step n. If greater than 0.25 millivolts, proceed to step k.

k. Use the following equation to calculate the value of R6.

Use same sign as sign of calculated offset from step j.

$$R6 = 10 \left[\frac{V_{REF} - V_{OFFSET}}{V_{OFFSET}} \pm 15 \right]$$

where

V_{REF} is the nominal switch voltage for the comparator

V_{OFFSET} is the voltage calculated in step j.

Use the proper amplitude and sign for these quantities.

If the calculated value of R6 is 100K ohms or greater, insert an RN55C resistor in position R6 that has the closest standard resistance value to the calculated value.

Connect R6 to +15 volts dc if the calculated value in step j is negative. Otherwise use -15 volts dc.

If the calculated value of R6 is less than 100K ohms, insert a 100K ohms, RN55C resistor in the R6 location and connect it to either ±15 volts dc as described above.

Then calculate the value of R5 and R8 using the following equation:

$$R5 = R8 = 10^5 \left[\frac{V_{OFFSET}}{V_{REF} - V_{OFFSET}} \pm 15 \right]$$

Use same sign as sign of calculated offset from step j.

Insert RN55C resistors in positions R5 and R8 that have the closest standard resistance value to the calculated value.

l. Confirm that the comparator switches within 0.25 millivolts of the nominal level by repeating steps d through j.

If it is not within this tolerance, change the value of the calculated resistor by one step in resistance value until the voltage at which the comparator switches is as close to nominal as obtainable.

m. Remove the 0.1 μf capacitor from R8.

n. The Minus Comparator Board has six comparators, all similar to the -d comparator just calibrated. Each of the remaining five comparators should be calibrated in a similar manner, using steps a through m.

When calibrating the -2d +a comparator (integrated circuit location 1D), ground connector P2-A3 (+a) and ground the junction of R20, R21 and C23. The purpose of this is to insure that the -2d comparator does not interfere with calibration of the -2d+a comparator. With P2-A3 grounded the -2d+a comparator should switch at -1.800 volts.

When calibrating the -2d comparator (integrated circuit location 2D), put +0.9 ±0.1 volt dc on connector pin P2-A3 (+a) to insure that the -2d+a comparator does not interfere with the -2d comparator.

3.6.3 Calibration Procedure For Plus Comparator Board (A7)

3.6.3.1 Digital to Analog Converter For "+a" Offset Adjustment

a. Supply TTL logic 1 signals to the following connector pins.

P1-1 through P1-6

P1-19 through P1-23

P1-37

b. Monitor the dc voltage at test point 8 and adjust the potentiometer R32 until the measured voltage is 0 ±0.0005 volts dc.

c. Disconnect the signals of step a. Calibration is complete.

3.6.3.2 "+2d" Reference Voltage Adjustment

a. With resistor R4 having a value 7.87K ohms, monitor the dc voltage at test point 3. Adjust potentiometer R31 until the monitored voltage is +1.8000 ±0.0005 volts dc.

If the potentiometer has insufficient range go to step b, otherwise calibration is complete.

b. Position potentiometer R31 in the middle of its range by adjusting it until the voltage at test point 3 is in the middle of its range. Measure and record this voltage.

c. Calculate the value of resistor R4 needed to give ±1.8 volts dc using the following equation.

$$R4 = \left[\frac{14166}{\text{VOLTAGE MEASURED IN STEP b}}\right]$$

d. Select an RN55C resistor with the closest nominal resistance value to that calculated in step c and insert it into the circuit at location R4 in place of the 7.87K ohms resistor. Then repeat step a.

3.6.4 Calibration Procedures For Relative Phase of Monitored Signal and Derived Clock For the BEM as a Unit

a. On the Input Board, A11, strap 2B-10 to 2A-1 and 2B-2 to 2A-10. This will select a nominal phase relationship.

b. Supply a sinewave to one of the BEM input ports, the test input on the front panel for instance. This signal should have a frequency of 3.13815 MHz and an amplitude of approximately 0.308 volts RMS (+2.78 dBm at 50 ohms).

c. Position the Maintenance switch to Maintenance. Select mode 2 and the input port used (Test Input is input 9).

d. Use an oscilloscope to monitor the voltage waveforms at test points 10 and 13 on the Sample and Hold Board, A5. (Monitor the signals on the circuit side of the 1K ohm test point isolation resistors so as to maintain the necessary signal bandwidth.)

   Test point 13 will be a sinewave approximately 1.8 volts peak and test point 10 will be samples of this waveform, from a sample and hold output.

   Position the waveforms on the oscilloscope screen so that they both have the same ground reference and the same amplitude scale. The waveforms will appear similar to those shown in Figure 3-26.

   When the phase of the clock is correct, the sinewave will be sampled at its zero crossings and at its peaks.

   As shown in Figure 3-26, the samples are being taken early, and therefore the clock is early. The samples closest to zero volts, which are the flat portions of the waveform closest to zero, are therefore offset from zero by V1.

   Measure the timing error in the clock by measuring the time it takes the sinewave to get from V1 to ground. When the clock is late V1 will be in the other direction.

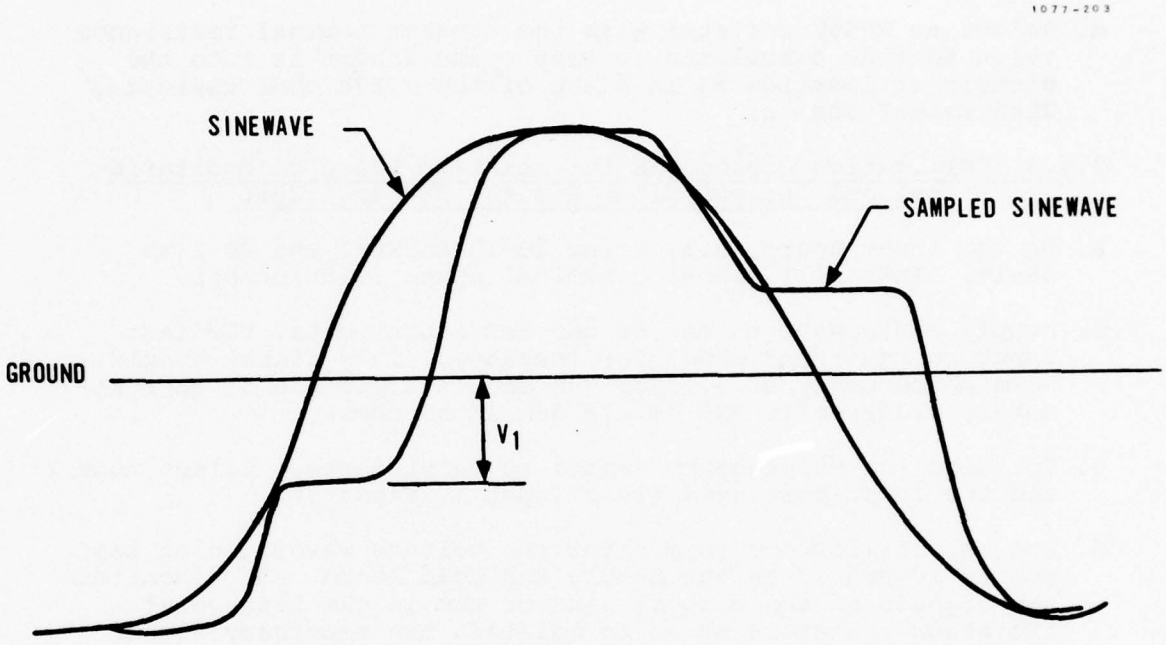

FIGURE 3-26. SAMPLE AND HOLD WAVEFORM (EARLY SAMPLING)

e. Divide the time measured in step d by 8 nanoseconds, and round the result to the nearest integer.

f. If the result in step e is zero, calibration is complete. If the result in step e is not zero, strapping on the Input Board, All needs to be modified. The source of the signal for 2B-2 should be moved the number of gates equal to the number calculated in step e. When the samples are too early as shown in the diagram, move the strapping wire to a gate preceding the existing strapping and vice versa for late samples.

   If more than two gate delays are required, remove the strap from 2B-10 to 2A-1 and add a strap from 2B-4 to 2A-1. Then repeat steps c through f.

g. Select mode - and the input port used.

h. Measure the dc voltage at test point 4 on the Input Board, All. Confirm that this voltage is +0.9 ±0.3 volts dc.

3.7 BEM AND ACTIVE COUPLER FIELD MODIFICATIONS FOR AVANTEK DR8A RADIO ADAPTATION

3.7.1 *BEM Modifications*

The BEM was modified in order to operate at the 6.3 MHz data rate in the AVANTEK DR8A instead of the 12.6 MHz data rate in the AN/FRC-162 radio. The change in data rates was accomplished by changing the crystal in the reference oscillator located on the clock recovery board in the BEM from 12.5533 MHz to 6.2765 MHz. The tuning inductor used to adjust the oscillator frequency was also changed to accommodate the new frequency range.

The dc output voltage representing EYE dispersion was further filtered to compensate for rapid changes in dispersion due to radio performance. The filtering was accomplished by the addition of a series resistor and shunt capacitor to the output signal thereby forming an RC time constant of approximately 10 seconds. This was found to be effective in accomplishing the necessary filtering.

3.7.2 BEM Active Coupler Modifications

The BEM active couplers were also changed to accommodate the test point level in the AVANTEK DR8A radio as opposed to that in the AN/FRC-162 radio. The DR8A radio monitor point signal level was of a lower value and higher impedance than the corresponding point in the AN/FRC-162 radio. Therefore, it was necessary to adapt the BEM active coupler to interface with the DR8A radio. The adaptation was performed by changing the buffer amplifier input impedance from 75 ohms to approximately 500 ohms. The voltage gain of the coupler was increased to 18 dB as a result of the impedance change.

REFERENCES

1. Robert C. Hanlon and Carl D. Reuter, "Signal Degradation Monitoring for a Digital Transmission System", Master of Science Thesis, University of Kansas, May 1973.

2. B. J. Leon, J. L. Hammond, T. C. Huang, and R. T. Kitahara, "Performance Monitors for Digital Communications Systems Summary", Defense Communications Engineering Office, DCEO H-700-1A, June 1973.

3. B. J. Leon, J. L. Hammond, T. C. Huang, and R. T. Kitahara, "Performance Monitors for Digital Communications Systems", Defense Communications Engineering Office, DCEO H-700-1, June 1973.

4. B. J. Leon, J. L. Hammond, R. B. Bode, and W. E. Sears, "Performance Monitors for Digital Communications Systems Part II", School of Engineering, Purdue University, TR-EE 74-33, August 1974.

5. W. J. Boxleitner, "Digital Communication System Improved Offset Timing Monitor", HQ Air Force Communications Service/ EPES, Richards-Gebaur AFB, Missouri 64030, DNFS-TR-101, 31 March 1975.

6. R. P. Stibor, "Digital Communication System Offset Threshold Monitor", HQ Air Force Communications Service/EPEX, Richards-Gebaur AFB, Missouri 64030, DNSF-TR-75-102, April 1975.

7. Digital Network Systems Facility (R. P. Stibor and D. Lindberg), "AFCS Modification Proposal No. 2 to VICOM 8 Port Multiplex" (stamped PRELIMINARY), Attachment No. 2 of "TDM and CY-104 Modifications", Communications Engineering Division, Digital Network Systems Facility, Richard-Gebaur AFB (HQ AFCS/EPES), 21 August 1975.

8. B. J. Leon, J. L. Hammond, R. B. Bode, and W. E. Sears, "Performance Monitoring for Digital Communication Systems Part II", Rome Air Development Center, Griffiss Air Force Base, New York, RADC-TR-74-318 Phase Report, December 1974 (a republication of Reference 4).

9. E. R. Kretzmer, "Generalization of Technique for Binary Data Transmission", IEEE Transactions on Communication Technology, February 1966, pp 67-68.

10. R. W. Lucky, J. Salz, and E. J. Weldon, Jr., "Principles of Data Communication", McGraw-Hill Book Co., 1968.

Section 4

FUNCTIONAL DESCRIPTION EVENT PER UNIT TIME (EPUT) MONITOR

4.1 INTRODUCTION

The Phase I ATEC Digital Adaptation Study recommended that a device be developed for the collection of error rate information from the Time Division Multiplexers used in the FKV. The study further recommended the adaptation of the existing ATEC VF/DC Form A scanner by adding new circuit boards which would measure event rates and latch transient digital events. This would functionally convert the Form A scanner to an Event Per Unit Time (EPUT) Monitor. The various outputs of the EPUT would then be performance related voltages for measurement by the existing Measurement Acquisition Controller. This section provides all study and design rationale involved in the conceptualization, design, construction and testing of the Event Per Unit Time monitor.

4.2 EPUT FUNCTIONAL REQUIREMENTS

From the Phase I study, functional requirements were established and later incorporated into the statement of work. The S.O.W. requirements and clarifying rationale follow.

4.2.1 Event Count and Fixed Time Base

S.O.W. requirement: Count the number of events over a time base which may be varied and output a dc voltage as a function of event rate.

The EPUT must be able to count transient digital system events, that is, frame error pulses, to permit frame error rate calculations. It must function as a sensor element in a continually scanning, asynchronous monitoring system, hence the need for a self-contained time base. It must also be able to interface with the Measurement Acquisition Controller which uses as its standard interface, dc voltages.

4.2.2 Field Strappable Time Base

S.O.W. requirement: The time base should be field strappable at four minutes or less.

The length of time events are to be collected for generating a single data point should be related to the amount of time between queries by the computer. The rate of updating the output dc

voltage should be slightly faster than the normal scan rate so that fresh data is always available. To allow for variations in scan rate due to system size, a strappable time base is therefore desirable.

4.2.3 Overflow Indication

S.O.W. requirement: A full scale indication shall be given if overflow occurs.

To prevent an ambiguous output from the EPUT should the rate of events being counted be such as to cause an overflow of the counting circuits, the output dc voltage should be locked at some maximum value. If the output voltage was simply allowed to follow the overflow condition of the event counter the result would most probably be a lower count indication.

4.2.4 Event Rate Measurement Capacity

S.O.W. requirement: Event rates of approximately 10^{-3} and less per T1-4000 frame bits should be measured without overflow.

The purpose of the EPUT is to detect degraded operation. Therefore, it is required that event rates be quantified accurately *under degraded operation*. Saturation of event rate measurement in the region of 10^{-3} allows quantifying very badly degraded operation and, therefore, is more than adequate. Given the T1-4000 frame rate of 9.65×10^4 frames/second, the total number of frame errors which must be counted in four minutes is 23,160.

4.2.5 Input Signals

S.O.W. requirement: Accept digital input pulses of 300 nanoseconds or more in width at a rate of 9.65×10^4 pulses/second or less.

The highest rate signal to be collected by the EPUT in the FKV is main frame bit miscompares from the T1-4000. Main framing bits occur at a rate of 9.65×10^4 bits/second. The shortest pulse width to be monitored is the T1WB1 framing bit error signal that has a width of 324 nanoseconds.

4.2.6 Latch Events

S.O.W. requirement: Latch transient digital events.

Knowledge of transient occurrences are important with regard to proper interpretation of other collected data, as well as to proper interpretation of network performance in general. As an example, transient loss of T1-4000 main frame synchronization will drastically affect T1-4000 main frame error counts thus significantly altering interpretation of this anomaly.

4.2.7 Clear - Reset

S.O.W. requirement: Clear latches and event rate counters at the same time.

The purpose of this is to report data taken simultaneously in order to provide for event correlation.

4.2.8 EPUT Latch Status Output

S.O.W. requirement: Output dc voltage to indicate state of latch.

Basis for this data reporting format is the same as for the event counters, namely, the MAC interface criteria is a dc voltage.

4.3 EVENTS PER UNIT TIME - CIRCUIT DESCRIPTION

4.3.1 EPUT Overall View

The function of the Event Per Unit Time (EPUT) option is to continuously monitor digital event occurrences over a strap selected time interval and output dc voltages indicative of the occurrences during the interval. The two types of monitoring operations are: (1) counting the number of pulse occurrences and outputting a dc voltage representative of the total count over the time interval; and (2) latching the occurrence of an event during the time interval and outputting a dc voltage to indicate the occurrence. At the end of each time interval, the state of the counters and latches are stored in buffers to provide dc outputs when interrogated during the next time interval and the counters and latches are reset for the next measurement interval.

As shown in Figure 4-1, there are three circuit boards utilized to adapt the Form A scanner to an EPUT. These are the Command Board, Counter Board and Latch Board. A fourth assembly, the remote buffer is located external to the EPUT. It is used to buffer and condition the input signals to the EPUT. The Command, Counter and Latch boards are located in the Analog Scanner (ANS). One command board is required per EPUT. The number of counter and latch boards are dependent on the type and number of signals monitored. Remote buffer assemblies are located physically as close to the monitored signal source points as possible. These units are discussed in more detail in the following paragraphs. Reference is made to simplified block diagrams during board descriptions. Detailed schematics are provided in Appendix A to this report.

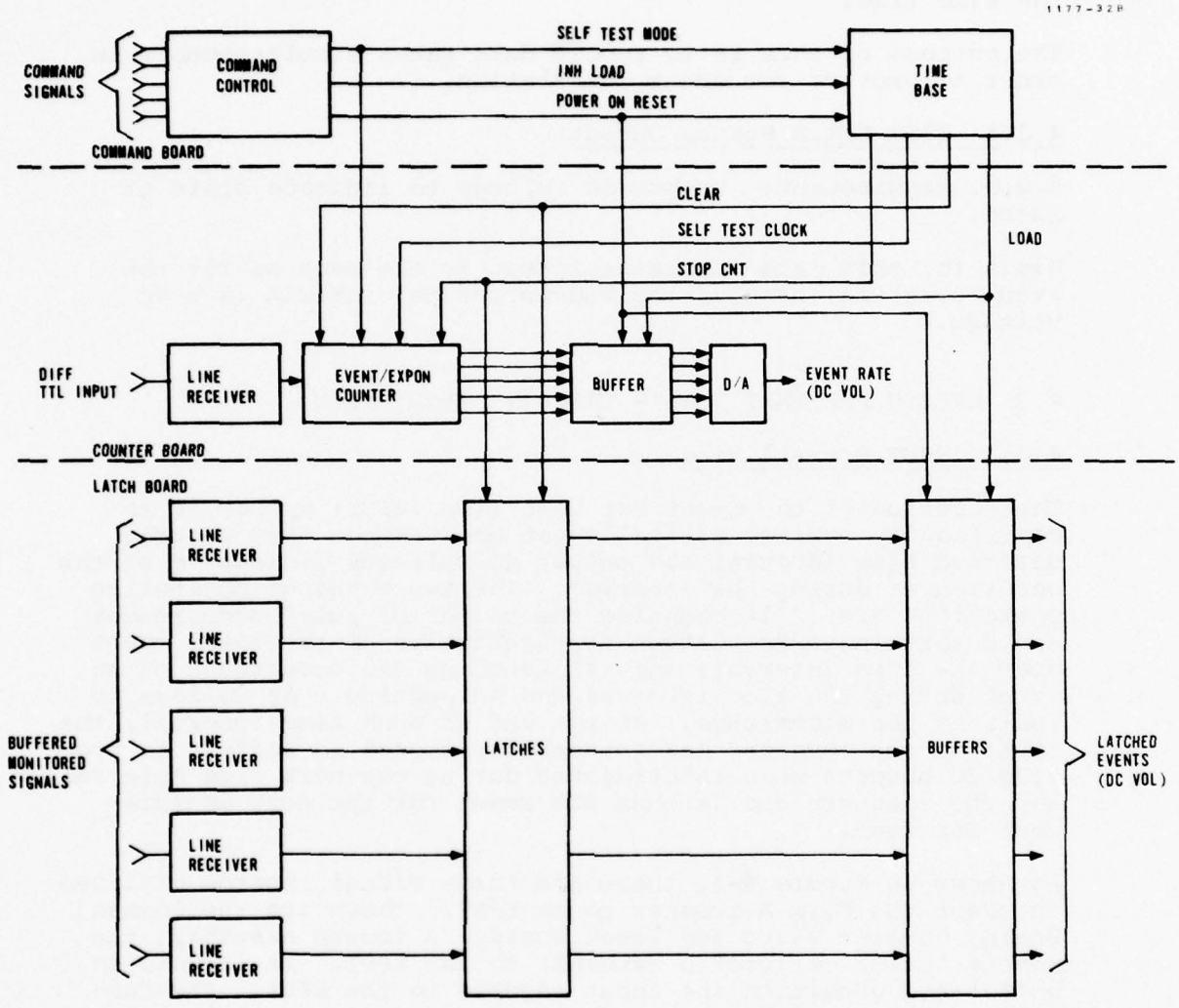

FIGURE 4-1. EPUT BLOCK DIAGRAM

4.3.2 Command Board

The Command board shown in Figure 4-2 contains two major functions. The first function is to receive control signals from the analog scanner control to provide mode control and self-test of the EPUT. The second function is the strappable time base, selectable in 1/16 minute increments to 16 minutes. One command board is required in each ANS equipped with an EPUT option.

4.3.3 Counter Board

The function of the Counter Board shown in Figure 4-3 is to count the number of event pulses received from a remote buffer assembly which occur during a time base interval and output a dc voltage representative of the total number of pulses received over the interval. At the end of each time interval a number (N), which is representative of the total count, is latched in a buffer and the counter is reset for the next measurement interval. The latched number (N) is presented to a Digital to Analog (D/A) converter which provides a dc voltage output during the next interval. The number (N) which is latched and the nominal voltage output (V_{out}) are related to the interval count as shown in Table 4-1.

TABLE 4-1. EPUT COUNTER OUTPUT

Count	N	V_{out}
0	0	0
1	1	-0.5
2-3	2	-1.0
4-7	3	-1.5
8-15	4	-2.0
16-31	5	-2.5
32-63	6	-3.0
64-127	7	-3.5
128-255	8	-4.0
256-511	9	-4.5
512-1023	10	-5.0
1024-2047	11	-5.5
2048-4095	12	-6.0
4096-8191	13	-6.5
8192-16383	14	-7.0
16384-32767	15	-7.5
32768 and above	16	-8.0

It can be seen that N is related to the greatest power of 2 which has not been exceeded.

N is defined by:

$N = 0 \quad Count = 0$

$N = n+1 \quad 2^n \leq count < 2^{n+1} \quad 0 \leq n \leq 14$

$N = 16 \quad 2^{15} \leq count$

One counter circuit is contained on each counter board.

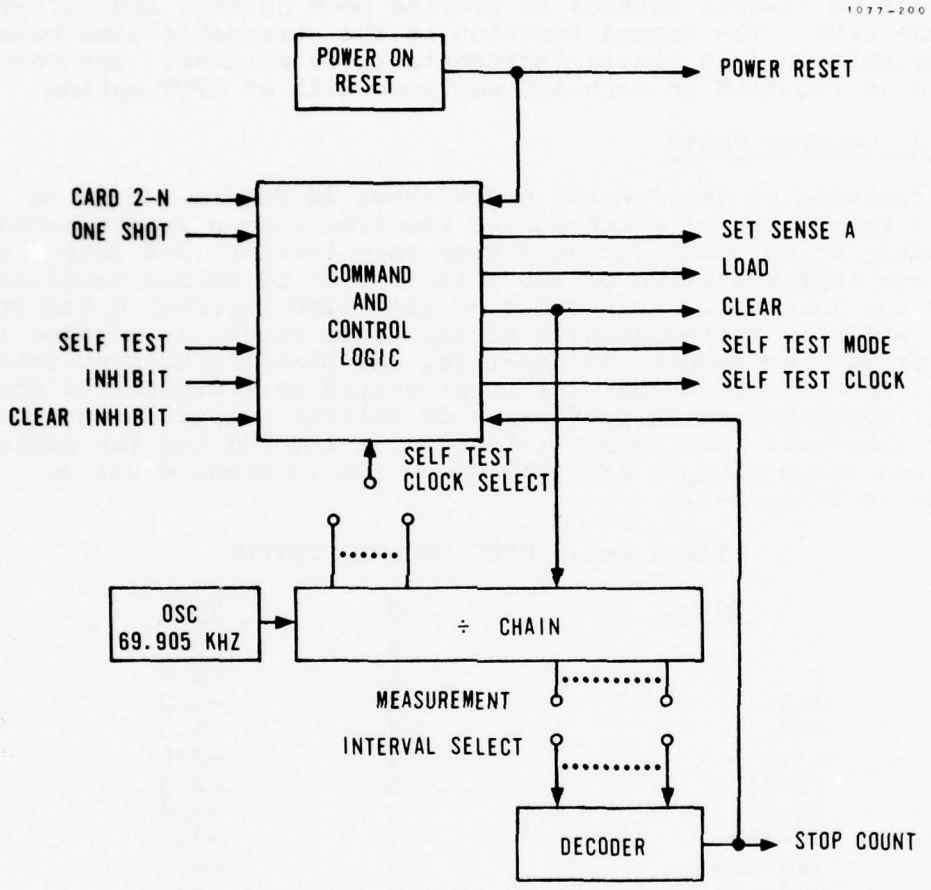

FIGURE 4-2. COMMAND BOARD

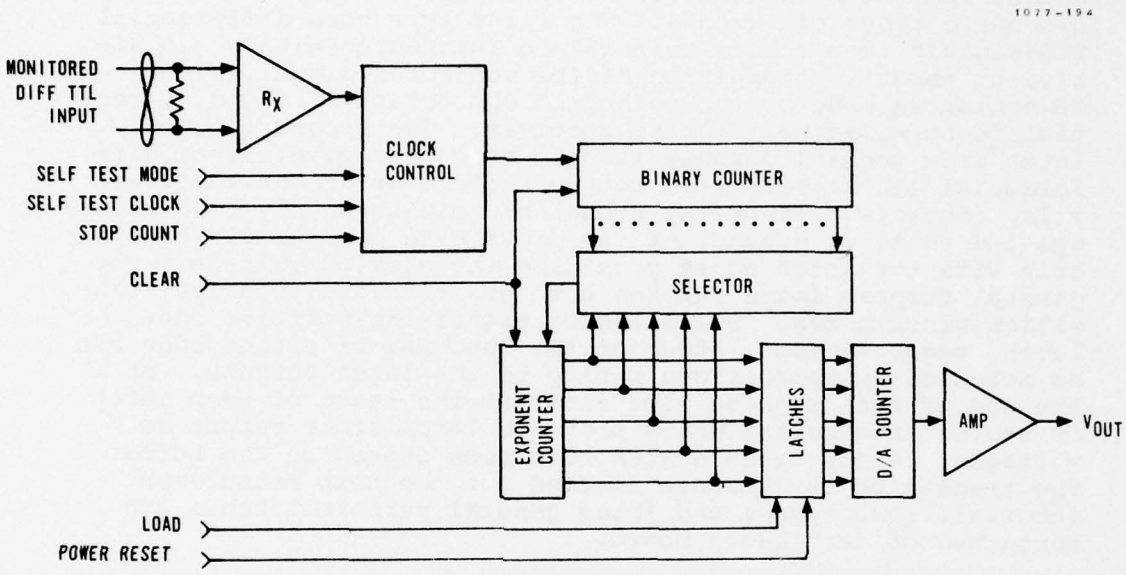

FIGURE 4-3. COUNTER BOARD

4.3.4 Latch Board

The function of the latch board shown in Figure 4-4 is to detect and latch the occurrence of signal changes. There are two basic types of latches. The first type uses differential TTL signals from remote buffers and latches on either a positive or negative transition of the monitored signal. The selection is made by the method of connection of the differential input wired pair to the receiver. The second type of latch is a general purpose latch. It can receive either differential TTL signals from remote buffers or it can receive relay contacts. The relay signal can either supply a dc voltage (+5 volts or ground) or can provide an open or closed circuit with the latch board providing the driving voltage. The general purpose latch latches both positive and negative transition occurrences. Selection of either the positive edge latch, negative edge latch, or the latching of either edge can be selected by appropriate wiring to the latch outputs. At the end of the selected time interval the state of each latch is stored in a buffer which provides latch state output dc voltages. After latch states have been stored in the buffer the transition latches are cleared for the next measurement interval. Two type 1 and three general purpose latches are contained on each latch board.

4.3.5 Remote Buffer

The function of the remote buffer shown in Figure 4-5 is to nonintrusively attach to TTL signals in the equipment being monitored and drive the monitored signal to the EPUT. Two monitor drivers are contained in each remote buffer. Bridgeon attachment to the TTL monitored signal is provided by high input impedance comparators which compare the monitored signal to a 1.4 volt reference with ±0.2 volts hysteresis incorporated around the reference. Power for the remote buffer is from the ANS power supply.

4.4 OPERATIONAL FUNCTIONS AND COMMANDS

The EPUT is functionally controlled by commands which are normally issued by the A scanner control boards to activate relay closures. (Refer to schematics in Appendix A.) These commands fall into three operational categories: Inhibit Load, Clear Inhibit, and Self-Test. In normal operation, when power is applied to the ANS all EPUT control flip-flops, event counters, latches and the time interval counter are reset by the power clear circuitry. Upon expiration of the power clear signal, the normal mode of continuous time interval measurements is entered. At the expiration of each time interval the control signal *STOP COUNT* is activated to inhibit inputs to the event counters and the latches while the buffers are being loaded. After the buffers are loaded the event counters,

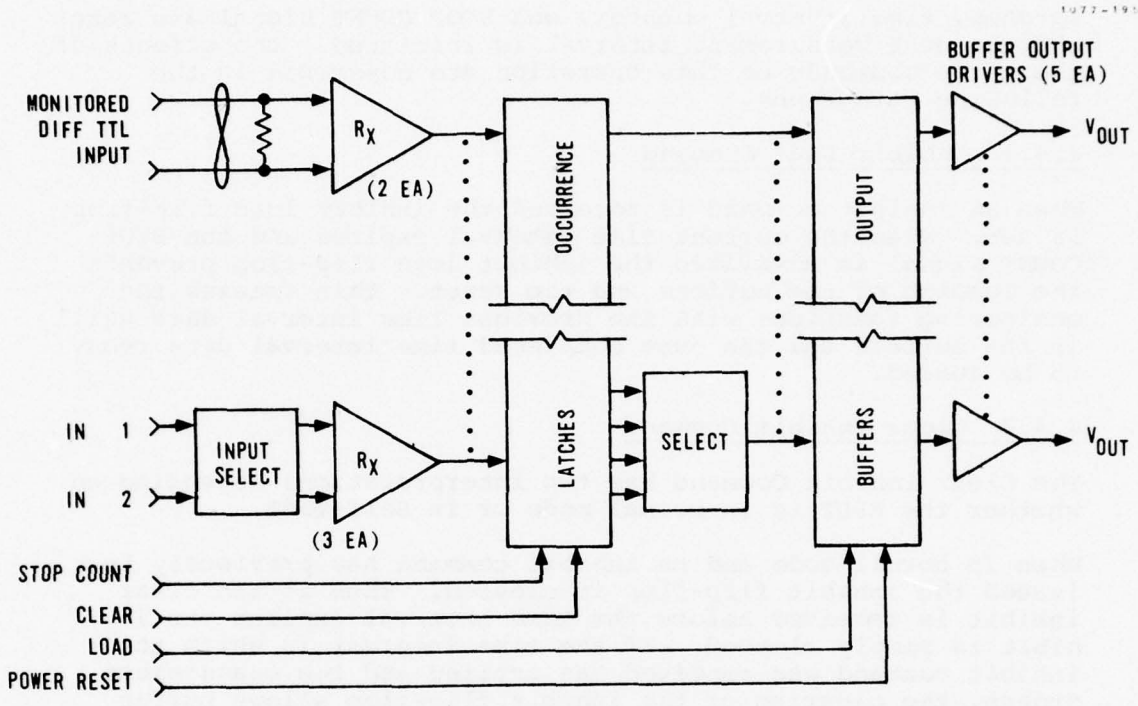

FIGURE 4-4. LATCH BOARD

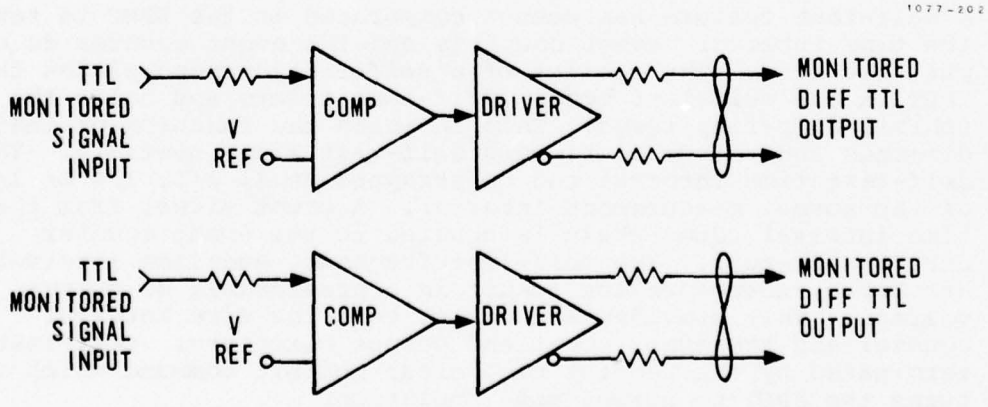

FIGURE 4-5. REMOTE BUFFER

latches, time interval counter, and STOP COUNT signal are reset and the next measurement interval is initiated. The effects of the three commands on this operation are described in the following paragraphs.

4.4.1 Inhibit Load Command

When an inhibit command is received the inhibit load flip-flop is set. When the current time interval expires and the STOP COUNT signal is activated the inhibit load flip-flop prevents the loading of the buffers and the reset. This freezes the monitoring functions with the previous time interval data still in the buffers and the just completed time interval data ready to be loaded.

4.4.2 Clear Inhibit Command

The Clear Inhibit Command has two interpretations depending on whether the EPUT is in normal mode or in Self-Test.

When in normal mode and an inhibit command has previously been issued the inhibit flip-flop is cleared. Thus if the clear inhibit is received before the time interval expires the inhibit is simply cleared. If the time interval in which the inhibit command was received has expired and the measurement frozen, the clearing of the inhibit flip-flop allows buffer storage and reset to occur and the next measurement interval to start.

When in Self-Test the receipt of Clear Inhibit immediately terminates Self-Test and begins the normal measurement mode.

4.4.3 Self-Test Command

A self-test feature has been incorporated in the EPUT to test the time interval, event counters and the event counter dc output circuitry. The receipt of a self-test command places the EPUT in the self-test mode. Self-test resets and holds the inhibit flip-flop reset. This inhibits the function of inhibit commands and allows continuous self-test time intervals. The self-test time interval can be strapped at 1, 1/2, 1/4 or 1/8 of the normal measurement interval. A count signal from the time interval count chain is applied to the event counter during self-test. The self-test frequency and time interval are known, therefore the result is a predictable dc output voltage. This provides a check of both the time interval counter and the event count and output circuitry. Self-test is terminated by the receipt of a clear inhibit command which returns the EPUT to normal mode operation.

4.5 FIELD TEST RESULTS

Operation of the two EPUT units located at Ft. Huachuca and Site Sibyl during field tests was satisfactory except for two problems. The first problem involving the EPUT at Sibyl was probably procedural rather than hardware related. The outputs of the counter boards involved in counting T1-4000 frame bit errors for both normal and standby units were resetting to 0.5 volt instead of zero volts. This is equivalent to having a count of one in the counters. This problem occurred on only one occasion, and because it was not critical to tests in progress at the time, it was not immediately corrected. It was never observed to occur again after the day it was first noted.

It is theorized that the problem occurred because phasing of the differential input signals to the input buffer amplifiers on the counter boards had been reversed. Tests were in progress at the time that required that T1-4000 frame error signals to the EPUT be disabled. This was accomplished by lifting the differential signals at the remote buffer assembly. If the leads had been reconnected such that signal high and low were reversed, it is possible that occurrence of the Stop Count signal could have acted as a strobe to generate a negative-going edge into the event counters. This would be interpreted as an event occurrence and would have placed a count of one in the counter. The Load pulse would then transfer this count to the latch in front of the D/A converter with the result that the output would appear to be resetting to 0.5 volt instead of zero.

The second problem involved a counter board in the EPUT at Ft. Huachuca. The discrepancy was first noted when the EPUT failed self-test. It output the wrong voltage at completion of the self-test interval. The trouble was traced to a connector problem. The board edge connector was cleaned and inserted and retracted several times to ensure it was seated properly. Operation of the EPUT was all right for the remainder of field tests.

As discussed in the Field Test and Evaluation Report, the EPUT time base was changed during field test operations. Initially, the EPUTs were strapped for a two minute sampling time interval. Tests indicated that latched data was being lost because the EPUT's time base relative to the DATEC system's normal scan time (approximately four minutes) was too short. The strapping of both EPUTs was changed in the field to obtain a 3-1/2 minute time base. Following the restrapping, the operation of the EPUTs was satisfactory. No lost data was subsequently observed, and the EPUTs were found to be highly effective in monitoring and latching transient events.

Section 5

SOFTWARE

This section describes the software development process used in the Digital ATEC Adaptation Study, Phase II. Structured programming is discussed in general followed by a description of the techniques selected for this project. Following this is a description of all phases of development including design, code, module test, integration, development monitoring, in-plant test and field test. The discussions include a description of the techniques used, their effectiveness and problems encountered. Concluding, and serving as a summary of this section, are several conclusions and recommendations.

5.1 STRUCTURED PROGRAMMING

With the realization that the major part of future communication systems will be software, Government agencies have been stressing the use of better techniques in the software development process. RADC has been a leader in this area and with the aid of private companies has developed a set of guidelines in the use of structured programming techniques for software development. Through the Statement of Work, RADC directed Honeywell to use such techniques in the development of the software adaptations for Digital ATEC. Section 1.3 of Annex II states that, "The software developed shall be in accordance with Annex 3." Annex 3 of the Statement of Work references sections of RADC Computer Software Development Specification CP-07877-96100. From this specification and a thorough literature search on structured programming, Honeywell chose the following.

5.1.1 Chief Programmer Team

A major problem associated with previous software development projects was lack of communications between programmers. There did not seem to be any one person knowledgeable about the entire program, only individuals with knowledge of their particular program. This led to serious interface problems during system integration and sometimes complete redesign, resulting in schedule slippages and irate customers.

The chief programmer team concept seemed to be a step in the right direction for solving these problems. The team consists of the following members:

- Chief Programmer
- Backup Programmer
- Librarian
- Support Programmer

Following is a description of each team member's responsibilities.

5.1.1.1 Chief Programmer

The chief programmer discharged managerial responsibilities for the entire development effort. Managerial responsibilities are identified for both the chief programmer's organization (internal) and the user or customer organization (external). The internal managerial responsibilities consist of both organizational and operational responsibilities:

1. Organizational - The chief programmer is the immediate manager for the backup programmer, librarian, and two or three support programmers. Specialized team support may require that the chief programmer manage two or three additional programmers for relatively short periods. He must maintain daily contact with other members of the team to circulate and evaluate ideas on the status of system development. The backup programmer must be kept informed of all decisions affecting project status.

2. Financial Responsibility - The chief programmer is responsible for establishing, monitoring and meeting cost and schedule goals for the entire development effort.

3. Operational - The chief programmer will:

   a. Prepare schedules and budgets with assistance of backup programmer or project manager, monitor progress, and reschedule tasks as necessary.

   b. Identify project resource requirements, plan the acquisition and allocation of these resources.

   c. Plan, schedule and distribute work assignments for team members.

   d. Establish and enforce project standards.

   e. Supervise closely the development of the system (design reviews, critiques of test plans, inspection of test results).

f. Plan and supervise development of computer programs and documentation.

4. User/Customer Relationship - The chief programmer will:

   a. Participate with customer's technical representatives in the definition of requirements and choices of solutions.

   b. Prepare and deliver written and oral reports as required to inform customer and customer management on project status and problems.

He will discharge technical responsibilities for the entire development effort through the following activities:

1. Confer with the team backup programmer in the formulation and implementation of concepts, design, procedures and programs for the system under development.

2. Identify and investigate complex problems, postulate solutions and innovate algorithms as necessary.

3. Design and code the software control modules and other similarly critical segments of the system.

4. Read and constructively criticize program source code produced by team members and provide technical direction.

5. Maintain an awareness of programming technology and tools, and incorporate these into project development where appropriate.

5.1.1.2 Backup Programmer

The backup programmer will assist the chief programmer in discharging management responsibilities. No direct managerial responsibility is assigned, but the backup programmer is expected to provide technical leadership through daily contact with other members of the team to circulate and evaluate ideas on and status of system development. Specific ways backup programmer assists the chief programmer are:

1. Planning project requirements and allocating resources.

2. Defining requirements and selecting solutions with the customer.

3. Reviewing technical progress and strategy in regular contact with customer counterpart.

4. Preparing reports on project status for higher levels of management both internal and customer.

5. Substituting for or participating with the chief programmer in giving presentations to higher levels of management.

6. Assisting the enforcement of project standards.

The backup programmer will assist the chief programmer in discharging technical responsibilities through the following activities:

1. Confer with the chief programmer in the formulation and implementation of concepts, design, procedures and programs for the system under development.

2. Investigate complex problem areas as assigned by the chief programmer, postulate solutions and analyze trade-offs.

3. Assist the chief programmer in the design and coding of critical segments of the system and develop major system programs assigned by the chief programmer.

4. Read and review the code of other team members, provide technical direction.

5. Integrate and check out modules.

6. Deliver presentations on technical subjects and project status to internal and customer management, as appropriate.

7. Maintain an awareness of programming technology and tools, evaluate their applicability to the system under development, and recommend their use as appropriate.

5.1.1.3 Librarian

The librarian is responsible for the creation and maintenance of project records. In discharging this responsibility the librarian will supply input to, or operate various hardware devices. Specific responsibilities are:

1. Establish, with the chief programmer, the project files and procedures for maintenance of the files.

2. Identify and obtain supplies and facilities necessary for file maintenance.

3. Inform team members of the procedures for submitting changes to the files.

4. Carry out change requests in an orderly and timely fashion.

5. Inform team members of status of all work requests in progress.

6. Validate project files as required. Identify procedural errors and correct if possible.

7. Maintain logs and retention schedules for project files.

8. Prepare various status and statistical reports.

9. Complete forms/reports to support the collection of management data.

10. Obtain additional clerical assistance (for example, keypunch support) as required.

11. Obtain other services as required to insure the proper working order of equipments utilized during the course of the project.

12. Perform other support duties as assigned. For example, type project documentation, order supplies, forward telephone messages.

5.1.1.4 Support Programmer

The support programmer is responsible for the production of computer programs. Specifically he will perform the following tasks:

1. Develop plans and schedules for the assigned program.

2. Review technical progress, work product and commitments with the chief programmer.

3. Estimate resource requirements such as equipment and computer time.

4. Analyze program objectives, develop or modify functional specifications as necessary.

5. Design and implement a feasible and efficient program to meet objectives.

6. Submit computer runs to secretary/librarian and utilize computer output as filed and prepared by librarian.

7. Learn and employ the specific standards on the project for use in top-down structured programming technology.

8. Identify and recommend design changes to hardware and software.

9. Prepare required program documentation.

5.1.2 Top-Down Design

Top-down design is a technique in which the Statement of Work or program specification is used to arrive at a set of initial functions that the software is to perform. Modules are designed to implement these functions and in the process new functions, usually of a simpler nature, are defined. The process is continued until no new functions are defined. The result of this process is a set of modules that together perform a complicated function but individually are rather easy to code, debug, test and document.

Following is a list of ways that a program can be modularized:

a. Functional. The case where a module performs a single, discrete, logical transformation.

b. Hierarchical. The case where a program is modularized on the basis of a hierarchy of the functions of the program.

c. Communicational. The case where a program is modularized by grouping input and output activities in the same module.

d. Multi-Use. The case of modularizing a program by logically grouping activities which are used several times in a program. This type of module usually will require a control data element to be passed to it to determine which of various types of processing is to be done.

e. Sequential. The case where a program is modularized on the basis of the time sequence of the operations of the program; that is, input data, process data and output data.

f. Coincidental. The case of modularizing in a rather arbitrary way (for example, each 200 lines constitute a module, totally disregarding functions).

The top-down approach to design usually leads to functional modularization. This consideration was almost always used in module determination for the Digital ATEC software because it led to uncomplicated modules which could be understood not only by support programmers but nonprogrammers as well.

5.1.3 Top-Down Testing

In top-down design the higher level or more complicated modules are designed first. They reference the lower level or less complicated modules. Top-down testing is a technique of checking out the higher level modules even though the lower ones are not yet coded. In this process, the uncoded modules are replaced by dummy programs called stubs which are coded to print out a message and other pertinent data when they are called to demonstrate that the module under test is working properly. When the

module represented by the stub is coded, it is incorporated into the system and checked out with the previously tested modules. By building up the system by testing new modules in the presence of previously tested modules, interface problems are detected and corrected early in the development process. This simplifies the system integration process considerably.

5.1.4 Walk-Throughs

The concept of walk-throughs, or informal reviews, has become an integral part of SP as a means of promoting high quality software. In its basic form, a programmer reviews his design or code with a peer by simply walking-through the segment or module. This simple technique has proven many times over, that the process of explaining to someone else the steps of a design or code will by itself uncover bugs that the programmer has overlooked.

A key aspect of the structured walk-through concept lies in its connection to top-down design and development. At a very early stage in a programming project, the programmer should be able to show to his peers, or to other members of his team, his design of the entire program. A great deal of the program may be in the form of dummy modules, but the overall logic and structure should be present. The purpose of the walk-through is to ensure that the overall logic of the program is correct, assuming that the dummy modules, when implemented, will work correctly. Rather than worrying about the details of low-level modules, the team concentrates its efforts, at the beginning of the project, on a review of the high-level structure of the program, thus exposing any major flaws that the programmer may have overlooked. This process then continues downward through the program hierarchy, as the top-down design progresses.

5.1.5 HIPO (Hierarchy-Input-Process-Output) Diagrams

Instead of traditional flow diagrams, Hierarchical-Input-Process-Output (HIPO) diagrams are used to show data flow through the program. After the structural design is complete, the HIPO diagrams can be used to show the detailed functions of each module and to provide a visual table of contents of the structure of the program. These HIPOs are generated during the design phase and are used as the primary documentation for the system design review.

A typical HIPO package contains a visual table of contents ("H" of HIPO) and the process charts ("IPO" of HIPO). The H-charts (Figure 5-1) present a top-down breakout of all the modules. The IPO charts (Figure 5-2) document the functions of each module. They are easy to read since they are entered at the top and exit at the bottom. The data transfer arrows show inputs to and outputs from the processing block. The flow of the processing always enters at the top of the process block and leaves from the bottom block. If control is passed to a lower level diagram, it

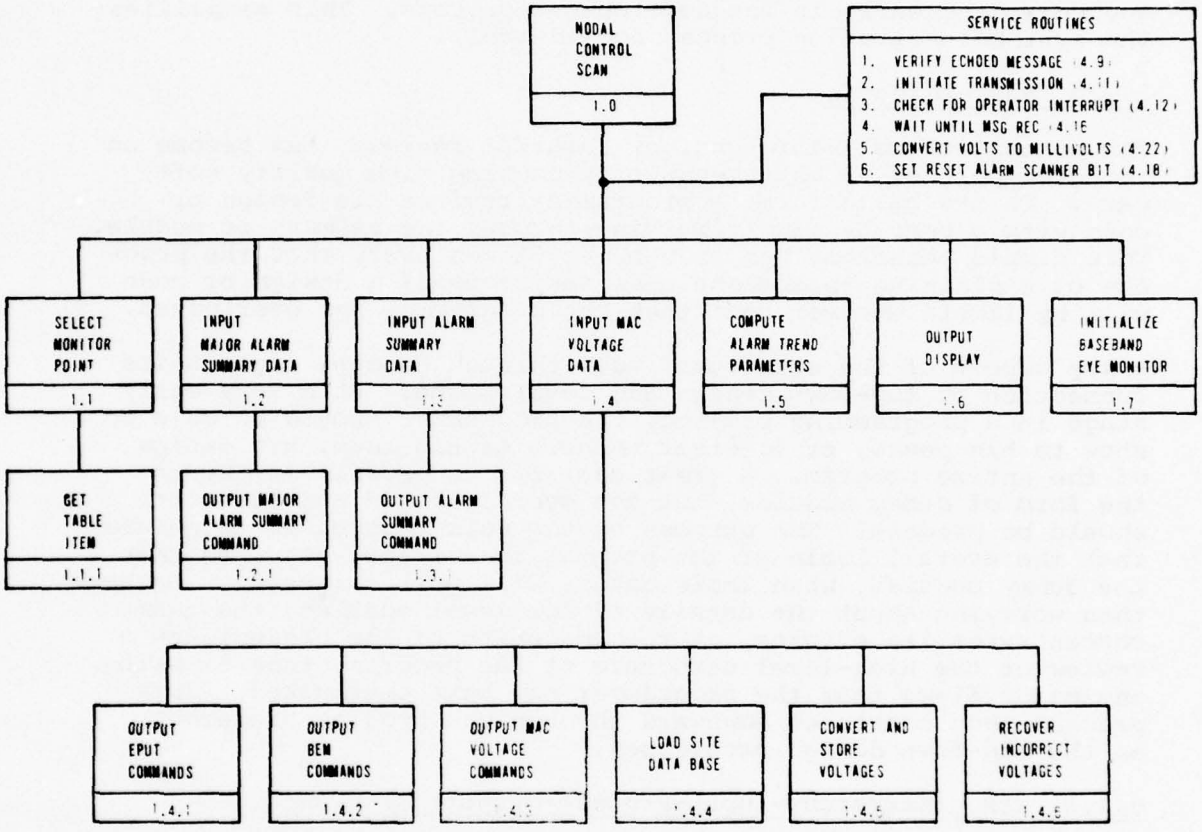

FIGURE 5-1. HIERARCHY DIAGRAM

HIPO NO.: 1.3 AUTHOR: DTD DATE: 7/27/76

TITLE: Input Alarm Summary Data

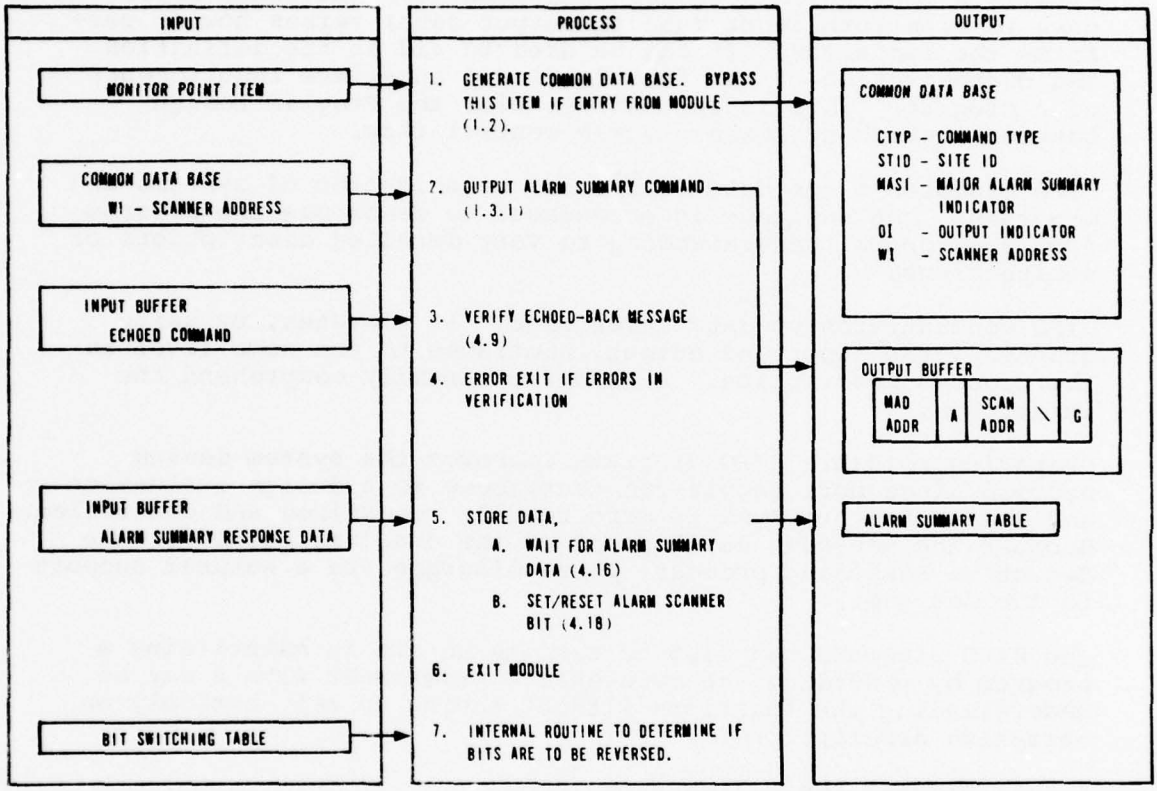

FIGURE 5-2. HIPO DIAGRAM

is always returned from the lower level diagram to the point of exit of the higher level diagram. Note how this HIPO diagram shows the nesting of functions within a specific process, thus reflecting the basic concepts of the structured design.

HIPO is a tool which stresses functions (that is, what a program does to transform input data to output data) versus how it performs the functions. It can be used to aid in the definition and documentation of the functional and interface requirements of a program. This is in contrast with the Program Design Language, which stresses program control flow.

HIPO promotes a top-down functional organization of systems and programs. The designer is encouraged to decompose the program from the general understanding to very detailed descriptions of subfunctions.

HIPO concentrates on data interfaces. It elevates, by using graphics, the input and output interfaces to the same level as the process description. A reader can easily comprehend the interfaces.

Preparing readable HIPO diagrams improves the system design process since more people can contribute to a design evaluation and the design progress is more readily recognized and controlled. Because the top-down development of the diagrams parallels the deductive reasoning process, these diagrams are a natural support to the designer.

The HIPO diagrams can also be used as an aid in maintaining a program by providing the maintenance programmer with a way of understanding the functions without having to rely entirely on narrative descriptions.

5.1.6 Program Design Language (PDL)

In a program design language, program functions are expressed in English statements. This approach to program design has several advantages. It replaces flow charts for the system documentation with easy to read descriptions. Moreover, there is a natural transition from the top-down design expressed in this manner to the actual top-down implementation process.

There are two forms of program design language, differing in complexity, pseudo code and playscript. Pseudo code is more structured in that it expresses the design only in a pre-selected set of structured program constructs such as If-Then-Else, Do While, Case and Do Until. This language is very good if a form of structured code available in higher order languages is going to be used. The playscript form is less structured in that it uses English statements in a well organized form to express a design. It is more applicable for programs to be coded in machine language in that it expresses the design while not dictating how it is to be coded. An example of the playscript form is shown in Figure 5-3.

PLAYSCRIPT

1.6.1.2 PROCESS T1-4000 SWITCH ITEM ($SPTSF)

This module processes T1-4000 switch display generator items for the system overview display.

1. Call ASBS to determine if major alarm set.

2. If set:

   A. If scanner bit number equals highest major alarm (FALT)

      1) Set blink indicator (BLIN).

   B. Set direction indicator (DIR=B).

   C. Set color indicator (COLR)=R.

   D. Call SFMS to format field and output to field file (DF).

   E. Exit module.

3. Call ASBS to determine if minor alarm set.

4. If set:

   A. Set direction indicator (DIR)-B. (Both)

   B. Set color indicator (COLR)=R. (Red)

   C. Call SFMS to output field to field file (DF).

   D. Exit module.

FIGURE 5-3. PLAYSCRIPT EXAMPLE

5.1.7 Program Support Library

A Program Support Library (PSL) serves as a repository for data necessary for the orderly development of computer programs using structured programming technology. The data exists in two forms:

- "Internal data" is stored in machine readable form accessible by computer.
- "External data" is stored in hardcopy (human readable) form in project notebooks.

Included with a PSL are the necessary computer and office procedures for manipulating this data.

The purpose of a PSL is to support the program development process. This involves the support of the actual programming process and the management of the process.

Support of the programming process involves support of the design, coding, testing, documentation and maintenance of computer programs and the associated data-base definitions. A PSL provides this support through:

- Storage and maintenance of programming data.
- Output of programming data and related control data.
- Support of the compilation and testing of programs.

Support of the management of the programming process also involves the storage and output of programming data. In addition, it involves:

- Collection and reporting of management data related to program development.
- Control over the integrity and security of the data stored in the PSL.
- Separation of the clerical activity related to the programming process.
- Archive of program development, to use as basis for future work.

A PSL supports an approach in which people work on a common, visible product rather than on independent pieces. The programmers communicate through this product in carrying out programmer and clerical interface activities. A PSL permits a programmer to exercise a wider span of detailed control and reduces explicit communication requirements. This makes it easier to bring new personnel on-board and to shift programmers from one part of the project to another.

A full- or part-time librarian is responsible for maintaining the internal and external libraries, but the programmers are responsible for their contents. This structure of responsibility permits standardization in project record-keeping and insures that the most current version of the system in machine readable form corresponds to the hard copy listing in the library.

5.2 SOFTWARE DESIGN

The purpose of this program, as the name implies (ATEC Digital Adaptation Study), is to adapt existing ATEC equipments and software to digital communications technology. From the previous study phases and the statement of work for Phase II, the initial software functions were determined to be:

a. Modify existing PATE software as required to accomplish Digital ATEC functions.

b. Write new software to perform nodal control functions for a digital system.

c. Write new software to provide operator interaction to support the nodal control functions.

5.2.1 PATE Software Modifications

The PATE system consists of a 316R computer with 16K of core memory and the ability to interface with a Caelus disk, an ADDS display, a nucleus subsystem through a 150 Baud data line controller and a Signal Parameter Converter drawer (see Figure 5-4). The Signal Parameter Converter is a computer controlled device used for circuit selection through A (bridge on) or C (break) type scanners and signal conversion as required by the particular software analysis task currently in core.

PATE software provides a task oriented operating system in which tasks are loaded and executed from queues. Tasks are scheduled from a scan sequencer, by the operator through operator interaction or by other tasks. The software also provides interrupt processing, real time clock processing, I/O for all interfaces and power fail recovery. The application tasks provide performance assessment and trend analysis on the following type circuits:

a. VF - 100 to 4000 kHz

b. DC - teletype

c. VFCT - frequency shift keying

d. FDM baseband.

Out-of-service tests such as impulse noise measurements, envelope delay, phase jitter, and net loss are available through the out-of-service application software scheduled and run at operator request.

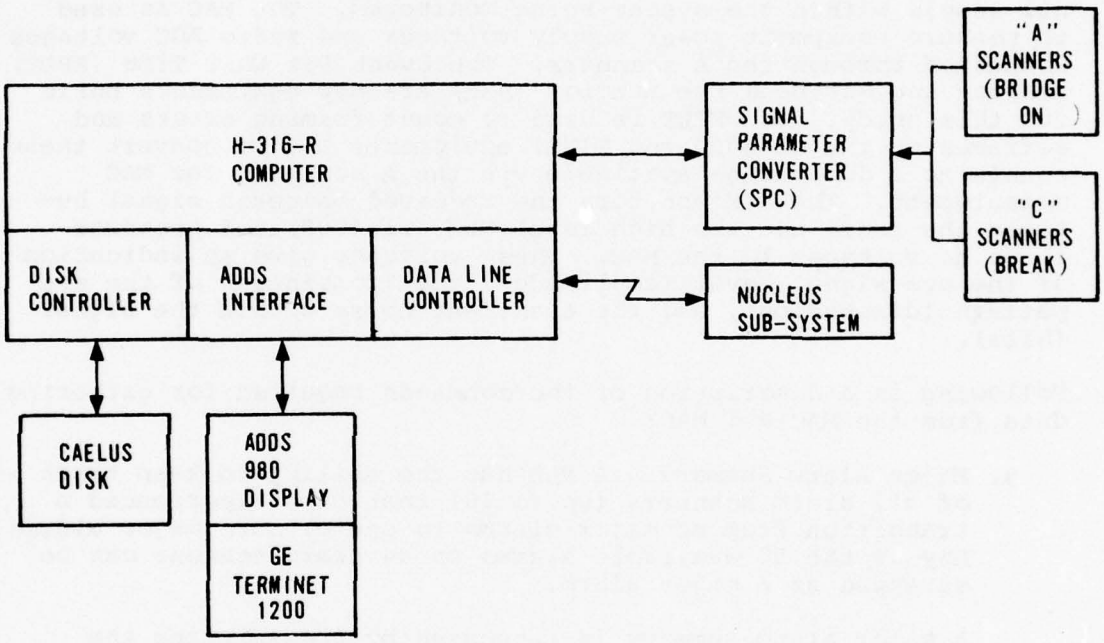

FIGURE 5-4. PATE HARDWARE ELEMENTS

Figure 5-5 shows the modifications made for the Digital Adaptation Study. The data line controller port is still used only it now interfaces the computer with the Master Alarm Display (MAD) and the Measurement Acquisition Controller (MAC) through a party line configuration.

The MAD is used for monitoring alarms and status on equipment at all levels within the system being monitored. The MAC is used to measure equipment power supply voltages and radio AGC voltages connected through the A scanners. The Event Per Unit Time (EPUT) Monitor and Baseband Eye Monitor (BEM) are new equipments built for this study. The EPUT is used to count framing errors and reframes on the T1-4000 and T1WB1 equipments and to convert these counts to a dc voltage available via the A scanners for MAC measurement. The BEM monitors the received baseband signal between the radio and the high level MUX (T1-4000) and presents three dc voltages to the MAC. These voltages give an indication of the eye signal level (amplitude), the "noisiness" of the eye pattern (dispersion), and the transient noise within the signal (hits).

Following is a description of the commands required for gathering data from the MAC and MAD:

a. Major Alarm Summary. A MAD has the ability to keep track of all alarm scanners (up to 10) that have experienced a transition from no major alarms to one or more major alarms. Any of the 50 available alarms on an alarm scanner can be strapped as a major alarm.

   A major alarm summary is requested by transmitting the following character stream to the MAD:

   Ⓢ a M\G

   where

   Ⓢ is a control S character which initializes the MAD.

   a represents the MAD address.

   As the MAD receives characters following the Ⓢ it echoes them back to the transmitting device. Upon receiving the G character the MAD transmits one character per alarm scanner representing its major alarm status. The number 1 indicates that the alarm scanner has one or more major alarms. The letter O indicates that the alarm scanner has no major alarms. The data is terminated with a backslash and a checksum character.

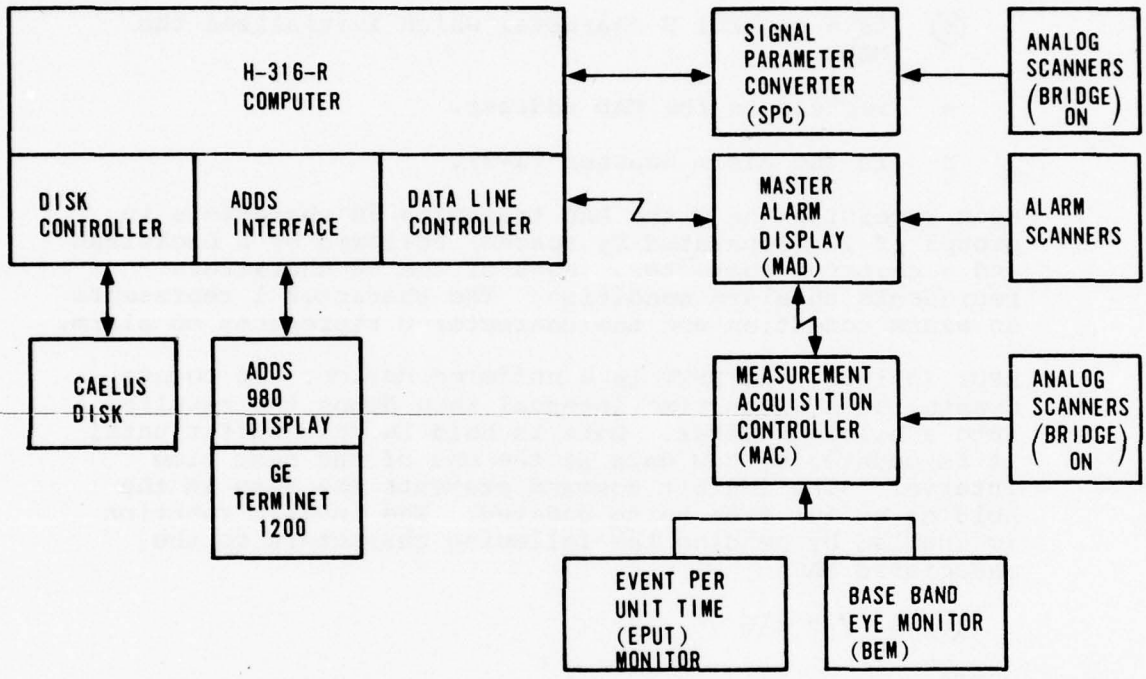

FIGURE 5-5. DIGITAL ATEC HARDWARE ELEMENTS

b. Alarm Summary. The MAD also has the ability to send the status of all 50 alarms on a particular alarm scanner. This is requested by sending the following characters:

Ⓢ a A n\G

where

Ⓢ is a control S character which initializes the MAD.

a represents the MAD address.

n is the Alarm Scanner (1-9).

Upon receiving the G the MAD transmits 50 characters in groups of 10 (separated by spaces) followed by a backslash and a checksum character. Each of the 50 characters represents an alarm condition. The character 1 represents an alarm condition and the character 0 represents no alarm.

c. EPUT Inhibit. An EPUT is a buffered device. It counts events for a given time interval then dumps the results *into a holding buffer.* Data is held in this buffer until it is updated by new data at the end of the next time interval. The inhibit command prevents the data in the holding buffer from being updated. The inhibit function is enabled by sending the following characters to the associated MAC:

Ⓢ a / 9 1\G

where

Ⓢ is a control S character which initializes the MAC.

a is the MAC address.

9 represents card nine of the scanner drawer. This is the EPUT control card.

1 is interpreted by the control card as the inhibit function.

All characters after the Ⓢ are echoed back to a transmitting device and there are no characters returned after the MAC receives the G.

d. Clear EPUT Inhibit. The clear inhibit function removes the effects of the inhibit command by allowing the holding buffer in the EPUT to be updated. The inhibit is removed by sending the following characters:

Ⓢ a / 9 2\G

where

Ⓢ is a control S character which initializes the MAC.

a is the MAC address.

9 represents card nine of the Scanner Drawer, the *EPUT control card.*

2 is interpreted by the EPUT control card as the clear inhibit function.

e. MAC Measurement (single channel). In order to make a voltage measurement on a single channel the following characters are sent to the MAC:

Ⓢ a D1 / cr\G

where

Ⓢ is a control S character which initializes the MAC.

a is the MAC address.

D1 is recognized by the addressed MAC as a dc voltage measurement command.

cr is the scanner card and relay to which the voltage is connected.

All characters following the Ⓢ are echoed back to the transmitting device. After receiving the G character the MAC closes the addressed relay and makes the voltage measurement. It then transmits the results in the following ASCII format:

Cr Lf 00 c r ± $X_1X_2 \cdot X_3X_4X_5V$

where

Cr is a carriage return character.

Lf is a line feed character.

00 c r is the scanner, card, and relay address.

$\pm X_1X_2 \cdot X_3X_4X_5V$ is the measured voltage returned as three significant figures. X_1X_2 are always present. X_5 is only present if significance requires it.

f. MAC Measurement (multiple channel). The MAC has the ability to automatically step through a number of voltage measurements. This is requested by sending the following characters:

Ⓢ a D1 / c_1r_1 / c_2r_2\G

where

Ⓢ is a control S character which initializes the MAC.

a is the MAC address.

D1 is recognized by the addressed MAC as a DC voltage measurement command.

c_1r_1 is the scanner card and relay of the first voltage to be measured.

c_2r_2 is the scanner card and relay of the last voltage to be measured.

All characters following the Ⓢ are echoed back to the transmitting device. After receiving the G character the MAC automatically measures each voltage from c_1r_1 to c_2r_2 and sends a set of characters representing the voltage as defined in e above.

g. BEM EPUT Inhibit. The BEM has been designed to operate as an option to the MAC. This means that the MAC serves as the interface for control information between the BEM and the transmitting device. The BEM has its own EPUT counter used for counting eye hits. In order to inhibit this EPUT the following characters must be sent to the MAC:

Ⓢ a 0 1 M 1\G

where

Ⓢ is a control S character which initializes the MAC.

a is the MAC address.

0 1 is recognized by the MAC as an option address.

M 1 is data sent to the BEM by the MAC. It is recognized by the BEM as the EPUT inhibit command.

All characters following the Ⓢ are echoed back to the transmitting device. After receiving the G character the MAC sends the M1 data to the BEM. If the BEM accepts the data the MAC transmits a + character to the transmitting device. If the BEM is not operable or for some reason does not accept the data, the MAC transmits the character Q to the transmitting device.

h. BEM Switch. The BEM has the ability to make eye measurements on any one of nine basebands. To switch the BEM to a particular baseband the following characters are sent to the MAC:

Ⓢ a 01 M0 In\G

where

Ⓢ is a control S character which initializes the MAC.

a is the MAC address.

01 is recognized by the MAC as an option command.

M0 is recognized by the BEM as the initialize mode.

In is recognized by the BEM as the command to switch the input to channel n.

The handshaking sequence between the MAC and BEM and the returned characters to the transmitting device are the same as in g above.

5.2.1.1 Data Line Controller (DLC) Software

The original PATE DLC software for communicating with the nucleus system was replaced with new code for communicating with the MAC and MAD devices. Figure 5-6 describes how the software interfaces with the data line controller. The DATEC software loads the output buffer with the appropriate command characters as described above along with a count of the number of characters

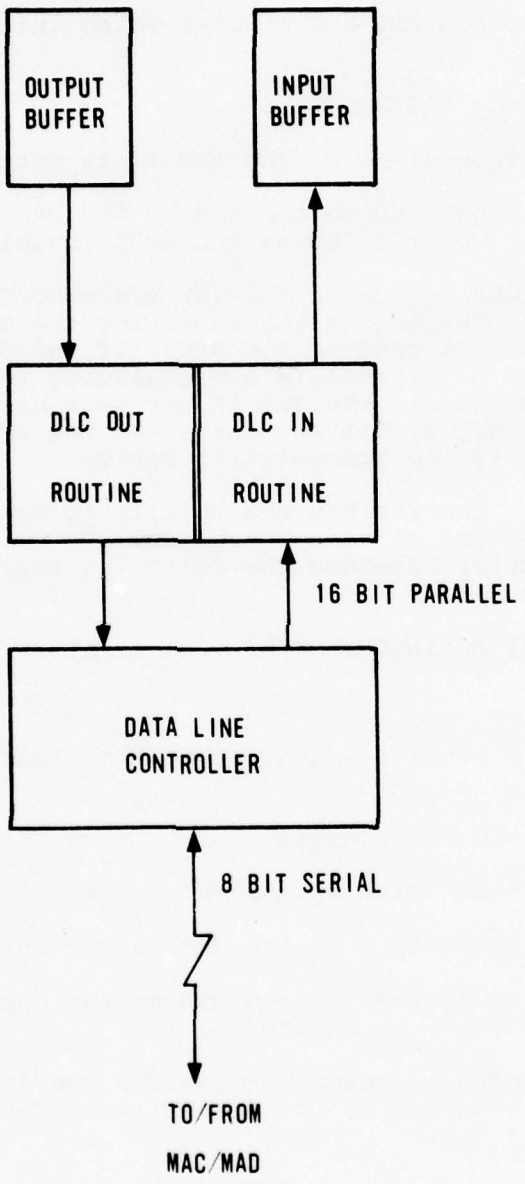

FIGURE 5-6. MAC/MAD

to be transmitted. Both the DLC input and output interrupts are then enabled. The data line controller hardware interrupts the computer which results in an entry into the DLC output routine. This routine transfers a word from the output buffer to the DLC which transmits the character contained in the lower eight bits of the word one bit at a time at a 150 Baud rate over the telemetry line. Upon completion the DLC again interrupts the computer. This process continues until the DLC output routine transfers the last word from the output buffer and removes the DLC output interrupt.

Each time the DLC receives eight bits of information and packs them into the lower eight bits of a 16 bit word it interrupts the computer. This results in an entry into the DLC input routine which checks for a parity error and puts the word into the input buffer. If the character has a parity error then the sign bit of the word is set before storage.

The DLC software was checked out during system integration. The corrections made at that time are described in the software log book No. 1159, page 71 (included as an Addendum to the DATEC Field Test and Evaluation Program Report). No other problems occurred in this software during in-plant test or field test.

5.2.1.2 IQCS Interface

The IQCS software is the PATE application task responsible for making VF measurements. The original PATE software was designed to be capable of passing data between tasks by means of disk buffers. The IQCS application task makes use of this feature by providing the capability of passing all calculated IQCS parameters to another task. A requirement of Digital ATEC software is to report on VF channel status of the CY-104. This involves making an IQCS measurement and determining the worst alarm color (R:red; A:amber or none: green) of all the parameters measured. This color is then used as the channel status.

The IQCS software was modified to include the worst alarm color in the disk buffer. This was a relatively simple modification in that it involved shuffling only some data base items. This software was checked out during module testing. It had no problems throughout in-plant and field testing.

5.2.1.3 Addition of Nodal Control Operator Interaction Command

Each application task in the PATE system has an associated operator interaction task providing the operator with the capability of accessing and changing the data base and changing system control. The first two characters of an application task command must be unique to that task. The operator interaction scheduler recognizes the task names and schedules the appropriate operator interaction task. The two character mnemonic NC was added to the list of acceptable mnemonics so that the nodal control operator interaction task could be scheduled when required.

5.2.2 Nodal Control Scan Software

The primary functions of the nodal control scan software are:

1. Input MAC/MAD/IQCS data in a timely sequence.

2. Compute, alarm and trend parameters from the data inputs.

3. Output the results in an easily understood set of displays that provide the nodal control operator a means of assessing system performance and isolating faults.

This is illustrated in the hierarchy diagram of Figure 5-7.

5.2.2.1 Input MAC/MAD/IQCS Data

By using the top down refinement process it was determined that the input software was to perform the following functions:

1. Select the next device from which to obtain data.

2. Output the appropriate command to the device.

3. Process the data received from the device.

4. Store the results of the processing.

An adequate device selection scheme was defined in the study phase of the Digital ATEC Program (ATEC Digital Adaptation Study, Volume III, Page 80) as:

a. Major alarm requests every 30 seconds.

b. An IQCS measurement at the nodal site every 30 seconds.

c. A complete alarm scanner update every minute.

d. Collection of all MAC voltages within a 3 minute period.

e. Collection of all power supply voltages (maintenance voltages) at least once an hour.

This scheme was implemented by the select monitor point module described in Figure 5-8. Each of the scan tables shown contain items with all data required to have a command sent to a measuring device (MAC/MAD/IQCS) and the returned data stored in the data base. All the scan tables have a common format so they can be accessed by the single module, Get Table Item. This module uses parameter TSEL to determine the table to be accessed. It then stores the address of the table item in parameter TBAD to be used by other modules. The type of command (MAC/MAD/IQCS) is also stored in parameter CTYP for other modules to reference. The parameter TSEL is then modified to point to the next table to be accessed. The normal selection sequence is AXTB, IQTB, and ADTB in a continuous cycle.

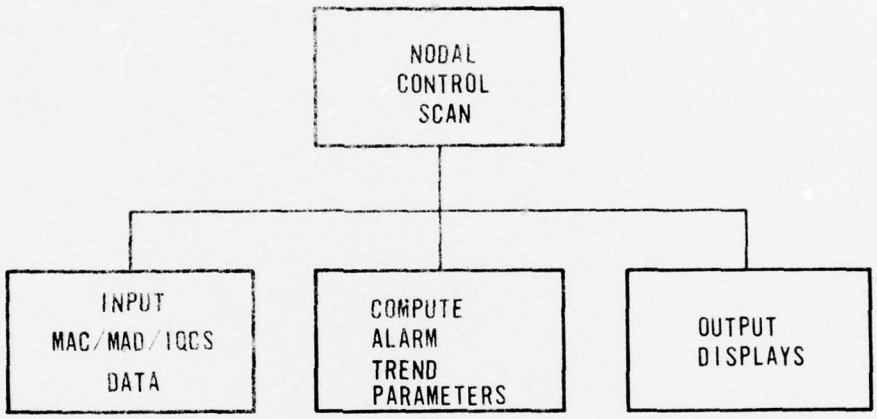

FIGURE 5-7. FIRST LEVEL HIERARCHY OF NODAL CONTROL SCAN PROCESS

The scan sequence used for the field tests as determined by the Select Monitor Point module is shown in Figure 5-9. The resulting cumulative scan time is slightly less than four minutes for both the nodal and remote sites. Of the target scan interval times determined in the study pphase, all but the Major Alarm Summary (MAS) occurs within or close to the desired interval. In one case the interval between the last MAS in the scan (occurring at cumulative elapsed time of 180.6 seconds) and the first MAS in the scan is 63.4 seconds as compared with the desired 30 second period. This longer interval results from the fact that it was decided just prior to in-plant checkout tests of DATEC to measure Maintenance Voltages for each site on every other scan (as opposed to once every hour). It is a simple matter to change the MAS interval as described in the following paragraph. It was not changed for the field tests because (1) the occurrence of a major alarm would have a uniform probability of occurring any time within the 63.4 second interval and therefore on the average would occur within 32 seconds of a MAS, and (2) the independent alarm system, SSFSS, would report all major alarms at the Alarm Display units within four seconds.

Another way of illustrating the scan update times is in terms of the alarm/parameter types as shown in Figure 5-10. This figure also shows scan times for a nodal control site with a jurisdiction of 16 stations, and update times for the Monitor Immediate scan mode. The Monitor Immediate mode was implemented just prior to field tests and replaced another similar mode called Temporary Scan, which was in use during in-plant tests at Honeywell. This model features an abbreviated scan which monitors only those parameters selected by the operator in the nodal command statement entered via the keyboard. The Monitor Immediate mode is discussed in Paragraph 5.2.3 of this report.

The Table ADTB contains data for MAC measurement commands. Each item in this table contains a maintenance bit. If it is set it causes the next item to be selected from the maintenance table MNTB before the return to AXTB. This scheme provides the capability of varying the rate at which maintenance voltages are scanned. Each item of all scan tables also has a bit that if set causes a major alarm summary command to be sent to the MAD before the next scan table is accessed. This provides the capability of varying the rate at which major alarms are interrogated.

The results of the refinement of the input function are shown in Figure 5-11. Module 1.3 is responsible for outputting the alarm summary command to the MAD and storing the results in the alarm summary table in the data base. Module 1.2 is responsible for outputting the major alarm summary command to the MAD and if major alarms have occurred, calling Module 1.3 to update the alarm scanner table. Module 1.4 is responsible for inputting MAC voltages. This involves outputting EPUT and BEM commands if required, outputting MAC voltage measurement commands, loading the site data base containing voltage tables and parameter tables for the site, converting and storing the returned voltages and recovering incorrect voltages due to telemetry problems if necessary.

	Command Mnemonic	Execution Time (Sec)	Cum Time (Sec)
1. Select nodal A radio	BEM-1-MO-I1	0.8	0.8
2. Select remote A radio	BEM-3-MO-I1	0.8	1.6
3. Alarm Summary - nodal	AS-1	10.6	12.2
4. Major Alarm Summary	MAS	0.6	12.8
5. IQCS - Chan 5	IQ-005	5.2	18.0
6. Inhibit EPUT - nodal	EPUT-1-1	0.6	18.6
7. Measure 6 voltages - nodal	MAC-1-01-06	19.4	38.0
8. Major Alarm Summary	MAS	0.6	38.6
9. Alarm Summary - remote	AS-2	10.6	49.2
10. IQCS - Chan 6	IQ-006	5.2	54.4
11. Measure 6 voltages - nodal	MAC-1-07-12	19.4	73.8
12. Alarm Summary - nodal	AS-1	10.6	84.4
13. Major Alarm Summary	MAS	0.6	85.0
14. IQCS - Chan 7	IQ-007	5.2	90.2
15. Measure 5 voltages - nodal	MAC-1-13-17	16.2	106.4
16. Clear inhibit - nodal	IPUT-1-2	0.6	107.0
17. Select nodal B radio (alternate with A)	BEM-1-MO-I2 (BEM-1-MO-I1)	0.8	107.8
18. Major Alarm Summary	MAS	0.6	108.4
19. Alarm Summary - remote	AS-2	10.6	119.0
20. IQCS - Chan 8	IQ-008	5.2	124.2
21. Inhibit EPUT - remote	EPUT-3-1	0.6	124.8
22. Measure 6 voltages - remote	MAC-3-01-06	19.4	144.2
23. Alarm Summary - nodal	AS-1	10.6	154.8
24. Major Alarm Summary	MAS	0.6	155.4

FIGURE 5-9. SCANNING SEQUENCE

	Command Mnemonic	Execution Time (Sec)	Cum Time (Sec)
25. IQCS - Chan 5	IQ-005	5.2	160.6
26. Measure 6 voltages - remote	MAC-3-07-12	19.4	180.0
27. Major Alarm Summary	MAS	0.6	180.6
28. Alarm Summary - remote	AS-2	10.6	191.2
29. IQCS - Chan 6	IQ-006	5.2	196.4
30. Measure 5 voltages - remote	MAC-3-13-17	16.2	212.6
31. Clear inhibit - remote	EPUT-3-2	0.6	213.2
32. Select remote B radio (Alternate with A)	BEM-3-MO-I2 (BEM-3-MO-I1)	0.8	214.0
33. Measure maintenance voltages - nodal (alternate with remote	MAC-I-I8-23 (MAC-3-18-23)	19.4	233.4
34. Go to 3.			

FIGURE 5-9. SCANNING SEQUENCE (Continued)

	Normal Update		Monitor Immediate
Major Alarm	Ft. Huachuca (2 sites)	16 Sites	
Loss of Service	<4 sec*	<4 sec*	
Alarm and Status			
2 state alarm or indicator	1 min	8 min	10 sec
Analog/Digital Parameters			
RSL, FER	4 min	32 min	8 sec**
Eye Parameters	8 min	64 min	8 sec***
Analog Maintenance Parameters	8 min	64 min	20 sec

* SSFSS

** FER update determined by EPUT Timebase

*** Eye Hits update determined by BEM EPUT Timebase

NOTE:

FIGURE 5-10. UPDATE TIMES

In the figure above with exception of Loss of Service, the update times for 16 sites are merely extrapolations of single link scan rates with a scan sequence such as that used at Fort Huachuca (see Figure 5-9). Loss of service major alarms are monitored by the Sudden Service Failure Sensing System and are reported in less than four seconds regardless of the number of sites. The update times of 64 minutes for eye and maintenance voltage parameters for instance assume only one update for an entire 16 site scan. Reducing the update time for a given parameter is simply a matter of changing the scan sequence. It takes approximately 2.5 seconds to obtain a MAC voltage measurement. The only restriction is that the update cannot be requested more frequently than the EPUT timebase frequency for those parameters where such a timebase is involved. This would be 90 seconds for eye hits and 3 1/2 minutes for multiplexer FER measurements.

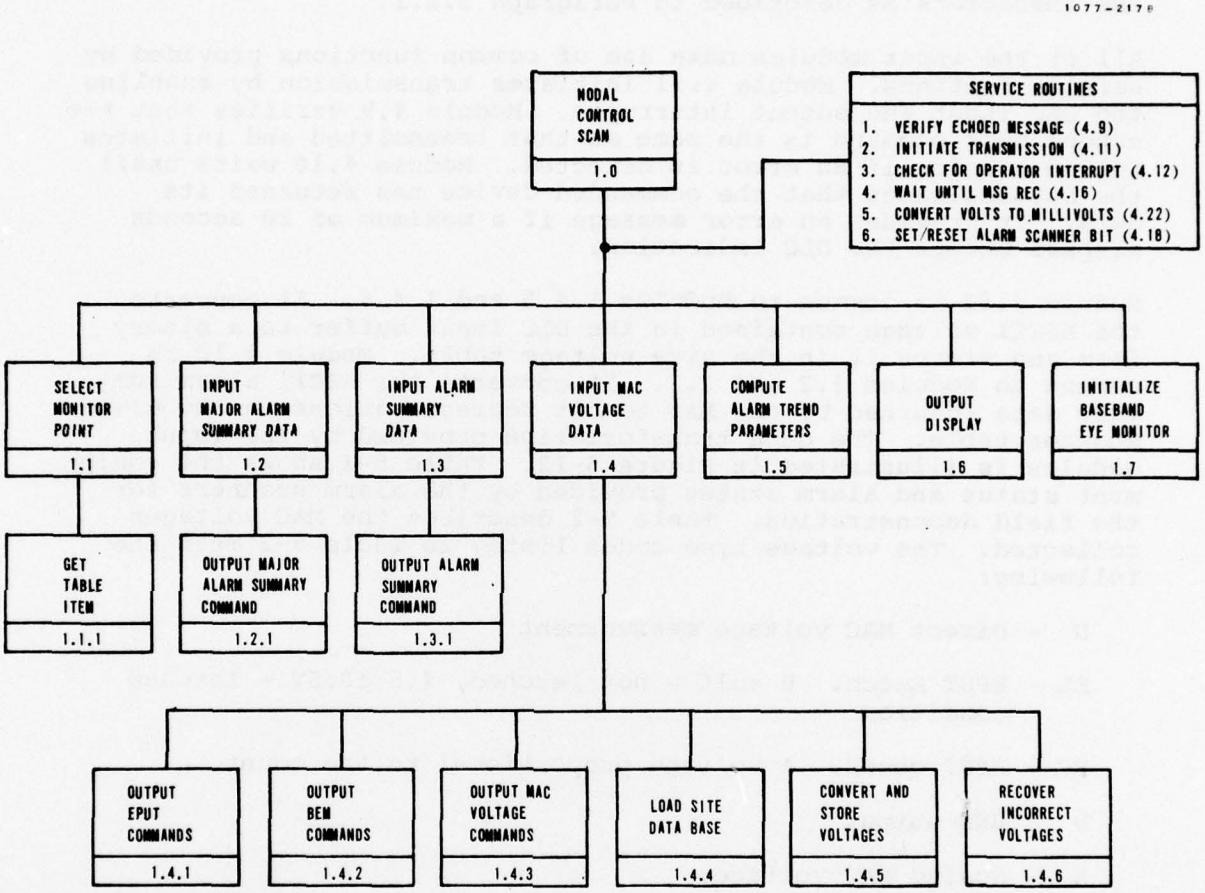

FIGURE 5-11. AFTER INPUT REFINEMENT

The output modules (1.2.1, 1.3.1, 1.4.1, 1.4.2, 1.4.3) are responsible for loading the output buffer used by the DLC software with the characters as described in Paragraph 5.2.1.

All of the input modules make use of common functions provided by service routines. Module 4.11 initiates transmission by enabling the DLC input and output interrupts. Module 4.9 verifies that the echoed back command is the same as that transmitted and initiates retransmission if an error is detected. Module 4.16 waits until the DLC indicates that the commanded device has returned its data. It provides an error message if a maximum of 20 seconds elapses before the DLC indication.

Module 4.22 is common to Modules 1.4.5 and 1.4.6. It converts the ASCII voltage contained in the DLC input buffer to a binary form and stores it in the site voltage table. Module 4.18 is common to Modules 1.2 and 1.3. It converts the ASCII alarm summary data returned by the MAD to bit representations in the alarm scanner table. The data transformation provided by the input modules is illustrated in Figure 5-12. Table 5-1 shows the equipment status and alarm states provided by the alarm scanners for the field demonstration. Table 5-2 describes the MAC voltages collected. The voltage type codes listed in Table 5-2 mean the following:

D - Direct MAC voltage measurement

EL - EPUT Latch. 0 volt = not latched, 4.5 ±0.5V = latched condition

EC - EPUT count. A voltage proportional to the count

B - BEM output

S - Scaled MAC voltage.

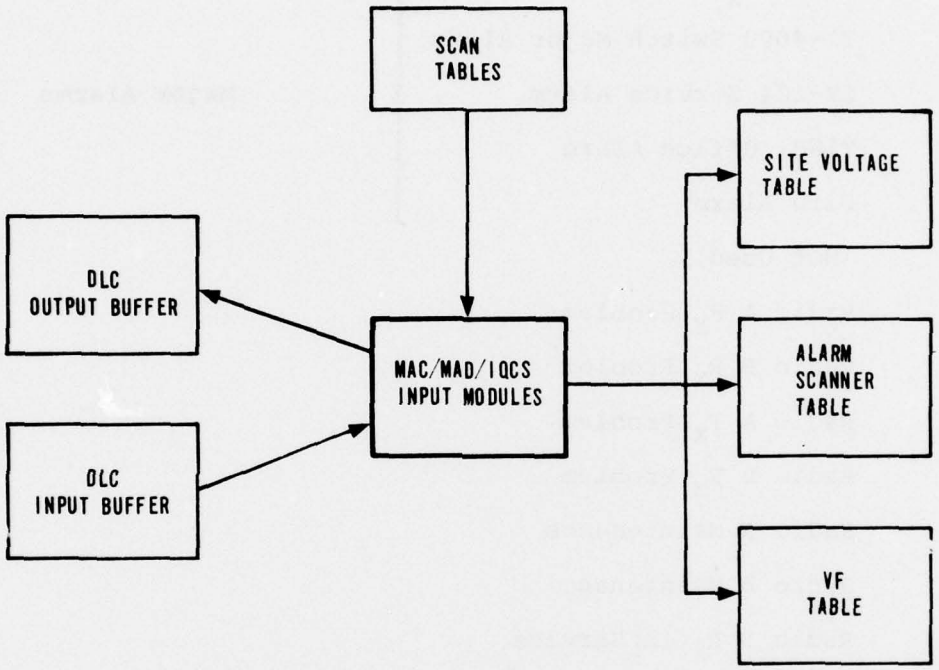

FIGURE 5-12. INPUT DATA TRANSFORMATION

TABLE 5-1. EQUIPMENT ALARMS AND STATUS
(HUA AND SBL)

Alarm No.	Description	
1	Radio R_X Alarm	Major Alarms
2	T1-4000 Switch Major Alarm	
3	CY-104 Service Alarm	
4	T1WB1 Office Alarm	
5	Site Alarm	
6	(Not Used)	
7	Radio A R_X Problem	
8	Radio B R_X Problem	
9	Radio A T_X Problem	
10	Radio B T_X Problem	
11	Radio A Maintenance	
12	Radio B Maintenance	
13	Radio B R_X In Service	
14	Radio B T_X In Service	
15	T1-4000 Norm Major Alarm	
16	T1-4000 Stby Major Alarm	
17	T1-4000 Switch Minor Alarm	
18	T1-4000 Stby R_X In Service	
19	T1-4000 Stby T_X In Service	
20	T1-4000 Norm Maintenance	
21	T1-4000 Stby Maintenance	
22	CY-104 Remote Alarm	
23	CY-104 Maintenance	
24	T1WB1 Maintenance	

TABLE 5-1. EQUIPMENT ALARMS AND STATUS
(HUA AND SBL) (Continued)

Alarm No.	Description
25	Entry Alarm
26	Fire Alarm
27	AC Power Alarm
28	Battery Alarm
29	Wave Guide Pressure Alarm
30	Wave Guide Humidity Alarm
31	Flood Alarm

TABLE 5-2. MAC VOLTAGES

MAC Channel	Description	Voltage Type
1	Radio A AGC	(D)
2	Radio B AGC	(D)
3	T1WB1 Reframe	(EL)
4	T1WB1 Frame Error Count	(EC)
5	Link Availability	(EL)
6	Radio R_X A Squelch	(EL)
7	Radio R_X B Squelch	(EL)
8	BEM A Amplitude	(B)
9	BEM A Dispersion	(B)
10	BEM A Hits	(B)
11	BEM B Amplitude	(B)
12	BEM B Dispersion	(B)
13	BEM B Hits	(B)
14	T1-4000 Reframe - normal	(EL)
15	T1-4000 Reframe - standby	(EL)
16	T1-4000 Frame Error Count - normal	(EC)
17	T1-4000 Frame Error Count - standby	(EC)
18	T1WB1 +15 VDC Supply	(S)
19	T1WB1 +12 VDC Supply	(S)
20	T1-4000 +5 VDC Supply	(S)
21	T1-4000 -6 VDC Supply	(S)
22	Radio +24 VDC Supply	(S)
23	Radio -20 VDC Supply	(S)

5.2.2.2 Compute, Alarm, Trend Parameters

The primary purpose of this function is to transform the voltages and alarm scanner data to a set of parameters, alarm colors and statistical values determined as useful for performance assessment, trend analysis and fault isolation within the digital communication environment. The results of the refinement of this function are shown in Figure 5-13. This was a rather straightforward process in that modules were defined to process each type of voltage collected. The data structure for this function is shown in Figure 5-14. For each voltage table item, there corresponds a pointer into the parameter directory file which leads to an item containing all the information required to compute, alarm and trend the parameter or parameters associated with that voltage. Table 5-3 describes the contents of the parameter value table and the voltages used in computing each item.

A parameter directory file item contains the following information:

a. Computation index. Used to determine which processing module to enter.

b. Voltage table pointers for accessing current voltage values.

c. Alarm scanner table pointers for determining equipment in service and maintenance status.

d. Conversion table indicators. Used to load the desired table for table look-up procedures when required.

e. Pointers into the parameter value table for results storage.

The service modules described in Figure 5-13 perform the following functions:

a. Module 4.4 (Convert voltages). Input to this module is a voltage value and a table indicator. It loads the indicated table into memory and uses a linear interpolation technique to produce a floating point resultant value.

b. Module 4.8.1 (Alarm parameter). This module is entered after a parameter is computed and it is determined from the site alarm trend table that it is enabled for alarming. It uses a threshold indicator found in the site alarm trend table for loading a set of thresholds from the alarm threshold file. An alarm color (red, amber, green) is then generated by determining where the parameter value fits in the alarm thresholds.

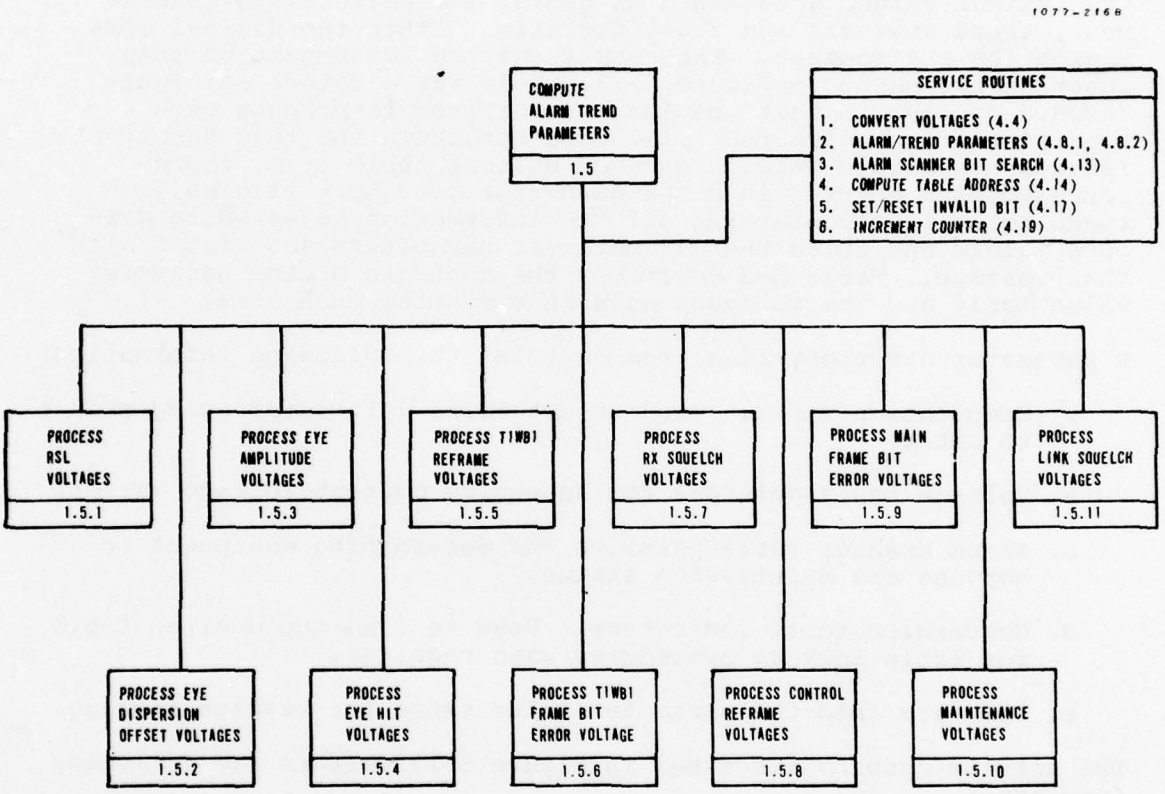

FIGURE 5-13. COMPUTE/ALARM/TREND PARAMETER HIERARCHY

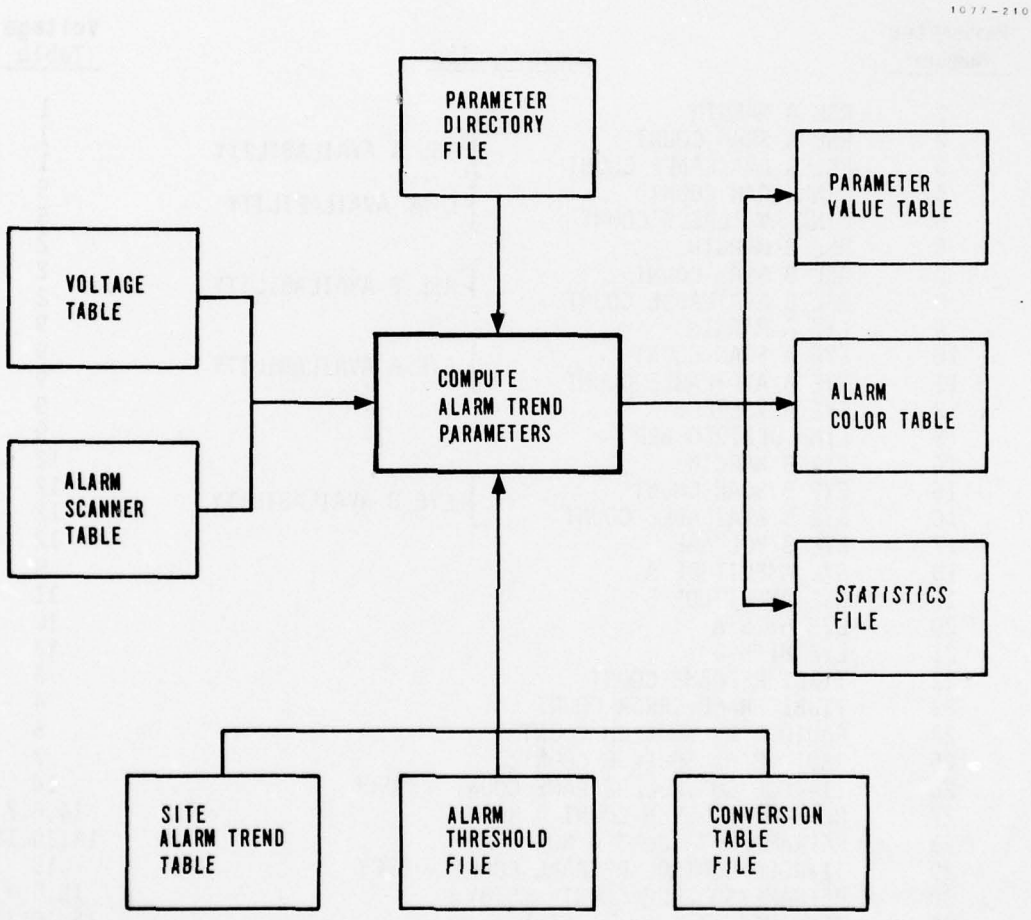

FIGURE 5-14. DATA STRUCTURE FOR COMPUTE, ALARM TREND PARAMETERS FUNCTION

AD-A051 925 HONEYWELL INC ST PETERSBURG FL AVIONICS DIV F/G 17/2
ATEC DIGITAL ADAPTATION STUDY, DEVELOPMENT AND FIELD EVALUATION--ETC(U)
JAN 78 T J CAMPBELL, W F ACKER, C L CHRISTNER F30602-75-C-0282
UNCLASSIFIED 1077-14813-VOL-1 RADC-TR-77-431-VOL-1 NL

3 OF 3
AD
A051925

END
DATE
FILMED
5-78
DDC

TABLE 5-3. PARAMETER VALUE TABLE

Parameter Number	Description	Voltage Table
1	RSL A MARGIN	1
2	RSL A SCAN COUNT } RSL A AVAILABILITY	1
3	RSL A AVAILABLE COUNT } RSL A AVAILABILITY	1
4	LINK SCAN COUNT } LINK AVAILABILITY	5
5	LINK AVAILABLE COUNT } LINK AVAILABILITY	5
6	RSL B MARGIN	2
7	RSL B SCAN COUNT } RSL B AVAILABILITY	2
8	RSL B AVAILABLE COUNT } RSL B AVAILABILITY	2
9	EYE A MARGIN	9
10	EYE A SCAN COUNT } EYE A AVAILABILITY	9
11	EYE A AVAILABLE COUNT } EYE A AVAILABILITY	9
12	EYE A VOLTAGE	9
13	LINK DERIVED BER	9
14	EYE B MARGIN	12
15	EYE B SCAN COUNT } EYE B AVAILABILITY	12
16	EYE B AVAILABLE COUNT } EYE B AVAILABILITY	12
17	EYE B VOLTAGE	12
18	EYE AMPLITUDE A	8
19	EYE AMPLITUDE B	11
20	EYE HITS A	10
21	EYE HITS B	13
22	T1WB1 REFRAME COUNT	3
23	T1WB1 FRAME ERROR COUNT	4
24	RADIO A RX SQUELCH COUNT	6
25	RADIO B RX SQUELCH COUNT	7
26	T1-4000 CONTROL REFRAME COUNT - NORM	14
27	REFRAME/SQUELCH COUNT - NORM	14,6,7
28	REFRAME/HIT COUNT - NORM	14,10,13
29	T1-4000 CONTROL REFRAME COUNT - STBY	15
30	REFRAME/SQUELCH COUNT - STBY	15,6,7
31	REFRAME/HIT COUNT - STBY	15,10,13
32	T1-4000 FRAME ERROR COUNT - NORM	16
33	FER SCAN COUNT - NORM } FER AVAILABILITY - NORM	16
34	FER AVAILABLE COUNT - NORM } FER AVAILABILITY - NORM	16
35	BER CORRELATION DIFF - NORM	16,9,12
36	T1-4000 FRAME ERROR COUNT - STBY	17
37	FER SCAN COUNT - STBY	17
38	FER AVAILABLE COUNT - STBY	17
39	BER CORRELATION DIFF - STBY	17,9,12
40	T1WB1 +15VDC SUPPLY VOLTAGE	18
41	T1WB1 +12VDC SUPPLY VOLTAGE	19
42	T1-4000 +5VDC SUPPLY VOLTAGE	20
43	T1-4000 -6VDC SUPPLY VOLTAGE	21
44	RADIO +24VDC SUPPLY VOLTAGE	22
45	RADIO -20VDC SUPPLY VOLTAGE	23

c. Module 4.8.2 (Trend parameters). This module is entered after a parameter is computed and it is determined from the site alarm trend table that its value is to be entered in the statistics file. This is done in one of three ways determined by the trend indicator.

1. The value is added to the current values list and the last hour, the last 24 hours, the last 30 days and the last 30 months sums are computed as required.

2. The value is added to the current values list and the last hour, the last 24 hours, the last 30 days and the last 30 months mean and standard deviation are computed as required.

3. The value is added to the current values list and the sum is computed for the last hour and last 24 hours and the mean and standard deviation is computed for the last 30 days and the last 30 months.

   Input to this module is the parameter number. This is used to obtain the parameter value and trend indicator. The statistics are updated and stored in the parameter statistics file on disk. Figure 5-15 shows the results of the refinement process for this and the alarm module. Table 5-4 describes the type of trending performed on each of the parameters computed.

4. Module 4.13 (Alarm scanner bit search). This module is used to determine an equipment's status and alarm states as indicated in the alarm summary table. Input is the alarm scanner number and alarm number. Output is the alarm state currently held in the table.

5. Module 4.14 (Compute table address). This module is used to compute the address of a table item given the starting address of the table and a relative word location.

6. Module 4.17 (Set/reset invalid bit). During input processing, a voltage is labeled invalid if it cannot be successfully input after three tries. When the computation modules detect this, they must set as invalid all parameters dependent on this voltage. This indication is set in the site alarm trend table and is used by the output display modules. This module (4.17) is used to set or reset the invalid indicator in the site alarm trend table.

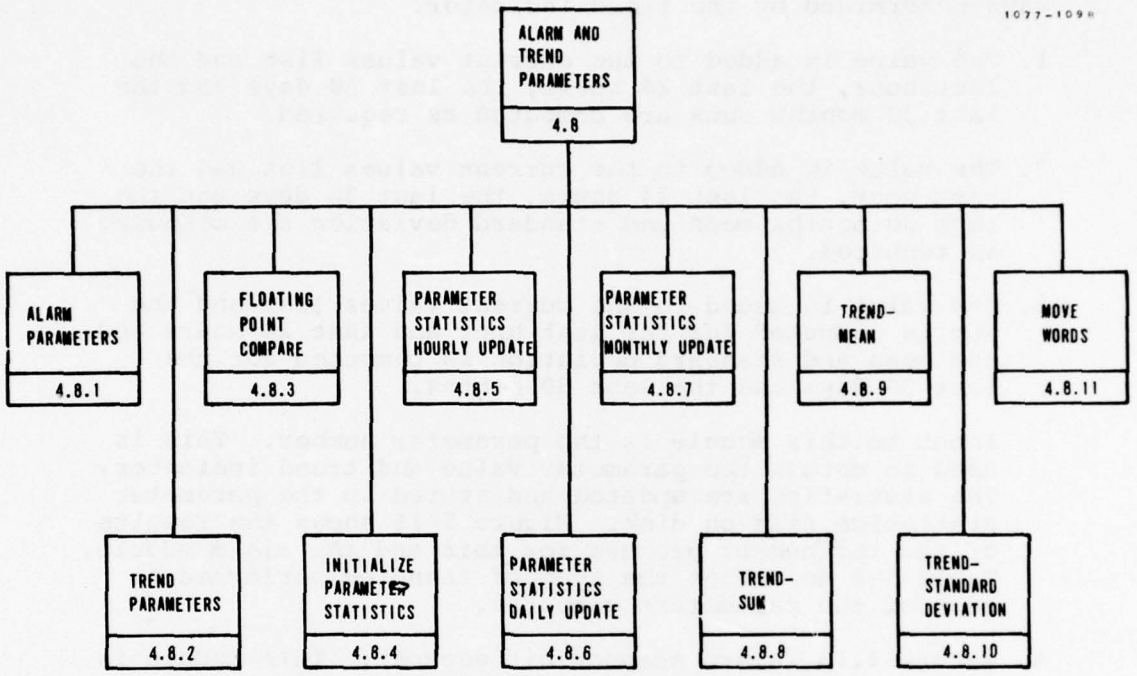

FIGURE 5-15. ALARM/TREND HIERARCHY

TABLE 5-4. TRENDING PER PARAMETER

Parameter Number	Description		Trend Level Indicator
1	RSL A MARGIN		2
2	RSL A SCAN COUNT	RSL A AVAILABILITY	1
3	RSL A AVAILABLE COUNT		1
4	LINK SCAN COUNT	LINK AVAILABILITY	1
5	LINK AVAILABLE COUNT		1
6	RSL B MARGIN		2
7	RSL B SCAN COUNT	RSL B AVAILABILITY	1
8	RSL B AVAILABLE COUNT		1
9	EYE A MARGIN		2
10	EYE A SCAN COUNT	EYE A AVAILABILITY	1
11	EYE A AVAILABLE COUNT		1
12	EYE A VOLTAGE		2
13	LINK DERIVED BER		2
14	EYE B MARGIN		2
15	EYE B SCAN COUNT	EYE B AVAILABILITY	1
16	EYE B AVAILABLE COUNT		1
17	EYE B VOLTAGE		2
18	EYE AMPLITUDE A		2
19	EYE AMPLITUDE B		2
20	EYE HITS A		2
21	EYE HITS B		2
22	T1WB1 REFRAME COUNT		3
23	T1WB1 FRAME ERROR COUNT		1
24	RADIO A RX SQUELCH COUNT		1
25	RADIO B RX SQUELCH COUNT		1
26	T1-4000 CONTROL REFRAME COUNT - NORM		3
27	REFRAME/SQUELCH COUNT - NORM		1
28	REFRAME/HIT COUNT - NORM		1
29	T1-4000 CONTROL REFRAME COUNT - STBY		3
30	REFRAME/SQUELCH COUNT - STBY		1
31	REFRAME/HIT COUNT - STBY		1
32	T1-4000 FRAME ERROR COUNT - NORM		1
33	FER SCAN COUNT - NORM	FER AVAILABILITY - NORM	1
34	FER AVAILABLE COUNT - NORM		1
35	BER CORRELATION DIFF - NORM		0
36	T1-4000 FRAME ERROR COUNT - STBY		1
37	FER SCAN COUNT - STBY		1
38	FER AVAILABLE COUNT - STBY		1
39	BER CORRELATION DIFF - STBY		0
40	T1WB1 +15 VDC SUPPLY VOLTAGE		2
41	T1WB1 +12 VDC SUPPLY VOLTAGE		2
42	T1-4000 +5 VDC SUPPLY VOLTAGE		2
43	T1-4000 -6 VDC SUPPLY VOLTAGE		2
44	RADIO +24 VDC SUPPLY VOLTAGE		2
45	RADIO -20 VDC SUPPLY VOLTAGE		2

5.2.2.3 Output Displays

The purpose of the output display function is to present the results of the data collection and parameter calculation functions in a meaningful way for the operator to assess system performance and isolate faults. It was determined in the study phase of the program that data could be presented adequately in four types of displays (see ATEC DIGITAL ADAPTATION STUDY - VOL. III, PG 42).

a. Overview Display. This is the highest level CRT display. It provides a current summary of system aberrations, by indicating equipment alarms not limited to service failure, and indications of parameters which are outside their tolerance. It is organized by link and site so that the relationship of failure or degradation to the communication system may be readily perceived (see Figure 5-16).

   The columns in the display represent network geography. A column of data is used to represent the conceptual middle of a site. Equipment to the right of the dots are elements of a link facing to the right.

   The higher level equipment is segregated by rows across the display. A row is used for the "A" radio, the "B" radio, the T1-4000 protective switch and the "A" and "B" T1-4000.

   For the lower level multiplex equipment, a slightly different method of display is used. In columns, to the proper side of the column of dots, the alarm states are displayed with the equipment number and the appropriate direction of transmission symbology.

   R - red alarm. Indicates an equipment alarm.

   A - amber alarm. Indicates a parameter out of tolerance.

   I - in-service equipment.

   S - standby equipment.

   M - out-of-service for maintenance.

   < > - both or ambiguous directions of transmission.

   > - transmit direction if on right side of column of dots receive direction if on left side of column of dots.

   < - transmit direction if on left side of column of dots receive direction if on right side of column of dots.

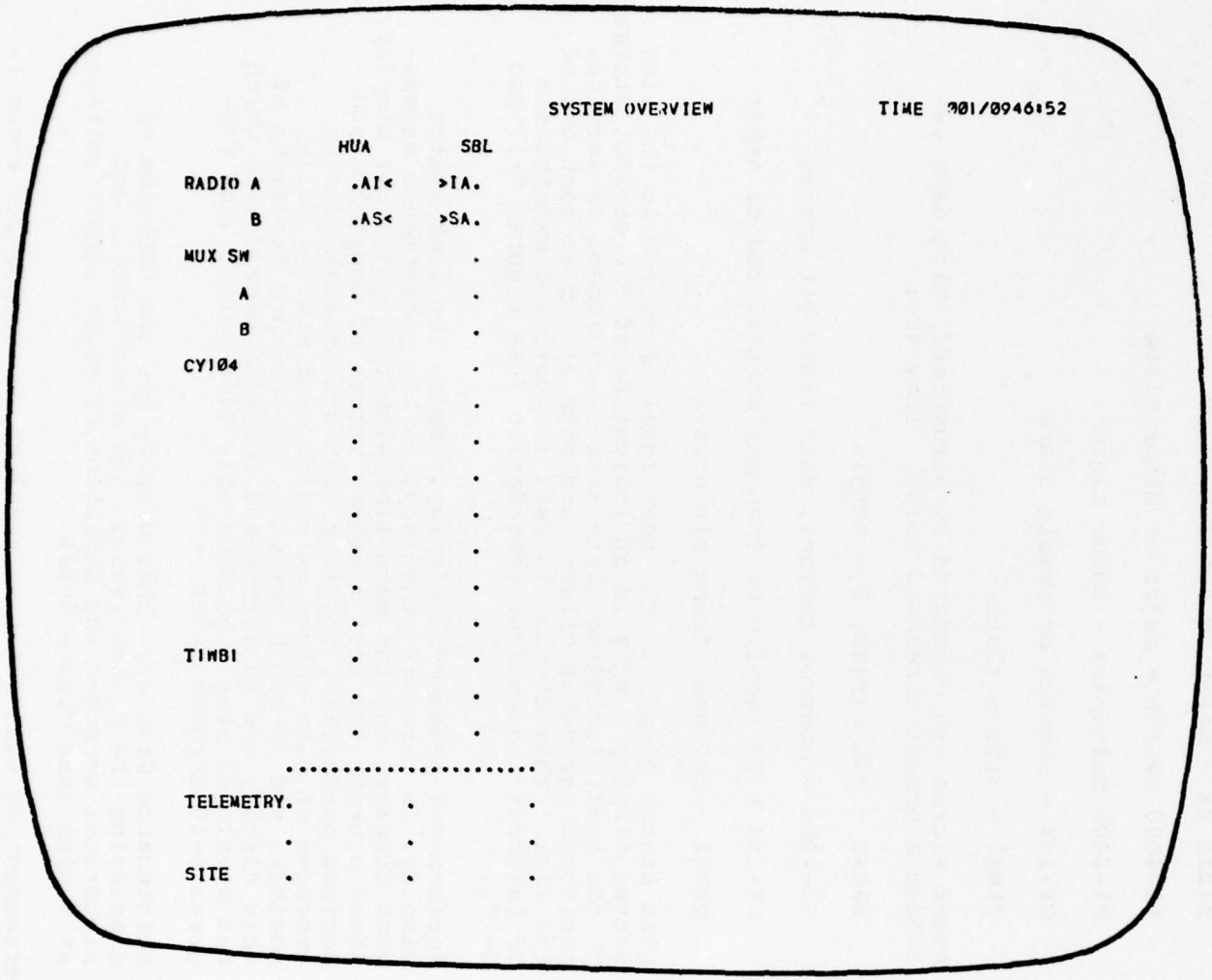

FIGURE 5-16. SYSTEM OVERVIEW DISPLAY

Red alarms are generated by the following conditions:

Radio TX - RF power or pilot or frequency alarm

Radio RX - pilot or squelch alarm

T1-4000 Switch - major or minor alarm

T1-4000 Multiplex - major alarm

CY-104 - service or remote alarm

T1WB1 - office alarm

Amber alarms are generated by parameters which have exceeded a preset threshold value. They are:

Radio - RSL margin, Eye margin

T1-4000 - control reframe, main frame bit errors

CY-104 - VF receive or transmit channel red or amber

T1WB1 - reframe, frame bit errors

b. Link Status Display. The next level of output is the link status display. This is an indication of the current status of the link, including alarm states, equipment in service, monitored parameter values, and site alarms at each end of the link. This display is used for detailed examination of failures and evident degradation (see Figures 5-17 and 5-18).

c. Performance Assessment Display. Below the link status display, in terms of immediacy, is the performance assessment display, one for each link with four pages per display. These provide the last measured values of monitored and derived parameters, together with statistical running averages of past values extending over hourly, daily, monthly, and 30 month periods. The primary functions of this display are to detect and localize degradation which has developed over a considerable time period (see Figures 5-19 through 5-21).

d. Maintenance Display. This display has the function of displaying the present value, the alarm limits, and historical averages and deviation of power supply voltages at a site (see Figure 5-23).

The refinement of this function resulted in the modules shown in Figure 5-24. The first level indicates that a module was defined to process each display type. All pages of the Link Performance Assessment Displays were so similar that only one module was

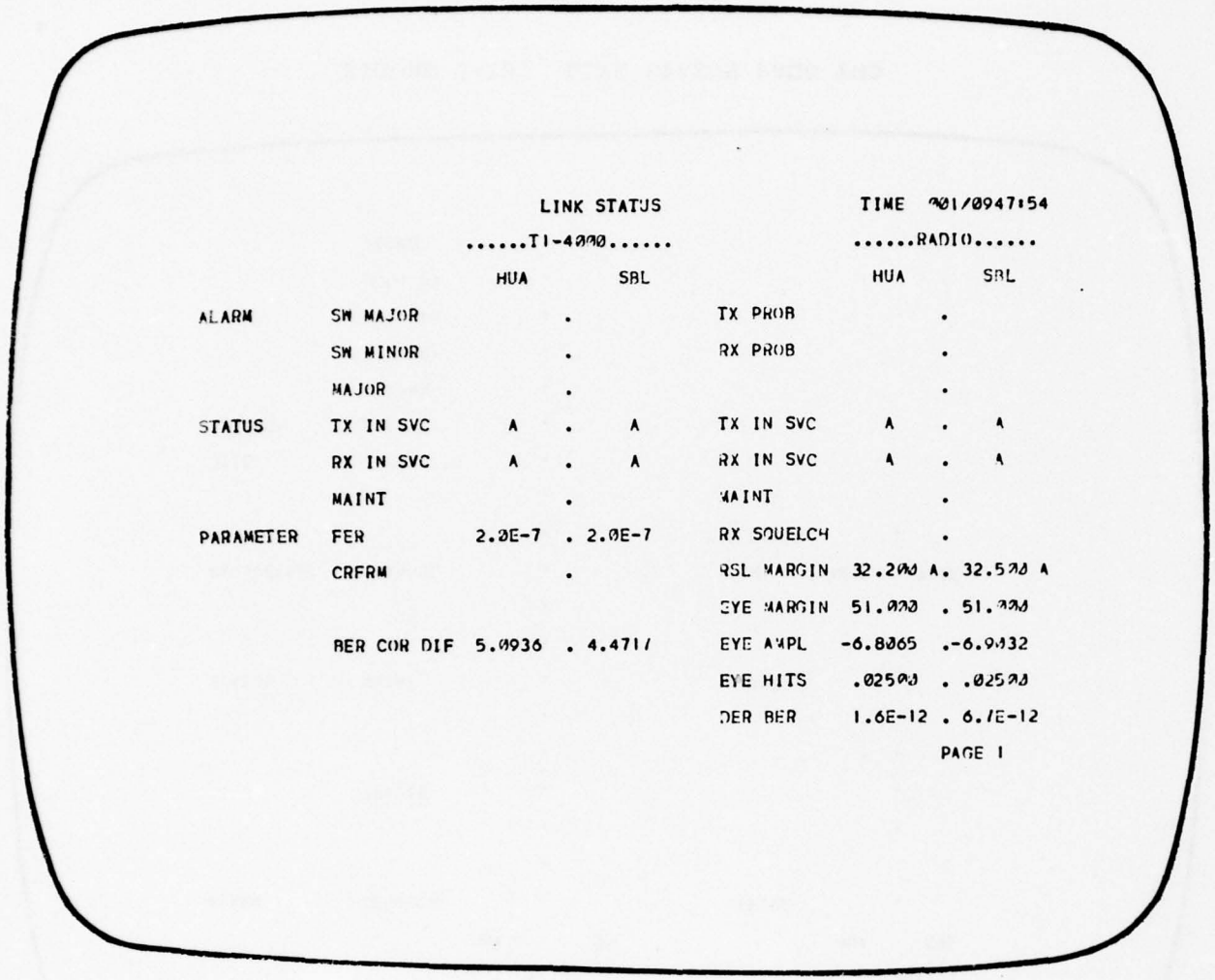

FIGURE 5-17. LINK STATUS PAGE ONE

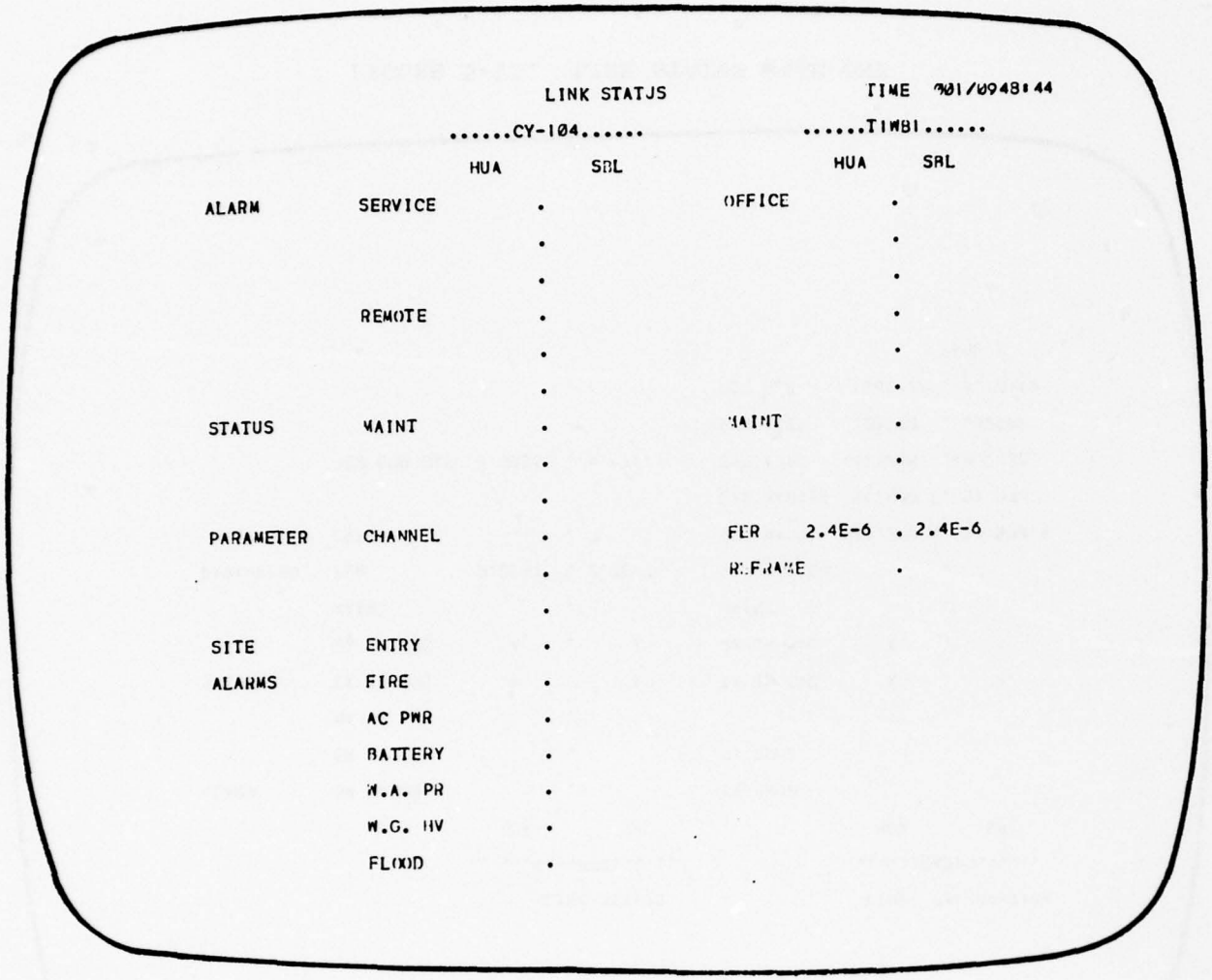

FIGURE 5-18. LINK STATUS PAGE TWO

LINK PERFORMANCE ASSESSMENT - RADIOS TIME 001/0949:37

		LAST SCAN	LAST HR MEAN	LAST 24 HR MEAN	LAST 24 HR DEV	LAST 30 DAYS MEAN	LAST 30 DAYS DEV	LAST 30 MTHS MEAN	LAST 30 MTHS DEV	
HUA	RSLMAR	32.200	32.200	32.290	.11136	30.240	11.534	30.366	.07310	DB
A	EYEMAR	51.000	27.900	29.900	.30000	30.600	.20000	30.700	.20000	DB
	RSLAVL	1.0000	1.0000	1.0000	--------	.97778	--------	.94313	--------	RATE
	EYEAVL	1.0000	.87500	.97500	--------	0.9975	--------	1.0412	--------	RATE
	EYEHIT	.02500	.00800	.00400	.00080	.00200	.00036	.00100	.00018	/SC
HUA	RSLMAR	32.500	32.500	32.400	.08944	30.340	11.563	30.448	.06191	DB
B	EYEMAR	6.8600	27.900	29.900	.30000	30.600	.20000	30.700	.20000	DB
	RSLAVL	1.0000	1.0000	1.0000	--------	1.2406	--------	1.1463	--------	RATE
	EYEAVL	1.0000	.87500	.97500	--------	0.9975	--------	1.0412	--------	RATE
	EYEHIT	.02500	.00800	.00400	.00080	.00200	.00036	.00100	.00018	/SC
SBL	RSLMAR	32.500	32.500	32.500	0.0	30.546	11.550	30.583	.02965	DB
A	EYEMAR	51.000	27.900	29.900	.30000	30.600	.20000	30.700	.20000	DB
	RSLAVL	1.0000	1.0000	1.0000	--------	.99876	--------	.95215	--------	RATE
	EYEAVL	1.0000	.87500	.97500	--------	0.9975	--------	1.0412	--------	RATE
	EYEHIT	.02500	.00800	.00400	.00080	.00200	.00036	.00100	.00018	/SC
SBL	RSLMAR	32.700	32.700	32.600	0.0	30.626	11.575	30.660	.02477	DB
B	EYEMAR	71.000	27.900	29.900	.30000	30.600	.20000	30.700	.20000	DB
	RSLAVL	1.0000	1.0000	1.0000	--------	1.3254	--------	1.2102	--------	RATE
	EYEAVL	1.0000	.87500	.97500	--------	0.9975	--------	1.0412	--------	RATE
	EYEHIT	.02500	.00800	.00400	.00080	.00200	.00036	.00100	.00018	/SC

FIGURE 5-19. LINK PERFORMANCE ASSESSMENT PAGE 1

LINK PERFORMANCE ASSESSMENT - RADIOS TIME 001/0950:18

		LAST SCAN	LAST HR MEAN	LAST 24 HR MEAN	LAST 24 HR DEV	LAST 30 DAYS MEAN	LAST 30 DAYS DEV	LAST 30 MTHS MEAN	LAST 30 MTHS DEV	
HUA	EYEVOL	-6.8065	81.400	82.100	.30000	83.500	.20000	82.600	.30000	MV
A	RXSQH	0.0	1.0000	5.0000	--------	.50000	.04300	.02600	.00330	RTE
HUA	EYEVOL	0.0	81.400	82.100	.30000	83.500	.20000	82.600	.30000	MV
B	RXSQH	0.0	1.0000	5.0000	--------	.50000	.04300	.02600	.00330	RTE
HUA	LNKAVL	1.0000	.90000	.98000	--------	0.9954	--------	0.9999	--------	RTE
SBL	EYEVOL	-6.9032	81.400	82.100	.30000	83.500	.20000	82.600	.30000	MV
A	RXSQH	0.0	1.0000	5.0000	--------	.50000	.04300	.02600	.00330	RTE
SBL	EYEVOL	-2.4286	81.400	82.100	.30000	83.500	.20000	82.600	.30000	MV
B	RXSQH	0.0	1.0000	5.0000	--------	.50000	.04300	.02600	.00330	RTE
SBL	LNKAVL	1.0000	.90000	.98000	--------	1.0954	--------	0.9999	--------	RTE

FIGURE 5-20. LINK PERFORMANCE ASSESSMENT PAGE 2

LINK PERFORMANCE ASSESSMENT - TI-4000 TIME 001/0951:05

		LAST SCAN	LAST HR MEAN	LAST 24 HR MEAN	LAST 24 HR DEV	LAST 30 DAYS MEAN	LAST 30 DAYS DEV	LAST 30 MTHS MEAN	LAST 30 MTHS DEV	
HUA	FER	2.0E-7	1.7E-7	4.3E-7	--------	8.6E-7	--------	2.3E-6	--------	RTE
A	FERAVL	0.0	.95000	0.9980	--------	0.9999	--------	0.9999	--------	RTE
	CRFRM	0.0	1.0000	5.0000	--------	.50000	.04300	.02600	.00330	RTE
	CR/SQH	0.0	1.0000	5.0000	--------	.50000	.04300	.02600	.00330	RTE
	CR/HIT	0.0	1.0000	5.0000	--------	.50000	.04300	.02600	.00330	RTE
HUA	FER	2.0E-7	1.7E-7	4.3E-7	--------	8.6E-7	--------	2.3E-6	--------	RTE
B	FERAVL	0.0	.95000	0.9980	--------	0.9999	--------	0.9999	--------	RTE
	CRFRM	0.0	1.0000	5.0000	--------	.50000	.04300	.02600	.00330	RTE
	CR/SQH	0.0	1.0000	5.0000	--------	.50000	.04300	.02600	.00330	RTE
	CR/HIT	0.0	1.0000	5.0000	--------	.50000	.04300	.02600	.00330	RTE
SBL	FER	2.0E-7	1.7E-7	4.3E-7	--------	8.6E-7	--------	2.3E-6	--------	RTE
A	FERAVL	0.0	.95000	0.9980	--------	0.9999	--------	0.9999	--------	RTE
	CRFRM	0.0	1.0000	5.0000	--------	.50000	.04300	.02600	.00330	RTE
	CR/SQH	0.0	1.0000	5.0000	--------	.50000	.04300	.02600	.00330	RTE
	CR/HIT	0.0	1.0000	5.0000	--------	.50000	.04300	.02600	.00330	RTE
SBL	FER	2.0E-7	1.7E-7	4.3E-7	--------	8.6E-7	--------	2.3E-6	--------	RTE
B	FERAVL	0.0	.95000	0.9980	--------	0.9999	--------	0.9999	--------	RTE
	CRFRM	0.0	1.0000	5.0000	--------	.50000	.04300	.02600	.00330	RTE
	CR/SQH	0.0	1.0000	5.0000	--------	.50000	.04300	.02600	.00330	RTE
	CR/HIT	0.0	1.0000	5.0000	--------	.50000	.04300	.02600	.00330	RTE

FIGURE 5-21. LINK PERFORMANCE ASSESSMENT PAGE 3

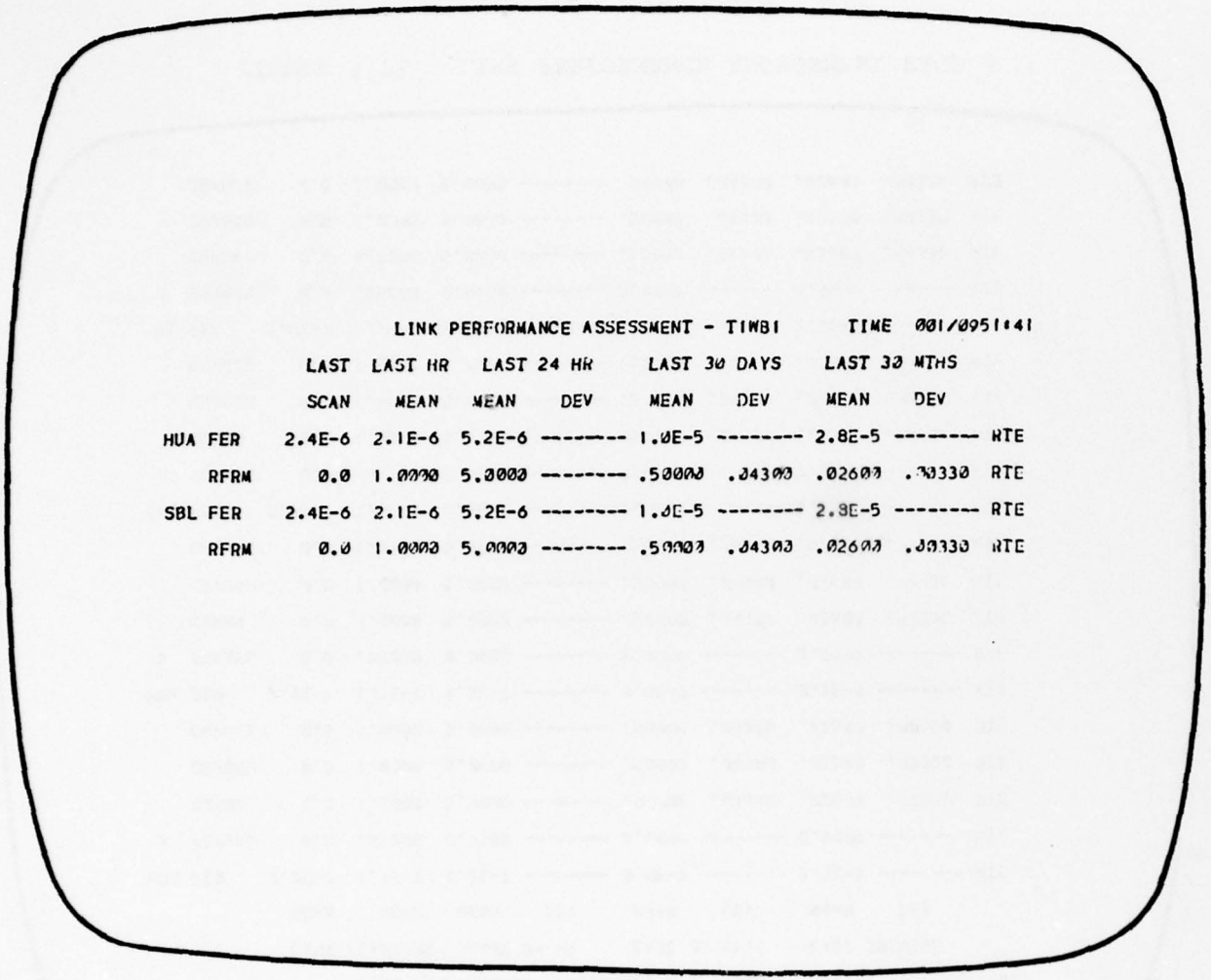

LINK PERFORMANCE ASSESSMENT - TIWB1 TIME 001/0951:41

	LAST SCAN	LAST HR MEAN	LAST 24 HR MEAN	LAST 24 HR DEV	LAST 30 DAYS MEAN	LAST 30 DAYS DEV	LAST 30 MTHS MEAN	LAST 30 MTHS DEV	
HUA FER	2.4E-6	2.1E-6	5.2E-6	--------	1.0E-5	--------	2.8E-5	--------	RTE
RFRM	0.0	1.0000	5.0000	--------	.50000	.04300	.02600	.00330	RTE
SBL FER	2.4E-6	2.1E-6	5.2E-6	--------	1.0E-5	--------	2.8E-5	--------	RTE
RFRM	0.0	1.0000	5.0000	--------	.50000	.04300	.02600	.00330	RTE

FIGURE 5-22. LINK PERFORMANCE ASSESSMENT PAGE 4

MAINTENANCE VOLTAGES - HUA TIME 001/0952:10

NO.	NAME	VOLTS	C	RH	AH	CG	AL	HL	MEAN	DEV	INITIAL DATE
01	TINBI+15	16.1	A	16.5	15.7	15.0	14.2	13.5	15.0	1.38	001/0301
02	TINBI-9	-9.76	A	-8.10	-8.55	-9.30	-9.45	-9.90	-9.10	.832	001/0301
03	TI4000+5	5.41	R	5.50	5.25	5.00	4.75	4.50	5.01	.475	001/0301
04	TI4000-6	-6.51	A	-5.40	-5.70	-6.00	-6.30	-6.60	-6.04	.557	001/0301
05	RADIO+24	25.9	A	26.4	25.2	24.0	22.8	21.6	24.1	2.21	001/0301
06	RADIO-20	-21.7	A	-18.8	-19.9	-20.9	-21.8	-22.8	-20.1	1.90	001/0301

FIGURE 5-23. MAINTENANCE VOLTAGES

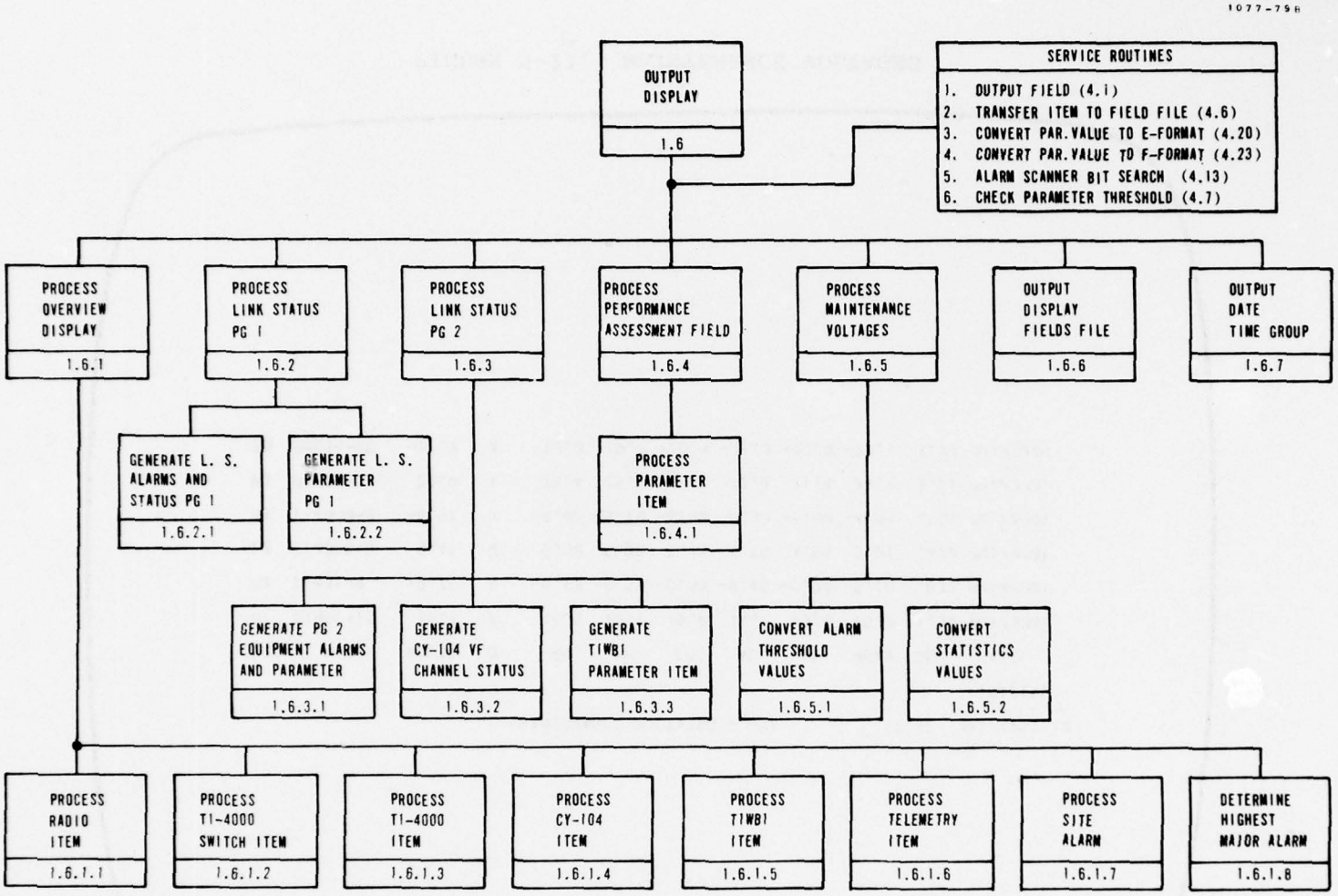

FIGURE 5-24. OUTPUT DISPLAY HIERARCHY

required to process all of them. Module 1.6.6 was defined to read a particular display field file after all fields have been generated and have it written on the ADDS display. Module 1.6.7 was defined to output the date/time group in the upper right hand corner of the ADDS screen. Further refinement was done on a functional basis resulting in modules that process individual fields of a display.

The data structure for the modules defined is shown in Figure 5-25. The display fields file contains all of the fields for each display type. Items within this file are variable in length and contain the following information.

a. The number of characters in the field.

b. An indicator used to determine if the field should blink.

c. An indicator telling whether the field has changed state or not.

d. The row and column at which the field is to begin on the screen.

e. The field contents.

The file is divided into two sections-- one containing only the fixed display fields for all displays and the other containing the variable fields to be generated by the processing modules. The reason for this separation was for speed of processing. It was felt that the base displays (i.e., fixed fields) would be painted on the screen less often than the variable fields. They would be brought up once and from then on only the variable fields updated. The base display would only be brought up if it was not currently on the screen. A complete pass must be made over the variable fields of a display each time the display is updated. By separating the fixed and variable fields, the number of items processed for an update is reduced, therefore, reducing the update time.

The display generator file is divided into eight sections, one for each display type. Each section is further divided into groups of items for each site in the system being monitored. Each item contains all information required to generate a variable field of the particular display. This information is in the form of pointers into the five data tables shown in Figure 5-25.

The output display module is entered as a result of operator request or a determination by the nodal control scan module that a display update is required. (This is determined by a bit in the scan table items providing for variability in the output interval.) If the requested display is not the one on the screen, then the fixed fields are transferred from the

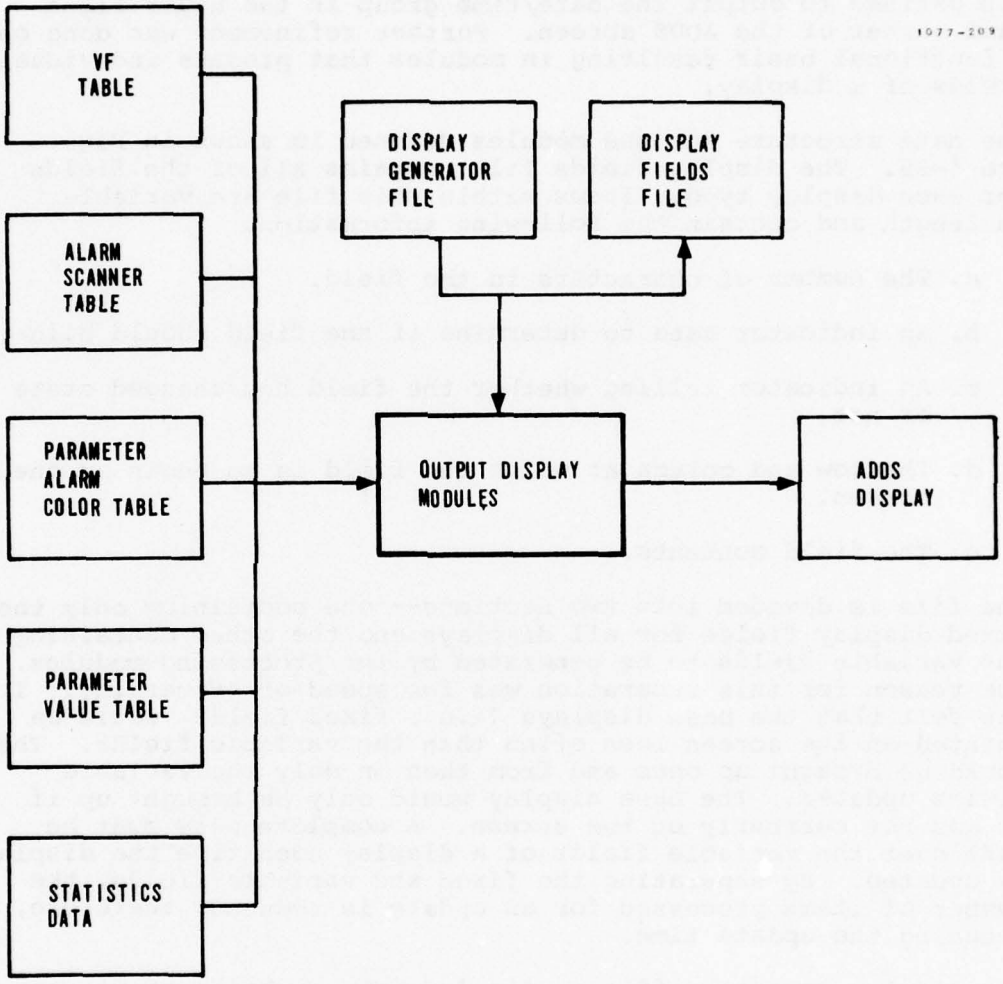

FIGURE 5-25. OUTPUT DISPLAY DATA STRUCTURE

display fields file to the screen by module 1.6.6 (Output Display Fields File) followed by the currently held variable fields. The appropriate processing modules are then called. They in turn use the site data from the display generator file for the display being processed to generate the variable fields and transfer them to the display field file. When all processing is complete, module 1.6.6 is again called to output the variable field to the screen. This time only those fields that have changed are output.

5.2.2.4 Functional Flow

Figure 5-26 shows how the modules of the nodal control scan process are functionally related. When an IQCS measurement is performed, it involves leaving the nodal control scan task and entering the PATE IQCS measurement task. It makes its VF measurement and reschedules the nodal control scan task, passing the channel alarm color through a disk buffer. The PATE modifications required to do this are described in Paragraph 5.2.1.2. Upon reentry, the channel alarm color is stored in the VF table for further processing.

The test for operator interrupt is made by module 4.12 (see Figure 5-11). If the operator has requested service, the nodal control operator interaction task is scheduled.

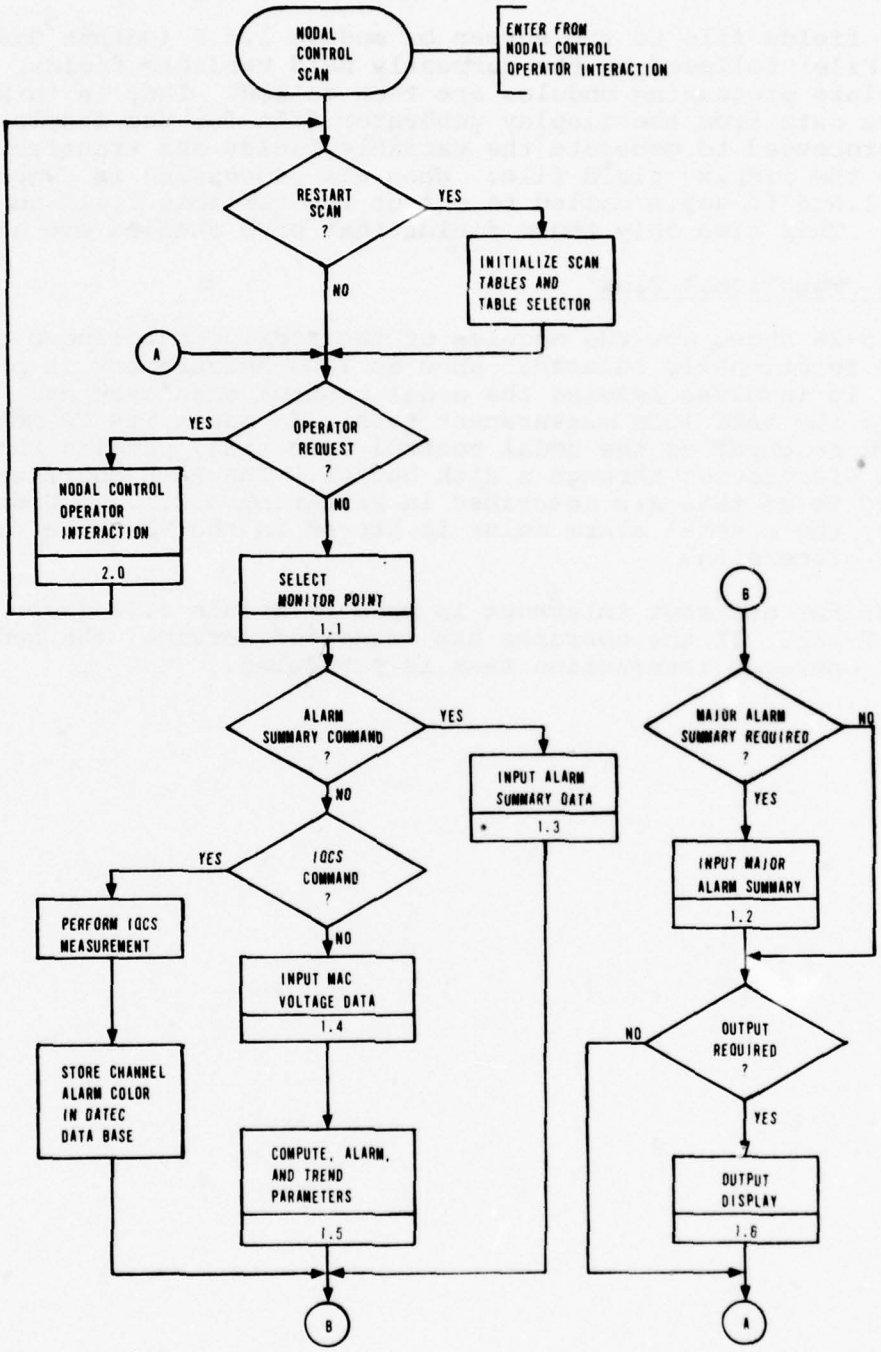

FIGURE 5-26. FUNCTIONAL FLOW OF NODAL CONTROL SCAN

5.2.3 Nodal Control Operator Interaction

The primary requirements of the nodal control operator interaction function are to provide the operator with a means of:

- Calling up the nodal control displays described in Section 5.2.2.3
- Adding/deleting maintenance voltages to/from the maintenance display
- Fault isolation by scanning selected equipments continuously
- Testing DATEC equipments
- Accessing and changing data base items.

The refinement of this function is shown in Figure 5-27. The PATE executive inputs the command as it is entered at the ADDS keyboard and stores it in an input buffer. The first two characters of the command are then checked to determine which operator interaction task is to be loaded. A modification was made in this area so that the characters NC would be recognized and the task containing module 2.0 and associated modules loaded. Module 2.0 uses the same input buffer to check the second argument of the command which is used to determine which processing module to enter. Each module in turn uses the remainder of the command buffer as required. Table 5-5 describes the command mnemonics and the processing module called.

As a means of describing the processing performed by each module, a description of the method of bringing up certain displays, accessing or changing files and entering special modes, similar to the content in the operator's manual written as a training aid in the field in the following paragraphs is included. Data contained in the brackets { } represent variable arguments. The ! symbol is not part of the keyboard entry made by the operator; it is the prompt character displayed on the CRT when the program is waiting on input information while in operator interaction mode.

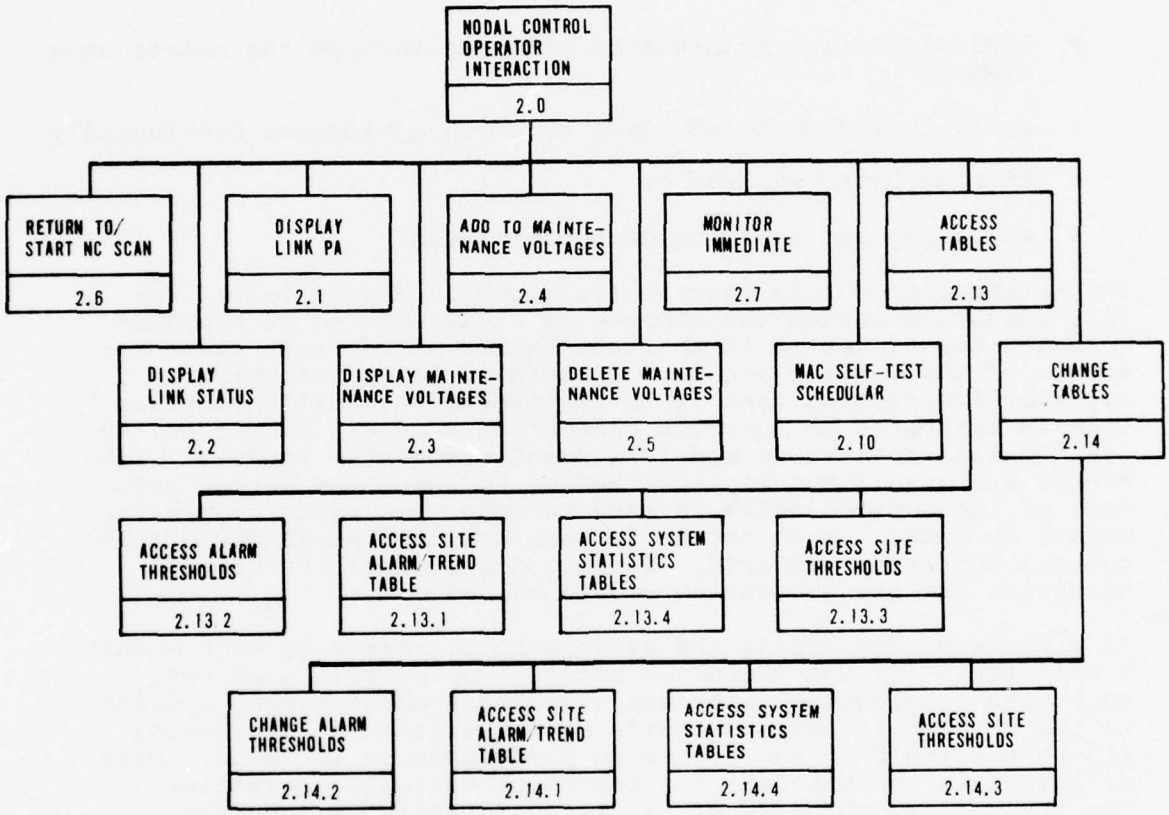

FIGURE 5-27. NODAL CONTROL OPERATOR INTERACTION HIERARCHY

TABLE 5-5. OPERATOR COMMAND MNEMONICS AND CORRESPONDING PROCESSING MODULES

Command Mnemonic	Processing Module
SN	2.6
RN	2.6
LS	2.2
LP	2.1
MV	2.3
AV	2.4
DV	2.5
MI	2.7
MS	2.10
AC	2.13
CH	2.14

5.2.3.1 Bringing Up The Overview Display

!NC, {SN / RN} [NEW LINE]

SN - Restarts Scan
RN - Resumes From Where Interrupted

Puts Processor In Normal Scan Mode

5.2.3.2 Bringing Up The Link Status Display

!NC,LS,1, {1 / 2} [NEW LINE]

1 - Brings up Page 1, T1-4000 & Radio

2 - Brings up Page 2, CY-104 & T1WB1

5.2.3.3 Bringing Up The Link Performance Assessment Display

!NC,LP,1, {1 / 2 / 3 / 4} [NEW LINE]

1 - Brings up Page 1, Radio Data

RSL Margin (RSLMAR)

EYE Margin (EYEMAR)

RSL Availability (RSLAVL)

EYE Availability (EYEAVL)

EYE Hits (EYE HIT)

2 - Brings up Page 2, Radio Data

EYE Voltage (EYEVOL)

Rx Squelch (RXSQH)

3 - Brings up Page 3, T1-4000 Data

Framing Error Rate (FER)

FER Availability (FERAVL)

Control Reframes (CRFRM)

Control Reframes + Squelch (CR/SQH)

Control Reframes + Hits (CR/HIT)

4 - Brings up Page 4, T1WB1 Data

Framing Error Rate (FER)

Reframes (RFRM)

5.2.3.4 Bringing Up The Maintenance Voltage Display

!NC,MV, {HUA / SBL} [NEW LINE]

HUA - Brings up Huachuca Voltages

SBL - Brings up Sibyl Voltages

5.2.3.5 Adding Voltages to the Maintenance Voltage Display

!NC,AV, {HUA / SBL} [NEW LINE]

HUA - Huachuca Maintenance Voltages

SBL - Sibyl Maintenance Voltages

Computer responds with:

NUMBER

Enter:

1-6 [NEW LINE] — To Enter Maintenance Voltages
[NEW LINE] — To Re-enter Operator Interaction

Computer responds with:

NAME

Enter:

Ten character voltage name [NEW LINE]

5.2.3.6 Deleting Voltages From the Maintenance Voltage Display

!NC,DV, {HUA / SBL} [NEW LINE]

HUA - Huachuca Maintenance Voltages

SBL - Sibyl Maintenance Voltages

Computer responds with:

NUMBER

Enter:

1-6 [NEW LINE] — To Delete Voltage
[NEW LINE] — To Re-enter Operator Interaction

5.2.3.7 Entering Monitor Immediate Mode

!NC,MI, |FI| , |TI| , |0/1| NEW LINE

FI = Starting Item in Monitor Immediate Table (1-14)

TI = Ending Item in Monitor Immediate Table (1-14)

NOTE: To Execute Only One Item Make FI = TI.

0 = Execute FI thru TI Continuously

1 = Execute FI thru TI One Time Only

TABLE 5-6. MONITOR IMMEDIATE ITEMS

Item	Description
1	Switch BEM to A Radio - HUA (Preceded by MAC-1-01)
2	Switch BEM to B Radio - HUA (Preceded by MAC-1-01)
3	Switch BEM to A Radio - SBL (Preceded by MAC-3-01)
4	Switch BEM to B Radio - SBL (Preceded by MAC-3-01)
5	Measure EYE Data A - HUA (Followed by MAS)
6	Measure RSL A & B - HUA (Followed by MAS)
7	Measure EYE Data B - HUA (Followed by MAS)
8	Measure EYE Data A - SBL (Followed by MAS)
9	Measure RSL A & B - SBL (Followed by MAS)
10	Measure EYE Data B - SBL (Followed by MAS)
11	Input Alarm Scanner Data - HUA
12	Input Alarm Scanner Data - SBL
13	Measure Maintenance Voltages - HUA
14	Measure Maintenance Voltages - SBL

5.2.3.8 Entering Self-Test Mode

!NC, MS, {MAC / EPUT / BEM} , {1 / 3} NEW LINE

MAC - MAC Self-Test
EPUT - EPUT Self-Test
BEM - BEM Self-Test

1 - HUA MAC Address
3 - SBL MAC Address

Computer responds with:

SELF-TEST RESULTS

5.2.3.9 Accessing Alarm Thresholds Table

!NC,AC,AT, {N} NEW LINE

N = Alarm Threshold Number (1-120)

Computer responds with:

RED HIGH THRESHOLD

RED HIGH HYSTERESIS VALUE

AMBER HIGH THRESHOLD

AMBER HIGH HYSTERESIS VALUE

CENTER GREEN VALUE

AMBER LOW HYSTERESIS VALUE

AMBER LOW THRESHOLD

RED LOW HYSTERESIS VALUE

RED LOW THRESHOLD

5.2.3.10 Accessing Site Alarm Trend Table

!NC,AC,SA, {HUA / SBL} [NEW LINE]

HUA - Access Huachuca SA Table
SBL - Access Sibyl SA Table

Computer responds with:

PARAMETER?

Enter:

1-39	[NEW LINE]	For Site Parameter
MV1-MV6	[NEW LINE]	For Site Maintenance Voltage
[NEW LINE]		To Re-enter Operator Interaction

Computer responds with:

{E / N} XXXX YY

PARAMETER?

Where:

E - Parameter Enabled for Alarming

N - Parameter Not Enabled for Alarming

XXXX - Alarm Threshold Indicator

YY - Trend Enable Level

5.2.3.11 Accessing System Statistics

!NC,AC,SS {HUA / SBL} [NEW LINE]

HUA - Huachuca System Statistics

SBL - Sibyl System Statistics

Computer responds with:

PARAMETER?

Enter:

1-39 [NEW LINE] For Site Parameter

MV1-MV6 [NEW LINE] For Site Maintenance Voltage

[NEW LINE] To Re-enter Operator Interaction

Computer responds with:

TIME PERIOD?

Enter:

{H / D / M / T} [NEW LINE] Where: H - Last Hour's Data Points

D - Last 24 Hours' Data Points

M - Last 30 Days' Data Points

T - Last 30 Months' Data Points

[NEW LINE] To Return To "PARAMETER?" Response

Computer responds with:

FLOATING POINT VALUES REQUESTED

TIME PERIOD?

5.2.3.12 Accessing Site Threshold Table

!NC,AC,ST, {HUA / SBL} NEW LINE

HUA - Access Huachuca ST Table

SBL - Access Sibyl ST Table

Computer responds with:

RSL A AVAILABILITY THRESHOLD VALUE

RSL B AVAILABILITY THRESHOLD VALUE

EYE A AVAILABILITY THRESHOLD VALUE

EYE B AVAILABILITY THRESHOLD VALUE

EYE A HIT COUNT THRESHOLD VALUE

EYE B HIT COUNT THRESHOLD VALUE

FER A AVAILABILITY THRESHOLD VALUE

FER B AVAILABILITY THRESHOLD VALUE

5.2.3.13 Changing Alarm Threshold Table

;NC,CH,AT, {N} NEW LINE

N = Alarm Threshold Number (1-120)

Computer responds with:

ENTER ITEM NUMBER

Enter:

{1 . . . 9} NEW LINE

Where:

1 = Red High Threshold

2 = Red High Hysteresis Value

3 = Amber High Threshold

4 = Amber High Hysteresis Value

5 = Center Green Value

6 = Amber Low Hysteresis Value

7 = Amber Low Threshold

8 = Red Low Hysteresis Value

9 = Red Low Threshold

NEW LINE To Return To Operator Interaction

Computer responds with:

ENTER FLOATING POINT VALUE

Enter:

Floating point number NEW LINE

Examples of Floating Point Numbers:

(1) 4.25

(2) 32.8E-2

(3) -32.75

(4) 2.7E+9

5.2.3.14 Changing Site Alarm Trend Table

!NC,CH,SA, {HUA / SBL} [NEW LINE]

HUA - Change HUA SA Table

SBL - Change SBL SA Table

Computer responds with:

PARAMETER?

Enter:

1-39 [NEW LINE]	For Site Parameter
MV-MV6 [NEW LINE]	For Site Maintenance Voltage
[NEW LINE]	To Re-enter Operator Interaction

Computer responds with:

ALARM ENABLE E or N

Enter:

E [NEW LINE]	To Enable Parameter Alarming
N [NEW LINE]	To Disable Parameter Alarming

Computer responds with:

ALARM THRESHOLD POINTER

Enter:

A number from 1-120 [NEW LINE]

Computer responds with:

TREND ENABLE LEVEL

Enter:

A number from 0-3 [NEW LINE]

5.2.3.15 Changing System Statistics

!NC,CH,SS, {HUA / SBL} NEW LINE

HUA - Huachuca System Statistics

SBL - Sibyl System Statistics

Computer responds with:

PARAMETERS?

Enter:

1-39 NEW LINE — For Site Parameters

MV1-MV6 NEW LINE — For Site Maintenance Parameters

NEW LINE — To Re-enter Operator Interaction

Computer responds with:

TIME PERIOD?

Enter:

{H / D / M / T} NEW LINE

Where:

H - Last Hour's Data

D - Last 24 Hours' Data

M - Last 30 Days' Data

T - Last 30 Months' Data

NEW LINE — To Return To "PARAMETER?" Response

Computer responds with:

ENTER ITEM NUMBER OR 'D'

Enter:

{N / D} NEW LINE

Where:

N = Item No. Within Time Period

D = Delete All Items In Time Period

5.2.3.16 Changing Site Thresholds

!NC,CH,ST, {HUA / SBL} NEW LINE

HUA - Change Huachuca ST Table

SBL - Change Sibyl ST Table

Computer responds with:

ENTER ITEM NUMBER

Enter:

{1 . . . 8} NEW LINE

Where:

1 = RSL A Availability Threshold

2 = RSL B Availability Threshold

3 = EYE A Availability Threshold

4 = EYE B Availability Threshold

5 = EYE A Hit Count Threshold

6 = EYE B Hit Count Threshold

7 = FER A Availability Threshold

8 = FER B Availability Threshold

NEW LINE To Re-enter Operator Interaction

Computer responds with:

ENTER FLOATING POINT VALUE

Enter:

Floating point item value NEW LINE

5.2.4 HIPO Diagrams

The results of the design process are made visible through Hierarchy diagrams and Input-Process-Output diagrams. The Hierarchy diagrams as seen in Figures 5-7, 5-11, 5-13, 5-15, 5-24 and 5-27 describe the organization of the software modules. An Input-Process-Output diagram exists for each module of the hierarchy. It tells what the module does by listing the steps it performs and showing the data flow through it. The complete set of diagrams are described in the final software data item DB002-2 (ATEC DIGITAL ADAPTATION STUDY - SOFTWARE DOCUMENTATION).

5.3 CODE

Making the transition from the HIPO diagrams to the machine code was accomplished by means of a generalized program design language known as playscripts. This is a detailed plan describing how the coding is to be done. It effectively replaces the function of the conventional flow chart. Programmers were required to generate a playscript and walk through it with the Chief Programmer before coding the module. In some instances, the module was layed out in playscript form by the Chief Programmer and then given to the support programmer to code and test.

This form of program design language was used instead of a more structured pseudo code with limited constructs because machine language was being used instead of a higher order language. All programmers on this program were excellent DAP (an assembly language peculiar to the -16 series Honeywell Computer) coders; therefore, they were given the freedom to implement the statements of the playscript as they wished as long as the end results were as defined. Programmers were, however, required to follow a standard format for organizing the code. This included the following:

a. Heading. The first line of each source code listing contains the module number and name as it appears in the hierarchy diagram, the source file name used for accessing the file for updating in the Program Support Library and the date that the source code was entered into the library.

b. Programmer's Name. The next information contains the name of the programmer that coded the module and the name of the last programmer to revise the file along with the date that the revision was made.

c. Abstract. Next appears an abstract in narrative form describing what the module does.

```
                    * 4.12    CHECK FOR OPERATOR INTERRUPT    ($SCOIN)      AUGUST 7 PAGE    1
                      (1)              (2)                      (3)              (4)
0001                *4.12   CHECK FOR OPERATOR INTERRUPT  ($SCOIN)      AUGUST 76
0002                *
0003                *     CODED BY: (5)          REVISED BY:(6)      DATE: (7)
0004                *
0005                *          TOM DOYLE
0006                *
0007                *     ABSTRACT:              (8)
0008                *
0009                *          THIS MODULE CHECKS FOR OPERATOR INTERRUPT.
0010                *          IF SERVICE IS DESIRED THE RETURN VECTOR IS SAVED AND
0011                *          THE CUPRENT TASK IS TERMINATED TO ALLOW NODAL CONTROL
0012                *          OPERATOR INTERACTION TO BE LOADED.
0013                *
0014                *     CALLING SEQUENCE:
0015                *
0016                *          JST*  OPCK  (9)
0017                *
0018                      REL
0019                      EXD
0020                      SUBR  OPCK
0021                *
0022 00000   0 000000  OPCK DAC   **          (10)
0023                *
0024                *     1. IF OPERATOR REQUIRES SERVICE
0025                *
0026 00001  -0 02 00013     LDA*  OPI                LOAD OPERATOR INTERRUPT FLAG
0027 00002   101040         SNZ
0028 00003  -0 01 00000     JMP*  OPCK         RETURN TO CALLING PROGRAM IF BIT NOT SET
0029                *
0030                *       A. SET WRITE BITS FOR LOADABLE DATA BASE
0031                *
0032 00004  -0 02 00014     LDA*  LDBB
0033 00005   140500         SSM
0034 00006  -0 04 00014     STA*  LDBB
0035                *
0036                *       B. CLEAR DISPLAY SCREEN
0037                *
0038 00007   0 02 00114     LDA   P12
0039 00010   74 0004        CTA   4
0040 00011   0 01 00010     JMP   *-1
0041                *
0042                *       C. RETURN TO EXEC FOR LOADING OF NODAL OPERATOR INTERACTION
0043                *
0044 00012  -0 01 00015     JMP*  NRRT
0045                *
0046                *          STORAGE - LINKAGE - EXTERNAL REFERENCES
0047                *
0048          000101    P1    EQU   *101   (11)
0049          000114    P12   EQU   *114
0050                *
0051 00013   0 000000  OPI   XAC   OPI          OPERATOR INTERRUPT FLAG
0052 00014   0 000000  LDBB  XAC   LDBB         LOADABLE DATA BASE WRITE FLAG
0053 00015   0 000000  NRRT  XAC   NRRT         SPECIAL EXEC RETURN (PATE)
0054                      FIN
0055                      END

LDBB   000014    NRRT   000015    OPCK   000000    OPI    000013
```

KEY

(1) MODULE NUMBER
(2) MODULE NAME
(3) SOURCE FILE NAME
(4) DATE ENTERED INTO LIBRARY
(5) CODERS NAME
(6) PERSON MAKING REVISION
(7) DATE REVISION MADE
(8) ABSTRACT
(9) CALLING SEQUENCE
(10) COMMENT
(11) STORAGE-LINKAGE-EXTERNAL REFERENCES

FIGURE 5-28. EXAMPLE OF CODING CONVENTIONS

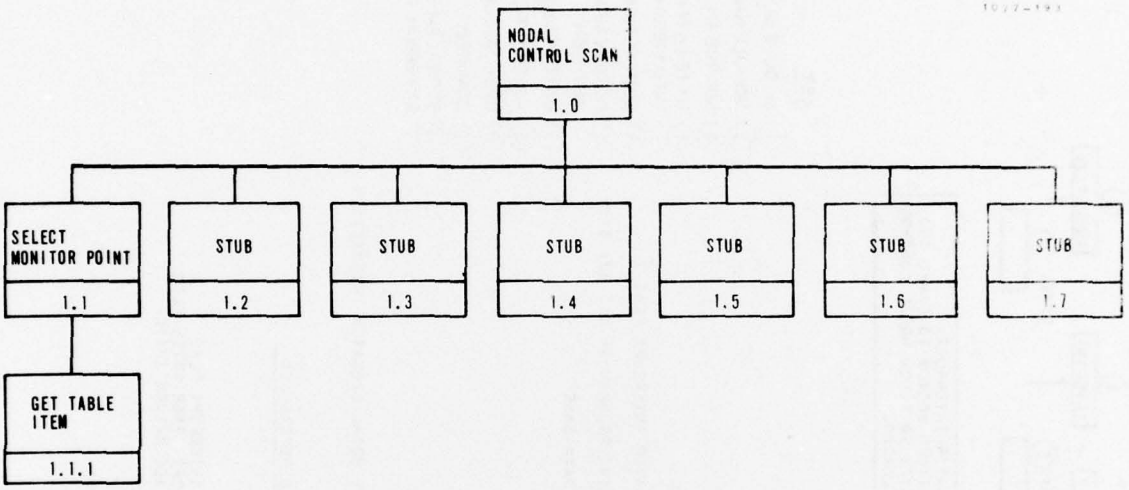

FIGURE 5-29. TEST CONFIGURATION FOR MODULE 1.0

monitor module. With this information, it could be determined that the control module was calling the correct input module. The scan tables were generated and the entire set of modules was loaded. The results of the testing verified that modules 1.0, 1.1 and 1.1.1 did the job that they were designed to do.

Next, the input modules (1.2, 1.3, 1.4) were tested. Processing is similar in all these modules in that they load the DLC output buffer with command characters and process the return data. It was decided that all these communication modules could be tested by bypassing the DLC communications. A stub was generated to replace module 4.11 which is called after the DLC output buffer is loaded. This stub printed out the contents of the DLC output buffer and generated data in the input buffer as it would have been received from the commanded device. This provided a scheme for testing all the output modules (1.2.1, 1.3.1, 1.4.1, 1.4.2, 1.4.3) as well as the processing sections of modules 1.2 and 1.3 and modules 1.4.4, 1.4.5, 1.4.6, 4.22 and 4.18. Stubs were also written for modules 4.9, 4.12 and 4.16 to allow the test program to run through a complete set of test data to exercise all modules.

Similar techniques were used to test other modules (1.5, 1.6, 2.0 and 4.8).

5.5 SYSTEM INTEGRATION

It was in the system integration phase of development that the benefits of using structured programming techniques were fully realized. By the time all the equipment was connected, the only software modules that were not thoroughly tested were the DLC communication software written to replace the PATE nucleus software and other modules associated with the communication process. An added benefit of top-down structured became recognized during the preparation of test procedures for both in-plant and field tests. Personnel not familiar with the software were responsible for writing the test procedures. Because of the visibility provided by the HIPO diagrams and playscripts, the procedures, many of which verified software algorithms (such as trending), as well as hardware operation, were prepared without having to disrupt the on-going software design process by unduly tying up programmers for information.

5.6 SUMMARY OF SOFTWARE EFFORT

The following is a summary of the effort expended to develop the software for the DATEC Program:

- The software development team was organized in the Chief Programmer Team Concept consisting of: chief programmer, backup programmer, three support programmers and a librarian.

- The design phase started in April 1976 and was completed in September 1976. Coding and testing/debugging were conducted concurrent with the design task. The calendar spread over which coding took place was from June through November 1976. Testing/debugging was accomplished in September through December 1976.

- System Integration also overlapped the design process--running from October 1976 into mid-February 1977.

- The breakdown percentage-wise of development effort was estimated to be: design - 60 percent; coding - 20 percent; and testing/integration - 20 percent.

- In the course of the software development, between 16,000 and 17,000 instructions of code were written. In addition, 15,000 words were written for the data base consisting of constants, flags, work spaces and tables. These data types were used in the loadable data base file, site data overlay files and the paged data files. The coding rate (including design, coding, debugging, and documentation) was between 10 and 11 instructions per day, per person. This is a conservative calculation, since all six members of the team were not on the program from beginning to end.

5.7 LESSONS LEARNED FROM STRUCTURED PROGRAMMING APPLICATION

There was no doubt that utilizing the top-down structured programming approach to software design resulted in an orderly, highly visible design process. Software program objectives and intermediate milestones were met in a timely fashion because the very nature of structured programming techniques dictated that they be highly definitized. The integration phase went smoothly and on-time because the time was spent in integrating - not in debugging the various modules. Field tests progressed without tie-ups due to software problems because these problems, when they did infrequently occur, were solved quickly by the chief programmer. The Chief Programmer Team (CPT) concept assured that one person had overall knowledge of the complete software effort.

The Digital ATEC software is written in machine language and is therefore restricted to the 316 computer. It should be pointed out though, that because of the highly visible documentation provided through the use of structured programming techniques, it would be a fairly easy job to convert the software to a higher order language. Rather than having to study listings and flow diagrams (which are the normal output of so-called traditional software development programs) to try to understand what the software was doing and then convert to higher language; the programmers would simply take the various modules which have already been structured into manageable functional blocks and,

using the self-explanatory HIPO diagrams and supporting playscripts, accomplish the conversion task.

Despite all the positive things resulting from applying structured programming, there were several areas where, if things had been done slightly differently, the results would have been even more impressive. These are summarized below:

a. The librarian should insist upon complete documentation consistency. Although everybody on the CPT knew the format requirements, there were occasional slips. The librarian is in the best position to enfore consistency.

b. The librarian should perform the editing function. It was found that an efficient way to handle program changes was to have the individual programmer red-line his listing with the desired changes and let the librarian handle the revisions completely from that point and place the revised listing into the library.

c. Walkthroughs should be conducted between the programmer and the chief programmer only-- not the entire team. This results in a faster review and lets the rest of the team free to carry their designs forward. As far as familiarity with the other team members' modules is concerned, it does not have to be obtained in this manner. The visibility of the software in the top-down structured programming method assures that any programmer can pick up another team member's output and gain the familiarity on his own in a short period of time.

d. Playscripts are more accurate if generated concurrent with the coding activity. The overall effort is accomplished in a shorter time span also. The playscripts act as a road map for the coding process; however, invariably as the coding took place, numerous improvements and required changes became evident. Changes to a previously completed playscript then had to be processed and entered in the library, which created additional effort for everyone involved.

e. Module testing should be flexible and make use of bottom-up as well as top-down test techniques. It was found early in the software module test phase that many of the lower tier modules could be checked out with relatively little input requirements from higher level modules. These modules, once verified, were then available for test of higher tier modules as opposed to additional software activity created by the necessity of generating stubs for testing purposes.

5.8 CONCLUSIONS AND RECOMMENDATIONS RELATIVE TO SOFTWARE PROGRAM

The following paragraphs present the software related conclusions and recommendations resulting from satisfactory completion of the ATEC Digital Adaptation Study. The recommendations, most of which arose as a result of the field test phase of the study, are presented with the primary objective of improving the overall usefulness and effectiveness of the DATEC system.

5.8.1 Conclusions

The specific requirements for the adaptation of PATE software for the digital ATEC Program were delineated in paragraph 1.3.1 of Attachment 2 to the revised S.O.W. for the ATEC Digital Adaptation Study. This attachment further invoked upon the software program the requirement that the software be developed in accordance with Annex III to the revised S.O.W. Among the more important requirements of this Annex was that of employment of structured programming techniques during the software development phase.

Upon completion of the ATEC Digital Adaptation Study through the field test phase, it is concluded that the software program accomplished all S.O.W. requirements and that all DATEC program software related milestones were met in a timely manner. These conclusions are evidenced by the successful operation of the DATEC software, both during in-plant and field tests; by the foregoing material presented in this section, and by software related material presented in Section 6 which is an excerpt from the Field Test and Evaluation Report.

Successful conclusion of the software program was due in large part to the application of top-down structured programming principles. This resulted in an accurate and orderly development process with a corresponding output of highly visible design documentation. The software development was accomplished in an efficient manner because the design group was organized in a Chief Programmer Team concept. This assured that each member of the team had explicit responsibilities.

5.8.2 Recommendations

The following recommendations, derived primarily from observations made during field tests and evaluations, are made with the thought of suggesting areas in which DATEC might be improved as a nodal control element.

a. Provide an immediate scan interrupt capability. This will allow the operator to gain immediate control without having to wait for an in-process measurement to be completed.

b. Streamline the scan sequence in order to shorten scan time.

c. Update CRT display with a single computer output as opposed to outputting display format and data separately.

d. Provide CRT paging within a single site to allow the operator to access various site displays using only a single page number.

e. Provide automatic self-test which is incorporated periodically as part of the scan sequence.

f. Make the following improvements to the Monitor Immediate mode:

- Provide a constructable scan sequence wherein the nodal controller selects the number and order of scanned monitor points.
- Add argument to Monitor Immediate command word to designate the display page which is desired to be observed.
- Add alarm scanner and T1WB1 FER commands.

g. Provide indication on CRT when Monitor Immediate mode is in progress; also an identification of what baseband, A or B, is being monitored by the BEM.

h. Show highest level system alarm as part of major alarm warning indicator.

i. Add alarm thresholds and flags to the key trend analysis parameters.

j. Add remote alarm status of the T1-4000 and T1WB1 multiplexers to the list of monitor points.

k. Provide an operator command to initialize the EPUTS to zero.

l. Add fault isolation routines to software.